# High-resolution reconstruction of Holocene climate variability and environmental changes in the North Pacific using bivalve shells

Dissertation

zur Erlangung des Grades

“Doktor der Naturwissenschaften“

im Promotionsfach Geologie/Paläontologie

am Fachbereich Chemie, Pharmazie und Geowissenschaften

der Johannes Gutenberg-Universität Mainz

von

Nadine Hallmann

geb. in Nauen

Mainz, 2011

(D77)

Dekan: Not displayed for reasons of data protection.

1. Berichterstatter: Not displayed for reasons of data protection.

2. Berichterstatter: Not displayed for reasons of data protection.

3. Berichterstatter: Not displayed for reasons of data protection.

Datum der mündlichen Prüfung: 09.06.2011

Ich erkläre hiermit, dass ich die vorliegende Arbeit

selbständig verfasst und keine anderen als

die angegebenen Quellen und Hilfsmittel benutzt habe.

Mainz, März 2011

Denken und Tun, Tun und Denken, das ist die Summer aller Weisheit,

von jeher anerkannt, von jeher geübt, nicht eingesehen von einem jeden.

Beides muß wie Aus- und Einatmen sich im Leben ewig fort hin und wider bewegen;

wie Frage und Antwort sollte eins ohne das andere nicht stattfinden.

-Johann Wolfgang von Goethe-

# PREFACE

This thesis presents results from a three years and seven months research on bivalve shells as climate proxy archives in the paleontological group of Prof. Dr. Bernd R. Schöne in Mainz. I started my Ph.D. in August 2007 in this group. The aim of this project is the reconstruction of Holocene climate variations in the North Pacific with a high spatial and temporal resolution using marine bivalve shells and the technique of high-resolution isotope sclerochronology. The purpose is to create a network of climate proxies based on bivalve shells to study large-scale climate variations during the Holocene. High-resolution proxy data from the marine environment of the mid- and high-latitudes are rare, therefore, this study contributes to the understanding of past climate and the improvement of the prediction of future climate.

This research was conducted under the supervision of Prof. Dr. Bernd R. Schöne. The accomplishment of this multidisciplinary project was made possible with the collaboration of research groups in Canada, The United States of America and Japan. Within the framework of this study a two-month research stay in Tokyo, Japan, from July to August 2009 permitted the collection of modern and archaeological shells and to maintain contact with our Japanese colleagues.

This thesis consists of three manuscripts, which are published in international peer-reviewed journals. The first paper, published in Palaeogeography, Palaeoclimatology, Palaeoecology, examines the reliability of the long-lived bivalve mollusk *Panopea abrupta* as a climate archive to reconstruct temperatures of the oxygen isotope values of the shells is tested. The second manuscript, published in the Journal of Archaeological Science, provides new insights into the biology, geochemistry and seasonal growth of the short-lived bivalve *Saxidomus gigantea*, which is crucial information for interpreting paleoenvironments and the season of shellfish collection in archaeological contexts. A combined approach of sclerochronology and stable isotope analysis helps to refine seasonality estimates and to improve the understanding of the gathering strategies of pre-historic coastal communities of hunter-gatherers. The third manuscript, published in PALAIOS, presents a model for reconstructing water temperatures and salinity from shell growth rates of the butter clam *S. gigantea* from south west Alaska, which allows us to disentangle the influence of freshwater and temperature on shell oxygen isotope values. An integrated growth pattern and isotope approach can be used to estimate salinity and temperature changes in freshwater-

influenced environments through time. Therefore, this study allows for a better understanding of hydrological changes related to the Alaska Coastal Current, and helps to interpret the meaning of oxygen isotope data in estuarine settings.

I would like to use this preface to thank all the people that contributed to this study. First of all, I am grateful to my supervisor Prof. Dr. Bernd R. Schöne for his guidance and support during this time. I wish to acknowledge the German Research Foundation (DFG) who funded this research project and the Japan Society for the Promotion of Science (JSPS) who provided financial support during my stay at the University of Tokyo. I want to thank all the numerous collaborators and providers of study material who made this project possible.

Mainz, 25 March 2011

Nadine Hallmann

# ABSTRACT

Bivalve mollusk shells are useful tools for multi-species and multi-proxy paleoenvironmental reconstructions with a high temporal and spatial resolution. They are valuable proxy archives to detect past environmental changes, since they record sensitive environmental information in their carbonate shells, but also these data can be used to gain new insights into the settlement and subsistence strategies of prehistoric people. Past environmental conditions can be reconstructed from shell growth and stable oxygen and carbon isotope ratios, which present an archive for temperature, freshwater fluxes and primary productivity. The purpose of this thesis is the reconstruction of Holocene climate and environmental variations in the North Pacific with a high spatial and temporal resolution using marine bivalve shells. This thesis focuses on several different Holocene time periods and multiple regions in the North Pacific, including: Japan, Alaska (AK), British Columbia (BC) and Washington State, which are affected by the monsoon, Pacific Decadal Oscillation (PDO) and El Niño/Southern Oscillation (ENSO). Such high-resolution proxy data from the marine realm of mid- and high-latitudes are still rare. Therefore, this study contributes to the optimization and verification of climate models. However, before using bivalves for environmental reconstructions and seasonality studies, life history traits must be well studied to temporally align and interpret the geochemical record. These calibration studies are essential to ascertain the usefulness of selected bivalve species as paleoclimate proxy archives. This work focuses on two bivalve species, the short-lived *Saxidomus gigantea* and the long-lived *Panopea abrupta*.

In the first part of this study, the sclerochronology and oxygen isotope ratios of different shell layers of *P. abrupta* were studied in order to test the reliability of this species as a climate archive and to reconstruct temperatures. The growing season lasts mainly during the warm period of the year from March/April through November/December with maximum growth rates in late spring and summer and negligible rates during the cold winter months. Shell growth patterns are clearly discernable in umbonal shell portions, but less so in the outer shell layer near the ventral margin. The $\delta^{18}O$ values recorded from the inner and outer shell layer are not the same. Temperatures reconstructed from the oxygen isotope values taken from the outer shell layer compare well with instrumental water temperature, however, values from the umbo differ by up to 3°C. The outer shell layer seems to be precipitated in isotopic equilibrium with the seawater. In contrast, the precipitation of the inner shell layer appears to

be in isotopic disequilibrium with the seawater. Therefore, annual increment widths should be measured in umbonal shell portions and a reliable reconstruction of paleotemperatures may only be achieved by exclusively sampling the outer shell layer of multiple contemporaneous specimens.

*S. gigantea* is one of the most commonly recovered bivalves from archaeological midden deposits along the west coast of North America. The second part of this thesis presents the first detailed analysis of life history traits and a stable isotope record of *S. gigantea*, which provides new insights into the growth of this species. Shell growth records and shell geochemistry can be used to reconstruct paleotemperature and paleoenvironmental conditions as well as to identify the season of shellfish collection and proxy the season of site occupation in archaeological contexts. However, this approach requires detailed knowledge of the life history traits, including regional variation in both shell growth and stable isotope values. Modern shells collected alive on a monthly basis for a period of one year in 1987-1988 from Pender Island (southern BC) and additional specimens from Dundas Islands in 2006 (northern BC) and Mink and Little Takli Islands (AK) in 1998, 2003 and 2007 were analyzed to determine the life history traits of this species, such as the timing of growth line formation, the duration of the growing season and seasonal varying growth rates, and geochemistry of live-collected *S. gigantea* shells. Intra-annual increments show clear seasonal oscillations with broadest increments in summer and very narrow increments or a growth cessation during winter months. Frequency analysis (multitaper method) revealed a fortnightly shell growth pattern with the formation of lunar daily growth increments. There is a latitudinal trend in shell growth with narrower annual increments and less lunar daily increments per year in shells from AK than in shells from BC. Shells from BC may grow throughout the whole year or may cease growth in some years for up to two months from mid November to the beginning of February. Alaskan shells may stop growth for six to seven months per year from approximately October/November to April/May. There is also a seasonal variation of oxygen isotopes with most positive $\delta^{18}O_{shell}$ values during winter and most negative values during summer. The range of $\delta^{18}O_{shell}$-derived temperatures is larger than the annual range of instrumental temperatures indicating a freshwater influx. A combined approach using sclerochronological and geochemical data can refine estimates for the season of shellfish collection and improve the understanding of resource procurement strategies of prehistoric people. Comparison of shell growth pattern and an appropriate tidal calendar permits precise estimates of collection circumstances, such as low or high tide, springs or

neaps, day- or nighttime and the relative position in the intertidal zone. However, the analysis of several shells from each locality is necessary due to intra-specific variability.

In the final part of this study a growth-temperature model based on *S. gigantea* shells from south west Alaska was established, which provides a better understanding of the hydrological changes related to the Alaska Coastal Current (ACC). This approach allows the independent measurement of water temperature and salinity from variations in the width of lunar daily growth increments of *S. gigantea*. Temperature explains 70% of the variability in shell growth. In combination with $\delta^{18}O_{shell}$ values, increment-derived temperatures were used to estimate salinity changes. The model was calibrated and tested with modern shells and then applied to archaeological specimens. The time period between 988 and 1447 cal yrs BP was characterized by colder (~1-2°C) and much drier (2-5 PSU) summers, and a likely much slower flowing ACC than at present. In contrast, the summers during the time interval of 599-1014 cal yrs BP were colder (up to 3°C) and fresher (1-2 PSU) than today. The Aleutian Low may have been stronger and the ACC was probably flowing faster during this time.

# ZUSAMMENFASSUNG

Muschelschalen eignen sich hervorragend für raumzeitlich hochaufgelöste Paläoumweltrekonstruktionen anhand verschiedener Proxies und basierend auf mehreren Arten. Ihre Karbonatschalen zeichnen Umweltinformationen auf und sie stellen somit wertvolle Proxyarchive zur Aufdeckung von Umweltveränderungen in der Vergangenheit dar. Des Weiteren erlauben Muschelschalen Einblicke in die Besiedlung und Subsistenz prähistorischer Völker. Umweltbedingungen der Vergangenheit können aus dem Schalenzuwachs und den stabilen Sauerstoff- und Kohlenstoffisotopenverhältnissen rekonstruiert werden, welche Archive für Temperatur, Süßwassereintrag und Primärproduktivität darstellen. Das Ziel dieser Doktorarbeit besteht darin, holozäne Klima- und Umweltschwankungen im nordpazifischen Sektor mit einer hohen räumlichen und zeitlichen Auflösung mittels Muschelschalen zu rekonstruieren. Diese Arbeit fokussiert sich dabei auf verschiedene holozäne Zeitabschnitte und mehrere Regionen im Nordpazifik, darunter Japan, Alaska (AK), Britisch-Kolumbien (BC) und Washington, welche vom Monsun, der Pazifischen Dekadischen Oszillation (PDO) und der *El Niño/Southern Oscillation* (ENSO) beeinflusst werden. Derartig hochauflösende Proxydaten aus dem marinen Bereich der mittleren und hohen Breiten sind jedoch selten. Somit trägt diese Arbeit zur Optimierung und Verifikation von Klimamodellen bei. Bevor Muschelschalen allerdings zur Umweltrekonstruktion und in Studien zur Saisonalität im archäologischen Kontext verwendet werden können, müssen *life-history*-Eigenschaften untersucht werden, um die geochemischen Daten zeitlich anzuordnen und zu interpretieren. Solche Kalibrierungsstudien sind notwendig, um die Nutzbarkeit ausgewählter Muschelarten als Paläoklimaarchiv zu untersuchen. Im Fokus dieser Arbeit stehen zwei Muschelarten: die kurzlebige Buttermuschel *Saxidomus gigantea* und die langlebige Elefantenrüsselmuschel *Panopea abrupta*.

Im ersten Teil dieser Arbeit wurden verschiedene Schalenlagen von *P. abrupta* sklerochronologisch und sauerstoffisotopisch untersucht, um die Eignung dieser Art als Klimaarchiv und die mögliche Rekonstruktion von Temperaturen zu prüfen. Die Wachstumssaison ist hauptsächlich während der warmen Jahreszeit und dauert von März/April bis November/Dezember mit maximalen Wachstumsraten im Spätfrühling und Sommer und geringfügigem Wachstum während der kalten Wintermonate. Wachstumsmuster sind im Schalenwirbel klar erkennbar, jedoch sind sie in der äußeren Schalenlage in der Nähe des ventralen Schalenrandes nur schlecht sichtbar. Die $\delta^{18}O_{Schale}$-Werte der inneren und

äußeren Schalenlage unterscheiden sich. Temperaturen, die von $\delta^{18}O_{Schale}$-Werten der äußeren Schalenlage rekonstruiert werden, stimmen gut mit den instrumentellen Wassertemperaturen überein. Rekonstruierte Temperaturen vom Schalenwirbel unterscheiden sich jedoch um bis zu 3°C von den gemessenen Temperaturen. Die äußere Schalenlage scheint sich im sauerstoffisotopischen Gleichgewicht mit dem Meerwasser zu bilden. Im Gegensatz dazu scheint sich die innere Schalenlage im isotopischen Ungleichgewicht mit dem Wasser zu bilden. Demzufolge sollten die jährlichen Inkrementbreiten im Schalenwirbel gemessen werden und eine verlässliche Rekonstruktion von Paläotemperaturen kann nur durch die ausschließliche Beprobung der äußeren Schalenlage von mehreren kontemporären Muschelschalen erreicht werden.

*S. gigantea* ist eine der häufigsten Muschelschalen in Küchenabfallhaufen (*shell middens*) entlang der Westküste Nordamerikas. Der zweite Teil dieser Arbeit beinhaltet die erste detaillierte Untersuchung der *life-history*-Eigenschaften und der stabilen Isotopenverhältnisse von *S. gigantea*, welche einen neuen Einblick in das Wachstum dieser Art gewährt. Schalenzuwachs und Schalengeochemie erlauben sowohl die Rekonstruktion von Paläotemperaturen und Paläoumweltbedingungen als auch die Bestimmung der Saison der Muschelaufsammlung und somit ein Verständnis über die Besiedlung durch prähistorische Völker. Dieser Ansatz erfordert jedoch ein detailliertes Wissen über die *life-history*-Eigenschaften unter Einbeziehung von regionalen Variationen im Schalenwachstum und in den stabilen Isotopenverhältnissen. Rezente Muschelschalen wurden monatlich für die Dauer von einem Jahr in 1987-1988 bei Pender Island (südliches BC) lebend gesammelt. Weitere Schalen wurden 2006 bei Dundas Islands (nördliches BC) und 1998, 2003 und 2007 bei Mink und Little Takli Islands (AK) aufgesammelt. Diese Muschelschalen wurden untersucht, um die *life-history*-Eigenschaften dieser Art, wie z.B. das Timing der gebildeten Wachstumslinien, die Dauer der Wachstumssaison und die saisonal variierenden Wachstumsraten, sowie die Geochemie von lebend gesammelten *S. gigantea* Schalen zu bestimmen. Intraannuelle Inkremente zeigen deutliche saisonale Oszillationen mit breiten Inkrementen im Sommer und sehr schmalen Inkrementen oder einer Wachstumspause während der Wintermonate. Eine Frequenzanalyse (Multitaper Methode) ergab ein *Fortnight*-Zuwachsmuster mit der Bildung von lunartäglichen Wachstumsinkrementen. Es besteht ein Trend im Schalenwachstum entlang der geographischen Breiten mit schmaleren Jahresinkrementen und weniger lunartäglichen Wachstumsinkrementen pro Jahr in Muschelschalen aus AK verglichen mit Schalen aus BC. Muschelschalen aus BC können das ganze Jahr über wachsen oder stellen das Wachstum in einigen Jahren für bis zu zwei Monate

von Mitte November bis Anfang Februar ein. Dagegen hören Schalen aus Alaska für sechs bis sieben Monate pro Jahr von ungefähr Oktober/November bis April/Mai auf zu wachsen. Des Weiteren besteht eine saisonale Variation in den Sauerstoffisotopenverhältnissen mit positivsten $\delta^{18}O_{Schale}$-Werten im Winter und negativsten Werten im Sommer. Der Bereich der von den $\delta^{18}O_{Schale}$-Werten abgeleiteten Temperaturen ist größer als die jährliche Spannbreite der instrumentellen Temperaturen. Das zeigt den Eintrag von Süßwasser an. Ein kombinierter Ansatz unter Verwendung von sklerochronologischen und geochemischen Daten kann die Genauigkeit der Bestimmung der Saison der Muschelaufsammlung und das Verständnis der Ressourcenbeschaffung prähistorischer Völker verbessern. Der Vergleich des Zuwachsmusters der Schalen mit einem geeigneten Gezeitenkalender erlaubt eine präzise Bestimmung der Umstände während des Aufsammelns der Schalen. Diese wären z.B. Ebbe oder Flut, Springfluten oder Nippfluten, Tag oder Nacht und die relative Position in der Gezeitenzone. Allerdings ist aufgrund der intraspezifischen Variabilität die Untersuchung von mehreren Muschelschalen von jeder Lokalität erforderlich.

Im letzten Teil dieser Arbeit wurde basierend auf *S. gigantea* Schalen aus Südwest-Alaska ein Wachstums-Temperatur-Modell aufgestellt, welches ein besseres Verständnis der hydrologischen Veränderungen der Strömung entlang der Küste Alaskas (*Alaska Coastal Current*, ACC) bietet. Dieser Ansatz erlaubt die unabhängige Messung von Wassertemperatur und Salinität aus Variationen in der Breite der Tagesinkremente in *S. gigantea*. Der Schalenzuwachs ist bis zu 70% temperaturgesteuert. In Kombination mit $\delta^{18}O_{Schale}$-Werten wurden die von den Wachstumsinkrementen abgeleiteten Temperaturen zur Rekonstruktion von Salinitätsveränderungen verwendet. Das Modell wurde mit rezenten Muschelschalen kalibriert und getestet und dann auf archäologische Schalen angewandt. Die Sommer in der Zeit zwischen 988 und 1447 Jahren vor heute waren kälter (~1-2°C) und viel trockener (2-5 PSU) und der ACC floss wahrscheinlich viel langsamer als heute. Im Gegensatz dazu waren die Sommer zwischen 599-1014 Jahren vor heute kälter (bis zu 3°C) und frischer (1-2 PSU) als heute. Das Aleutentief war wahrscheinlich stärker zu dieser Zeit und der ACC floss voraussichtlich schneller.

# ACKNOWLEDGEMENTS

For reasons of data protection the content of the acknowledgements is not displayed in the online version of this thesis.

# TABLE OF CONTENTS

# LIST OF FIGURES

**CHAPTER 2**



**CHAPTER 3**

**CHAPTER 4**

**CHAPTER 6**

# LIST OF TABLES

**CHAPTER 2**



**CHAPTER 3**

**CHAPTER 4**

# Chapter 1: INTRODUCTION

This chapter introduces the climate regimes of the North Pacific, the climate variability in this region during the Holocene and the use of proxy archives for the reconstruction of past climate and environmental variability. The research field of sclerochronology is described and the advantage of bivalve shells over other proxy archives is outlined. Furthermore, the importance of shell middens is explained. This chapter also gives a brief introduction to the use of stable oxygen and carbon isotopes for environmental reconstructions from shells and summarizes the relevant sclerochronological methods. Finally, the key aims and objectives of this study together with an overview of the research are presented.

## *1.1. The North Pacific climate*

The North Pacific Ocean extends from the Arctic in the north to the equator in the south and from Asia in the west to North America in the east. There are two major climate oscillations occurring in the North Pacific: the Pacific Decadal Oscillation (PDO) and the El Niño/Southern Oscillation (ENSO). The PDO is the leading mode of North Pacific sea surface temperature (SST) variability (MANTUA et al., 1997). This inter-decadal climate pattern oscillates between positive (warm) and negative (cold) phases, which persist for 20 to 30 years and are characterized by distinctive SST, surface wind and sea level pressure (SLP) anomalies (MANTUA, 1997; MANTUA and HARE, 2002). During a positive PDO phase, the SSTs in the central North Pacific are anomalously cool but along the American west coast they are anomalously warm. Low pressures over the North Pacific from November to March lead to strong counterclockwise winds while high SLPs over the northern subtropical Pacific cause clockwise winds (MANTUA and HARE, 2002). A negative PDO phase is characterized by the opposite patterns. During a warm PDO phase, precipitation and river discharge are enhanced over south central Alaska and are reduced over the Pacific Northwest and British Columbia (MANTUA et al., 1997; DETTINGER et al., 2001; MUNDY, 2005). This large-scale climate system is responsible for changes in marine ecosystems (FRANCIS et al., 1998), e.g., the PDO influences the biological productivity of the oceans (HARE and MANTUA, 2000) and is correlated with salmon productivity (MANTUA et al., 1997; HARE et al., 1999).

PDO and ENSO have teleconnections and affect global climate with their characteristic temperature, wind, pressure and precipitation patterns, and also biological

productivity (e.g., MANTUA et al., 1997; STENSETH et al., 2002). BARNETT et al. (1999) describe an atmospheric teleconnection between the North Pacific and the Tropical Pacific. Here, decadal oscillations over the North Pacific modulate ENSO on a decadal time scale.

ENSO is a weather pattern which originates in the Equatorial Pacific and has three phases: warm (El Niño), normal and cold (La Niña). The Equatorial Pacific is warm during El Niño; SSTs are high in the East Pacific and low in the West Pacific. This leads to lower pressures over the East Pacific and higher pressures over Southeast Asia and the West Pacific. Consequently, the trade winds weaken and precipitation is thereby increased in the East Pacific and decreased in the West Pacific. In contrast, during La Niña, the Equatorial Pacific is cold. Decreased SSTs in the East and Central Pacific, and increased SSTs in the tropical West Pacific, lead to higher pressures over the East Pacific and lower pressures over Indonesia and Australia. Trade winds strengthen due to the high pressure gradient, and as a consequence, less precipitation occurs in the East Pacific while precipitation is increased in the West Pacific.

There is a clear relationship between PDO and ENSO. Cold PDO is correlated with La Niña-like climate patterns, and warm PDO with El Niño-like climate (MANTUA et al., 1997; ZHANG et al., 1997). Furthermore, El Niño is stronger during a highly positive PDO phase (GERSHUNOV and BARNETT, 1998). In contrast to the PDO, ENSO has secondary effects on the climate of the North Pacific. ENSO signals occur in the northern North Pacific eight to twelve months after the initiation of an ENSO event in the Tropical Pacific (SPIES, 2007). Therefore, ENSO signals in the Gulf of Alaska are strongest during autumn and winter (SPIES, 2007). PDO and ENSO have different time scales. In contrast to the multidecadal PDO, ENSO exhibits frequencies of three to seven years (CANE, 2005), and typical ENSO events last for six to eighteen months.

The climate over the North Pacific is determined by the Aleutian Low (AL) and the North Pacific High (NPH). The AL is located near the Aleutian Islands and is most intense during spring and winter, whereas the NPH is strongest in summer (MUNDY, 2005; SPIES, 2007). The NPH moves southward during the winter when the AL dominates (SPIES, 2007). This low pressure area reveals decadal variability (OVERLAND et al., 1999). Both atmospheric pressure systems, AL and NPH, are associated with the PDO. The AL is stronger during a PDO warm phase than during a cold phase (SPIES, 2007). As described by HARE and MANTUA (2000), the strength of the AL can be measured with the following atmospheric indices: the Pacific/North American (PNA) teleconnection index (WALLACE and GUTZLER, 1981), the

North Pacific Index (NPI, TRENBERTH and HURRELL, 1994) and the Aleutian Low Pressure Index (ALPI, BEAMISH and BOUILLON, 1993). An intense AL during a positive PDO leads to a warming of the ocean, an increase in precipitation and stormy weather (EMERY and HAMILTON, 1985; MUNDY, 2005; SPIES, 2007). In contrast, during a negative PDO the weather is colder, drier and less stormy (MUNDY, 2005; SPIES, 2007).

Variations in the amount of precipitation influence the transport of the Alaska Coastal Current (ACC), which is one of the major circulation systems in the Gulf of Alaska (ROYER, 1981). The ACC extends from southern British Columbia, around the Gulf of Alaska to Unimak Pass, where it flows into the Bering Sea (MUENCH et al., 1978; SCHUMACHER et al., 1982; KIPPHUT, 1990; SPIES, 2007). This alongshore flow is affected by freshwater influx (melt water and precipitation) along the Alaskan coast and wind (ROYER, 1982; JOHNSON et al., 1988; STABENO et al., 2004). The ACC brings freshwater to the Bering Sea, the Arctic Ocean and finally to the northern North Atlantic (KEIGWIN and COOK, 2007; HU et al., 2010). The ACC is therefore important in determining climate through the transport of cool and fresh waters. This coastal current, of relatively low salinity, also transports sediments and nutrients and therefore influences the productivity of the surrounding ecosystems.

## *1.2. Climate reconstructions using proxy archives*

Knowledge of past climate and environmental variations is essential for the prediction of future climate. Meteorological records are limited to the past 150 years and are too short to study long-term climate variability. In addition, instrumental data for the marine realm exist only for the past 100 years. An improved understanding of long-term climate oscillations, such as PDO, requires longer time series than those obtainable from the instrumental records. For longer environmental reconstructions it is necessary to use proxy archives for temperature and other environmental parameters. There is a variety of natural climate archives that grow periodically and record environmental conditions through variations in growth and geochemistry. These can be divided in abiogenic and biogenic archives. Abiogenic proxy archives are ice cores (e.g., PETIT et al., 1990, 1999; THOMPSON et al., 1998), speleothems (e.g., HENDY and WILSON, 1968; SPÖTL and MATTEY, 2006) and marine, lake and river sediments (e.g., HOUGH, 1953; LAMOUREUX, 2000; NEDERBRAGT and THUROW, 2001). Ice cores contain proxies for environmental parameters such as temperature (JOHNSEN et al., 1995; VIMEUX et al., 2002), precipitation (STEIG et al., 1994) and insolation (PETIT et al., 1999). Gas bubbles trapped in the cores provide information about the ancient atmosphere (in

particular $CO_2$; FRIEDLI et al., 1986; BATTLE et al., 1996; MONNIN et al., 2004). Speleothems are an important terrestrial climate archive. They allow precise (uranium) dating and their geochemistry (stable oxygen and carbon isotopes, and trace elements) and laminations reveal information about temperature, precipitation and vegetation history (e.g., LAURITZEN and LUNDBERG, 1999; MCDERMOTT, 2004). Furthermore, the lamination and geochemistry of sediments also serve as proxies for temperature (MOORE et al., 2001), precipitation (NEDERBRAGT and THUROW, 2001), sea/lake level (ABBOTT et al., 2000) and biological productivity (SCHELSKE et al., 1988).

Biogenic proxy archives include trees (FRITTS, 1976; BECKER et al., 1991), corals (BECK et al., 1992; REN et al., 2003), pollen (ALLEY, 1976; HEBDA, 1995), fish otoliths (KALISH, 1991), ostracods (HU et al., 1998), diatoms (CHANG and PATTERSON, 2005; KHIM et al., 2005), midges (PALMER et al., 2002; ROSENBERG et al., 2004), stromatolites (PAERL et al., 2003), coralline sponges (FALLON et al., 2005; ROSENHEIM et al., 2005), coralline red algae (HALFAR et al., 2007, 2011; HETZINGER et al., 2009) and bivalves (e.g., DAVENPORT, 1938; JONES et al., 1989). Trees are a terrestrial archive and their rings contain information about variations in precipitation (GRAUMLICH, 1987; D'ARRIGO and JACOBY, 1991) and temperature (BRIFFA et al., 1990; WILES et al. 1996, 1998; BARBER et al., 2004). Tree rings allow the reconstruction of long master chronologies and therefore, the analysis of long-term climate oscillations. BECKER et al. (1991) constructed an extremely long master chronology of about 10 000 years using Holocene oaks from south central Europe. However, the longest master chronology currently available for the North Pacific region is only approximately 1000 years long (BARCLAY et al., 1999). In the marine realm, corals can provide particularly long-term environmental records since some coral colonies may exceed several hundred years of age. They may even reveal a higher temporal (i.e., subseasonal) resolution than trees. Sea surface temperatures can be reconstructed from the oxygen isotopes (ZINKE et al., 2009) or trace element ratios (Mg/Ca, Sr/Ca; BECK et al., 1992; MITSUGUCHI et al., 1996; PFEIFFER et al., 2009) of their skeletons. However, the construction of master chronologies based on coral growth patterns is much more difficult than for trees. Nevertheless, both archives (trees and corals) allow the reconstruction of PDO (D'ARRIGO et al., 2001; GEDALOF, 2002; MANTUA and HARE, 2002) and ENSO (LOUGH and FRITTS, 1985; URBAN et al., 2000; LAROCQUE and SMITH, 2005) and therefore, they can be used to better understand natural climate oscillations.

Pollen is also widely studied and can be used to reconstruct past vegetation and climate changes. Palynological studies allow inferences to be made about temperature,

precipitation and sea-level changes (MATHEWES and HEUSSER, 1981; WILLIAMS and HEBDA, 1991). Additional proxy archives, which can be used to reconstruct paleotemperatures, are fish otoliths (WURSTER and PATTERSON, 2001) and chironomid midges (WALKER and CWYNAR, 2006; CHASE et al., 2008). Midges are very sensitive indicators of environmental change because they respond very quickly to these changes. The head capsules of chironomids also allow paleosalinity reconstructions (HEINRICHS et al., 1997). The calcareous shells of ostracods also contain information about past temperatures and salinities (Mg/Ca and Sr/Ca; HU et al., 1998; ENGSTROM and NELSON, 1991). Furthermore, sediment cores containing microorganisms such as diatoms can provide valuable insights into past climate variability. For example, environmental changes can be inferred from the abundance and distribution of warm- and cold-water species (KHIM et al., 2005). Their well-preserved siliceous skeletons can also be used to derive information about salinity (HEINRICHS et al., 1997), precipitation and upwelling (CHANG and PATTERSON, 2005). Coralline sponges are also sources of proxy climate data. Sclerosponges have a long life span of several hundred years and therefore their skeletons allow long-term reconstructions of temperature and salinity from oxygen isotopes and Sr/Ca ratios (FALLON et al., 2005; ROSENHEIM et al., 2004, 2005). A relatively new climate archive is the coralline red algae. They provide long-term records with a relatively high temporal resolution. Changes in temperature can be inferred from Mg/Ca and oxygen isotope ratios (HALFAR et al., 2007; HETZINGER et al., 2009). It is also possible to detect PDO and ENSO signals from those proxy data and therefore, to reveal teleconnections (HALFAR et al., 2007). Finally, bivalve mollusks are excellent high-resolution multi-proxy archives. They can be used to reconstruct temperature (UREY, 1947; GROSSMAN and KU, 1986; BÖHM et al., 2000), the carbon isotopic composition of dissolved inorganic carbon ($\delta^{13}C_{DIC}$; GILLIKIN et al., 2006), salinity (MCCONNAUGHEY and GILLIKIN, 2008) and precipitation (DAVIS and MUEHLENBACHS, 2001) and to detect upwelling events (KILLINGLEY and BERGER, 1979; JONES and ALLMON, 1995). In addition to the aforementioned proxy archives, bivalve shells can also be used to reconstruct PDO and ENSO from oxygen isotopes or growth increment time series (STROM et al., 2004; CARRÉ et al., 2005; LAZARETH et al., 2006).

## *1.3. The North Pacific during the Holocene*

As discussed in the previous section there are many different proxy archives that can be used to reconstruct past climate variability and environmental changes. This study focuses on the

environmental variability of the Holocene, which represents the last ~10 000 years of the Earth's history. During the early Holocene, the North Pacific coast was warmer and drier than it is today. The Mid-Holocene is a period of climate transition (PELLATT et al., 2000, 2001). In the course of the middle Holocene it became cooler and wetter although the Northwest coast was still warmer and drier than at present (MOSS et al., 2007). The Neoglaciation reached a maximum after 3000 cal yrs BP (MANN and HAMILTON, 1995). Mid-Holocene climate change affected the people at the Northwest Coast of North America and therefore, the middle Holocene interval (around 4850 cal yrs BP) is a time of cultural transition (MOSS et al., 2007).

During the Mid-Holocene, the Aleutian Low was weaker (and more westwards) and the North Pacific High was stronger (and more northwards) than at present. This study is based on terrestrial and marine proxy archives (BARRON and ANDERSON, 2010). According to BARRON and ANDERSON (2010), a climate transition occurred between ca. 4200 and 3000 cal yrs BP. The Late Holocene was more El-Niño-like and characterized by positive PDO. The AL became stronger (and more eastwards) and the NPH became weaker (and more southwards). Furthermore, the frequency and intensity of ENSO changed during the Holocene. The frequency of ENSO increased until about 1200 years ago and then declined toward the present day (MOY et al., 2002). In addition, the ENSO amplitude increased from the Mid-Holocene up until the beginning of the last millennium (WANNER et al., 2008).

This research focuses on four regions in the North Pacific sector that are affected by ENSO, PDO and a monsoon system: Washington State, British Columbia (BC), Alaska and Japan. The glacial-interglacial transition in coastal BC occurred around 12 500 and 9000 $^{14}$C yrs BP (WALKER and PELLATT, 2003). A warm and dry early Holocene in BC, and also Washington State, is evident from many studies (e.g., WALKER and MATHEWES, 1987; HEBDA, 1995; PELLATT and MATHEWES, 1994; MANN and HAMILTON, 1995). WALKER and PELLATT (2003) postulate a period between 9000 and 7000 $^{14}$C yrs BP in coastal BC, which was 3°C warmer than today with minimal precipitation. The timing of maximum postglacial warmth, however, differs from site to site (especially for coastal vs. interior sites). Based on fossil midges from southern BC, ROSENBERG et al. (2004) describe a climate transition between 7800 and 3800 cal yrs BP. Cooling at the BC coastal sites started ca. 5000 $^{14}$C yrs BP, however, warm temperatures were prolonged at interior sites (WALKER and PELLATT, 2003). Pollen analysis from southern interior BC indicates cooler and wetter conditions after ca. 6600 cal yrs BP (ALLEY, 1976; MATHEWES and KING, 1989). In addition, lake sediments indicate wetter conditions between 6000 and 3000 cal yrs BP (NEDERBRAGT and THUROW,

2001; SPOONER et al., 2002). There was a continued cooling from the Mid- to Late Holocene (PALMER et al., 2002; ROSENBERG et al., 2004). The AL intensified and enhanced precipitation occurred during this time interval (CHANG and PATTERSON, 2005). The subsequent Neoglacial (after ca. 3500 $^{14}$C yrs BP) was cool and wet and glaciers started to advance (PELLATT et al., 2000, 2001; WALKER and PELLATT, 2003).

Southern Alaska was also warm and dry in the early Holocene (HEUSSER et al., 1985; MANN and HAMILTON, 1995), while moist conditions prevailed in the Mid- and Late Holocene (HEUSSER et al., 1985). The Late Holocene is characterized by increased storm activity and precipitation and by decreased temperature. During this time period it was colder and more humid at the coasts compared to the interior (HEUSSER et al., 1985). The cool and wet Neoglacial was accompanied with glacier expansion around ca. 3600-3000 cal yrs BP (southeastern Alaska, CALKIN et al., 2001). Lake sediments from southwestern Alaska indicate a maximum glacial expansion around 700 cal yrs BP (LEVY et al., 2004).

The warmest period in Japan occurred around 6500-5000 $^{14}$C yrs BP (LUTAENKO et al., 2007). SAKAGUCHI (1983) reports a similar time period of maximum warmth from 7000 to 5000 cal yrs BP (= Jomon Transgression Period). Significant cooling started ca. 4500-4000 $^{14}$C yrs BP (LUTAENKO et al., 2007). Water temperatures reconstructed from Holocene bivalve shells reveal the same climatic pattern: the lowest reconstructed temperature was at around 9000 cal yrs BP, the highest at 7000 cal yrs BP; low temperatures were also recorded between 4500 and 4000 cal yrs BP and ca. 2000 cal yrs BP (CHINZEI et al., 1987).

## *1.4. Sclerochronology*

Sclerochronology is the marine equivalent of dendrochronology (FRITTS, 1976). The term sclerochronology was introduced by BUDDEMEIER (1975) and HUDSON et al. (1976). It is the study of physical and chemical variations in periodically-grown, accretionary hard tissues of invertebrates, stromatolites and coralline red algae, and the temporal context in which they formed. The aim is to understand the life history traits of the studied species as well as to reconstruct environmental and climatic changes. The focus of sclerochronological research is principally on growth patterns, which reflect annual, monthly, fortnightly, tidal, daily and subdaily periods. Growth is controlled by environmental (e.g., temperature, salinity and food) and astronomical parameters. Only periodic growth patterns allow the exact dating of portions. Biological clocks trigger periodic growth (PITTENDRIGH, 1979; RICHARDSON, 1988a;

RODLAND et al., 2006). Triggers include the day-night rhythm (solar 24 h day, CLARK II, 1975), tides (EVANS, 1972), the seasons (TRUTSCHLER and SAMTLEBEN, 1988) and reproduction (JONES, 1980). Growth lines result from periodic growth breaks and divide the growth pattern into segments containing the same amount of time, i.e., annual, monthly, fortnightly, daily and subdaily increments (PANNELLA and MACCLINTOCK, 1968; JONES, 1980; LUTZ and RHOADS, 1980).

Mollusk shells have been studied as environmental archives for more than 70 years (e.g., DAVENPORT, 1938; EPSTEIN et al., 1953; CLARK II, 1974; HUDSON et al., 1976; JONES, 1983). They form periodic growth patterns in their skeletons and reveal distinctive growth lines and growth increments, to which an exact calendar date can be attributed. Mollusk shells are multi-proxy archives that can provide a high temporal resolution (weekly, daily and even hourly). However, mollusk shells only record environmental, climatic and life-history information during their growth (JONES et al., 1983, 1984) and they preserve this as variations in growth rate and geochemistry. Variations in shell growth rate, and geochemical proxies, i.e., oxygen and carbon isotopes and trace elements, such as Mg/Ca and Sr/Ca (e.g., FREITAS et al., 2005; GILLIKIN et al., 2005) are therefore useful indicators of environmental conditions and can be utilized as proxies for temperature (UREY, 1947; KENNISH and OLSSON, 1975; GOODWIN et al., 2001), salinity (DAVIS and CALABRESE, 1964; MARSDEN, 2004; MCCONNAUGHEY and GILLIKIN, 2008) and phyto-/zooplankton abundance (SATO, 1997; WANAMAKER et al., 2009). Shell growth has to be studied for an exact alignment of the geochemical data, i.e., increments need to be identified and their periodicity (subdaily to annual) needs to be verified. A combination of growth pattern and stable isotopes analyses is therefore the best approach for providing a reliable and detailed interpretation of the shell record (e.g., JONES et al., 1983, 1984; GOODWIN et al., 2001).

## *1.5. Why bivalves?*

Bivalve mollusks are valuable environmental and climatic multi-proxy archives. Growth increments are broadest when environmental conditions (e.g., temperature and food availability) are optimal. Bivalve shells can be used to reconstruct PDO and ENSO from oxygen isotopes or increment time series (CARRÉ et al., 2005; LAZARETH et al., 2006). Furthermore, bivalves are excellent biomonitors, for instance, they can act as perfect monitors of environmental pollution (e.g., PRICE and PEARCE, 1997; BOENING, 1999). Variations in bivalve growth and geochemistry are also controlled by physiological factors (RICHARDSON,

1988a). A thorough knowledge of the physiology of the studied species (life history traits such as growing season, growth rate and reproduction) is therefore essential for the interpretation of the geochemical record (SCHÖNE, 2008).

In contrast to the majority of climate archives, bivalves provide a high temporal resolution. They reveal precise intra-annual records with a seasonal up to subdaily resolution (PANNELLA and MACCLINTOCK, 1968; LUTZ and RHOADS, 1980). Other archives are often temporally limited and only provide an annual resolution and as such, they do not allow the detection of seasonal variability.

Bivalve shells grow through periodic accretion of calcium carbonate, i.e., they form by incremental growth and therefore, they function as an excellent calendar. This allows very precise dating of shell portions because the growth patterns reflect annual, monthly, fortnightly, tidal, daily, and subdaily increments of time (PANNELLA and MACCLINTOCK, 1968; EVANS, 1972; PANNELLA, 1976; LUTZ and RHOADS, 1980; RICHARDSON, 1988b). Bivalve growth lines are the result of growth breaks. Tide-controlled growth patterns are formed because bivalves only grow when they are submerged during high tides (GOODWIN et al., 2001). During aerial exposure at low tide, however, shell growth stops and a microgrowth line forms (EVANS, 1972; OHNO, 1985). A typical tidal growth pattern exhibits narrow increments and distinct growth lines formed during spring tides and broad increments with less defined growth lines formed during neap tides (GOODWIN et al., 2001). In addition, bivalves may reduce or stop their growth under suboptimal temperatures during the summer or winter months (JONES and QUITMYER, 1996; GOODWIN et al., 2001; SCHÖNE et al., 2002a), which leads to the formation of annual growth lines. Furthermore, random events, such as storms and predation, and periodic events, such as spawning, are clearly recorded in the shell microstructure (RHOADS and PANNELLA, 1970; CLARK II, 1974; KENNISH and OLSSON, 1975). They cause the formation of so-called disturbance lines, which complicate the correct alignment of the geochemical record and therefore, require a precise analysis of shell growth pattern. However, specimens of the same species living in the same habitat typically reveal synchronous growth patterns and similar geochemistry.

Another advantage of using bivalves as proxy archives is that some species, such as *Arctica islandica* and *Panopea abrupta* are extremely long-lived. *P. abrupta* for example may exceed 160 years in age (BUREAU et al., 2002; STROM et al., 2004). The longest recorded lifespan for the ocean quahog *A. islandica* is 405 years (WANAMAKER et al., 2008a) so this bivalve is potentially the oldest solitary animal in the world. The analysis of such long-lived

species makes it theoretically possible to construct master chronologies, which can be extended back in time for several centuries or even millennia, by combining contemporaneous specimens with overlapping lifespans. The longest marine shell master chronology to date extends over 489 years and was constructed by BUTLER et al. (2009, 2010) using *A. islandica*. However, researchers from Bangor University (UK) are currently developing a 1000-year long master chronology. These long master chronologies provide the potential to analyze natural low-frequency climate oscillations.

Bivalves are very well suited as climate archives because of their broad geographic distribution. They inhabit nearly all aquatic environments from the low to high latitudes and from shallow water to the deep sea. In contrast, trees and corals have a far more limited spatial distribution. Trees only provide a terrestrial record and the majority of corals are limited to the tropics.

## 1.6. The bivalves *Panopea abrupta* and *Saxidomus gigantea*

The present study focuses on aragonitic shells of two bivalve species in the North Pacific, the long-lived geoduck *Panopea abrupta* (Conrad) and the short-lived butter clam *Saxidomus gigantea* (Deshayes). The long-lived geoduck may reach an age of more than 150 years, which provides the potential to reconstruct long-term natural climate oscillations, such as PDO, on an annual scale. The short-lived butter clam may attain an age of twenty years or more (MC LEAN FRASER and SMITH, 1928; QUAYLE and BOURNE, 1972), which allows high-resolution environmental reconstructions on a seasonal up to daily time-scale.

NOAKES and CAMPBELL (1992) were the first who identified *P. abrupta* as a potential climate proxy. This species occurs in high-latitudes where few other marine organisms are available for climate reconstructions. *P. abrupta* has many different names. The name geoduck has a Native American origin and means “dig deep”. Additional names are the king clam and elephant trunk clam. This infaunal suspension feeder is the largest burrowing bivalve in the world. In the first two years of life they can burrow one meter into the substrate, however, adults are not capable of digging. They are distributed from Alaska to Baja California and around Japan, where they are commercially harvested.

The butter clam, *S. gigantea*, is a North American species, which is distributed from San Francisco Bay, California to the Bering Sea, Alaska. *S. gigantea* is an infaunal bivalve, which lives in the intertidal to subtidal zone (QUAYLE and BOURNE, 1972) and may be buried

to a depth of approximately 30 cm below the surface (PAUL et al., 1976; NICKERSON, 1977). Like geoducks, this species is commercially harvested and furthermore, butter clams are commonly found in prehistoric midden sites.

## *1.7. Shell middens*

Well-preserved bivalve shells often occur in archaeological midden deposits. Shell middens occur throughout the world and they are a valuable source of information regarding paleoenvironment, paleoclimate and subsistence strategies of past populations (e.g., BAILEY, 1975; KOIKE, 1980; BONOMO and AGUIRRE, 2009; MARTINDALE et al., 2009). Shell middens have traditionally been used to interpret paleo-diet and the utilization of shellfish resources, since shellfish constitutes an important part of the human diet (KOIKE, 1980; ELLIS and SWAN, 1981). Past people were dependent on seafood. Shellfish was a seasonally important food resource and patterns of site occupation are strongly related to shellfish availability. *S. gigantea* occurs in shell middens along the west coast of North America. Archaeological midden deposits accumulated over several thousands of years on the coast of British Columbia and the butter clam is the shellfish most commonly recovered from these deposits. However, shellfish may also have caused illness and mortality. Harmful algal blooms occurred throughout the Holocene (MUDIE et al., 2002) and they may be a reason for the avoidance of shellfish collection during certain seasons. Butter clams in particular, may contain a high amount of the toxin saxitoxin, which is particularly enriched in the siphon and, in contrast to other species that become nontoxic within a few weeks, may stay at lethal levels for humans for more than two years (KVITEK, 1991; KVITEK and BEITLER, 1991; KITTS et al., 1992; KVITEK and BRETZ, 2004).

The sclerochronological analysis of archaeological shells from shell midden deposits can reveal information about local environmental changes and the seasonality of shellfish collection. Several studies propose the use of oxygen isotopes from archaeological shells for the determination of the season of collection (e.g., SHACKLETON, 1973; KILLINGLEY, 1981; BAILEY et al., 1983; KENNETT and VOORHIES, 1996), a proxy for season of site occupation. The precision of these seasonality studies has improved considerably over the years due to advances in sampling techniques on a micrometer scale (DETTMAN and LOHMANN, 1995; WURSTER et al., 1999).

Shell middens can provide a lot of information about past activities of local populations. They can supply information on subsistence strategies, settlement patterns, timing of resource use and trade. Hunting and gathering economies require mobility so if a food source was exploited people had to move to a different place. Many questions may therefore be answered by analyzing shell middens: Was a site inhabited only on a seasonal basis or year-round? During which season of the year were shells collected? Were shells collected during spring or neap tides? Were they preferentially collected during the day or night? Where did they collect the shells from? At what distance from the coast? Is there a change of the shell collection pattern over time? Furthermore, reconstructing coastal environmental conditions from shell midden bivalves may also allow us to understand the human adaptation to changing climates (e.g., DEMENOCAL, 2001).

## *1.8. Stable oxygen and carbon isotopes*

Stable oxygen and carbon isotopes of bivalve shells can provide useful information about modern and past environments, since many species precipitate their shell in isotopic equilibrium with the ambient water (EPSTEIN et al., 1953; MOOK and VOGEL, 1968; WEFER and BERGER, 1991). The fractionation of oxygen isotopes is largely controlled by temperature (GROSSMAN and KU, 1986) with temperature and $\delta^{18}O$ being negatively correlated. This $^{18}O/^{16}O$ thermometer was first established by UREY (1947), and since then, many studies have used oxygen isotope records from marine invertebrates to reconstruct seawater temperatures (e.g., WILLIAMS et al., 1982; SCHÖNE et al., 2004a; WANAMAKER et al., 2008b; ULLMANN et al., 2010). Since the oxygen isotope value of the surrounding water contributes to the oxygen isotope ratios of the precipitated shell carbonate (EPSTEIN et al., 1953; WEFER and BERGER, 1991), shell oxygen isotopes can be used to reconstruct hydrological changes in the ocean, such as evaporation and the influx of freshwater (e.g., meltwater and precipitation) (DAVIS and MUEHLENBACHS, 2001; SCHÖNE et al., 2003). Freshwater is enriched in $^{16}O$ relative to ocean water and therefore leads to more negative isotopic values in the water and in the precipitated shell carbonate and consequently, may also lead to elevated temperature reconstructions.

Although many taxa, e.g., corals and bivalves, typically precipitate their carbonate close to oxygen isotopic equilibrium with ambient water, carbon isotopes often reveal disequilibrium fractionation (WEFER and BERGER, 1991). Nevertheless, carbon isotopes have been used to reconstruct $\delta^{13}C_{DIC}$ (MOOK and VOGEL, 1968; GILLIKIN et al., 2006), primary

productivity (KRANTZ et al., 1987), salinity (MCCONNAUGHEY and GILLIKIN, 2008) and to detect upwelling events (more negative $\delta^{13}C_{DIC}$ and $\delta^{13}C_{shell}$ values; KILLINGLEY and BERGER, 1979; JONES and ALLMON, 1995). However, the interpretation of shell carbon isotopes remains controversial especially since a number of studies have revealed that shell carbon isotopes are also influenced by metabolism (TANAKA et al., 1986) and growth (LORRAIN et al., 2004).

Disequilibrium deposition of oxygen and carbon isotopes results from kinetic or metabolic effects (TURNER, 1982; MCCONNAUGHEY, 1989a, b; OWEN et al., 2002). Kinetic disequilibrium occurs due to the discrimination against heavier isotopes at higher precipitation rates and affects both oxygen and carbon isotopes, while metabolic disequilibrium, which is due to biological processes such as photosynthesis and respiration, only affects carbon isotopes (MCCONNAUGHEY, 1989a, b). According to MCCONNAUGHEY and GILLIKIN (2008) mollusk shells rarely exhibit strong kinetic effects. Slow shell growth due to relatively low water temperatures (or high ontogenetic age) reduces the influence of kinetic effects (leading to depletions from isotopic equilibrium) on the isotope record (KRANTZ et al., 1987; MCCONNAUGHEY, 1989a, b; MCCONNAUGHEY et al., 1997; RAHIMPOUR-BONAB et al., 1997). Carbon precipitated in the shell can be derived from dissolved inorganic carbon (DIC), therefore recording an environmental signal, or from metabolic carbon, which would mask the $\delta^{13}C_{DIC}$ record of the shell. The shells usually reflect changes in ambient $\delta^{13}C$ of the DIC exactly (MCCONNAUGHEY et al., 1997; MCCONNAUGHEY and GILLIKIN, 2008). However, metabolic $CO_2$ may also be an important factor in controlling the carbon isotope composition of biogenic carbonates (e.g., TANAKA et al., 1986; DETTMAN et al., 1999; OWEN et al., 2008). In fact, TANAKA et al. (1986) determined that about 50% (but potentially up to 85%) of the carbon in shell carbonate was derived from metabolic sources such as food, which has a more negative $\delta^{13}C$ value than that of DIC. The incorporation of respired $CO_2$ into the shell usually leads to depletion of $\delta^{13}C_{shell}$ by as much as 2‰ in aquatic invertebrates (MCCONNAUGHEY et al., 1997).

## *1.9. Sclerochronological methods*

For sclerochronological and stable isotope analyses, the shells were mounted on plexiglass cubes using a two-component adhesive and coated with metal epoxy resin to prevent shell fracture during cutting. Two three-millimeter thick slabs were cut from the shells using a low-

speed precision saw. The slabs were cut perpendicular to the growth lines and along the axis of maximum growth from the umbo to the ventral margin. For each shell, both slabs were mounted on glass slides with metal epoxy resin, then ground and polished.

One polished section of each specimen was immersed in Mutvei's solution (SCHÖNE et al., 2005a) for sclerochronological analyses. Mutvei's solution simultaneously etches the shell, preserves organic matrices and stains the intercrystalline organic envelopes blue (SCHÖNE et al., 2005b). The growth lines are etch-resistant and richer in organics and therefore they stain dark blue. In contrast, the growth increments between two consecutive growth lines are more strongly etched and appear lighter blue. Immersion in Mutvei's solution therefore facilitates the analysis of shell growth patterns by reflected-light microscopy. To analyze shell growth patterns, digital images of the shell slabs were taken with a Nikon Coolpix 995 camera attached to a binocular microscope. The number and widths of the growth increments were determined using the image analysis software Panopea (© 2004 PEINL and SCHÖNE).

The remaining polished cross-sections were used for oxygen isotope analysis of the shell carbonate. Shell powder samples were obtained either by high resolution milling, conducted parallel to the growth lines and perpendicular to the direction of growth or by drilling consecutive holes. Each powder sample weighed between 30 and 130 µg. Analyses were conducted using a Thermo Finnigan MAT 253 isotope ratio mass spectrometer coupled with a Gas Bench II (University of Frankfurt/Main and University of Mainz, Germany). Results are reported in the usual δ-notation. Carbonate samples were calibrated against an NBS-19 calibrated Carrara marble standard. The isotope values of the shells and $\delta^{13}C_{DIC}$ were calculated against the VPDB (Vienna Pee Dee Belemnite) standard and expressed as parts per mil (‰). The oxygen isotope values of the seawater are reported in per mil (‰) with respect to VSMOW (Vienna Standard Mean Ocean Water) standard. The paleothermometry equation by BÖHM et al. (2000) for biogenic aragonite was used to reconstruct temperatures from $\delta^{18}O_{shell}$ values.

In order to obtain radiocarbon ages from the archaeological shells, the most recent years of shell growth were sampled from the ventral margin or umbo. First, the periostracum was mechanically removed, and then at least 40 mg of shell carbonate was sampled for the radiocarbon analysis. Ages were determined by $^{14}C_{AMS}$ dating performed by the Poznań Radiocarbon Laboratory (Poland). Conventional radiocarbon ages were converted to

calibrated $^{14}C_{AMS}$ ages by the program Calib 6.0 (STUIVER and REIMER, 1993) using the Marine09 calibration dataset (REIMER et al., 2009).

## *1.10. Aim and research questions*

The goal of this thesis is to reconstruct climate and environmental variations in the North Pacific during the Holocene, and to do this with a high spatial and temporal resolution using the shells of bivalve mollusks. This thesis focuses on many different Holocene time slices and multiple regions in the North Pacific: Japan, Alaska (AK), British Columbia (BC) and Washington State, which are all affected by a monsoon system, Pacific Decadal Oscillation (PDO) and/or El Niño/Southern Oscillation (ENSO). The results of this study contribute to the construction of a paleoclimate network of proxy data for the North Pacific that can be used to examine large-scale Holocene climate variability. These data will also have a multidisciplinary impact because they are of interest for paleontologists, geochemists, biologists, (paleo)climatologists, (paleo)oceanographers and archaeologists. These data help to improve the understanding of major pressure and circulation systems, as well as natural climate oscillations, such as PDO and ENSO. To date, such high-resolution proxy data, from the marine realm and of the mid and high latitudes, are still scarce. This study therefore provides a significant contribution to the understanding of past climate changes and the optimization and verification of climate models for future scenarios. Knowledge of climate variability prior to anthropogenic forcing is essential to test and validate these climate models because changes due to natural climate oscillations and human impact must be distinguished. This Ph.D. research also has significant implications for archaeologists. Sclerochronological data resolve many archaeological questions, e.g., the season, timing and water depth of shellfish collection. Shellfish procurement strategies and seasonal settlement patterns of prehistoric people can be reconstructed. The obtained data contribute to the understanding of life strategies and migration of prehistoric people, cultural developments and reasons for sociocultural changes.

A major component of this Ph.D. research is calibration studies, which are essential in order to ascertain the usefulness of selected bivalve species as paleoclimate proxy archives. Prior to using archaeological mollusk shells for paleoclimate reconstructions, a detailed analysis of the life history traits of live-collected specimens is required. This includes the analysis of, for example, the timing of growth line formation, the duration of the growing season and seasonally varying growth rates. The analysis of life history traits is necessary for

the correct alignment and interpretation of shell geochemical data. The aim of which is to understand the influence of environmental parameters (e.g., temperature, freshwater and food) on shell growth and geochemical properties (e.g., stable oxygen and carbon isotopes). This knowledge then needs to be transferred to archaeological shells for each species and for every region. Such calibration studies are therefore essential for understanding and interpreting the environmental and climatic signals preserved in archaeological shells.

The following key research questions are addressed:

- Do shell oxygen isotope values of *P. abrupta* and *S. gigantea* allow reliable temperature reconstructions?
- Do oxygen isotope values differ among contemporaneous specimens?
- Which shell portions are most suitable as geochemical proxy archives of environmental change?
- How does freshwater influence shell growth and geochemistry?
- What is the timing of growth line formation?
- How long does the growing season last?
- How do shell growth rates vary during different seasons?
- How precisely can the time of collection be determined?
- Can the distance of shellfish collection from the coast be reconstructed?
- Is there a latitudinal trend in the shell growth?
- Is it possible to reconstruct the past flow of the Alaska Coastal Current from shells?
- Can quantifiable temperature and salinity data be reconstructed from shell growth patterns and shell oxygen isotope data?

## *1.11. Overview of research*

The results of this Ph.D. research are presented in chapters two to four, with each chapter representing individual publications in high-impact, peer-reviewed journals. Chapter five contains the main conclusions and reveals possibilities for further research. The three publications presented in this manuscript are as follows:

Chapter 2: HALLMANN, N., SCHÖNE, B.R., STROM, A., and FIEBIG, J., 2008. An intractable climate archive — Sclerochronological and shell oxygen isotope analyses of the Pacific geoduck, *Panopea abrupt*a (bivalve mollusk) from Protection Island (Washington State, USA). Palaeogeography, Palaeoclimatology, Palaeoecology 269, 115–126.

> The main focus of this study was to analyze oxygen isotopes of *P. abrupta* shells in order to test the reliability of this species as a climate archive and to reconstruct regional temperatures. The key objectives were as follows: firstly, to determine whether the oxygen isotope values recorded from the inner and outer shell layers were the same and secondly, to investigate any intra-specific differences within contemporaneous specimens.

Chapter 3: HALLMANN, N., BURCHELL, M., SCHÖNE, B.R., IRVINE, G.V., and MAXWELL, D., 2009. High-resolution sclerochronological analysis of the bivalve mollusk *Saxidomus gigantea* from Alaska and British Columbia: techniques for revealing environmental archives and archaeological seasonality. Journal of Archaeological Science 36, 2353–2364.

> This chapter presents the first detailed analysis of the life history traits and stable isotope records of *S. gigantea*, which provides new insights into the growth of the butter clam. Shell growth records and geochemistry are used to reconstruct paleotemperature as well as to identify the season of shellfish collection, a proxy for the season of site occupation. This approach requires a detailed knowledge of the life history traits of this species. Therefore, the timing of growth line formation, the duration of the growing season, the seasonally varying growth rates and the geochemistry of live-collected *S. gigantea* shells were analyzed. Comparison of the shell growth patterns with an appropriate tidal calendar permits precise estimates of collection circumstances, such as low or high and spring or neap tides, day- or nighttime collection and the relative position in the intertidal zone. The combined sclerochronological and geochemical approach refines estimates for the season of

shellfish collection and improves the understanding of procurement strategies of prehistoric people.

Chapter 4: HALLMANN, N., SCHÖNE, B.R., IRVINE, G.V., BURCHELL, M., COKELET, E.D., and HILTON, M.R., 2011. An improved understanding of the Alaska Coastal Current: the application of a bivalve growth-temperature model to reconstruct freshwater-influenced paleoenvironments. PALAIOS, In press (accepted, pending minor to moderate revisions).

This study establishes a growth-temperature model based on *S. gigantea* shells from south west Alaska, which provides a better understanding of the hydrological changes related to the Alaska Coastal Current. We tested the hypotheses that the independent measurement of water temperature and salinity can be used to estimate seasonal to inter-annual changes in paleosalinity and paleotemperature revealed in the sclerochronological records of *S. gigantea* shells. Water temperatures were reconstructed from variations in the width of lunar daily growth increments, and in combination with $\delta^{18}O_{shell}$ values, these increment-derived temperatures were used to reconstruct salinity changes. The model was calibrated and tested with modern shells and then applied to archaeological shells.

Bivalve shell proxy data from different study regions have to be compared, and regional shell records need to be compared to other proxy archives in order to detect large-scale climate patterns, to investigate land-sea interactions and to study teleconnections between Japan, Alaska, British Columbia and further study areas in the North Pacific.

# Chapter 2: An intractable climate archive — Sclerochronological and shell oxygen isotope analyses of the Pacific geoduck, *Panopea abrupta* (bivalve mollusk) from Protection Island (Washington State, USA)

Nadine Hallmann[1], Bernd R. Schöne[1], Are Strom[2], Jens Fiebig[3]

[1] Department of Applied and Analytical Paleontology and INCREMENTS Research Group, Institute of Geosciences, University of Mainz, Johann-Joachim-Becher-Weg 21, 55128 Mainz, Germany

[2] WDFW Point Whitney Shellfish Lab, 1000 Point Whitney Rd., Brinnon, WA. 98320, USA

[3] Department of Paleontology, Institute of Geosciences, University of Frankfurt, Altenhöferallee 1, 60438 Frankfurt, Germany

HALLMANN, N., SCHÖNE B.R., STROM, A., and FIEBIG, J., 2008. An intractable climate archive – Sclerochronological and shell oxygen isotope analyses of the Pacific geoduck, *Panopea abrupta* (bivalve mollusk) from Protection Island (Washington State, USA). Palaeogeography, Palaeoclimatology, Palaeoecology 269, 115–126.

## *ABSTRACT*

**Annual growth increment patterns of cardinal teeth (CT) of *Panopea abrupta* (Conrad) can reportedly provide information about past climate variations. However, little is known about the intra-annual timing and rate of shell growth necessary to interpret such records. In addition, it remains unclear whether actual temperatures can be reliably inferred from $\delta^{18}O$ values of geoduck {goo'e-duk} shells. This study compared high-resolution environmental records (hourly to monthly resolved temperature, bi-weekly to monthly $\delta^{18}O_{water}$ and salinity data) with temperatures reconstructed from oxygen isotope values of the outer shell layer ($T\delta^{18}O_{OSL}$) and cardinal tooth portions ($T\delta^{18}O_{CT}$) of different contemporaneous specimens alive at the same locality. Results indicate that shell growth mainly occurred between March/April and November/December with a maximum during May–August. This finding must be considered when comparing the "annual" growth increment width chronologies to environmental parameters. In addition, intra-annual $\delta^{18}O_{shell}$ values require the calculation of weighted averages instead of arithmetic means. During ontogeny, the duration of the growing season remained nearly unchanged; an important finding for paleoclimate studies based on inter-annual growth patterns. Seasonal shell growth was strongly correlated with temperature ($R = 0.93$, $R^2 = 0.86$, $p < 0.0001$). Presumably due to individual differences in the exchange rate between the extrapallial fluid (EPF) and the ambient water, the outer shell layer of some specimens formed out of oxygen isotopic equilibrium, particularly during summer (high growth rates, increased $^{18}O$ depletion of the EPF). This resulted in a $T\delta^{18}O_{OSL}$ difference of up to 2°C among different specimens. In addition, a bias was observed in different specimens toward daytime or nighttime temperatures, particularly during summer. Such a bias may be related to**

**individual differences in the physiological activity at ultradian time-scales or to elevated predation pressure. More importantly, CT portions (= inner shell layer) formed in isotopic disequilibrium with the ambient water. Typically, reconstructed temperatures differed by more than 3–4°C from actual water temperatures. Within specimens, $T\delta^{18}O_{OSL}$ and $T\delta^{18}O_{CT}$ were offset by ca. 2°C. Some $T\delta^{18}O_{CT}$ also exhibited unexplained inter-annual trends, so that $T\delta^{18}O_{CT}$ among specimens varied by up to 4°C. Given the $\delta^{18}O_{shell}$ inconsistency between and among shells, a small seasonal temperature amplitude barely exceeding 4°C and the error bars of $T\delta^{18}O$ of geoducks at this setting on the order of ±2°C (error bars of the paleothermometry equation + variable $\delta^{18}O_{water}$ values + precision error of the mass spectrometer), the geochemical record of a single *P. abrupta* may not serve as a suitable paleoclimate archive. A reliable approximation to paleotemperatures may only be achieved by exclusively sampling the outer shell layer of multiple contemporaneous specimens, so that the $T\delta^{18}O_{OSL}$ variance among shells can be quantified.**

**Keywords: Temperature, Bivalve, Oxygen isotopes, Disequilibrium fractionation, Climate, North Pacific**

## 2.1. INTRODUCTION

Skeletons of many aquatic organisms function as recorders of environmental and climate change. Particularly, long-lived bivalve mollusks such as *Arctica islandica* (Linnaeus), *Cucullaea raea* (Zinsmeister), *Margaritifera margaritifera* (Linnaeus), or *Panopea abrupta* (Conrad) are increasingly used to reconstruct climate variations prior to anthropogenic forcing in the North Atlantic or North Pacific, respectively (MARCHITTO et al., 2000; SCHÖNE et al., 2003; BUICK and IVANY, 2004; SCHÖNE et al., 2004a,b; STROM et al., 2004; SCHÖNE et al., 2005a; STROM et al., 2005; WANAMAKER et al., 2007). Such data is relevant because knowledge of natural low frequency climate oscillations (e.g., the Pacific Decadal Oscillation, PDO, or the El Niño/Southern Oscillation, ENSO) prior to the extensive anthropogenic forcing is needed to test and validate climate models. The interest in using bivalve sclerochronology s.l. (analyses of growth patterns, crystallography and geochemistry) for paleoclimate analyses partly results from significantly improved microanalytical techniques (e.g., micromilling: DETTMAN and LOHMANN, 1995; mass spectrometry: SPÖTL and VENNEMANN, 2003; FIEBIG et al., 2005), but also from the recognition that mollusks provide several advantages over other environmental and climate proxy archives. Bivalves form their valves by periodic accretion of skeletal hard parts, analogous to annual growth bands in corals (HUDSON et al., 1976; DODGE and VAIŠNYS, 1980) or tree rings (FRITTS, 1972). In addition, they inhabit nearly every aquatic environment. Thus, bivalve sclerochronology can potentially link proxy records from different settings, for example, high-latitude dendrochronology and tropical coral sclerochronology. Some bivalve species grow shell carbonate uninterruptedly for several centuries permitting the reconstruction of quasi- and multi-decadal climate oscillations (SCHÖNE et al., 2003; STROM et al., 2004; WANAMAKER et al., 2007). During growth, bivalve mollusks faithfully archive environmental changes in their skeletons in the form of variable growth rates and variable geochemical properties (e.g., EPSTEIN et al., 1953; JONES et al., 1989; GOODWIN et al., 2001; SURGE and WALKER, 2006). Furthermore, shell growth patterns function as a calendar that places the environmental proxy record in a temporal context (CLARK, 1975; JONES, 1980; JOHNSON et al., 2000; ELLIOT et al., 2003).

However, a reliable interpretation of proxy records acquired from mollusk shells first and foremost requires precise knowledge of the timing and rate of biomineralization during different seasons. Typically, shells grow faster at warmer temperatures and when food supply is higher (e.g., HENDERSON, 1929; KENNISH and OLSSON, 1975; PAGE and HUBBARD, 1987; SATO, 1997). Therefore, powder samples taken from these shells at equidistant spatial intervals typically represent different amounts of time. Shell portions near the annual growth

lines grew slower, whereas those from about half-way between two consecutive growth lines were deposited in shorter time intervals. Consequently, calculation of annual averages from such samples requires weighted averaging (SCHÖNE et al., 2005b). Furthermore, individual differences in the response to environmental forcings are likely to exist. GILLIKIN et al. (2005) noted a $\delta^{18}O$ difference of up to 0.2‰ in three contemporaneous shells of *Saxidomus giganteus* (Deshayes) from the same habitat indicating that a single specimen may not be sufficient to reliably reconstruct the climate of the past. Finally, it is necessary to know which portions of the shell are suitable geochemical proxy archives of climate change. For example, previous studies reported significant differences in trace element and stable isotope composition in the inner and outer shell layers (GILLIKIN et al., 2005; SURGE and WALKER, 2006). Therefore, life history traits and the basic mechanisms of shell deposition are prerequisite for a state-of-the-art sclerochronology-based paleoclimate analysis.

Here, we studied the growth patterns and oxygen isotope geochemistry of shells of the bivalve mollusk *P. abrupta* from the Northwest Pacific. Our primary goals were to identify the average duration of the growing season and variable rates of shell formation during different seasons. In addition, we asked the following questions: (1) Do shell $\delta^{18}O$ values of this species provide reliable temperature estimates; (2) If so, do such records differ among specimens; (3) Which shell portions are suitable for shell growth and isotope analyses, the cardinal tooth (inner shell layer) or the outer shell layer? Results of the present study are indispensable to properly utilize the Pacific geoduck as a paleoclimate proxy archive.

## 2.2. MATERIALS AND METHODS

Ten shells of *Panopea abrupta* were collected alive during 2005 and 2006 from a subtidal tract west of Protection Island (N48°08.4, W122°57; water depth of ca. 14 m) near the mouth of Discovery Bay in the Strait of Juan de Fuca, Washington State, USA (Fig. 1, Tab. 1). Shells lived ca. 70–100 cm below the sediment water interface. The Strait of Juan de Fuca lies between the Pacific Ocean and Puget Sound and the Strait of Georgia (Fig. 1). This passage is characterized by strong currents and an intense tidal mixing which results in relatively constant water temperatures and an unstratified surface water body (MACKAS and HARRISON, 1997). Growth of bivalve shells from Protection Island such as *P. abrupta* is thus strongly linked to sea surface temperatures (SST) (STROM et al., 2005).

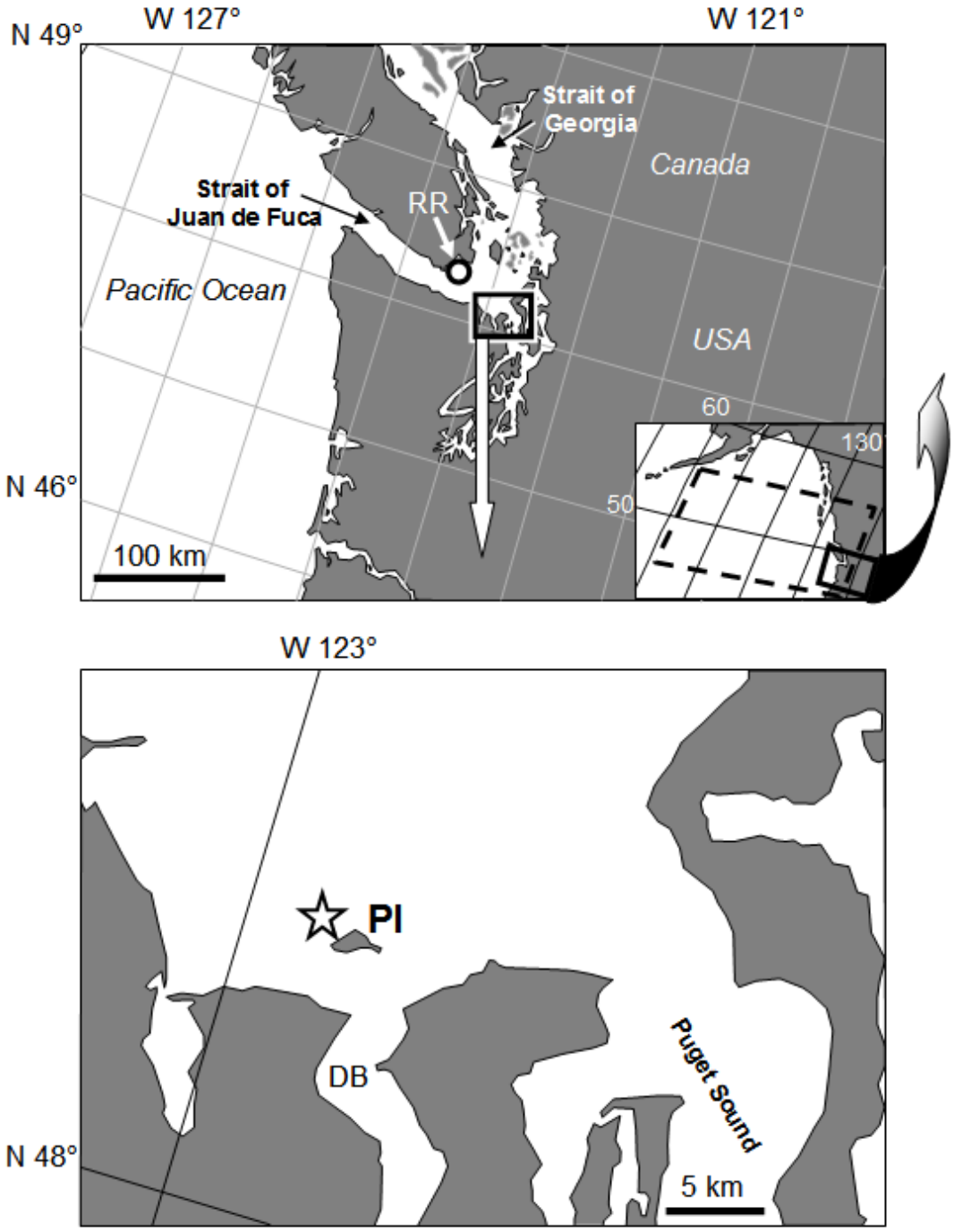


Figure 1. Map showing the sample locality (star in lower panel) of the *Panopea abrupta* specimens (Tab. 1) and water samples (Tab. 2) NW of Protection Island (PI) near Discovery Bay (DB). Two temperature loggers were deployed at PI as well. Additional salinity data came from Race Rocks (RR) and were used to calculate $\delta^{18}O_{water,\ reco}$ values. The rectangle in the small map of the upper panel indicates the data grid of the $\delta^{18}O_{water}$ and salinity values that were used to calculate the freshwater mixing line and the region of the $SST_{satellite}$ data used to reconstruct bottom water temperatures from shell oxygen isotopes and salinity (Tab. 2) at PI.

Table 1. List of *Panopea abrupta* specimens used in this study. Four shells were isotopically analyzed.

| Specimen | Date of collection | Ontogenetic age [yrs] | Ventral margin thickness [mm] | $\delta^{18}O_{shell}$ analysis (number of samples, time interval, shell portion) |
|---|---|---|---|---|
| AS-Mar-A1L | 28 Mar 2005 | 6 | 0.83 | 70, 1999 – March 2004, CT |
| AS-Apr-A1L | 8 April 2005 | 6 | 0.63 | 108, January 2004 – April 2005, OSL |
| … - A1R | | | | 27, 1999 – April 2004, CT |
| AS-0806-A1L | 18 Aug 2006 | 73 | 2.00 | |
| AS-0806-A2L | 18 Aug 2006 | 25 | 1.60 | 27, April 2005 – August 2006, OSL |
| AS-0806-A3L | 18 Aug 2006 | 41 | 1.33 | |
| AS-0806-A4L | 18 Aug 2006 | 63 | 2.23 | |
| AS-0806-A5L | 18 Aug 2006 | 41 | 1.64 | |
| AS-0806-A6R | 18 Aug 2006 | 16 | 1.67 | 46, September 2004 – August 2006, OSL |
| AS-0806-A7L | 18 Aug 2006 | 71 | 2.00 | |
| AS-0806-A8L | 18 Aug 2006 | 62 | 1.84 | |

### 2.2.1. Geoducks — bivalve(d) Methuselahs

The Pacific geoduck {goo'e-duk}, *P. abrupta* (Fig. 2), is extremely long-lived and reaches a lifespan of up to 160 years (BUREAU et al., 2002; STROM et al., 2004). Each year a sharply delimited growth line is deposited in the cardinal tooth (Fig. 3A) enabling a reliable estimate of ontogenetic ages of the shells (SHAUL and GOODWIN, 1982; STROM et al., 2004, 2005; GOMAN et al., 2008). Variations in annual shell growth reflect climate and environmental fluctuations (STROM et al., 2004). Geoducks were first identified as a potential climate proxy by NOAKES and CAMPBELL (1992). These authors postulated that shell growth co-varies with temperature. Modified dendrochronological methods were then applied to retrieve temperature estimates from geoducks (STROM et al., 2004). *P. abrupta* is broadly distributed in shallow waters in the entire North Pacific (GOODWIN and PEASE, 1989). This subtidal, infaunal suspension feeder occurs in marine and estuarine waters at depths of over 110 m from Alaska to Baja California, along the west coast of North America, around Japan (GOODWIN and PEASE, 1989) and New Zealand (GRIBBEN and CREESE, 2003) as well as in the South Atlantic (MORSÁN and CIOCCO, 2004). In Japan and the American Northwest, *Panopea sp.* is commercially harvested and considered a delicacy. The geographic center of

geoducks' distribution, however, is Puget Sound, USA and British Columbia, Canada. Preferentially, *P. abrupta* lives in soft substrates such as mud and sand, but also in pea gravel or gravel substrates and mixtures of these. As shown by mark-and-recovery experiments, geoducks in Puget Sound grow primarily from March through October (SHAUL and GOODWIN, 1982; STROM et al., 2004) and reproduce from April to July with peaks in May and June (GOODWIN, 1976).

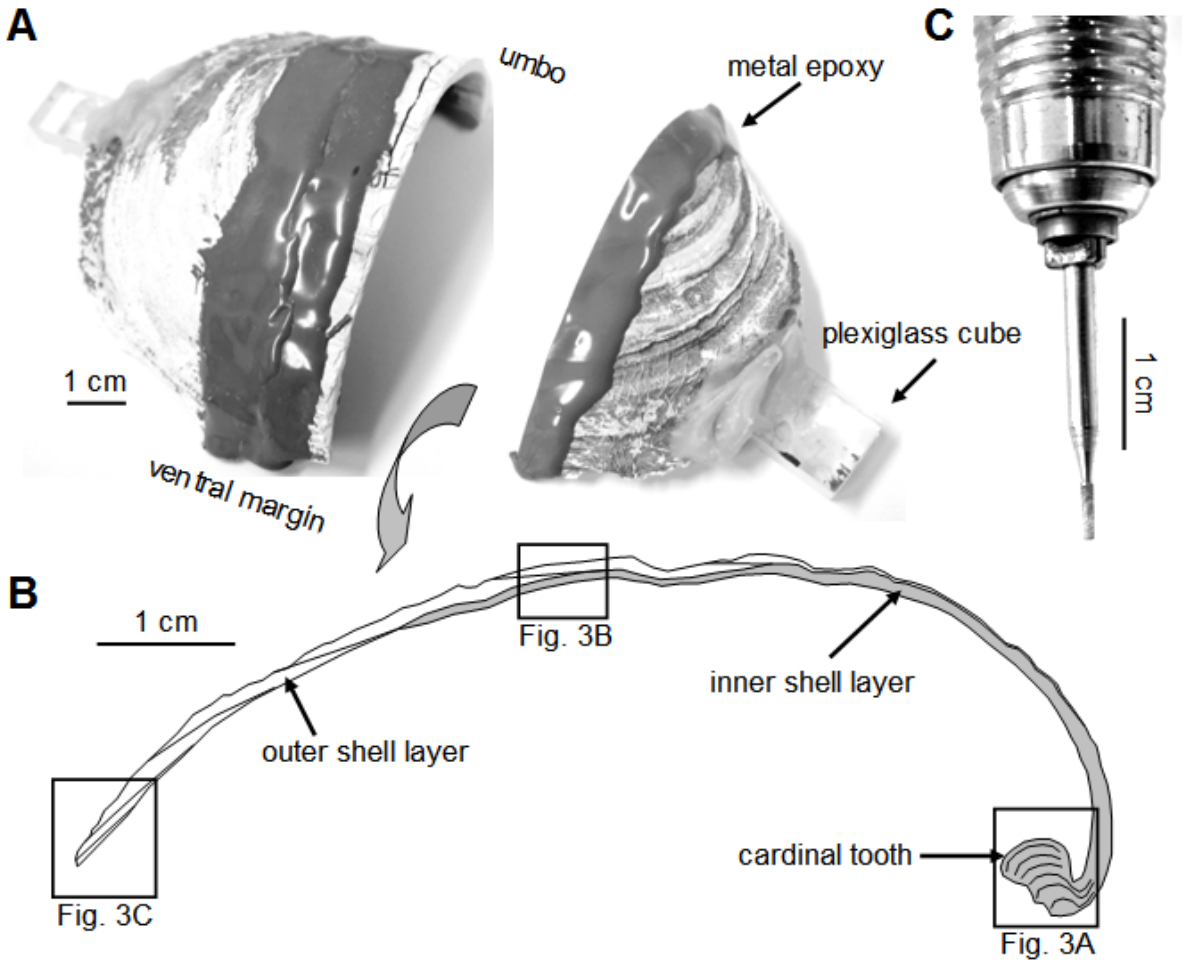


Figure 2. Sample preparation of *Panopea abrupta* shells. (A) The shell was mounted on a plexiglass block, covered with metal epoxy and cut along the height axis perpendicular to the growth lines. Two immediately adjacent slabs (2–3 mm thick) were then mounted on glass slides. (B) Typical cross-section of the shells depicting the outer and inner shell layer (including the cardinal tooth) that were precipitated by the outer and inner extrapallial fluid, respectively. (C) Micromilling equipment that was used to obtain powder samples from the shells for stable isotope analyses.

### 2.2.2. Preparation

For sclerochronological and isotope analyses, the ten studied shells (Tab. 1) were mounted on plexiglass cubes with plastic welder (Multipower, GlueTec). Preparation and analytical steps are shown in Figure 2. After coating with metal epoxy resin (WIKO), the shells were cut perpendicular to the axis of growth along the shell height axis from the umbo to the ventral margin (Fig. 2A) using a low-speed precision saw (Buehler, IsoMet 1000) and 0.4 mm thick diamond-coated saw blades. Two sections of each valve were mounted on glass slides. In order to visualize the internal growth patterns (Fig. 3), the radial cross-sections (Fig. 2B) were ground on glass plates (800, 1200 grit powder) and polished with 1 µm $Al_2O_3$ powder. After each step, the valves were ultrasonically rinsed in de-ionized water to remove any adhering grinding powder from the shells.

### 2.2.3. Shell growth patterns

For sclerochronological analyses, one polished section of each specimen was cleaned with water-free ethanol and immersed in Mutvei's solution for 20 min under constant stirring at 37°C to 40°C (SCHÖNE et al., 2005c). Stained sections were then carefully rinsed with de-ionized water and air-dried. Immersion in Mutvei's solution gently etches the carbonate and differentially stains the glycoproteins of the biominerals (SCHÖNE et al., 2005c). Etch-resistant, organic-rich growth lines (dark blue) and stronger etched growth increments (light blue) can now easily be identified (Fig. 3).

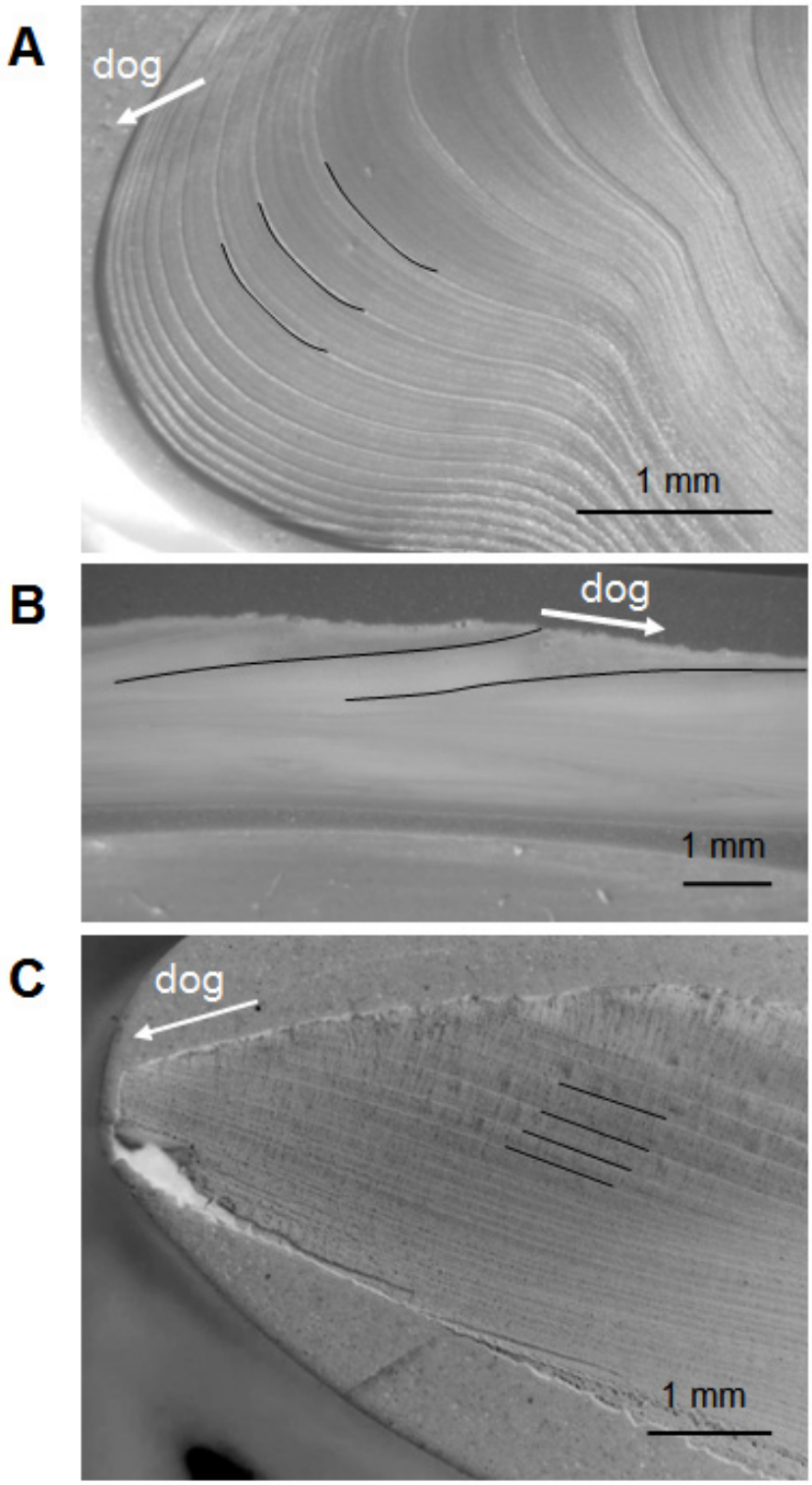


Figure 3. When viewed under a binocular microscope, cross-sections of *Panopea abrupta* shells immersed in Mutvei's solution reveal annual growth patterns. These consist of distinct growth lines (black lines) that delimit growth increments and are best viewed in the cardinal tooth portion (A). (B and C) In the outer shell layer, these growth patterns are less well developed and difficult to recognize. (B) About half-way between the umbo (A) and the ventral margin (C) annual growth lines approach the outer shell surface at an angle of about 10° suggesting that the shell was growing rapidly in size. dog = direction of growth.

Digital images of the growth patterns were taken from the umbonal shell regions (Fig. 3A) and from the outer shell layer approx. half-way between the umbo and the commissure (Fig. 3B) and from the ventral margin (Fig. 3C) with a Nikon Coolpix 995 camera attached to a binocular microscope (Wild HeerbruggM3Z). Subsequently, the widths of the growth increments were measured in the direction of growth to the nearest 8 μm using the image analysis software Panopea (© Peinl and Schöne). Ontogenetic age and annual increment widths (SHAUL and GOODWIN, 1982) were determined by counting and measuring the distance between major growth lines. The ventral margin thickness was measured 2–7 mm away from the ventral margin (Tab. 1).

## 2.2.4. Oxygen isotope analyses

For the analysis of the oxygen isotope values of the shells, $\delta^{18}O_{shell}$, powder samples were taken from the remaining polished cross-sections of four bivalves (Figs 3A and 3C). We sampled the outer shell layer near the ventral margin ($\delta^{18}O_{OSL}$) of three individuals and the cardinal tooth sections ($\delta^{18}O_{CT}$) of two specimens (Figs 4-7). Ontogenetic ages of the sampled specimens ranged from six to 25 years (Table 1). Prior to sampling, the slabs were ultrasonically rinsed in de-ionized water. Shell powder samples were obtained by milling parallel to the growth lines and perpendicular to the direction of growth with a cylindrical drill bit (1 mm diameter, Komet/Gebr. Brasseler GmbH & Co. KG, model no. 835 104 010; Figs 2C, 3A and 3C). Samples were taken from the growing edge back toward youth portions of the shells. Each sample represents spatially equidistant shell portions ranging from 13 to 21 μm in the outer shell layer and ca. 60 to 120 μm in the cardinal teeth. Each powder sample weighed between 40 and 130 μg. Samples were processed in a Thermo Finnigan MAT 253 isotope ratio mass spectrometer equipped with a Gas Bench II following the method described by SPÖTL and VENNEMANN (2003). Results are reported in the usual δ-notation. The samples were measured against the NBS-19 calibrated Carrara marble standard ($\delta^{18}O = -1.74‰$). Per day, we measured 52 shell carbonate samples and twelve Carrara marble standards. Four Carrara standards were placed at the beginning of each daily run, after 24 shell samples and at the end of the remaining 28 samples. On average, the 1σ error of each shell carbonate analyses was better than 0.06‰. The $\delta^{18}O$ values of the shells ($\delta^{18}O_{shell}$) were calculated against the VPDB (Vienna Pee Dee Belemnite) standard and expressed as parts per mil.

If the oxygen isotopy of the water ($\delta^{18}O_{water}$) is known, $\delta^{18}O_{shell}$ values can provide detailed information on the ambient temperature during growth (EPSTEIN et al., 1953). The shell mineralogy of *P. abrupta* is the $CaCO_3$ polymorph aragonite (COAN et al., 2000). This was confirmed by the present study. According to Raman analyses the outer and inner shell layers equally consist of more than 95% aragonite. Thus, we utilized the paleothermometry equation by BÖHM et al. (2000) for biogenic aragonite to reconstruct temperatures from $\delta^{18}O_{shell}$ values:

(1) $$T_{\delta^{18}O}(°C) = (20 \pm 0.2) - (4.42 \pm 0.1) \cdot (\delta^{18}O_{shell} - \delta^{18}O_{water}).$$

A one per mil shift in the $\delta^{18}O_{shell}$ value corresponds to a temperature change of the ambient water by 4.42°C. The equation by BÖHM et al. (2000) is superior to the GROSSMAN and KU (1986) function because it provides more reliable data and reduces the error. If the $\delta^{18}O_{shell}$ and $\delta^{18}O_{water}$ values are the same, the temperature error equals ±0.2°C. With each one per mil increase in the difference between the two values, the temperature error increases by ±0.1°C. For temperature error estimates, the precision error of the mass spectrometer was also considered. In the present study, the average error was ±0.5°C.

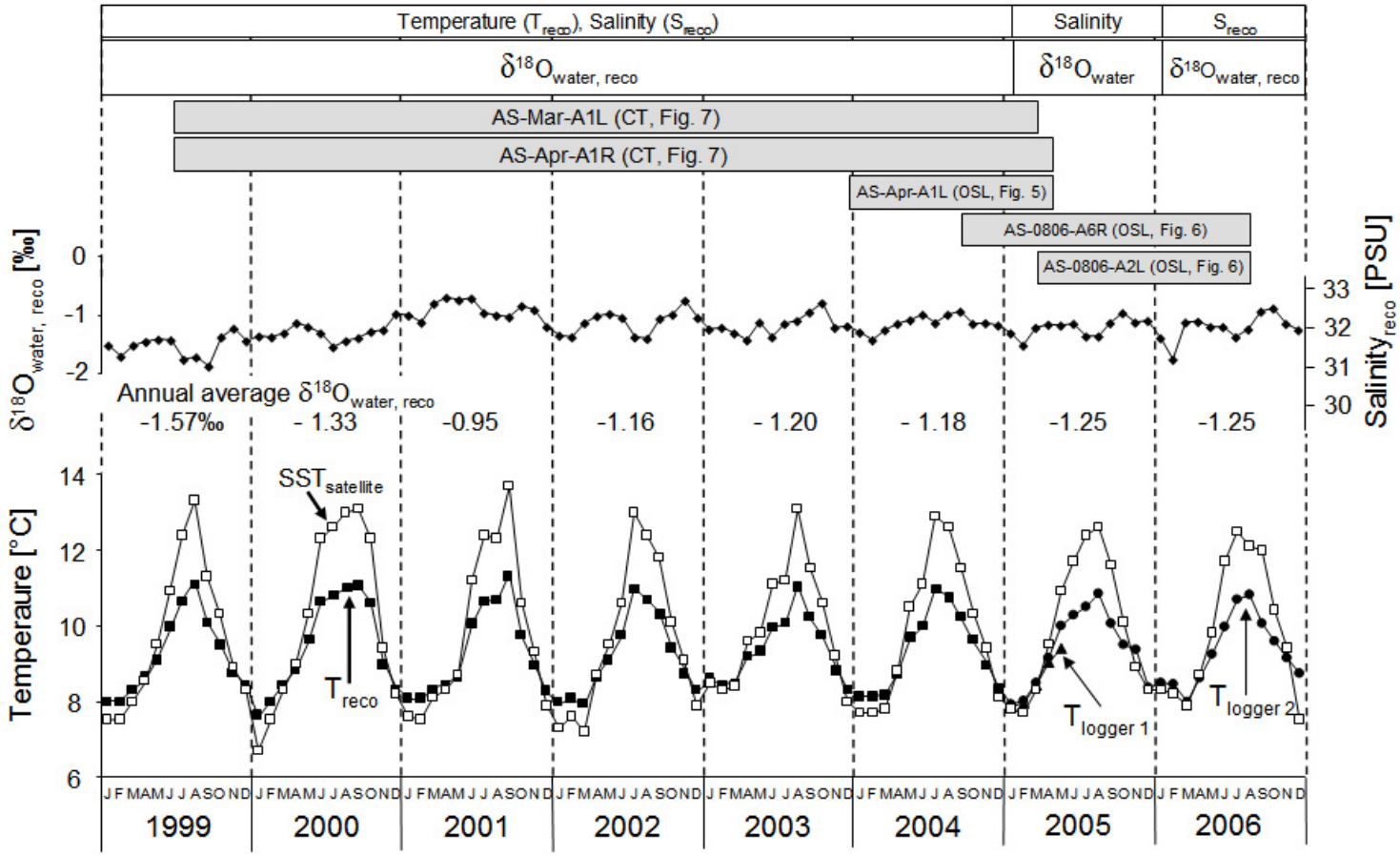


Figure 4. Hourly resolved temperature data ($T_{logger}$, 2005–2006; logger 1: triangles, logger 2: filled circles) and bi-weekly to monthly water samples ($\delta^{18}O_{water}$+salinity, 2005) were obtained from the position where the shells lived. For other time intervals from 1999–2006, monthly resolved environmental records were reconstructed ($T_{reco}$: filled squares; $S_{reco}$ + $\delta^{18}O_{water, reco}$: filled diamonds) from satellite data (open squares), published data and meteorological stations nearby (for details see text). The temporal coverage of the shell oxygen isotope records of the outer shell layer (OSL) and cardinal tooth (CT) records is indicated by the grey bars.

### 2.2.5. Environmental recordings

In order to calibrate shell growth and the $\delta^{18}O_{shell}$ data, we recorded temperature, salinity and the oxygen isotope composition ($\delta^{18}O_{water}$) at the locality where the shells lived (Figs 4 and 6, Tab. 2). Two temperature loggers (HOBO Water Temp Pro v2) were deployed near Protection Island at water depths of 11 and 14 m, respectively. The first logger (11 m) recorded bottom water temperatures on an hourly basis from 27 January to 3 May 2005 before it was lost. The second temperature logger was deployed approximately 0.9 km north of the first logger at N48°07.253, W122°57.156 (14 m) and provided seawater temperature data at hourly intervals for almost two years (27 January 2005 to 4 December 2006) (Figs 4 and 6). An arithmetic average, $T_{logger}$, was calculated from the two loggers and used for the comparison with the shell data (Fig. 6). Aside from a seasonal oscillation, $T_{logger}$ data fluctuated on a fortnightly time-scale. During spring tides, temperatures were higher than during neap tides (Fig. 6). Daily temperature ranges were as large as 2.3°C during summer, but negligibly small (0.1°C) during winter (Fig. 6). The minimum and maximum recorded temperatures were 7.8°C (6 February 2005, 3:00 PM) and 12.3°C (8 July 2006, 7:00 AM), respectively. The average $T_{logger}$ equaled ca. 9.5°C in 2005 (Tab. 3). The precision of the logger data was ±0.2°C. Because no bottom water temperature data were available for Protection Island for the time interval of January 1999 to January 2005, we used monthly resolved satellite data, $SST_{satellite}$ (AVHRR Pathfinder SST v5 Product 216; Physical Oceanography DAAC at podaac-www.jpl.nasa.gov), to reconstruct these values for Protection Island ($T_{reco}$) (Figs 1, 2 and 4–7). $SST_{satellite}$ and $T_{logger}$ data were linearly correlated ($R = 0.98$, $R^2 = 0.96$, $p < 0.0001$). Based on the linear regression analysis, $T_{reco}$ can be inferred from $SST_{satellite}$ with the following equation:

$$T_{reco} = \frac{SST_{satellite} + 7.21}{1.83}. \quad (2)$$

For $\delta^{18}O_{water}$ analyses, SCUBA divers collected water samples in close vicinity to the shells on a bi-weekly to monthly basis from January 2005 to January 2006 (Tab. 2, Fig. 4). Bottles were rinsed several times and the lid was tightly closed. Samples were refrigerated at 4°C prior to the analyses. 7 ml of water was equilibrated in 13 ml headspace with gaseous $CO_2$ in an automated equilibration device connected to a Finnigan MAT Delta-S mass spectrometer. The $\delta^{18}O_{water}$ values are reported against VSMOW (Vienna Standard Mean Ocean Water). Average 1SD error was better than 0.03‰. Slight variations in $\delta^{18}O_{water}$ can significantly alter temperature estimates from shell oxygen isotopes. For example, a change in $\delta^{18}O_{water}$ of 0.1‰ results in a temperature difference of more than 0.4°C. Because $\delta^{18}O_{water}$ values fluctuated with the tides, annual $\delta^{18}O_{water}$ averages were computed in order to reconstruct water temperatures from $\delta^{18}O_{shell}$ values. Seasonal minimum and maximum $\delta^{18}O_{water}$ values were used for an additional error calculation of the shell oxygen isotope-derived temperatures (here, on average, ±2°C). Salinity of the water samples was measured to the nearest of 1 PSU. The $\delta^{18}O_{water}$ values varied between −1.44‰ and −1.05‰ (Tab. 2) with an average value of −1.27‰ during 2005, and salinity ranged from 31 to 32 PSU (2005 average: 31.9 PSU).

Oxygen isotope values of the water for the time interval of January 1999 to December 2006 were reconstructed ($\delta^{18}O_{water,\ reco}$) from monthly salinity (S) records of a lighthouse, Race Rocks (W 123° 31.548, N 48° 17.541), ca. 50 km northwest of Protection Island (Fig. 1). We used a linear regression model of salinity and $\delta^{18}O_{water}$ of the Northwest Pacific (Fig. 1, N44–54°, W126–158°). These data (EPSTEIN and MAYEDA, 1953; CRAIG and GORDON, 1965) were obtained from NASA Goddard Institute for Space Studies from their homepage at http:// data.giss.nasa.gov/o18data/:

(3) $$\delta^{18}O_{water,reco} = 0.67 \cdot S - 22.8 \quad (R = 0.81;\ R^2 = 0.66,\ p = 0.004,\ n = 10).$$

Measured and reconstructed oxygen isotope values of the water during 2005 showed a constant offset of ca. 0.7‰ indicating that seawater at Race Rocks was about 1 PSU fresher than at Protection Island. Therefore, we added 1 PSU to each Race Rock salinity value und used these data to calculate the $\delta^{18}O_{water,\ reco}$ for Protection Island. During 1999–2006, the $\delta^{18}O_{water,\ reco}$ ranged from −1.92‰ to −0.75‰, while salinity values were between ca. 31.06 PSU and 32.82 PSU (Fig. 4). A seasonal cycle does not exist. However, from 1999 to 2001, waters became more saline (seasonal averages; 31.5 to 32.5 PSU), thereafter a shift toward slightly fresher conditions was observed (32 PSU). $\delta^{18}O_{water,\ reco}$ values of 2005 (−1.25‰) were in perfect agreement with the average $\delta^{18}O_{water}$ value of −1.27‰.

Table 2. List of water samples used in the present study. Salinity (S) was measured to the nearest 1 PSU. The freshwater mixing line enabled a calculation of salinity ($S_{reco}$) values from isotope values of the water ($\delta^{18}O_{water}$).

| Date of collection | Locality | Water depth [m] | $\delta^{18}O_{water}$ [‰] | S [PSU] | $S_{reco}$ [PSU] |
|---|---|---|---|---|---|
| 27 January 2005 | N48°07.794, W122°57.400 | 11 | -1.37 ± 0.012 | 32 | 31.98 |
| 2 February 2005 | N48°08.753, W122°57.156 | 14 | -1.30 ± 0.01 | 31 | 31.88 |
| 9 February 2005 | N48°08.278, W122°57.164 | 15 | -1.44 ± 0.025 | 32 | 31.78 |
| 23 February 2005 | N48°08.198, W122°57.194 | 14 | -1.27 ± 0.014 | 32 | 32.04 |
| 24 March 2005 | N48°08.253, W122°57.156 | 13 | -1.09 ± 0.029 | 32 | 32.31 |
| 7 April 2005 | N48°08.768, W122°57.091 | 12 | -1.28 ± 0.009 | 32 | 32.02 |
| 15 June 2005 | N48°08.253, W122°57.156 | 13 | -1.19 ± 0.002 | 32 | 32.15 |
| 2 August 2005 | N48°07.794, W122°57.400 | 11 | -1.41 ± 0.014 | 32 | 31.83 |
| 8 December 2005 | N48°08.253, W122°57.156 | 15 | -1.05 ± 0.009 | 32 | 32.37 |
| 11 January 2006 | N48°08.253, W122°57.156 | 15 | -1.36 ± 0.012 | 32 | 31.90 |

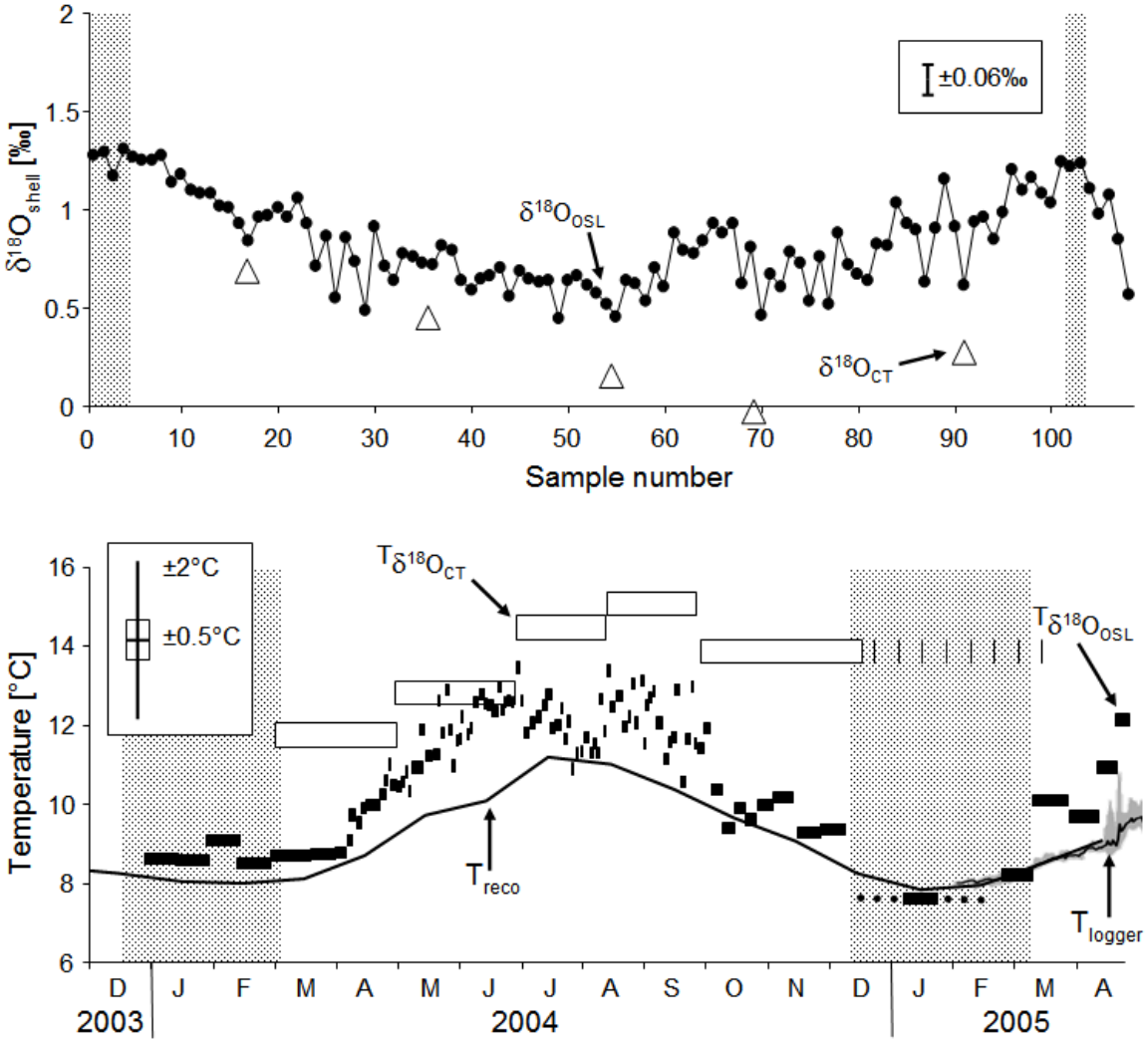


Figure 5. Specimen AS-Apr-A1L: Shell oxygen isotope record (upper panel) and temperatures reconstructed thereof (lower panel). Black circles and black squares are data from the outer shell layer (OSL) near the ventral margin, open triangles and open squares represent data from the cardinal tooth (CT). The temporal coverage of each sample is indicated by the length of the bars (lower panel). Whether the shells grew during winter at extremely low rates or entirely ceased growing is difficult to tell (stippled or dotted lines). Shaded portions represent samples taken from the within annual growth lines. $T_{reco}$ = monthly temperatures reconstructed from satellite data, $T_{logger}$ = hourly resolved data (grey) and daily averages (black) from temperature loggers recorded from 27 January 2005 onwards. Error bar in the upper panel refers to the precision error of the mass spectrometer. Error bars in the lower panel represent the average errors of all $T_{\delta 18O}$ data of this study. The 0.5°C error is computed from the Böhm et al. (2000) paleotemperature equation including the precision error of the mass spectrometer. The 2°C error considers the seasonal salinity and oxygen isotopy of the water ($\delta^{18}O_{water}$ or $\delta^{18}O_{water,\ reco}$) variability. $T_{\delta 18O}$ calculation is based on annual average $\delta^{18}O_{water}$ or $\delta^{18}O_{water,\ reco}$. In general, $T_{reco}$ are fairly well reproduced by $T\delta^{18}O_{OSL}$, but overestimated by $T\delta^{18}O_{CT}$. Note the different temporal resolution of the data sets. $T_{reco}$ is monthly resolved, each $T\delta^{18}O_{OSL}$ represents up to two days, and $T\delta^{18}O_{CT}$ approx 1.5 to two months per sample. Note, that the daily temperatures during summer exhibit a range of up to 2.3°C (see Fig. 6, lower panel).

## *2.3. RESULTS*

Specimens immersed in Mutvei's solution permitted an easy identification of shell internal growth patterns (Fig. 3). In cardinal tooth sections, sharply delimited annual growth lines separated consecutive annual growth increments from each other (Fig. 3A). In the outer shell layer, however, these annual growth structures were much more difficult to track, because the growth lines approached the outer shell surface at a very narrow angle (approx. 10°; Fig. 3B). During the first ten to fifteen years of life, *Panopea abrupta* shells grew predominantly in shell size and formed the broadest annual increments (up to 956 µm in the cardinal tooth). Subsequently, the shells grew mainly in ventral margin thickness (= "inward growth", ZOLOTAREV, 1980). After the age of fifteen, increment widths in the cardinal tooth measured only between 8 and 172 µm. The ventral margin thicknesses ranged from 0.6 mm in a six year-old shell (AS-Apr-A1L) to 2.23 mm in a 63 year old specimen (AS-0806-A4L) (Tab. 1).

The first few centimeters of the shells (measured along the outer shell surface and along shell height) were dominated by the inner shell layer (Fig. 2B). Only at approximately 2 cm from the umbo could the outer shell layer be identified. The inner shell layer vanished at ca. 7 cm from the umbo while the outer shell layer continued to increase in thickness toward the ventral margin (Fig. 2B). It should be noted that the cardinal tooth only yielded a minimum estimate of the ontogenetic age of the bivalve. According to a comparison of relative annual increment widths of the outer shell layer and the cardinal tooth, the first ca. three years of life may be missing in the cardinal tooth due to dissolution.

### 2.3.1. Shell oxygen isotope data

A total of 278 oxygen isotope samples of four different shells ($\delta^{18}O_{shell}$) were analyzed (Tab. 1, Fig. 4). 181 samples came from the outer shell layer near the ventral margin ($\delta^{18}O_{OSL}$) of three specimens, namely AS-Apr-A1 (n = 108; Fig. 5), AS-0806-A2L (n = 27; Fig. 6), and AS-0806-A6R (n = 46; Fig. 6). The $\delta^{18}O_{OSL}$ values exhibited very high temporal resolution of up to two days per sample as they only covered the years of 2004–2006. The remaining 97 samples were taken from the cardinal tooth sections ($\delta^{18}O_{CT}$; inner shell layer) of specimens ASMar-A1L (n = 70; Fig. 7) and AS-Apr-A1 (n = 27; Fig. 7), respectively, representing mainly the time interval of 1999 to 2004 (little shell material had formed between winter 2004/2005 and the date of collection in spring 2005).

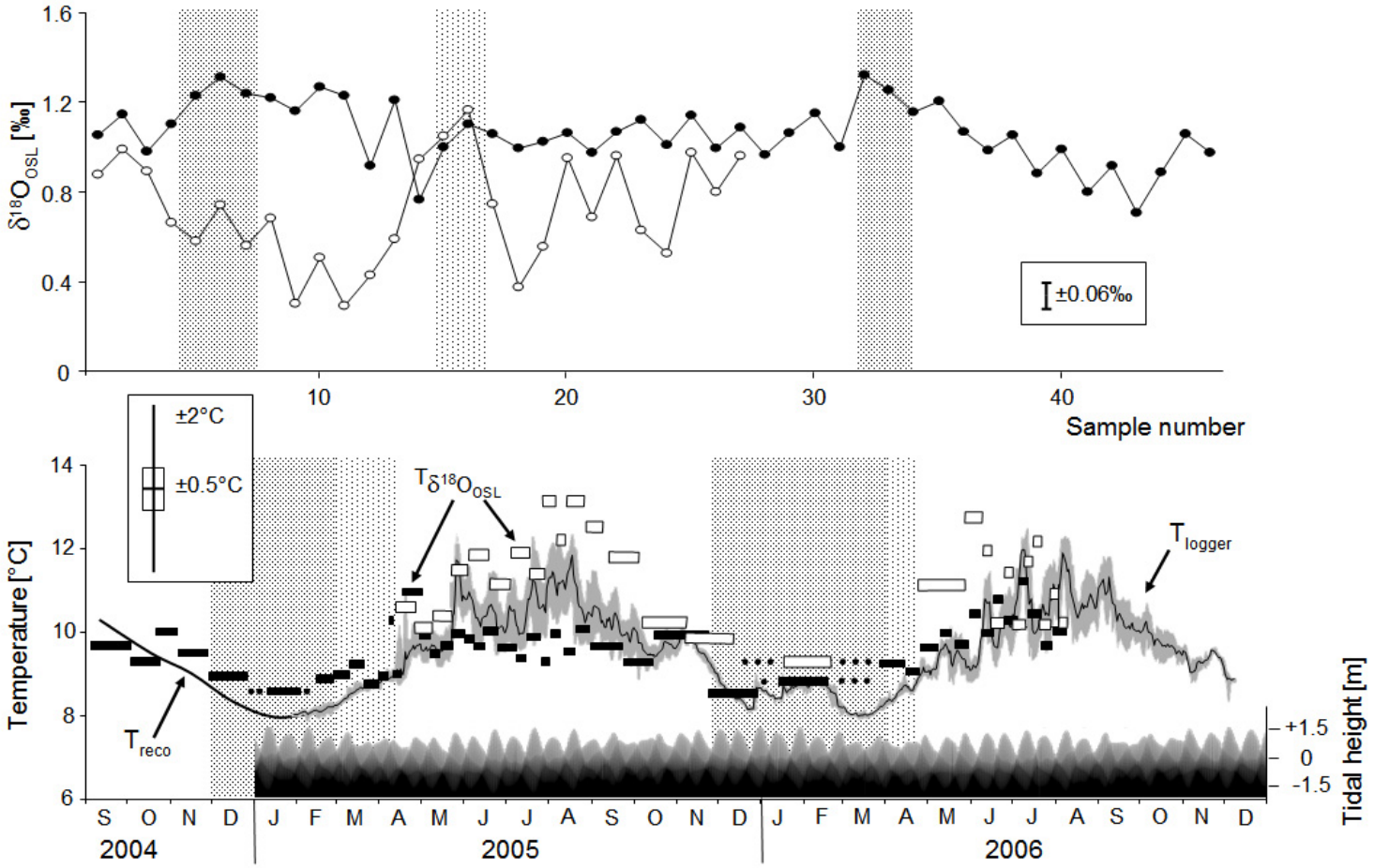


Figure 6. Specimens AS-0806-A2L (filled circles and squares) and AS-0806-A6R (open circles and squares): Shell oxygen isotope records from the outer shell layers (upper panel) and temperatures reconstructed thereof (lower panel). Despite both shells occurred contemporaneously at the exact same locality, their isotope records and $T\delta^{18}O_{OSL}$ data differ greatly from each other. The temperature record of specimen AS-0806-A2L appears truncated, whereas specimen AS-0806-A6R overestimates the temperature logger data, particularly during summer. Dark shading represents position of annual growth lines in specimen AS-0806-A2L, light shading that of specimen AS-0806-A6R. Note that daily summer temperatures exhibit a range of up to 2.3°C (grey curve in lower panel; average daily $T_{logger}$ data in black). This variability is strongly related to the tides. For other details of the graphs see description in caption of Fig. 5.

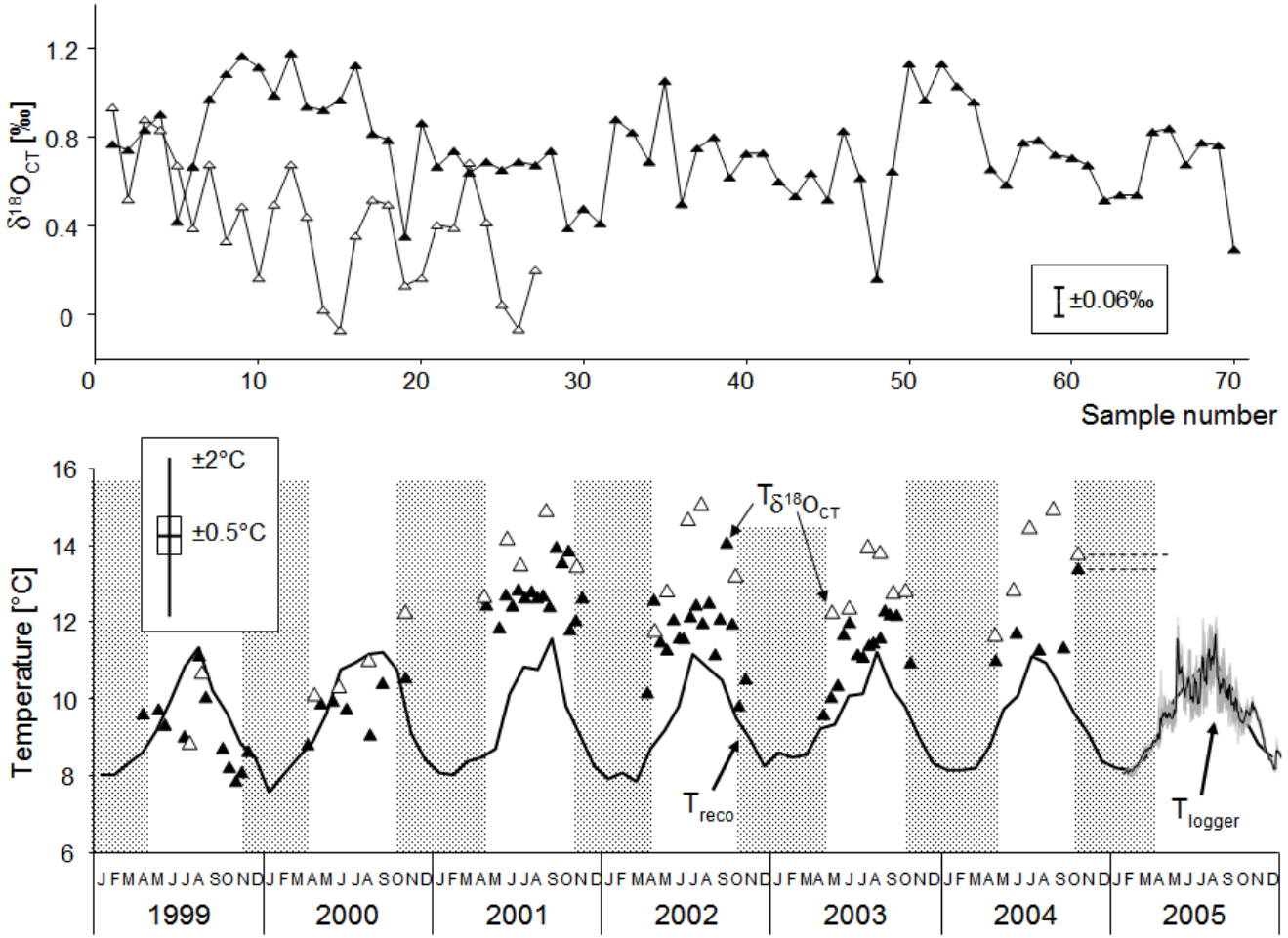


Figure 7. Specimens AS-Mar-A1L (filled triangles) and AS-Apr-A1L (open triangles): Shell oxygen isotope records from the cardinal teeth (CT) (upper panel) and temperatures reconstructed thereof (lower panel). Actual temperatures were greatly overestimated by the shell record during 2001 to 2004, particularly from specimen AS-Apr-A1L. Note that this specimen exhibited a distinct trend toward less positive $\delta^{18}O_{CT}$ values with increasing age. For other details of the graphs see description in caption of Figure 5.

### 2.3.2. Differences between $\delta^{18}O$ records of the inner and outer shell layer

Distinct seasonal oscillations were observed in all oxygen isotope chronologies from the outer shell layer with most positive values near the annual growth lines and least positive values half-way between two consecutive annual growth lines (Figs 5 and 6). However, the $\delta^{18}O_{CT}$ curves showed less clear sinusoidal oscillations, particularly specimen AS-Mar-A1 (Fig. 7). In addition, the $\delta^{18}O_{CT}$ curve of specimen AS-Apr-A1 exhibited a distinct trend from an annual average of 0.73‰ in 1999 to 0.26‰ in 2004 (Fig. 7). Specimen AS-Mar-A1, however, showed a much weaker trend from 0.88‰ to 0.67‰ during the same time interval (Fig. 7). A direct comparison of the $\delta^{18}O_{CT}$ and $\delta^{18}O_{OSL}$ data was possible for specimen AS-Apr-A1 (Fig. 5). On average, $\delta^{18}O_{CT}$ values of 2004 of this specimen were 0.58‰ more negative than the $\delta^{18}O_{OSL}$ data. Extreme $\delta^{18}O_{CT}$ values equaled −0.06 and 0.69‰ (n = 5; Tab. 4), whereas those of the outer shell layer were 0.44 and 1.31‰ (n = 102). Seasonal amplitudes recorded in the cardinal tooth (0.75‰) compared well to those of the outer shell layer record (0.87‰) (Tab. 4). Note that these differences occurred despite much lower sampling resolution in cardinal tooth sections than in the outer shell layer (five versus 102 samples).

### 2.3.3. Variability of $\delta^{18}O$ records among different contemporaneous specimens

Notably, the $\delta^{18}O$ values of contemporaneous shells from the same habitat differed significantly from each other (Figs 6 and 7). As mentioned above, the $\delta^{18}O_{OSL}$ data showed differences of up to 0.40‰ among individuals AS-0806-A2 and AS-0806-A6 (Fig. 6). Although both specimens grew contemporaneously at the same locality their oxygen isotope profiles varied in respect to amplitude and absolute values (Fig. 6, Tab. 4). The average value of 2005 calculated from specimen AS-0806-A6 (1.10‰; n = 28) was 0.40‰ more positive than that of AS-0806-A2 (0.70‰, n = 16; Tab. 4). During 2005, minimum and maximum $\delta^{18}O_{OSL}$ values of specimen AS-0806-A6 were 0.76 and 1.32‰ (amplitude of 0.56‰), whereas specimen AS-0806-A2 exhibited extremes of 0.29 and 1.17‰ (amplitude of 0.88‰). Notably, the isotope record obtained from AS-0806-A6 was ca. 80% higher resolved than that of its neighbor. Likewise, the cardinal tooth records differed from each other. The record of specimen AS-Apr-A1 showed a distinct trend over the time interval of 1999–2004 (Fig. 7). Consequently, the average $\delta^{18}O_{CT}$ values of the shells AS-Mar-A1 (0.75‰; n = 70) and AS-Apr-A1 (0.42‰; n = 27) differed by 0.33‰ (Tab. 4).

### 2.3.4. Timing of shell growth

In order to assign precise calendar dates to each portion of the shells, expected $\delta^{18}O$ values ($\delta^{18}O_{exp}$) were computed from instrumental or modeled temperatures ($T_{logger}$, $T_{reco}$) and oxygen isotope values of the water ($\delta^{18}O_{water}$, $\delta^{18}O_{water,\ reco}$) values using the equation by Böhm et al. (2000). The $\delta^{18}O_{shell}$ values from the very tip of the shells (= date of collection) functioned as one important anchor point. Then, shell oxygen isotope data of the shells were so arranged that measured and expected oxygen isotope curves closely matched each other, and the best fit was obtained between the $\delta^{18}O_{exp}$ and $\delta^{18}O_{shell}$ data (qualitative wiggle matching, linear regression analyses). Correlation coefficients were as high as $R = 0.82$ ($p < 0.0001$; AS-Apr-A1, OSL). After the temporal alignment of the data was completed, temperatures were calculated from shell oxygen isotope data and plotted against time (Figs 5-7).

### 2.3.5. Temperature reconstructions from shell oxygen isotopes

As seen from Figs 5 and 6, shell growth of the outer shell layer (OSL) mainly occurred between March/April and November/December. Lowest $T_{\delta 18O}$ fell together with the annual growth lines. The agreement between temperatures derived from shell oxygen isotopes of the OSL ($T\delta^{18}O_{OSL}$) and instrumental or modeled temperatures varied from shell to shell.

The $T\delta^{18}O_{OSL}$ of the youngest sampled specimen (AS-Apr-A1, six years old) showed the closest match with $T_{reco}$ (Fig. 5). $T\delta^{18}O_{OSL}$ overestimated actual minimum (8.1°C) and maximum (11°C) temperatures during 2004 by 0.9°C and 1.8°C, respectively, and the seasonal range (2.8°C) by 1°C (Tabs 3 and 4). Note the different time averaging of both data sets: $T_{reco}$ are monthly values, whereas the temporal resolution of the $T\delta^{18}O_{OSL}$ of this specimen was ca. two days during summer and about one to two weeks during winter. $T_{logger}$ data from 2005 suggested a large daily temperature range during summer of more than 2.3°C and 1°C larger seasonal amplitude than that calculated from monthly values (Tab. 3, Fig. 6). Although the reconstructed summer temperatures of AS-Apr-A1 tended to slightly overestimate the actual values, winter temperatures were almost perfectly reproduced. Notably, the error bars of the $T\delta^{18}O_{OSL}$ encompass the observed monthly temperatures.

Table 3. Temperature data. Seasonal amplitudes, average and extreme temperatures from logger data ($T_{logger}$) during 2005 and satellite-based reconstructed temperatures ($T_{reco}$) during 2004.

| 2005 | $T_{logger}$ (°C) | | |
|---|---|---|---|
| | Monthly resolution | Daily resolution | Hourly resolution |
| Average | 9.37 | 9.49 | 9.49 |
| Minimum | 7.93 | 7.91 | 7.77 |
| Maximum | 10.84 | 11.72 | 12.22 |
| Amplitude | 2.91 | 3.81 | 4.45 |

| 2004 | $T_{reco}$ (°C) |
|---|---|
| | Monthly resolution |
| Average | 9.31 |
| Minimum | 10.97 |
| Maximum | 8.13 |
| Amplitude | 2.84 |

Table 4. Shell (*Panopea abrupta*) oxygen isotope-derived temperatures. Seasonal amplitudes, average and extreme oxygen isotope values ($\delta^{18}O_{shell}$) and temperatures reconstructed thereof ($T_{\delta 18O}$). OSL = outer shell layer, CT = cardinal tooth.

| Shell portion | Time interval ($\delta^{18}O_{water,reco}$ or $\delta^{18}O_{water}$ [‰]) | | $\delta^{18}O_{shell}$ [‰] ($T_{\delta 18O}$ [°C]) | | | |
|---|---|---|---|---|---|---|
| | | | AS-Mar-A1 | AS-Apr-A1 | AS-0806-A2 | AS-0806-A6 |
| OSL | 2004 (-1.18) | Average | | 0.84 (11.1) | | |
| | | Maximum | | 1.31 (9) | | |
| | | Minimum | | 0.44 (12.8) | | |
| | | Amplitude | | 0.87 (3.8) | | |
| | 2005 (-1.27) | Average | | | 0.7 (11.3) | 1.1 (9.5) |
| | | Maximum | | | 1.17 (9.2) | 1.32 (8.6) |
| | | Minimum | | | 0.29 (13.1) | 0.76 (11) |
| | | Amplitude | | | 0.88 (3.9) | 0.56 (2.4) |
| CT | 2004 (-1.18) | Average | 0.67 (11.8) | 0.26 (13.6) | | |
| | | Maximum | 0.84 (11.1) | 0.69 (11.8) | | |
| | | Minimum | 0.30 (13.5) | -0.06 (15.1) | | |
| | | Amplitude | 0.54 (2.4) | 0.75 (3.3) | | |
| | 1999-2004 | Average | 0.75 (11.4) | 0.42 (12.9) | | |
| | (see Fig. 4) | Maximum | 1.18 (7.9) | 0.94 (8.9) | | |
| | | Minimum | 0.16 (14.2) | -0.07 (15.1) | | |
| | | Amplitude | 1.02 (6.3) | 1.00 (6.2) | | |

The $T\delta^{18}O_{OSL}$ records of the other two shells that lived contemporaneously at the same locality differed significantly from one another in range, average and summer values (Fig. 6). Specimen AS-0806-A6 (16 years old) showed a truncated seasonal temperature amplitude barely exceeding 2.4°C (winter and summer extremes of 8.6°C and 11°C; Tab. 4). Despite that, the upper error bars of the reconstructed temperatures of this shell were still in the

bounds of measured temperatures (Fig. 6). However, the $T\delta^{18}O_{OSL}$ curve of the 25 year-old specimen AS-0806-A2 was shifted toward warmer temperatures by an average of 2°C during summer with the error bars plotting outside the daily temperature variance (Fig. 6). The reconstructed seasonal temperature range of 3.9°C was in good agreement with daily $T_{logger}$ data, but both daily winter (7.9°C) and summer (11.7°C) extremes were overestimated by the shell isotope record (about two weeks resolution) by ca. 1.4°C (Tabs 3 and 4). The annual average $T\delta^{18}O_{OSL}$ of the two shells differed by 1.8°C.

Temporally aligned temperature estimates from cardinal teeth ($T\delta^{18}O_{CT}$) differed greatly from each other (up to 4°C) and exceeded actual temperatures by more than 3–4°C in some years (Fig. 7). Seasonal temperature extremes showed less severe discrepancies (Tab. 4). For example, summer $T\delta^{18}O_{CT}$ maxima during 2004 were 13.5°C and 15.1°C in the six year-old specimens AS-Mar-A1 and ASApr-A1, respectively. Note that each sample from AS-Apr-A1 represented more than one month, whereas a ca. bi-weekly resolution was achieved for specimen AS-Mar-A1. Lowest $T\delta^{18}O_{CT}$ values (2004) of specimen AS-Apr-A1 equaled 11.8°C which is ca. 2.5°C warmer than observed during winter. Its $T\delta^{18}O_{CT}$ range (3.3°C), however, was almost identical to the observed seasonal amplitude (monthly resolution).

It was difficult to confidently add a time axis the $T\delta^{18}O_{CT}$ data, particularly in the case of specimen AS-Mar-A1. The record may be incomplete and did not display seasonal oscillations. Over the time interval of 2001–2004, however, both reconstructed temperature curves plotted above the $T_{reco}$, while actual temperatures were underestimated during 1999.

### 2.3.6. Intra-annual shell growth rates and relation to temperature

Based on the temporal alignment of the $\delta^{18}O_{OSL}$ data it was possible to estimate the time represented by each isotope sample. In turn, this enabled us to estimate the relative monthly growth rates during different seasons (Fig. 8). Growth rate increased rapidly after the winter cessation and reached a maximum in late spring and summer. After August shell growth quickly slowed down and reached minimum rates in November or December. Shell growth and temperature were highly positively correlated. For example, reconstructed monthly shell growth of the 25 year-old specimen AS-0806-A2 showed a strong positive linear correlation with water temperature ($R = 0.93$, $R^2 = 0.86$, $p < 0.0001$).

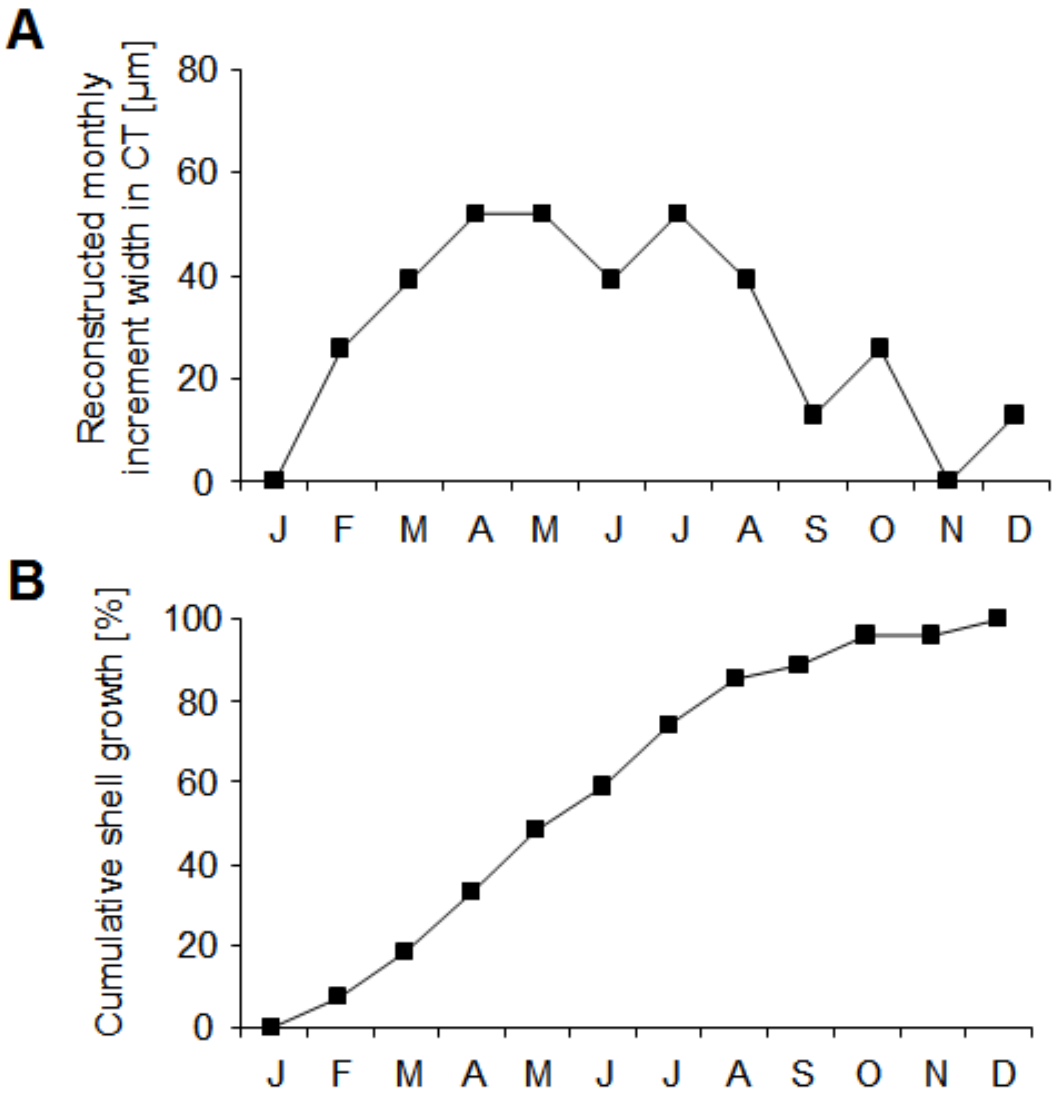


Figure 8. Relative monthly shell growth rates (A = differential; B = integral, cumulative growth curve) during different seasons. Growth rate increased rapidly after the winter cessation and reached a maximum in late spring and summer. After August shell growth quickly slowed down and reached minimum rates in November or December (specimen AS-0806-A2L).

## *2.4. DISCUSSION*

Owing to its remarkably long lifespan, *Panopea abrupta* has recently become the focus of paleoclimate reconstructions (STROM et al., 2004, 2005). These studies have demonstrated that shell growth of this species is influenced by the PDO (STROM et al., 2004). However, little is known about intra-annual growth rates and whether geochemical proportions of geoducks can be used to quantitatively reconstruct past water temperatures and other environmental variables (compare GOMAN et al., 2008). The present study is the first to

compare the high-resolution (up to two days per sample) oxygen isotope records of contemporaneous shells from the same habitat with each other and with high-resolution environmental data, including hourly resolved instrumental temperatures and near-monthly $\delta^{18}O_{water}$ records. Results of our study suggest that shell oxygen isotopes of this species may be more challenging to interpret than previously thought (GOMAN et al., 2008). For example, the study by GOMAN et al. (2008) did not take into account that $\delta^{18}O_{water}$ values can change significantly on seasonal and inter-annual time-scales. The authors reported only a single $\delta^{18}O_{water}$ measurement. Furthermore, their study was only based on two specimens and did not address possible inter-individual differences of $\delta^{18}O_{shell}$ values. In addition, analyses were only performed on the hinge plate, a shell portion that should not be used for chemical analyses.

### 2.4.1. Timing of shell growth

Temporally aligned shell oxygen isotope profiles indicated that the ain growing season (= formation of the annual growth increment) of *P. abrupta* lasts from March or April through November or December (Figs 5 and 6). During the remainder of the year, however, the annual growth line seems to form. These findings compare well with the work by SHAUL and GOODWIN (1982). In fact, geoducks are less active in winter and have their siphons retracted most of the time (GOODWIN, 1977) so that shell growth is reduced to extremely low rates (SHAUL and GOODWIN, 1982). Slight variations in the duration of the growing season may be explained by year-to-year environmental variability (temperature, food etc.) or different individual physiological needs. However, there is no trend toward shorter growing periods with increasing ontogenetic age as in some short-lived bivalve species (e.g., MIYAJI et al., 2007). Knowledge of the timing of shell growth and its possible changes throughout life is relevant to interpret long-term climate data gathered from biogenic hard parts (SCHÖNE et al., 2005c). Former studies have provided indirect evidence for a temporally invariable growing period of geoduck shells. STROM et al. (2004, 2005) showed that annual increment chronologies from contemporaneous specimens of different ontogenetic ages matched each other perfectly. If the duration of the growing season was reduced with increasing age, the corresponding annual increments would be narrower and the growth curves of these individuals would not have compared well with each other.

## 2.4.2. Oxygen isotope variability among shells

Oxygen isotope-derived temperature records of the OSL of contemporaneous shells from the exact same habitat varied by up to 2°C from each other (Fig. 6). This can barely be explained by microhabitat differences, because the surface waters were well-mixed at the locality where the shells dwelled. Near Protection Island, temperature and salinity values are unlikely to vary on scales of nearly 2°C (= 50% of the seasonal temperature amplitude; compare Fig. 4) or 0.7 PSU (= 140% of the seasonal salinity amplitude; compare Fig. 4) within a few meters. Furthermore, differences in sample resolution cannot account for the observed differences in $\delta^{18}O_{OSL}$ values. Yet, the lowest number of samples came from specimen AS-0806-A2 (Fig. 6), this shell was isotopically most depleted. Vital effects (UREY et al., 1951; WEINER and DOVE, 2003) can also be ruled out, because shell calcium carbonate utilizes the oxygen isotopes of the water and not oxygen of the food. A more likely explanation for the discrepancies is that variable exchange rates between the outer EPF (extrapallial fluid) and the ambient water vary among different specimens. During $CaCO_3$ precipitation, the EPF becomes isotopically depleted, because $^{18}O$ is preferably incorporated into the shell. This has been demonstrated by numerous experimental (e.g., EPSTEIN et al., 1953; GROSSMAN and KU, 1986) and theoretical studies (O'NEIL et al., 1969). The $\delta^{18}O_{OSL}$ values of newly forming shell will therefore be more negative. The observed greater discrepancy between expected and measured shell oxygen isotope values can be explained by higher growth rates in summer which will cause a stronger depletion in $^{18}O$ of the EPF. Although bivalves are generally believed to precipitate their hard parts (at least the outer shell layer) in isotopic equilibrium with the ambient water, slight between-specimen differences have been also reported in various other studies (GOODWIN et al., 2001; SCHÖNE et al., 2006; GILLIKIN et al., 2005).

In addition, we observed some variability in the seasonal temperature amplitudes of up to 1.5°C (Figs 5 and 6, Tabs 3 and 4). The $T\delta^{18}O_{OSL}$ curve of specimen AS-0806-A6 appeared flatter than that of specimen AS-0806-A2 (Fig. 6). The latter overestimated summer temperatures more than winter temperatures (Tabs 3 and 4). It is possible that the specimens deposited shell at different times during the day. Analyses of physiological activity patterns of bivalves held in tanks revealed considerable variability in the timing of shell gaping between different species (RODLAND et al., 2006), but also among different individuals of the same species (unpublished data by one of us, BRS). No specimen grew uninterruptedly during the day, but showed clear circadian and ultradian activity cycles. For example, *Anodonta cygnea* (Linnaeus) is physiologically active and precipitates shell carbonate only during ca. 8–12 h

per day. In settings with intra-annual temperature variations, the timing of shell formation during one day/night cycle can result in very different shell oxygen isotope curves. In this study, temperature loggers indicated an intra-daily temperature variability of up to 2.3°C during summer (Fig. 6), which corresponds to more than 50% of the seasonal temperature amplitude. If one geoduck, for example, grew preferentially during midday, the resulting $T\delta^{18}O_{OSL}$ curve would exhibit a greater seasonal amplitude (see AS-0806-A6; Fig. 6) than the temperature record of a specimen that grew preferentially at night (see AS-0806-A2; Fig. 6).

It remains unclear what caused these individual differences in ultradian timing of shell growth. Variable ultradian activity patterns could be linked to genetically predetermined or environmentally entrained physiological differences. The underestimation of summer temperatures by the $T\delta^{18}O_{OSL}$ values of specimen AS-0806-A6 may also be explained by siphon-cropping. According to NAKAOKA (2000) the presence of predators can alter the feeding behavior of bivalves. Siphon-cropping by epibenthic vertebrates and invertebrates like crabs, sea stars and gastropods may not directly result in death, but can have negative, sublethal effects on bivalve growth and feeding. While more energy is spent on tissue regeneration, the feeding rate is reduced and thus shell growth rates are lower (PETERSON and QUAMMEN, 1982). Foraging predators may be particularly abundant and active during the warm season of the year. Subtidal predation of geoducks by epibenthic predators such as sea stars (*Pycnopodia spp.*) and Dungeness crabs (*Cancer magister* Dana) has been observed in the Puget Sound region (Lynn Goodwin, pers. communication), and geoduck siphon tips have been recovered from the stomachs of cabezon and rockfish.

### 2.4.3. Oxygen isotope variability within shells

Cardinal teeth and the adjacent hinge plate of geoducks have previously been identified as the most suitable shell portions for growth pattern analyses (SHAUL and GOODWIN, 1982; STROM et al., 2004, 2005). However, our results suggest that the $\delta^{18}O_{shell}$ data from these shell portions should not be used for paleotemperature estimates. The $\delta^{18}O_{CT}$ ranges were shifted away from equilibrium and the $\delta^{18}O_{OSL}$ values by up to approx. 0.7–0.9‰ toward less positive values in most years (Fig. 7). This translates into a temperature overestimation of more than 3–4°C and results in $T\delta^{18}O_{CT}$ values far outside the bounds of the instrumental temperatures and $T\delta^{18}O_{OSL}$. Note that the offset was also particularly high during our water

sampling campaign and can hence not be explained by unrealistic estimates of the oxygen isotope values of the water. Whether this offset increases over a lifetime has yet to be shown. Moreover, the $\delta^{18}O_{CT}$ values of different contemporaneous specimens from the same habitat can also vary by nearly 4°C (Fig. 7). One of the two sampled shells (AS-Apr-A1) showed a ca. 0.5‰ shift in its $\delta^{18}O_{CT}$ values while the oxygen isotope curve of the other specimen from the exact same locality showed only a minor negative shift of 0.2‰ during the same time interval (Fig. 7).

Although the cardinal tooth and outer shell layer consist of exact same mineralogy (> 95% aragonite), the isotopic difference between the records of the two shell portions was not completely unexpected. The inner shell layer – which includes the cardinal tooth – and outer shell layer of many other bivalve mollusk species have been shown to vary considerably in respect to elemental composition and stable isotope ratios. For example, the outer prismatic and middle crossed-lamellar shell layers of *Mercenaria campechiensis* (Gmelin) differ greatly in respect to their Sr/Ca profiles (SURGE and WALKER, 2006). Likewise, the inner and outer shell layers of *Saxidomus giganteus* show a 0.2‰ difference in oxygen and carbon isotope data (Gillikin et al., 2005). It is well known that the cardinal tooth is precipitated from the inner EPF while the outer shell layer is formed from the outer EPF. These two fluids are probably not in elemental or isotopic equilibrium. Moreover, they may exhibit within- and among-specimen differences in the exchange rate between the EPF and the ambient water. Therefore geochemical analyses are commonly performed on shell material from the outer shell layer (JONES and QUITMYER, 1996).

### 2.4.4. Shell growth and water temperature

Seawater temperature is commonly the most important factor controlling shell growth in bivalves (GOODWIN et al., 2001). For geoducks at Protection Island the fastest growth corresponded to the highest temperatures in July and August. During winter, however, growth was reduced or came to a complete cessation (Figs 5, 6 and 8). The relation between temperature and growth in geoduck shells was also postulated in previous studies (NOAKES and CAMPBELL, 1992; STROM et al., 2004) and demonstrated by laboratory experiments (STROM et al., 2004).

## 2.5. CONCLUSIONS

Paleoclimate reconstructions based on single geoduck shells appear to be highly problematic. Given a typical seasonal temperature range from about 8 to 12°C, a nearly 2°C discrepancy among the $T\delta^{18}O_{OSL}$ records of different specimens is a significant error and makes reliable paleotemperature estimates based on $\delta^{18}O_{shell}$ of *P. abrupta* nearly impossible. Another challenge encountered in this study was the need to interpret shell records that may have been biased towards higher or lower temperatures because the shells grew preferentially during night or day, or were exposed to high predation pressure. If additional shells from the same location and time-period were analyzed it may have been possible to provide a more robust estimate of the actual temperatures and to quantify the vital effects. Most paleoclimate analyses, however, are dependent on single specimens, because due to time-averaging contemporaneity of shells from the same stratigraphic horizon is almost impossible to prove.

Unknown paleo-$\delta^{18}O_{water}$ values further aggravate temperature estimates from $\delta^{18}O_{shell}$ values of this species. During a single year, $\delta^{18}O_{water}$ values can vary by ca. 0.39‰. This translates into a shell oxygen isotope-based temperature difference of 1.7°C. Furthermore, ENSO and PDO strongly impact precipitation patterns in the Pacific Northwest (WALKER, 1923; KURTZMAN and SCANLON, 2007), freshwater discharge and hence the oxygen isotope composition of the water in which the shells live. Therefore, salinity and $\delta^{18}O_{water}$ values not only fluctuate on seasonal time-scales, but on decadal to multi-decadal time-scales as well.

Finally, although it may be more convenient to sample the same shell portion for isotope analyses that was used for growth pattern analysis, the cardinal teeth of geoducks exhibit strong vital effects in $\delta^{18}O_{shell}$ values. Temperature estimates from these inner layer shell portions may be incomplete and are usually precipitated out of equilibrium. This can result in a temperature overestimation by 3–4°C and more.

Subsequent studies should analyze if the minor element to calcium ratios (Sr/Ca, Mg/Ca) of shells of *P. abrupta* can provide better paleotemperature estimates than stable oxygen isotope data. Perhaps, metal to calcium ratios can be used in conjunction with $\delta^{18}O_{shell}$ values to eliminate the adverse effect of variable $\delta^{18}O_{water}$ values on temperature reconstructions from oxygen isotopes.

## 2.6. ACKNOWLEDGMENTS

We wish to acknowledge the late Tom O'Rourke for his critical contributions to the successful completion of this study. This work could not have been accomplished without the cooperation of the Jamestown S'Klallam Tribe and the efforts of their employees Tom, his wife Lohna O'Rourke and Aleta Erickson who together obtained all bottom samples of water and deployed and maintained the temperature loggers. We also thank Bob Lona, David Nguyen and the staff of the Washington Department of Health Biotoxin lab in Shoreline Seattle, who provided all shell samples. Analía Soldati is kindly acknowledged for her help with the Raman spectroscopy and A. Mackensen (Alfred Wegener Institute for Polar and Marine Research) for determining the $\delta^{18}O_{water}$ and salinity values. SST data (AVHRR) came from the PO.DAAC — NASA Jet Propulsion Laboratory from their Web site at http://www-sci.pac.dfo-mpo.gc.ca and salinity of Race Rocks from Fisheries and Oceans Canada — Pacific Region (http://www-sci.pac.dfo-mpo.gc.ca). Salinity and $\delta^{18}O_{water}$ values for the northwest Pacific were obtained from the NASA-Goddard Institute for Space Studies (http://data.giss.nasa.gov/o18data/). We thank two anonymous reviewers for their comments that helped further improving the manuscript. Financial support for this study was provided by the German Research Foundation, DFG (SCHO 793/3).

## 2.7. REFERENCES

BÖHM, F., JOACHIMSKI, M.M., DULLO, W.-Ch., EISENHAUER, A., LEHNERT, H., REITNER, J., and WÖRHEIDE, G., 2000. Oxygen isotope fractionation in marine aragonite of coralline sponges. Geochimica et Cosmochimica Acta 64, 1695–1703.

BUICK, D.P., and IVANY, L.C., 2004. 100 years in the dark: extreme longevity of Eocene bivalves from Antarctica. Geology 32, 921–924.

BUREAU, D., HAJAS, W., SURRY, N.W., HAND, C.M., DOVEY, G., and CAMPBELL, A., 2002. Age, size structure and growth parameters of geoducks (*Panopea abrupta*, Conrad 1849) from 34 locations in British Columbia sampled between 1993 and 2000. Canadian Technical Report of Fisheries and Aquatic Sciences 2413, 1–84.

CLARK II, G.R., 1975. Periodic growth and biological rhythms in experimentally grown bivalves. *In*: ROSENBERG, G.D., RUNCORN, S.K. (eds.), Growth Rhythms and the History of the Earth's Rotation. Wiley, London, 103–117.

COAN, E.V., SCOTT, P.V., and BERNARD, F.R., 2000. Bivalve Seashells of Western North America. Santa Barbara Museum of Natural History, Santa Barbara. 764 p.

CRAIG, H., and GORDON, L.I., 1965. Deuterium and oxygen 18 variations in the ocean and the marine atmosphere. *In*: TONGIORGI, E. (ed.), Stable Isotopes in Oceanographic Studies and Paleotemperatures. Consiglio Nazionale delle Ricerche, Spoleto, Italy, 9–130.

DETTMAN, D.L., and LOHMANN, K.C., 1995. Microsampling carbonates for stable isotope and minor element analysis; physical separation of samples on a 20 micrometer scale. Journal of Sedimentary Research 65, 566–569.

DODGE, R.E., and VAIŠNYS, J.R., 1980. Skeletal growth chronologies of recent and fossil corals. *In*: RHOADS, D.C., LUTZ, R.A. (eds.), Skeletal Growth of Aquatic Organisms. Plenum, New York, 493–517.

ELLIOT, M., DEMENOCAL, P.B., LINSLEY, B.K., and HOWE, S.S., 2003. Environmental controls on the stable isotopic composition of *Mercenaria mercenaria*: potential application to paleoenvironmental studies. Geochemistry Geophysics Geosystems 4, 1–16.

EPSTEIN, S., BUCHSBAUM, R., LOWENSTAM, H.A., and UREY, H.C., 1953. Revised carbonate-water isotopic temperature scale. Bulletin of the Geological Society of America 64, 1315–1326.

EPSTEIN, S., and MAYEDA, T., 1953. Variation of $O^{18}$ content of waters from natural sources. Geochimica et Cosmochimica Acta 4, 213–224.

FIEBIG, J., SCHÖNE, B.R., and OSCHMANN, W., 2005. High-precision oxygen and carbon isotope analysis of very small (10–30 μg) amounts of carbonates using continuous flow isotope ratio mass spectrometry. Rapid Communications in Mass Spectrometry 19, 2355–2358.

FRITTS, H.C., 1972. Tree-rings and climate. Scientific American 226, 93–100.

GILLIKIN, D.P., DE RIDDER, F., ULENS, H., ELSKENS, M., KEPPENS, E., BAEYENS, W., and DEHAIRS, F., 2005. Assessing the reproducibility and reliability of estuarine bivalve shells (*Saxidomus giganteus*) for sea surface temperature reconstruction: implications for paleoclimate studies. Palaeogeography Palaeoclimatology Palaeoecology 228, 70–85.

GOMAN, M., INGRAM, B.L., and STROM, A., 2008. Composition of stable isotopes in geoduck (*Panopea abrupta*) shells: a preliminary assessment of annual and seasonal paleoceanographic changes in the northeast Pacific. Quaternary International 188, 117–125.

GOODWIN, C.L., 1976. Observations on spawning and growth of subtidal geoducks (*Panope generosa*, Gould). Proceedings of the National Shellfisheries Association 65, 49–58.

GOODWIN, C.L., 1977. The effects of season on visual and photographic assessment of subtidal geoduck clam (*Panope generosa*, Gould) populations. Veliger 20, 155–158.

GOODWIN, D.H., FLESSA, K.W., SCHÖNE, B.R., and DETTMAN, D.L., 2001. Cross-calibration of daily growth increments, stable isotope variation, and temperature in the Gulf of California bivalve mollusk *Chione cortezi*: implications for paleoenvironmental analysis. PALAIOS 16, 387–398.

GOODWIN, C.L., and PEASE, B., 1989. Species profiles: life histories and environmental requirements of coastal fish and invertebrates (Pacific Northwest): Pacific geoduck clam. U.S. Fish and Wildlife Service Biological Report 82 (11.120), U.S. Army Corps of Engineers, TR EL-82-4. 14 p. (available at http://www.nwrc.usgs.gov/wdb/pub/species_profiles/ 82_11-120.pdf).

GRIBBEN, P.E., and CREESE, R.G., 2003. Protandry in the New Zealand geoduck, *Panopea zelandica* (Mollusca, Bivalvia). Invertebrate Reproduction and Development 44, 119–129.

GROSSMAN, E.L., and KU, T.-L., 1986. Oxygen and carbon isotope fractionation in biogenic aragonite; temperature effects. Chemical Geology (Isotope Geoscience Section) 59, 59–74.

HENDERSON, J.T., 1929. Lethal temperatures of Lamellibranchiata. Contributions to Canadian Biology and Fisheries 4, 399–411.

HUDSON, J.H., SHINN, E., HALLEY, R., and LIDZ, B., 1976. Sclerochronology: a new tool for interpreting past environments. Geology 4, 361–364.

JOHNSON, A.L.A., HICKSON, J.A., SWAN, J., BROWN, M.R., HEATON, T.H.E., CHENERY, S., and BALSON, P.S., 2000. The Queen Scallop *Aequipecten opercularis*: a new source of information on late Cenozoic marine environments in Europe. Geological Society, London, Special Publications 177, 425–439.

JONES, D.S., 1980. Annual cycle of shell growth increment formation in two continental shelf bivalves and its paleoecologic significance. Paleobiology 6, 331–340.

JONES, D.S., ARTHUR, M.A., and ALLARD, D.J., 1989. Sclerochronological records of temperature and growth from shells of *Mercenaria mercenaria* from Narragansett Bay, Rhode Island. Marine Biology 102, 225–234.

JONES, D.S., and QUITMYER, I.R., 1996. Marking time with bivalve shells: oxygen isotopes and season of annual increment formation. PALAIOS 11, 340–346.

KENNISH, M.J., and OLSSON, R.K., 1975. Effects of thermal discharges on the microstructural growth of *Mercenaria mercenaria*. Environmental Geology (Springer) 1, 41–64.

KURTZMAN, D., and SCANLON, B.R., 2007. El Niño — Southern Oscillation and Pacific Decadal Oscillation impacts on precipitation in the southern and central United States: evaluation of spatial distribution and predictions. Water Resources Research 43, W10427, doi:10.1029/2007WR005863.

MACKAS, D.L., and HARRISON, P.J., 1997. Nitrogenous nutrient sources and sinks in the Juan de Fuca Strait/Strait of Georgia/Puget Sound estuarine system: assessing the potential for eutrophication. Estuarine, Coastal and Shelf Science 44, 1–21.

MARCHITTO, T.A., JONES, G.A., GOODFRIEND, G.A., and WEIDMAN, C.R., 2000. Precise temporal correlation of Holocene mollusk shells using sclerochronology. Quaternary Research 53, 236–246.

MIYAJI, T., TANABE, K., and SCHÖNE, B.R., 2007. Environmental controls on daily shell growth of *Phacosoma japonicum* (Bivalvia: Veneridae) from Japan. Marine Ecology Progress Series 336, 141–150.

MORSÁN, E., and CIOCCO, N.F., 2004. Age and growth model for the southern geoduck, *Panopea abbreviata*, off Puerto Lobos (Patagonia, Argentina). Fisheries Research 69, 343–348.

NAKAOKA, M., 2000. Nonlethal effects of predators on prey populations: predatormediated change in bivalve growth. Ecology 81, 1031–1045.

NOAKES, D.J., and CAMPBELL, A., 1992. Use of geoduck clams to indicate changes in the marine environment of Ladysmith Harbor, British Columbia. Environmetrics 3, 81–97.

O'NEIL, J.R., CLAYTON, R.N., and MAYEDA, T.K., 1969. Oxygen isotope fractionation in divalent metal carbonates. Journal of Chemical Physics 51, 5547–5558.

PAGE, H.M., and HUBBARD, D.M., 1987. Temporal and spatial patterns of growth in mussels *Mytilus edulis* on an offshore platform: relationships to water temperature and food availability. Journal of Experimental Marine Biology and Ecology 111, 159–179.

PETERSON, C.H., and QUAMMEN, M.L., 1982. Siphon nipping: its importance to small fishes and its impact on growth of the bivalve *Protothaca staminea* (Conrad). Journal of Experimental Marine Biology and Ecology 63, 249–268.

RODLAND, D.L., SCHÖNE, B.R., HELAMA, S., NIELSEN, J.K., and BAIER, S., 2006. A clockwork mollusc: ultradian rhythms in bivalve activity revealed by digital photography. Journal of Experimental Marine Biology and Ecology 334, 316–323.

SATO, S., 1997. Shell microgrowth patterns of bivalves reflecting seasonal change of phytoplankton abundance. Paleontological Research 1, 260–266.

SCHÖNE, B.R., FREYRE CASTRO, A.D., FIEBIG, J., HOUK, S., OSCHMANN, W., and KRÖNCKE, I., 2004a. Sea surface temperatures over the period 1884–1983 reconstructed from oxygen isotope ratios of a bivalve mollusk shell (*Arctica islandica*, southern North Sea). Palaeogeography Palaeoclimatology Palaeoecology 212, 215–232.

SCHÖNE, B.R., DUNCA, E., FIEBIG, J., and PFEIFFER, M., 2005c. Mutvei's solution: an ideal agent for resolving microgrowth structures of biogenic carbonates. Palaeogeography Palaeoclimatology Palaeoecology 228, 149–166.

SCHÖNE, B.R., DUNCA, E., MUTVEI, H., and NORLUND, U., 2004b. A 217-year record of summer air temperature reconstructed from freshwater pearl mussels (*M. margaritifera*, Sweden). Quaternary Science Reviews 23, 1803–1816.

SCHÖNE, B.R., FIEBIG, J., PFEIFFER, M., GLEß, R., HICKSON, J., JOHNSON, A.L.A., DREYER, W., and OSCHMANN, W., 2005a. Climate records from a bivalve Methuselah (*Arctica islandica*, Mollusca; Iceland). Palaeogeography Palaeoclimatology Palaeoecology 228, 130–148.

SCHÖNE, B.R., OSCHMANN, W., RÖSSLER, J., FREYRE CASTRO, A.D., HOUK, S.D., KRÖNCKE, I., DREYER, W., JANSSEN, R., RUMOHR, H., and DUNCA, E., 2003. North Atlantic Oscillation dynamics recorded in shells of a long-lived bivalve mollusk. Geology 31, 1237–1240.

SCHÖNE, B.R., PFEIFFER, M., POHLMANN, T., and SIEGISMUND, F., 2005b. A seasonally resolved bottom-water temperature record for the period AD 1866–2002 based on shells of *Arctica islandica* (Mollusca, North Sea). International Journal of Climatology 25, 947–962.

SCHÖNE, B.R., RODLAND, D.L., FIEBIG, J., OSCHMANN, W., GOODWIN, D., FLESSA, K.W., and DETTMAN, D., 2006. Reliability of multitaxon, multiproxy reconstructions of environmental conditions from accretionary biogenic skeletons. Journal of Geology 114, 267–285.

SHAUL, W., and GOODWIN, L., 1982. Geoduck (*Panope generosa*: Bivalvia) age as determined by internal growth lines in the shell. Canadian Journal of Fisheries and Aquatic Sciences 39, 632–636.

SPÖTL, C., and VENNEMANN, T.W., 2003. Continuous-flow isotope ratio mass spectrometric analysis of carbonate minerals. Rapid Communications in Mass Spectrometry 17, 1004–1006.

STROM, A., FRANCIS, R.C., MANTUA, N.J., MILES, E.L., and PETERSON, D.L., 2004. North Pacific climate recorded in growth rings of geoduck clams: a new tool for

paleoenvironmental reconstruction. Geophysical Research Letters 31, L06206, doi:10.1029/2004GL019440.

STROM, A., FRANCIS, R.C., MANTUA, N.J., MILES, E.L., and PETERSON, D.L., 2005. Preserving low-frequency climate signals in growth records of geoduck clams (*Panopea abrupta*). Palaeogeography Palaeoclimatology Palaeoecology 228, 167–178.

SURGE, D., and WALKER, K.J., 2006. Geochemical variation in microstructural shell layers of the southern quahog (*Mercenaria campechiensis*): implications for reconstructing seasonality. Palaeogeography Palaeoclimatology Palaeoecology 237, 182–190.

UREY, H.C., LOWENSTAM, H.A., EPSTEIN, S., and MCKINNEY, C.R., 1951. Measurement of paleotemperatures and temperatures of the Upper Cretaceous of England, Denmark, and the southeastern United States. Bulletin of the Geological Society of America 62, 399–416.

WALKER, G.T., 1923. Correlation in seasonal variations of weather, VIII: a preliminary study of world weather. Memoirs of the India Meteorological Department 24, 75–131.

WANAMAKER JR., A.D., KREUTZ, K.J., SCHÖNE, B.R., PETTIGREW, N., BORNS, H.W., INTRONE, D.S., BELKNAP, D., MAASCH, K.A., and FEINDEL, S., 2007. Coupled North Atlantic slope water forcing on Gulf of Maine temperatures over the past millennium. Climate Dynamics 31, 183–194.

WEINER, S., and DOVE, P.M., 2003. An overview of biomineralization processes and the problem of the vital effect. *In*: DOVE, P.M., DEYOREO, J.J., WEINER, S. (eds.), Biomineralization. Reviews in Mineralogy and Geochemistry 54, 1–29.

ZOLOTAREV, V.N., 1980. The life span of bivalves from the Sea of Japan and Sea of Okhotsk. The Soviet Journal of Marine Biology 6, 301–308.

# Executive summary and conclusions

The long-lived bivalve *Panopea abrupta* provides a long-term environmental record with an annual resolution. The linkage of temporal overlapping growth records of shells collected in one region allows the construction of master chronologies, which permit long-term reconstructions of the climate history. However, interpreting proxy archives requires precise knowledge of how such information is recorded. The sclerochronological and oxygen isotope analysis of different shell layers of *P. abrupta* revealed that it is important to know where to sample the shell for isotope analysis. Temperatures are reliably recorded by the oxygen isotope ratios of the outer shell layer, however, the inner shell layer is not formed in equilibrium with the ambient water. In contrast, growth lines are only clearly discernable in umbonal shell portions (inner shell layer), but less so in the outer shell layer.

The short-lived bivalve *Saxidomus gigantea* is an environmental archive with a high temporal resolution on a seasonal up to subdaily time scale. In addition, the butter clam serves as an ideal paleoweather archive. This species opens several windows into both the environmental and cultural past since its analysis permits us to gain detailed insights into past climate changes and also subsistence strategies of indigenous peoples. For *S. gigantea*, I tested if there is a difference in sampling the outer shell layer near the shell surface (periostracum) or near the inner shell layer. The obtained oxygen isotope records from these different portion of the outer shell layer were the same, i.e. the whole outer shell layer may be sampled. In a calibration study the seasonal growth of *S. gigantea* was studied. As well as for *P. abrupta*, life history traits, such as the timing of growth pattern formation, the duration of the growing season and growth rates, were analyzed in *S. gigantea* shells. Growth increment analyses are required to place the geochemical data in a temporal context and to resolve important questions on life history traits of the species of interest.

# Chapter 3: High-resolution sclerochronological analysis of the bivalve mollusk *Saxidomus gigantea* from Alaska and British Columbia: techniques for revealing environmental archives and archaeological seasonality

Nadine Hallmann[1], Meghan Burchell[2], Bernd R. Schöne[1], Gail V. Irvine[3], David Maxwell[4]

[1] Earth System Science Research Centre, Department of Applied and Analytical Paleontology (INCREMENTS), Institute of Geosciences, University of Mainz, Johann-Joachim-Becherweg 21, 55128 Mainz, Germany

[2] Department of Anthropology, McMaster University, 1280 Main Street West, Hamilton, Ontario, Canada

[3] U.S. Geological Survey, Alaska Science Center, 4210 University Dr., Anchorage, AK 99508, USA

[4] 5331 Meadedale Drive, Burnaby, British Columbia V5B 2E6, Canada

HALLMANN, N., BURCHELL, M., SCHÖNE, B.R., IRVINE, G.V., and MAXWELL, D., 2009. High-resolution sclerochronological analysis of the bivalve mollusk Saxidomus gigantea from Alaska and British Columbia: techniques for revealing environmental archives and archaeological seasonality. Journal of Archaeological Science 36, 2353–2364.

## *ABSTRACT*

**The butter clam, *Saxidomus gigantea*, is one of the most commonly recovered bivalves from archaeological shell middens on the Pacific Coast of North America. This study presents the results of the sclerochronology of modern specimens of *S. gigantea*, collected monthly from Pender Island (British Columbia), and additional modern specimens from the Dundas Islands (BC) and Mink and Little Takli Islands (Alaska). The methods presented can be used as a template to interpret local environmental conditions and increase the precision of seasonality estimates in shellfish using sclerochronology and oxygen isotope analysis. This method can also identify, with a high degree of accuracy, the date of shell collection to the nearest fortnightly cycle, the time of day the shell was collected and the approximate tidal elevation (i.e., approx. water depth and distance from the shoreline) from which the shell was collected.**

**Life-history traits of *S. gigantea* were analyzed to understand the timing of growth line formation, the duration of the growing season, the growth rate, and the reliability of annual increments. We also examine the influence of the tidal regime and freshwater mixing in estuarine locations and how these variables can affect both incremental structures and oxygen isotope values. The results of the sclerochronological analysis show that there is a latitudinal trend in shell growth that needs to be considered when using shells for seasonality studies.**

**Oxygen isotope analysis reveals clear annual cycles with the most positive values corresponding to the annual winter growth lines, and the most negative values corresponding to high temperatures during the summer. Intra-annual increment widths demonstrate clear seasonal oscillations with broadest increments in summer and very narrow increments or no growth during the winter months. This study provides new**

**insights into the biology, geochemistry and seasonal growth of *S. gigantea*, which are crucial for paleoclimate reconstructions and interpreting seasonality patterns of past human collection.**

**Keywords: Seasonality, Shellfish harvesting, Bivalve growth, Sclerochronology, Stable isotopes, Pacific Northwest, Paleoclimate**

## 3.1. INTRODUCTION

Knowledge of local climate and environmental conditions are essential for understanding seasonal procurement strategies of past populations. Incorporating seasonality into archaeological analyses provides insight as to how specific resources were used within a subsistence-settlement system, and information pertaining to seasonal patterns of site occupation. Sclerochronological analyses of shell growth patterns (JONES, 1983; KOIKE, 1973, 1975, 1980; MILNER, 2001; QUITMYER et al., 1997; RHOADS and PANNELLA, 1970; SCHÖNE et al., 2002a) and their geochemical properties can be used to identify shifts in local climates such as precipitation and temperature (ANDRUS and CROWE, 2000; DAVIS and MUEHLENBACHS, 2001; JONES and QUITMYER, 1996; SCHÖNE et al., 2002b; SCHÖNE et al., 2005a). This information can be used to identify the season of shellfish collection and to proxy the season of site occupation. Identifying seasonal patterns of procurement addresses not only patterns of site use, but it also contributes to understanding how shellfish were incorporated into prehistoric diets.

Prior to using archaeological mollusk shells for seasonality and paleoclimate reconstructions, a detailed analysis of the life history traits of living specimens from the species in question is required. This includes identifying the timing of shell growth and the duration of the growing period during different life stages. Modern specimens should be obtained from different environmental regimes since growth rate, duration of the growing season and timing of annual growth line formation strongly depend on local environmental conditions. Local climates likely have changed over time. Therefore, the growth pattern and geochemical record of archaeological shells may deviate from modern ones.

The butter clam, *Saxidomus gigantea* is one of the most commonly recovered bivalves in archaeological shell middens from the Pacific Coast of North America. This species exhibits a broad biogeographic distribution from northern California to the Aleutian Islands, and has played an important role in prehistoric, historic and modern clam fisheries (QUAYLE and BOURNE, 1972). The long-term occupation at some shell midden sites represents thousands of years of continual shellfish collection (CANNON et al., 2008; CANNON and BURCHELL, 2009), and the sclerochronological and geochemical analyses of shells from these sites can reveal information pertaining to both local climate and subsistence practices over the course of several millennia.

This paper presents the first detailed analysis of the life history traits and stable isotope record of *S. gigantea*. A major focus is on the seasonal timing and rate of shell growth

of butter clams collected alive along a latititudinal gradient. Using high-resolution sclerochronology and oxygen isotope profiles obtained through microdrilling technique, we tested the following questions: (1) Is it possible to constrain the time of shellfish collection to a precise calendar date, either full/new moon or half moon, or low or high tide? and (2) Is it possible to reconstruct the distance from the coast at which the shells were harvested? This paper also provides an example of the necessary experimentation required before attempting to use shellfish for seasonality studies.

## *3.2. SCLEROCHRONOLOGY AND MICROANALYTICAL TECHNIQUES*

Controlled by biological clocks and environmental conditions, shell growth slows at regular time intervals resulting in the formation of distinct growth lines. Consecutive growth lines delimit growth increments [periods of fast shell growth]. Therefore, discernible growth lines and increments can divide growth pattern into time slices of equal duration, i.e., tidal cycles, days, fortnights and years. The regularity in bivalve growth permits a precise calendar dating of each shell portion.

Changes in the ambient environment are recorded in the geochemistry of the shells and associated variable growth rates. Oxygen isotopes can be used to quantify changes in precipitation and temperatures (EPSTEIN et al., 1953; GROSSMAN and KU, 1986; ROMANEK et al., 1992), and season of mollusk collection (e.g., DEITH, 1983; KENNETT and VOORHIES, 1996; MANNINO et al., 2003). During the past decade significant advances in sclerochronology and microanalytical techniques have been made that may greatly benefit archaeological studies.

Analysis of annual shell growth patterns has been used for seasonality studies in archaeology (COUTTS, 1970; CUSTER and DOMS, 1990; DEITH, 1983; KOIKE, 1973, 1975, 1980; QUITMYER et al., 1997). Seasonality using growth increment data is typically calculated by comparing translucent growth increments (or growth lines) to opaque growth increments under transmitted light, by dividing the size of the pre-death increment by the last complete increment or by calculating growth ratios (MONKS and JOHNSTON, 1993). Using growth increments alone to establish seasonality in older shells can produce ambiguous results because the growth rate of the animal slows with ontogeny, thereby reducing precision when estimating the time between the last growth line and death. The analysis of growth structures

is meaningless without confirming the timing of growth lines and identifying the time represented by each growth increment. Previous attempts to determine seasonality using bivalves from the coast of British Columbia have produced ambiguous results since the analytical techniques applied did not have sufficient resolution (e.g., HAM and IRVING, 1975; KEEN, 1979; MAXWELL, 1989), or variation in growth rates have caused difficulty in interpreting significant quantities of the shellfish population (COUPLAND et al., 1993). The application of sclerochronology has been applied widely in geological studies to examine environmental patterns of seasonality, but its potential has not been fully realized by archaeologists working in coastal settings.

## *3.3. MATERIALS AND METHODS*

A total of 28 *S. gigantea* clams were collected alive from intertidal zones at different localities in Alaska, as well as northern and southern British Columbia for sclerochronological analysis (Tab. 1, Fig. 1). Sixteen specimens were gathered from Mink Island and Little Takli Island in southwestern Alaska (Tab. 1, Fig. 1B). In addition, clams were collected on a monthly basis (total n = 10) from Pender Island, in the Gulf of Georgia, near the archaeological site DeRt-1 (Maxwell, 1989), southern British Columbia (Tab. 1, Fig. 1C), between 21 February 1987 and 24 January 1988. Two additional clams collected in July 2006 came from the Dundas Islands Group near archaeological sites GcTr-5 and GcTr-8, northern British Columbia (Tab. 1, Fig. 1D).

Table 1. List of live collected *S. gigantea* specimens used in this study.

| Locality | Specimen | Date of collection | Ontogenetic age [years] | Length [mm] | Height [mm] | Width [mm] |
|---|---|---|---|---|---|---|
| Mink Island, AK | GI-MI0898-A2L | 9 Aug 1998 | 19 | 68 | 57 | 17 |
| | GI-MI0898-A5R | 9 Aug 1998 | 11 | 60 | 47 | 13 |
| | GI-MI0903-A2R | 11 Sep 2003 | 8 | 46 | 38 | 10 |
| | GI-MI0903-A3L | 11 Sep 2003 | 15 | 55 | 43 | 13 |
| | GI-MI0903-A5L | 11 Sep 2003 | 7 | 44 | 37 | 11 |
| | GI2-MI0707-A3L | 3 Jul 2007 | 4 | 32 | 28 | 8 |
| | GI4-MI0907-A2L | 11 Sep 2007 | 7 | 44 | 37 | 10 |
| | GI4-MI0907-A4L | 11 Sep 2007 | 5 | 46 | 36 | 12 |
| Little Takli Island, AK | GI1-LTI0707-A1L | 3 Jul 2007 | 5 | 43 | 32 | 10 |
| | GI1-LTI0707-A2L | 3 Jul 2007 | 5 | 39 | 30 | 8 |
| | GI1-LTI0707-A3L | 3 Jul 2007 | 3 | 28 | 24 | 8 |
| | GI1-LTI0707-A4L | 3 Jul 2007 | 6 | 51 | 42 | 12 |
| | GI1-LTI0707-A7L | 3 Jul 2007 | 4 | 36 | 29 | 10 |
| | GI1-LTI0907-A1L | 9 Sep 2007 | 7 | 46 | 37 | 11 |
| | GI1-LTI0907-A2L | 9 Sep 2007 | 4 | 41 | 30 | 9 |
| | GI1-LTI0907-A8L | 9 Sep 2007 | 5 | 43 | 37 | 10 |
| Dundas Island, northern BC | MB1-DI61-A1L | 10 Jul 2006 | 20 | | | |
| | MB2-DI271-A1L | 9 Jul 2006 | 15 | | | |
| Pender Island, southern BC | DeRt-1-0188-A15L | 24 Jan 1988 | 6 | 63 | 54 | 18 |
| | DeRt-1-0287-A30L | 21 Feb 1987 | 5 | 75 | 59 | 25 |
| | DeRt-1-0387-A1R | 20 Mar 1987 | 4 | 56 | 50 | 17 |
| | DeRt-1-0487-A18R | 2 Apr 1987 | 4 | 56 | 48 | 17 |
| | DeRt-1-0587-A26L | 15 May 1987 | 3 | | | |
| | DeRt-1-0687-A15R | 12 Jun 1987 | 2 | 45 | 38 | 13 |
| | DeRt-1-0787-A3L | 9 Jul 1987 | 2 | 48 | 39 | 13 |
| | DeRt-1-0987-A21R | 6 Sep 1987 | 5 | 62 | 51 | 18 |
| | DeRt-1-1087-A1R | 4 Oct 1987 | 5 | 48 | 41 | 14 |
| | DeRt-1-1187-A10R | 1 Nov 1987 | 5 | 56 | 48 | 19 |

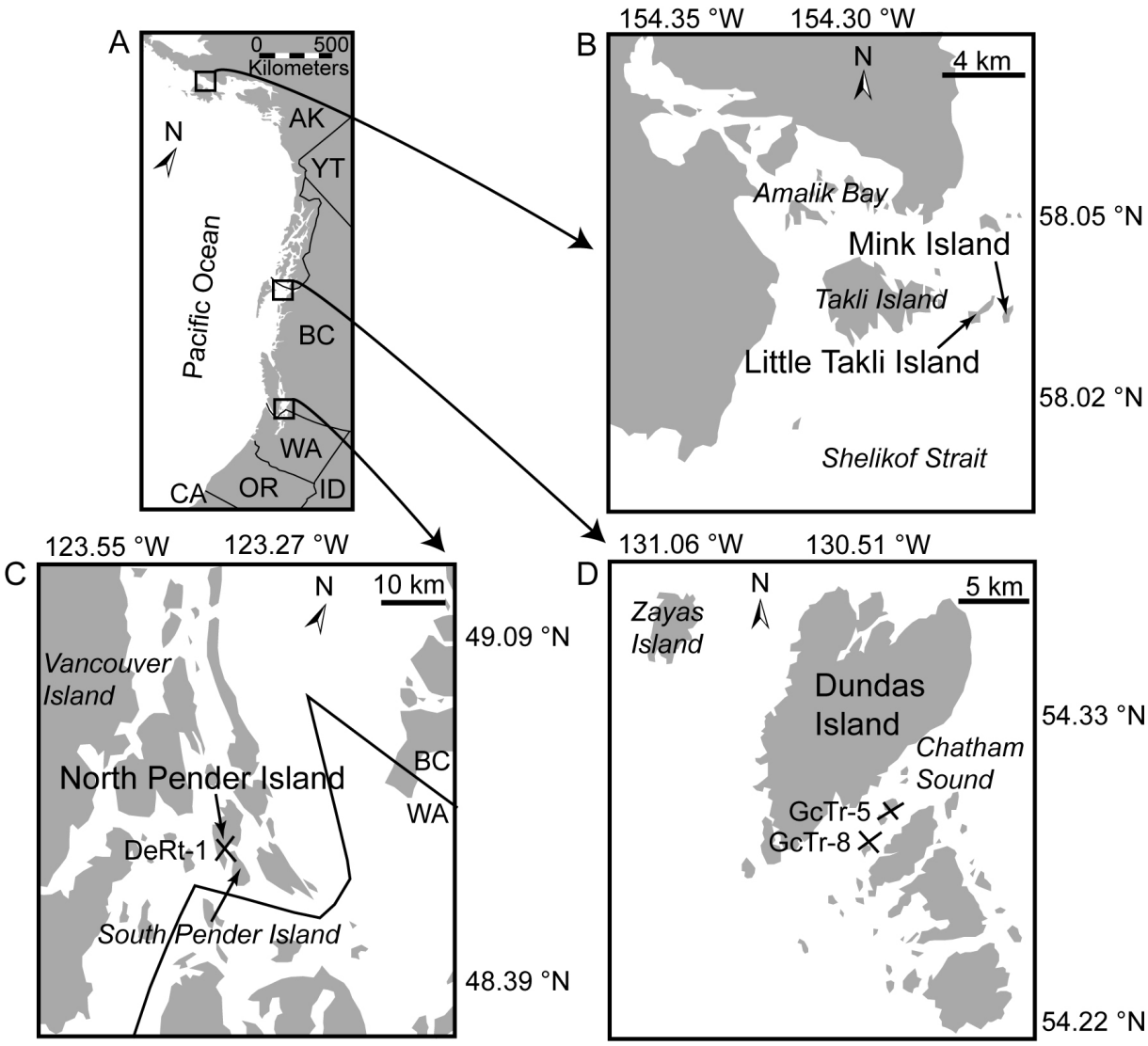


Figure 1. (A) Map of American Pacific Northwest Coast and the three study sites: (B) Mink Island and Little Takli Island in Shelikof Strait, Alaska; (C) Pender Island in the Strait of Georgia, southern British Columbia; and (D) Dundas Islands in northern British Columbia. AK = Alaska, YT = Yukon, BC = British Columbia, WA = Washington, OR = Oregon, ID = Idaho, CA = California.

### 3.3.1. The butter clam, *S. gigantea*

*S. gigantea* is a temperate marine species that burrows to a depth of approximately 30 cm below the surface (NICKERSON, 1977; PAUL et al., 1976). In specimens from the Pacific Coast of North America, major dark lines form during winter. According to winter line counts, *S. gigantea* may attain an age of twenty years or more (QUAYLE and BOURNE, 1972). However, it remains unclear how much time is represented by these winter growth checks and whether the time interval of no or slow growth (growth line) and rapid growth (growth increment) varies among different geographic settings. Variability in growth rates and the formation of major growth bands present significant problems when attempting to identify season of death when using low-resolution methods that rely solely on the identification of a winter line.

### 3.3.2. Preparation of shell cross-sections

One valve of each specimen was mounted on plexiglass cubes with plastic welder (Multipower, GlueTec). After coating with metal epoxy resin (WIKO) to avoid shell fracture during sectioning, two three-millimeter thick slabs were cut from the shells perpendicular to the growth lines along the axis of maximum growth from the umbo to the ventral margin using a low-speed precision saw (Buehler, IsoMet 1000) and a 0.4 mm thick diamond-coated saw blade (Fig. 2A). Both slabs of each shell were mounted with metal epoxy resin on glass slides, ground on glass plates (800 and 1200 grit powder, respectively) and polished with 1 mm $Al_2O_3$. Shell cross-sections (Fig. 2B) were cleaned by ultrasonic rinsing after each grinding and polishing step. All samples were then cleaned with water-free ethanol and air-dried.

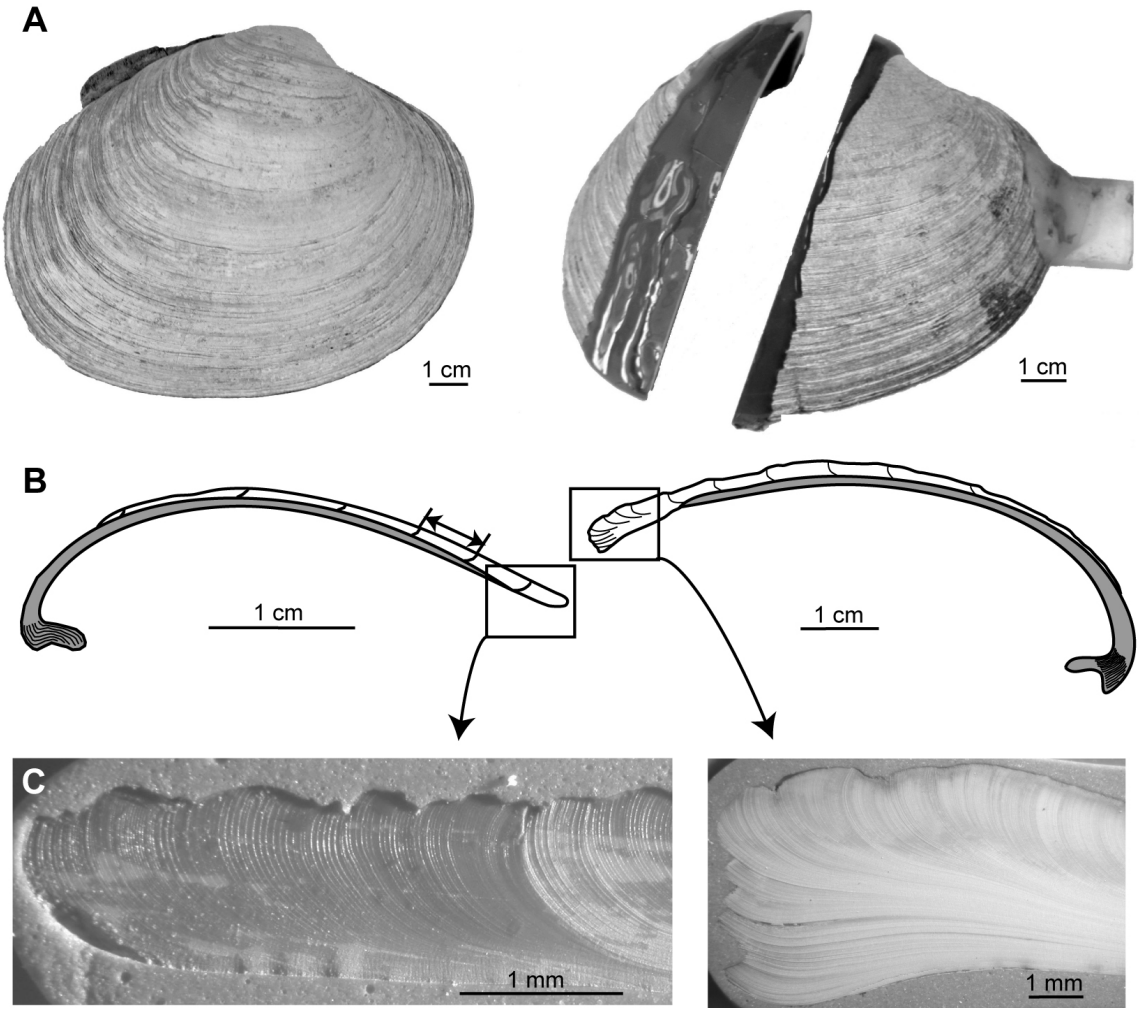


Figure 2. Preparation of *S. gigantea* shells. (A) The valves were cut perpendicular to the growth lines along the axis of maximum growth after coating with metal epoxy resin. (B) The polished cross sections show a mature (GI4-MI0907-A2L; ontogenetic age of seven years, magnification 10x) and a senile shell (MB1-DI61-A1L; ontogenetic age of approximately 20 years, magnification 6.5x). The arrow marks the measured distance between two consecutive annual winter growth lines (= annual growth increment). Inner shell layer = grey, outer shell layer = white. (C) Growth lines at the ventral margin of the mature and the senile shell (inward growth).

### 3.3.3. Sclerochronological analyses

One polished section of each specimen was immersed in Mutvei's solution for 20 min under constant stirring at 37–40°C (SCHÖNE et al., 2005b). Mutvei's solution simultaneously etches the shell, preserves organic matrices and stains the intercrystalline organic envelopes (i.e., chitin, mucopolysaccharides, glucosamids) blue (SCHÖNE et al., 2005b). The growth lines are etch-resistant and richer in organics and therefore stain dark blue. In contrast, the growth increments between two consecutive growth lines are more strongly etched and appear light

blue. Immersion in Mutvei's solution therefore facilitates the analysis of shell growth patterns by reflected-light microscopy.

To analyze shell growth patterns, digital images of shell slabs were taken with a Nikon Coolpix 995 camera attached to a binocular microscope (Wild Heerbrugg M3Z). Widths of the growth increments were measured in the direction of growth to the nearest 2 mm using the image analysis software Panopea (© 2004 Peinl and Schöne) to determine the duration of the growing season. Fast Fourier Transformation (Multitaper Spectral Analysis) was applied to identify possible periodic variations of the growth increment widths. The F-value indicates the significance of a detected signal (high amplitude or variance). Only revealed frequencies with a high amplitude or variance and a high F-value are considered as significant (= signals). Analysis of variance (ANOVA) was used to test for significant growth differences (shell height, length and weight) of specimens from British Columbia and Alaska.

### 3.3.4. Oxygen isotopes

For oxygen isotope analysis of shell carbonate ($\delta^{18}O_{shell}$), 479 powder samples were taken from the outer (Fig. 2B) shell layer of eleven unstained polished cross-sections. Shell powder samples were obtained by drilling holes with a cylindrical drill bit (300 mm diameter, Komet/Gebr. Brasseler GmbH & Co. KG, model no. H52 104 003). The drilled holes had an approximate diameter of 350 mm, and the distance between the sample spots varied between 200 and 500 mm. Each powder sample weighed between 48 and 125 mg. Analysis was conducted using a Thermo Finnigan MAT 253 isotope ratio mass spectrometer coupled with a Gas Bench II. Results are reported in the usual δ-notation. Samples were calibrated against a NBS-19 calibrated Carrara marble standard ($\delta^{18}O = -1.74‰$) with a 1σ precision error of 0.06‰. The $\delta^{18}O_{shell}$ values were calculated against the Vienna Pee Dee Belemnite (VPDB) standard and are given as parts per mil. The $\delta^{18}O_{shell}$ values reflect changes in sea surface temperatures (SST) and the oxygen isotope ratio of seawater ($\delta^{18}O_{water}$). They also reflect changes in salinity. If the $\delta^{18}O_{water}$ value is known (typical modern seawater $\delta^{18}O_{water} = 0‰$), the temperature of the water in which the shell lived can be reconstructed (EPSTEIN et al., 1953). For the reconstruction of temperatures from $\delta^{18}O_{shell}$ values ($T_{\delta 18O}$) of *S. gigantea* (aragonite; GILLIKIN et al., 2005a), we used the paleothermometry equation by BÖHM et al. (2000):

$$T_{\delta^{18}O}(°C) = (20 \pm 0.2) - (4.42 \pm 0.1) \cdot (\delta^{18}O_{shell} - \delta^{18}O_{water})$$

A variation in the $\delta^{18}O_{shell}$ value of one per mil implies a change of ambient water temperature by 4.42°C. We used the equation by BÖHM et al. (2000) instead of that from GROSSMAN and KU (1986) because it reduces the error of the calculated temperature. Furthermore the precision error of the mass spectrometer had to be considered which resulted in an average $T_{\delta 18O}$ error of ±0.5°C. In shallow water environments, the $\delta^{18}O_{water}$ value can underlie significant variations that make precise temperature reconstructions from shell oxygen isotopes difficult unless the $\delta^{18}O_{water}$ value is closely monitored. The $\delta^{18}O_{water}$ value becomes more positive with evaporation and more negative with freshwater influx or strong precipitation (CRAIG and GORDON, 1965). Therefore, we measured the $\delta^{18}O_{water}$ value at the localities where the shells lived; these ranged between −2.38‰ (3 July 2007) and −3.05‰ (10 September 2007) for Little Takli Island, Alaska (winter $\delta^{18}O_{water}$ values are not available).

### 3.3.5. Environmental recordings

To reconstruct the timing of shell growth and determine the duration of the growing period, shell data (growth patterns and $\delta^{18}O_{shell}$) were cross-calibrated with environmental variables, specifically instrumental sea surface temperatures (SST) and the tides (Figs 3 and 4). Weekly SST data (NOAA_OI_SST_V2) were obtained from NOAA/OAR/ESRL PSD, Boulder, Colorado, USA (http://www.cdc.noaa.gov) (REYNOLDS et al., 2002). Minimum temperatures in southern British Columbia were recorded from December to February and in Alaska from December to March. Highest temperatures were recorded in July and August (AK and BC). The minimum and maximum recorded temperatures for Mink Island and Little Takli Island, Alaska, were 3.2°C (March) and 14°C (July), respectively (1990–2007), while temperatures near Pender Island, southern BC, ranged between 5.9°C (January) and 16.5°C (July). Tidal ranges at stations close to the position where the shells grew were computed with the software WXTide32 ver. 4.7.

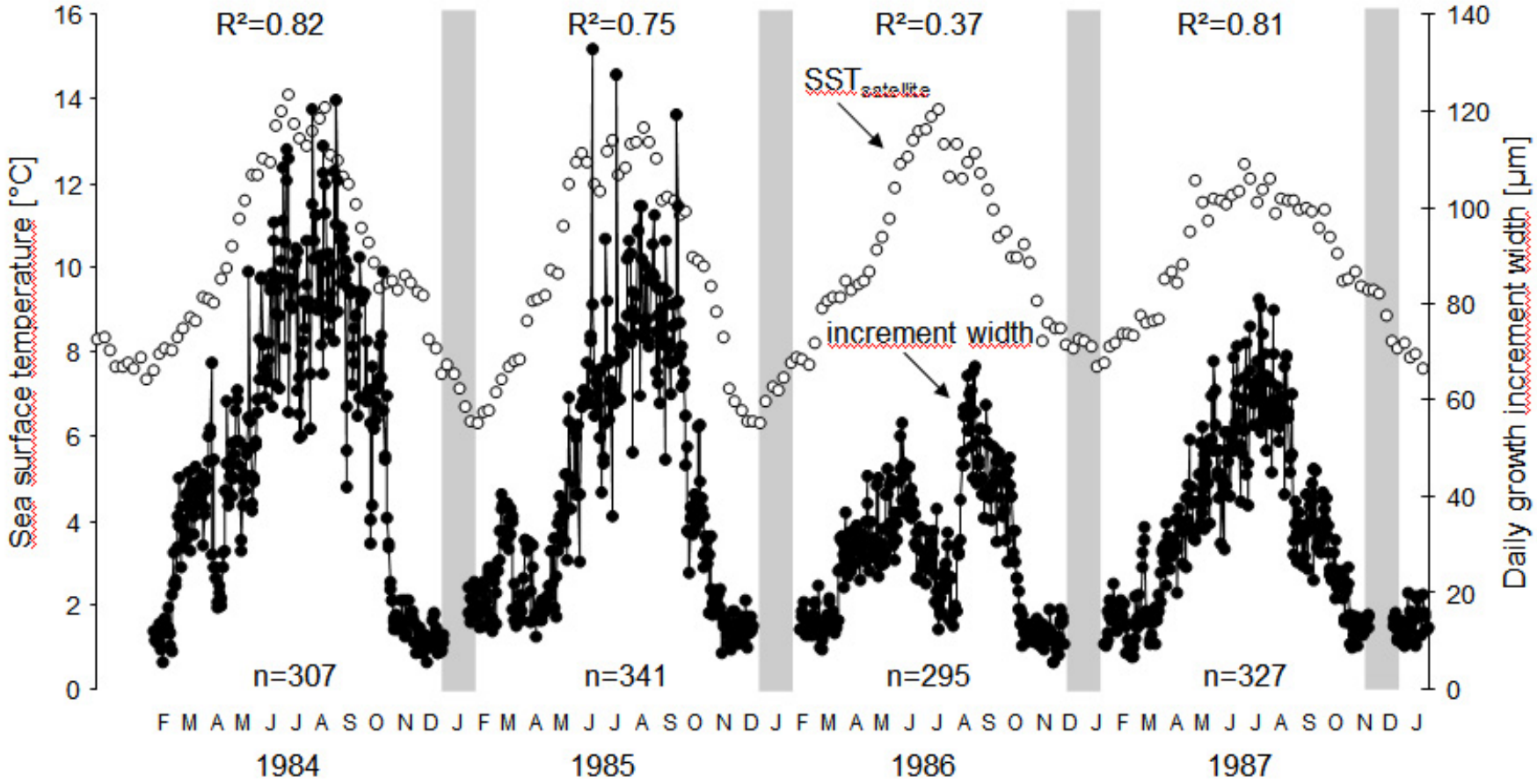


Figure 3. Seasonal temperature and growth pattern of the *S. gigantea* specimen DeRt-1-0188-A15L from Pender Island from 1984 to January 1988. Open circles show weekly sea surface temperature (SST) data from www.cdc.noaa.gov and filled circles present daily growth increment width. $R^2$ represents the variation of the daily growth increments width explained by the sea surface temperature data and n is the number of increments per year. Grey bars represent winter growth lines.

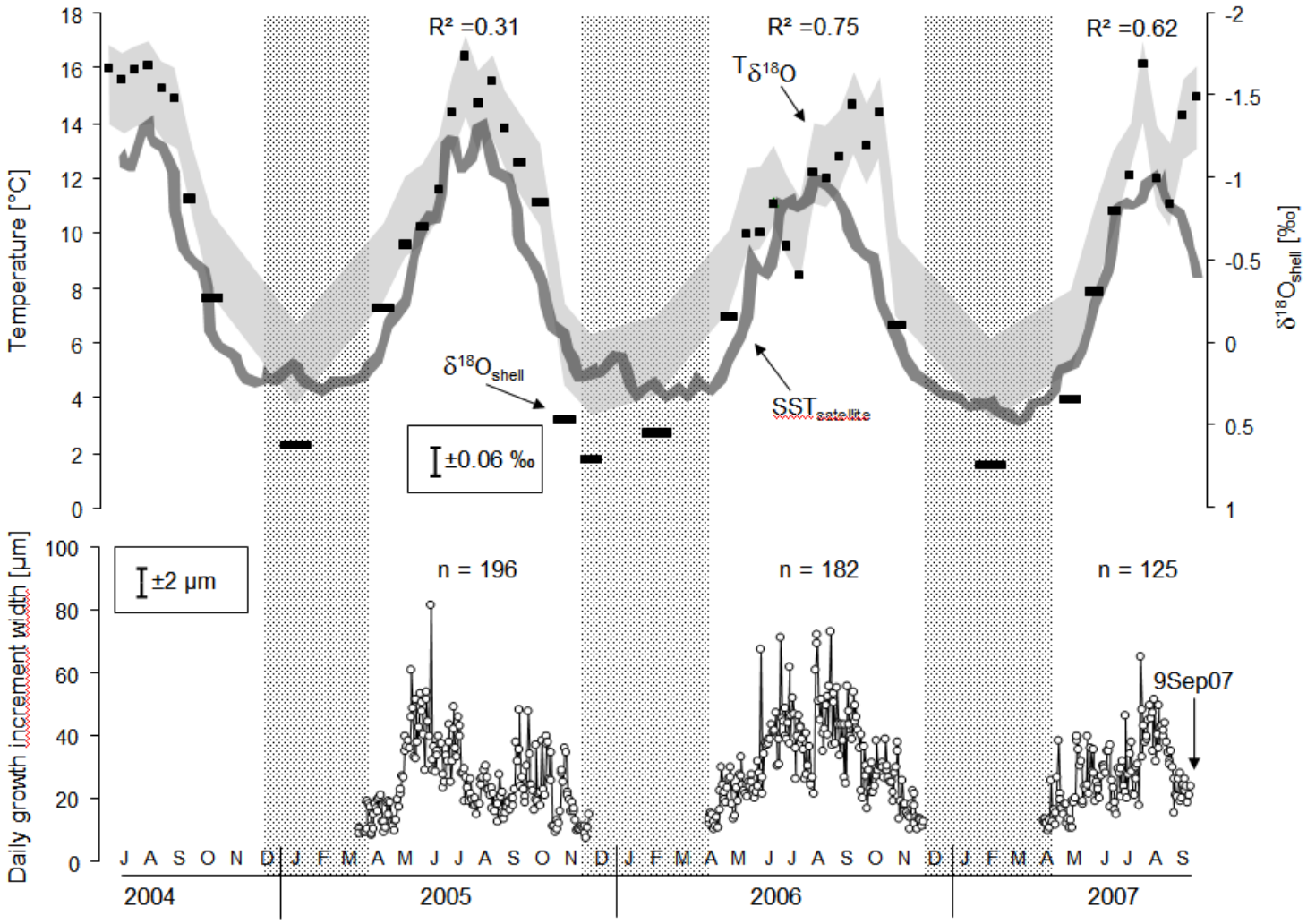


Figure 4. Oxygen isotope and sclerochronological data are shown for the *S. gigantea* specimen GI1-LTI0907-A2L from 2004 to 2007 which was collected alive on 9 September 2007 from Little Takli Island, Alaska. Upper panel: Shell oxygen isotope record ($\delta^{18}O_{shell}$, black bars, inverted scale) with an error bar of 0.06‰ which refers to the precision error of the mass spectrometer. Reconstructed temperatures ($T_{\delta 18O}$, light grey curve) include the error of the Böhm et al. (2000) paleotemperature equation and the variability in the oxygen isotopy of the water. Weekly sea surface temperature data ($SST_{satellite}$, dark grey curve) were used from www.cdc.noaa.gov. $R^2$ represents the variation of the daily growth increment width explained by the sea surface temperature data. Lower panel: Daily growth increment width time series with a measurement error of approximately 2 mm. n = number of increments per year. The annual winter growth lines are confirmed by the oxygen isotope data. The most positive oxygen isotope values were measured at the growth lines, i.e., shell portions that formed during winter. The most negative oxygen isotope values were measured between two consecutive growth lines which correspond to highest temperatures during summer. Shaded bars represent annual winter growth lines.

## *3.4. RESULTS*

### 3.4.1. Annual growth patterns

Analyzed *S. gigantea* specimens showed distinct dark growth lines on external shell surfaces and in cross-sections (Fig. 2). After immersion in Mutvei's solution, these major growth lines were stained dark blue and stood out significantly from the remaining growth patterns. In specimens collected between December and March, a distinct major growth line was visible near the ventral margin, i.e., the last formed shell portion (Fig. 5A). We refer to these lines as winter lines and to the portions between two consecutive winter lines as annual growth increments. Shells that were collected during the summer months showed approximately 60–75% of the newly formed annual growth increment.

Typically, the annual increment width decreased from the umbo to the commissure, therefore the distance between the annual growth lines became smaller toward the ventral margin. Annual increments were broadest during the first and second year of growth and gradually became narrower toward the ventral margin. When plotted against ontogenetic age, cumulative annual increment width is best described by an exponential function (Fig. 6A). During approximately the first ten to twelve years of life, *S. gigantea* shells grew mainly in shell size, thereafter, predominantly in ventral margin thickness (Figs 2B and 2C).

Clams from Alaska reached nearly the same age as specimens from British Columbia, approximately 20 years (Tab. 1). Despite that, specimens in British Columbia grew significantly larger and heavier shells (Tab. 1). *S. gigantea* shells collected in British Columbia (age 2–12) differed significantly from Alaskan specimens (age 2–19) with respect to their shell height (ANOVA, $F = 34.082$, $p < 0.0001$), length (ANOVA, $F = 30.206$, $p < 0.0001$) and weight (ANOVA $F = 16.009$, $p < 0.001$). Average annual increment widths of shells from British Columbia clams exceeded those of shells from Alaska specimens by more than 55% during years two to four (Fig. 6A, Tab. 2).

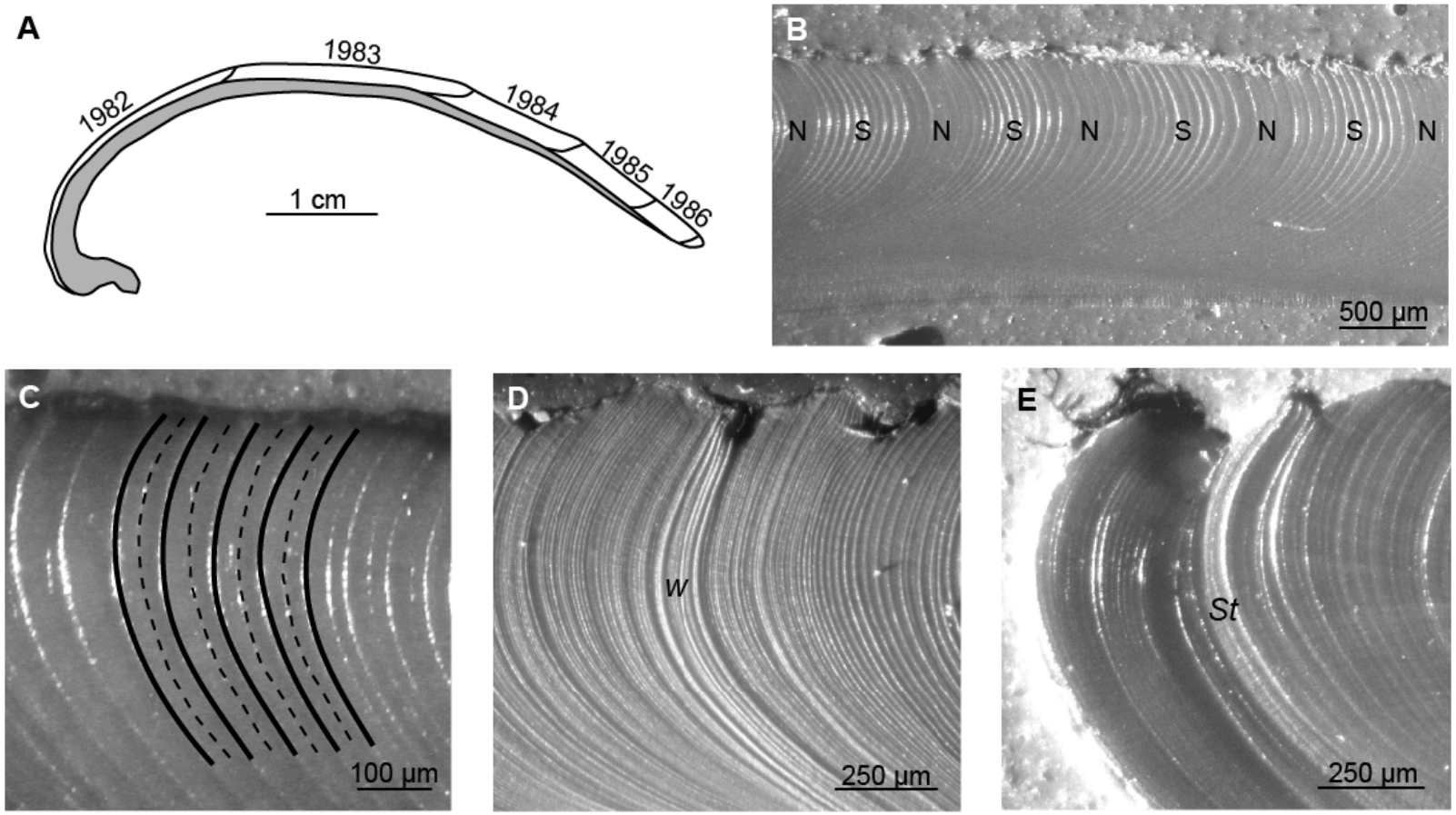


Figure 5. (A) Cross-section of the *S. gigantea* specimen DeRt-1-0287-A30L collected in February from Pender Island, B.C., which reveals a winter growth line near the ventral margin. (B) Tidal growth pattern of DeRt-1-0787-A3L (magnification 10x) with distinct growth lines and narrow increments during spring tide (S) and shell portions with less defined growth lines and broad increments during neap tide (N). (C) Formation of two circatidal increments which are separated by a faint line and correspond to one circalunidian increment (GI1-LTI0707-A2L, magnification 40x). (D) A winter growth line (*w*) is formed by a slow decrease and slow recovery of shell growth (DeRt-1-0188-A15L, magnification 10x). (E) A probable storm event (St) covers just several days and is characterized by a sudden break and fast recovery of shell growth (GI1-LTI0707-A7L, magnification 40x).

Table 2. Number of daily increments per year and annual growth rate for portions of live collected *S. gigantea* specimens from Alaska (AK) and British Columbia (BC) having an ontogenetic age ranging between two and six years. The ontogenetic age of the clam for the year being assessed is presented in the rightmost column. Note that for some individual clams sequential years are evaluated (e.g., ages 3, 4, 5, 6 for DeRt-1-0188-A15L). n.c. = not computed.

| Locality | Specimen | No. increments/year | Growth rate [mm/year] | Ontogenetic age of year assessed |
|---|---|---|---|---|
| AK | GI2-MI0707-A3L | 170 | 5.7 | 3 |
| | GI4-MI0907-A2L | 152 | 4.5 | 6 |
| | GI1-LTI0707-A2L | 168 | 7.3 | 4 |
| | GI1-LTI0907-A2L | 196 | n.c. | 2 |
| | | 182 | 9.2 | 3 |
| | GI1-LTI0907-A8L | 149 | 6.5 | 4 |
| BC | MB2-DI271-A1L | 350 | 10.4 | 3 |
| | DeRt-1-0188-A15L | 332 | 16.3 | 3 |
| | | 316 | 14.4 | 4 |
| | | 295 | 6.5 | 5 |
| | | 327 | 8.1 | 6 |
| | DeRt-1-0387-A1R | 333 | n.c. | 4 |
| | DeRt-1-0487-A18R | 353 | n.c. | 3 |
| | DeRt-1-0987-A21R | 290 | 14.0 | 3 |
| | | 303 | 15.0 | 4 |
| | DeRt-1-1087-A1R | 309 | 9.9 | 4 |

### 3.4.2. Intra-annual growth patterns

When viewed under higher magnification (40x) micrometer-scale patterns and microgrowth patterns became visible within annual increments (Figs 5B to 5E). Dark blue stained microgrowth lines alternated with lighter blue stained microgrowth increments. Periodically, microgrowth lines appeared considerably less distinct (Fig. 5B). The number of microgrowth

increments between two less distinctly structured shell portions equaled on average approximately 13–15. Furthermore, in such shell portions a much fainter line was developed between adjacent microgrowth lines (Fig. 5C). Specimens collected during spring tides showed distinct microgrowth lines near the ventral margin. The weakly structured shell portions were only found in specimens gathered during the neap tide cycle.

The width of microgrowth increments varied considerably within annual growth increments and over a lifetime. As demonstrated by spectral analyses of the intra-annual growth curves, the widths of the microincrements fluctuated with a periodicity of about 12–16 as well (Tab. 3, Fig. 7). Only signals with periods that had a high amplitude, variance and a high F-value were considered as significant (Fig. 7). Thereby, the broadest microgrowth increments coincided with the weakly structured growth portions and occurred in shells obtained during neap tides. Contrary, the narrowest microgrowth increments within each bundle of 13–15 microgrowth increments fell together with the spring tide cycles. Within annual increments, the narrowest microgrowth increments were found near annual growth lines (Fig. 5D) and the broadest microgrowth increments approximately half-way between two annual growth lines, i.e., shell portions that were formed during summer (Figs 6 and 8). Intra-annual growth curves often appeared bell-shaped and closely resembled the seasonal temperature cycle (Figs 3, 4 and 6B). A significant and strong positive correlation exists between microgrowth increment widths and water temperature ($R = 94.6$, Fig. 6B). In some specimens, however, a strong and sudden reduction in shell growth occurred during different times of the year. Shell growth commenced slowly after such growth cessations. Furthermore in some shells we observed a sudden and short growth stop with a fast recovery of growth (Fig. 5E). In such cases we found the same number of daily growth increments between the ventral margin (same collection date of GI1-LTI0707-A4L and -A7L) and the observed sudden growth break. Macroscopically, however, the respective shell portions showed dark growth lines that were nearly indistinguishable from winter growth breaks.

Table 3. Results of frequency analysis (Multitaper method) of *S. gigantea* specimens from Little Takli Island and Mink Island (Alaska), from Dundas Island (northern British Columbia) and Pender Island (southern British Columbia). The analyzed time period and the number of measured increments are shown. The signals range from 6.6 to 16.0 daily increments revealing a fortnightly growth pattern developed to a greater or lesser extent depending on the intertidal elevation where the clams lived.

| Locality | Specimen | Time period | Number of increments | Signals |
|---|---|---|---|---|
| Mink Island, AK | GI-MI0903-A2R | 1997-September 2003 | 1082 | 9.8 |
| | GI4-MI0907-A2L | 2002-September 2007 | 884 | 14.0 |
| | GI4-MI0907-A4L | 2003-September 2007 | 814 | 14.0 |
| Little Takli Island, AK | GI1-LTI0707-A3L | 2005-2006 | 586 | 12.2 |
| | GI1-LTI0707-A4L | 2002-2006 | 1128 | 16.0 15.0 |
| | GI1-LTI0907-A1L | 2002-September 2007 | 878 | 13.9 |
| | GI1-LTI0907-A2L | 2005-September 2007 | 671 | 12.9 |
| | GI1-LTI0907-A8L | 2005-September 2007 | 533 | 8.3 6.6 14.0 |
| Dundas Island, northern BC | MB1-DI61-A1L | undated | 390 | 15.0 |
| | MB2-DI271-A1L | 1992-1994 | 699 | 11.8 15.2 |
| Pender Island, southern BC | DeRt-1-0188-A15L | 1984-January 1988 | 1302 | 14.2 |
| | DeRt-1-0787-A3L | 1986-July 1987 | 391 | 13.5 |
| | DeRt-1-1087-A1R | 1986-October 1987 | 464 | 13.6 |
| | DeRt-1-1187-A10R | 1986-November 1987 | 660 | 14.7 |

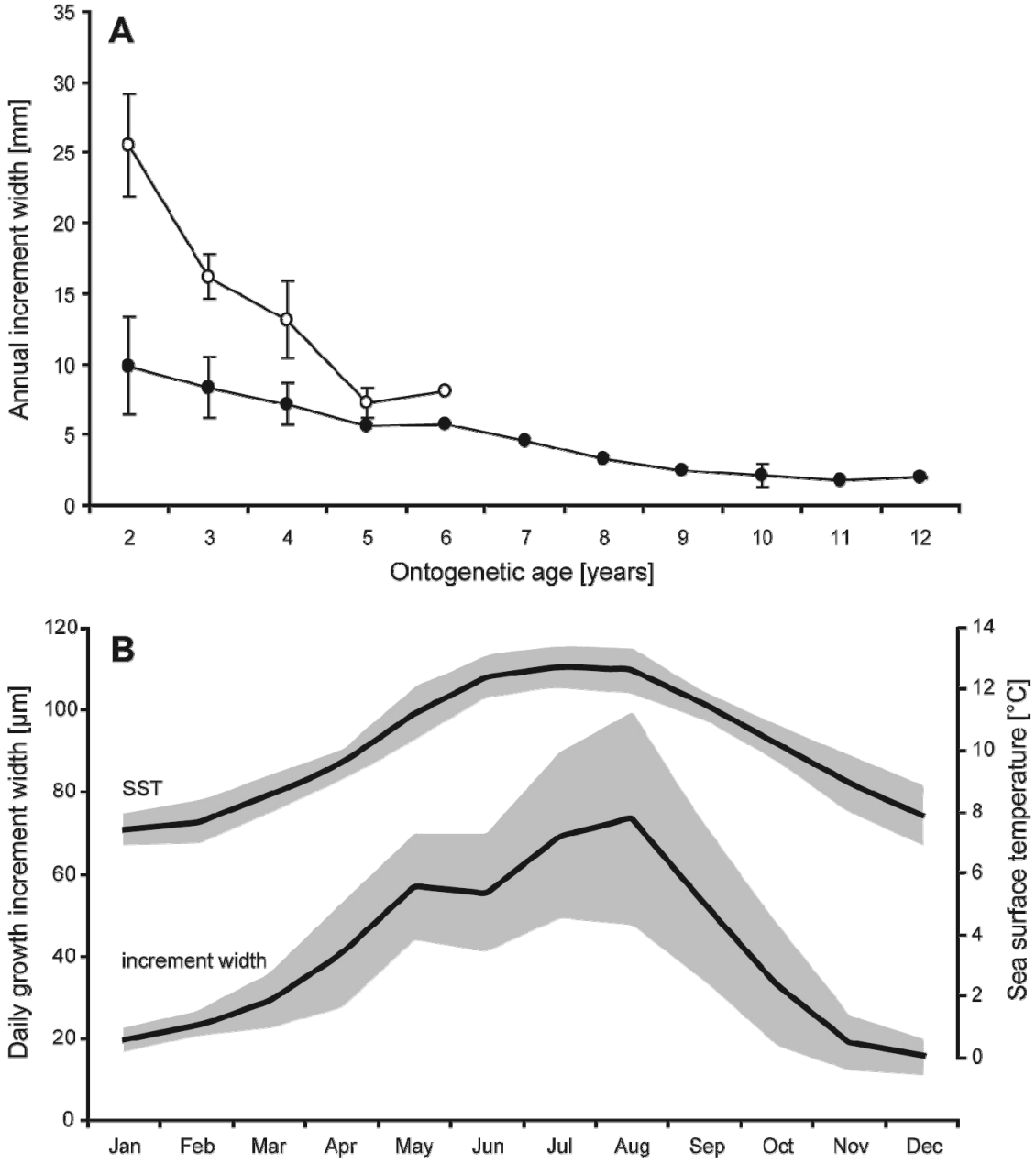


Figure 6. (A) Annual growth rate during ontogeny of seven *S. gigantea* specimens from Pender Island, southern BC (open circles) and eight specimens from Little Takli Island and Mink Island, AK (filled circles). (B) Measurement of the width of daily growth increments of eight shells from Pender Island (age two to six, 1984–1987) yields a seasonal growth curve that illustrates the growing season (lower grey curve = 4413 daily growth increments). Upper grey curve presents weekly sea surface temperature (SST) data from www.cdc.noaa.gov (1984–1987). Shell growth increases in spring and reaches a maximum growth rate in summer. In autumn growth slows down and reaches its minimum or may cease during winter months. Temperature explains 94.6% of daily growth increment variation. Black lines represent the average values and the grey areas represent one standard deviation.

The broadest microgrowth increments of 106 ± 27 µm (southern BC; Tab. 4) and 95 ± 12 µm (AK) were observed in the younger portions of shells. Toward the ventral margin, the broadest microgrowth increments measured less than ca. 82 ± 11 µm (southern BC). Minimum daily increment width is 9 ± 3 µm in southern British Columbia and 8 ± 2 µm in Alaska. Shells from Alaska formed significantly fewer microincrements each year than specimens from British Columbia. On average, we counted 321 ± 22 and 170 ± 18 microincrements in shells from British Columbia and Alaska, respectively (Tab. 2, Figs 3 and 4). We determined the number of daily growth increments per year of shells with an ontogenetic age between three and six years. An ontogenetic change, such as a decreasing number of increments and a shortening of the growing season (e.g., a later onset and an earlier stop of the growing season) was not observed within that age range. However, the number of microincrements changes and reveals inter-annual and inter-individual variability (Tab. 2, Figs 3 and 4). Shells from Pender Island, southern BC, may grow throughout the whole year. Nevertheless some specimens may cease growth in some years for up to two months from mid November to the beginning of February. Maximum growth proceeds during highest summer temperatures from mid June to the beginning of September (Fig. 6). Due to the lower temperatures Alaskan shells stop their growth six or seven months per year from approximately October/November to April/May.

Table 4. Maximum and minimum daily growth increment width of monthly collected *S. gigantea* specimens from Pender Island, British Columbia. The ontogenetic age ranges from two to six years.

| Specimen | Daily increment width [µm] | | Number of increments |
|---|---|---|---|
| | Maximum | Minimum | |
| DeRt-1-0188-A15L | 122 | 6 | 1299 |
| DeRt-1-0387-A1R | 99 | 6 | 410 |
| DeRt-1-0487-A18R | 80 | 6 | 492 |
| DeRt-1-0687-A15R | 147 | 12 | 350 |
| DeRt-1-0787-A3L | 134 | 13 | 384 |
| DeRt-1-0987-A21R | 107 | 7 | 892 |
| DeRt-1-1087-A1R | 83 | 6 | 617 |
| DeRt-1-1187-A10R | 73 | 12 | 652 |

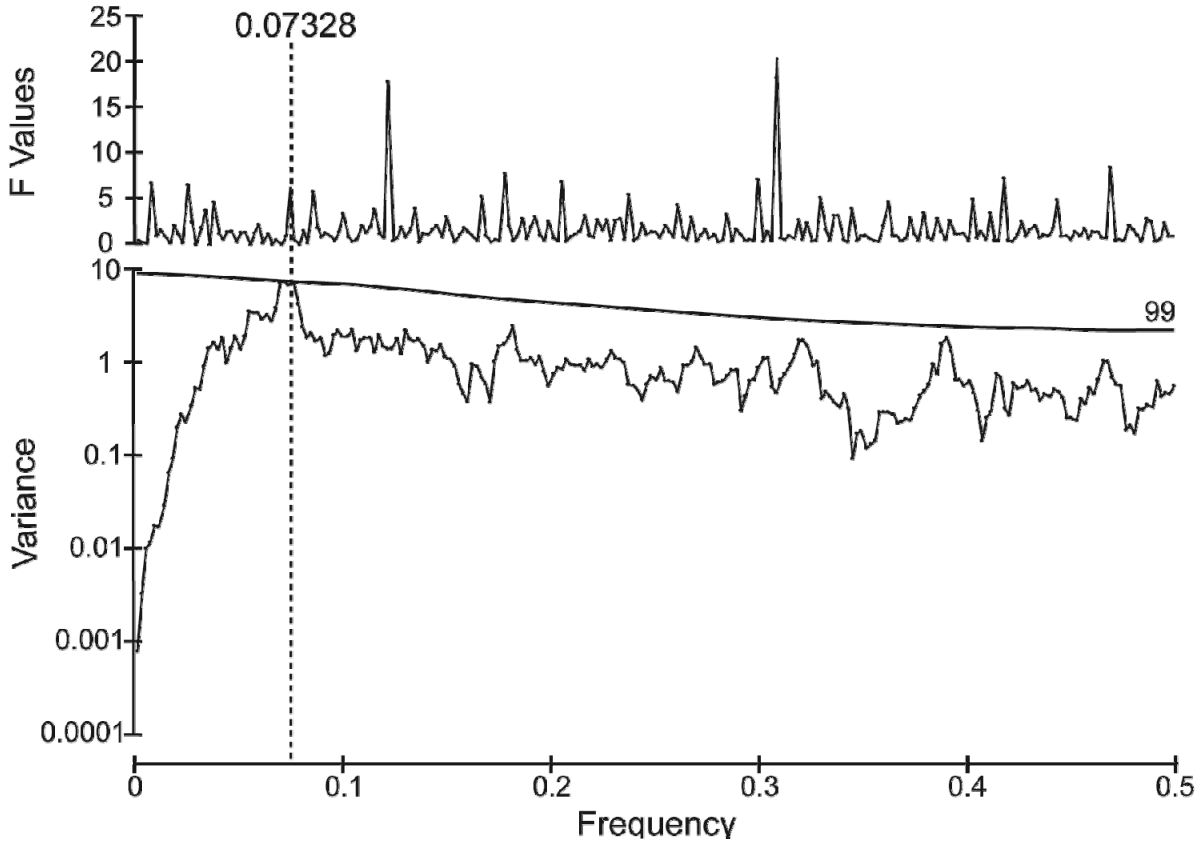


Figure 7. Multitaper spectrum of time series from standardized growth increment width of the *S. gigantea* specimen DeRt-1-1087-A1R from Pender Island along with 99% significance level and F-test values for this multitaper spectrum above. The frequency of 0.07328 refers to a signal of 13.6 increments indicating a fortnightly shell growth pattern (Variance = 6.33, F-value = 6.23, amplitude = 0.23, degrees of freedom = 8.01). We consider only signals with periods that have a high amplitude, variance and a high F-test as significant.

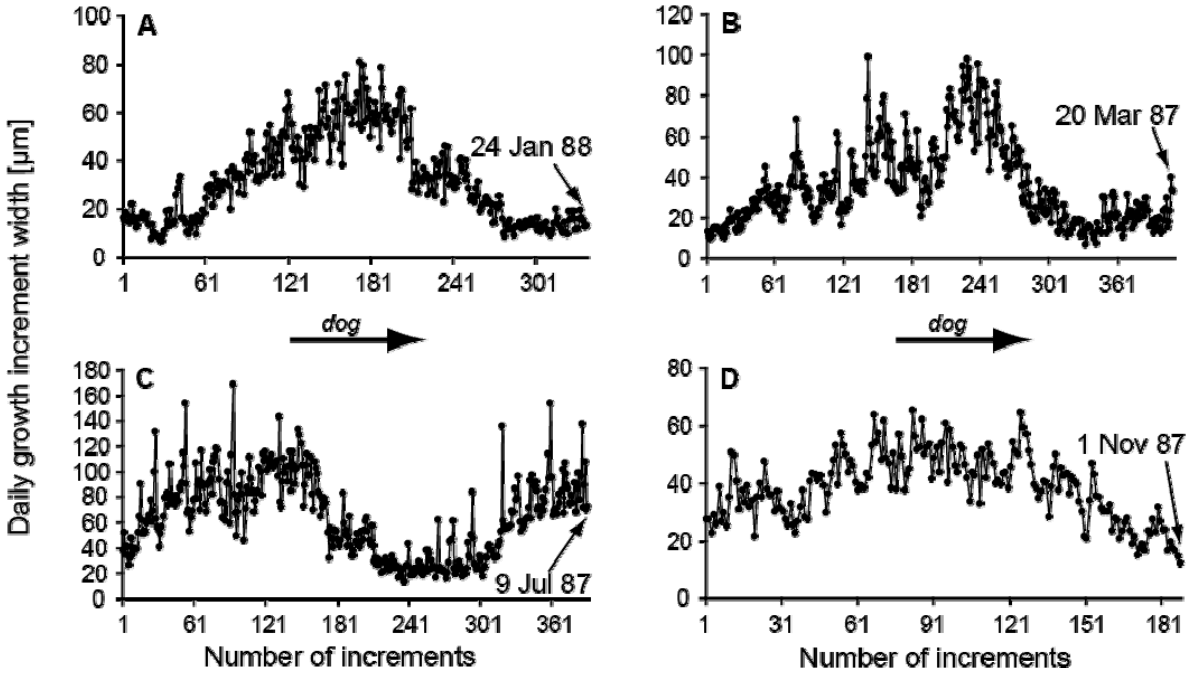


Figure 8. Daily growth increment width for four *S. gigantea* specimens from Pender Island. (A) DeRt-1-0188-A15L, (B) DeRt-1-0387-A1R, (C) DeRt-1-0787-A3L and (D) DeRt-1187-A10R. The width of the last formed increment at the ventral margin reveals information about the season of shell collection. The arrow marks the direction of growth (*dog*).

### 3.4.3. Shell oxygen isotopes

Shell oxygen profiles reflected distinct annual cycles (Fig. 4) with most positive values of −0.48 ± 0.37‰ (southern BC) and 0.80 ± 0.12‰ (AK) near the winter lines. Most negative $\delta^{18}O_{shell}$ values were observed approximately half-way between consecutive winter lines when seasonal shell growth attained a maximum (southern BC: −3.60 ± 0.37‰; AK: −1.97 ± 0.45‰). Absence of measured $\delta^{18}O_{water}$ and salinity prevents reliable reconstruction of temperature at this time. It can be stated that the range of the reconstructed temperatures exceeded the range of the instrumental temperatures in British Columbia and Alaska by 7.6 and 5.7°C, respectively. Reconstructed summer temperatures from British Columbia overestimate instrumental temperatures by 5.9–7.5°C.

## *3.5. DISCUSSION*

Periodic growth patterns provide the basis of sclerochronology and have been described in hard parts of many different organisms (MIYAJI et al., 2007; SCHÖNE et al., 2003). If the timing of growth increments and growth lines is known, precise calendar dates can be assigned to each portion of the shells.

### 3.5.1. Annual growth checks and disturbance breaks

Previous studies assumed that major dark lines on external shell surfaces of *S. gigantea* form during winter (NICKERSON, 1977; PAUL et al., 1976; QUAYLE and BOURNE, 1972). The first compelling evidence for this assertion, however, was provided by GILLIKIN et al. (2005a) for *S. gigantea* from Puget Sound, Washington, USA. These authors showed that most positive oxygen isotope values (i.e., the lowest $T_{\delta 18O}$) of each annual cycle were associated with major dark lines. Results of our study extend the findings of GILLIKIN et al. (2005a) and demonstrate that clams from British Columbia and Alaska also form winter lines. The formation of winter lines is initiated at temperatures below ca. 5–6°C, i.e., the lowest recorded intra-annual oxygen isotope-derived temperature in all studied shells. The minimum temperature near Pender Island, BC is 5.9°C (1990–2007) leading to a growth break of up to two months. Winter temperatures near Little Takli Island and Mink Island, AK can drop to 3.2°C initiating shell growth breaks of six to seven months. GILLIKIN et al. (2005b) reported that *S. gigantea* does not seem to have a threshold where they stop growing. However, the minimum temperature recorded at their shell collection site was 7°C. We reconstructed temperatures from $\delta^{18}O_{shell}$ using $\delta^{18}O_{water}$ summer values because no $\delta^{18}O_{water}$ data are available from October to June in Alaska. It has to be considered that salinity is higher during winter months than during summer, because the freshwater is locked up as snow and ice due to the low winter temperatures. In winter the evaporation and wind stress is high and water layers are deep mixed (SARKAR et al., 2005). Therefore reconstructed winter temperatures have to be higher than our calculated minimum temperature of 3.2°C shown in Fig. 4. QUAYLE and BOURNE (1972) reported that *S. gigantea* tolerates temperatures just above the freezing point up to 25°C. Reconstructed summer temperatures from British Columbia overestimate instrumental temperatures by 5.9–7.5°C (1.3–1.7‰). This overestimation may be due to freshwater influx (melt water, rivers) because precipitation is lowest in summer.

However, not all major dark lines of *S. gigantea* corresponded to positive $\delta^{18}O_{shell}$ values. GILLIKIN et al. (2005a) revealed that most positive $\delta^{18}O_{shell}$ values correspond to low winter temperatures and most negative $\delta^{18}O_{shell}$ values to high summer temperatures. However, they also found up to three growth lines per year. Such growth patterns were often termed disturbance lines (CLARK, 1974) and may result from major storms (MC LEAN FRASER and SMITH, 1928) or predation (CLARK, 1974). According to our findings, temperature-mediated growth cessations can be distinguished from disturbance lines through a careful analysis of microgrowth patterns. As shown in Fig. 5D, microgrowth increment width decreased gradually before these growth lines and commenced gradually thereafter. Disturbance breaks, however, were preceded by an abrupt change from broad to narrow microgrowth increments (Fig. 5E). Sometimes, disturbance breaks formed at the exact same time in different shells at the same place suggesting that shell growth was disturbed by a common environmental factor such as a major storm (Fig. 5E). In such cases, the same number of microgrowth increments was found between the disturbance line and the ventral margin (same date of collection). Examining shells collected in July 2007 in Alaska (see 4.2) and counting daily growth increments back reveals in both shells a disturbance line caused by a storm at the beginning of June 2007. Storms or other individual accidents are characterized by a sudden break and a fast recovery of growth. We observed a slowing down of growth for several days up to two weeks. In contrast, spawning breaks are characterized by a sudden break and a slow recovery (RHOADS and PANNELLA, 1970). In some years and in some shells from British Columbia we detected a $\delta^{18}O_{shell}$ peak (most positive values corresponding to winter), but we did not observe a dark growth line or it was just a barely visible line indicating that no or just a short growth break occurred. It is possible that the actual control is food availability, which might vary with temperature. The influence of food availability might be a topic for further research.

### 3.5.2. Tide-controlled growth patterns: daily and fortnightly growth patterns

Similar to other bivalve species from the intertidal zone (SCHÖNE et al., 2003), *S. gigantea* shells produced distinct circatidal (low tide-high tide cycle), circalunidian (lunar daily) and fortnightly growth patterns. This interpretation is substantiated as follows.

(1) The number of microgrowth increments within annual increments never exceeded the number of days per year (Tab. 2).

(2) In specimens collected on a monthly basis, the number of microgrowth increments between the ventral margin and the last winter line increased nearly by the number of days between collection dates. This suggests that each microgrowth increment roughly corresponds to one day.

(3) As demonstrated by Fast Fourier Transformation of the microgrowth increment chronologies, broader and narrower increments alternated regularly and formed bundles of ca. 13–15. These bundles are commonly ascribed as fortnight bundles and are related to tidal oscillations (EVANS, 1972; OHNO, 1985). Comparison of the tidal calendar with the microgrowth pattern at the ventral margin clearly demonstrated that specimens gathered at low tide during the spring tide cycle (new moon) showed distinct microgrowth lines near the ventral margin and relatively narrow microgrowth increments. The exact same pattern was observed ca. 15 microgrowth increments away from the ventral margin toward the umbo and can be cross-matched with the full moon cycle. Each spring tide-to-spring tide-cycle equals 14 days (13.5 lunar days, new moon to full moon) or 15.5 days (15 lunar days, full moon to new moon). The lunar day is ca. 50 min longer than a solar day on earth and describes the time that elapses until the moon is visible on the following day at the exact same position on the horizon. Therefore, we conclude that each microgrowth increment corresponds to precisely one lunar day (circalunidian increment = lunar daily growth increment, SCHÖNE et al., 2003).

(4) Bivalves only grow when they are submerged during high tide. During aerial emersion at low tide, however, shell growth stops and a microgrowth line forms (EVANS, 1972; OHNO, 1985). Predominantly in circalunidian increments that formed during neap tides (mid intertidal, Pender Island), we observed a faint line in the middle of the increment (Fig. 5C). According to the tidal calendar, these shells were exposed to semidiurnal tides during the neap tide cycle, i.e., they were aerially exposed twice per lunar day. The second emersion, however, was only for a very short time interval, so that the duration of shell closure remained short and resulting growth line much weaker than the adjoining microgrowth lines that formed during extended time intervals of shell closure. The faint growth lines separates two so-called circatidal increments from each other (two circatidal increments correspond to one circalunidian increment, Fig. 5C). During the remainder of each fortnight cycle the shells at this locality were exposed to diurnal tides. Circatidal growth patterns in such shell portions are rare.

(5) During neap tides, the shells were submerged for a longer time interval than during spring tides. Hence, circalunidian increments formed during neap tides were broader than those formed during spring tides.

### 3.5.3. Recommendations for increasing precision of seasonality estimates of collected archaeological shells

Low-resolution methods can only provide rough approximations, such as 'cold' or 'warm' collection (CLAASSEN, 1983; HERBERT and STEPONAITIS, 1998) spanning a time frame of several months, and potentially over-estimating the length of time an activity occurred. Improving the resolution of seasonality estimates using stable-isotope sclerochronology provides greater precision for identifying the potential variability in monthly patterns of shellfish collection. By refining seasonal estimates, it is possible to construct a more accurate picture of the occupational history of shell midden sites, and the activities that took place at shellfish gathering locations.

Microgrowth patterns of *S. gigantea* can be used to estimate the time of collection of an archaeological shell to the nearest day. This requires the following steps:

(1) The annual nature of the major dark lines has to be confirmed by oxygen isotope analysis.

(2) The duration of the growing season, ($g$), during the year of shell collection needs to be estimated from the number of lunar days counted in previous years of the shell ($g_1$, $g_2$, $g_3$ . $g_n$). This is required because the duration of the growing season may decrease with increasing age. We did not observe an ontogenetic change in the number of increments up to an age of six years. As shown in the present study, the middle of $g$ corresponds to approximately 1 July ± 14 days (Pender Island, southern BC). The maximum growth occurs around 25 July ± 40 days during the warmest days of the year. The growing season started $g$/2 days prior to 1 July, and ended $g$/2 days after this anchor point.

(3) It is necessary to estimate the time represented by the last formed winter growth line, $w$. This is given by $w = 353 - g$, where 353 is the number of lunar days per year. Shells from Pender Island, southern BC, cease their growth up to 63 days between 12 November and 27 January. We assume that the middle of $w$ corresponds to 22 December ± 8 days for shells from Pender Island, i.e., the coldest days of the year. Hence the growing season started $w$/2 days after 22 December.

(4) If the number of lunar daily increments, *i*, between the ventral margin and the last winter line is greater than *g*/2, $i - g/2$ gives the number of lunar days that passed after 1 July. However, if *i* is smaller than *g*/2, $i + w/2$ gives the number of lunar days that passed after 22 December. If a winter line is developed at the ventral margin, shell collection may have occurred *w*/2 lunar days before or after the winter anchor point. Data can be double checked by oxygen isotope analysis. During the first half of the year until summer, $\delta^{18}O_{shell}$ values become increasingly more negative, thereafter, values become more positive.

### 3.5.4. Additional information on the circumstances of shell collection

Aside from the date of collection, shell microgrowth patterns at the ventral margin can reveal if the shells were obtained during neap tides or spring tides. Distinct microgrowth lines at the commissure suggest collection during spring tides, weakly structured microgrowth patterns, indicate collection during neap tides. Distinguishing between shell portions deposited during full moon and new moon is more challenging. Because the full-to-new moon period (apogee) is ca. 1.5 days longer than the new-to-full moon period (perigee), the respective fortnightly growth increments contain different amounts of circalunidian increments. If a microgrowth line is developed at the ventral margin, the shell was gathered during low tide. However, if an incomplete lunar daily increment is found at the ventral margin, the shell was obtained by diving during high tides. Shell collection during spring tide is more dangerous than during neap tide, and this type of information and can be used to interpret strategies for obtaining shells, such as collecting shells during a full moon when it is brighter at night. Even shell collection during day or night can be estimated by comparison of the shell growth pattern with the tidal calendar.

Shell microgrowth patterns can also be used to identify the approximate tidal location (i.e., approx. water depth and distance from the shoreline) where the clams lived. Bivalves collected from high intertidal settings may have been aerially exposed for some days during neap tides and not grown shell carbonate during this time. These shells will show less than 14 lunar daily increments per fortnight period (some Alaskan shells; Tab. 3). In addition, at high intertidal settings the number of semidiurnal tides is larger than at settings farther offshore. Correspondingly, shells from such settings will exhibit a greater number of circatidal growth increments. In low intertidal settings, however, shells mainly experience diurnal tides and

produce only one growth line per day. During neap tides, these habitats may not fall dry, so that only faint growth lines are developed during such times. Identifying the approximate location of shellfish collection in the intertidal zone can be used to understand the range and extent of shellfish harvest.

When comparing the shell growth pattern and the tidal calendar for the locality where the shell lived, the observed lunar daily growth increment pattern coincides with the expected pattern (Fig. 9). By comparison of the observed and the expected shell growth the tidal height above the mean low-water level can be estimated (approx. 2 m). The studied shell in Fig. 9 shows distinct microgrowth lines near the ventral margin implying collection during spring tide (full or new moon). A growth line is visible at the edge of the ventral margin indicating shell collection during ebb. Furthermore the time of collection can be estimated by comparing the position of the last formed growth line and the last formed growth increment with the tidal calendar. According to that the shell was collected during the early evening at 9 July 1987.

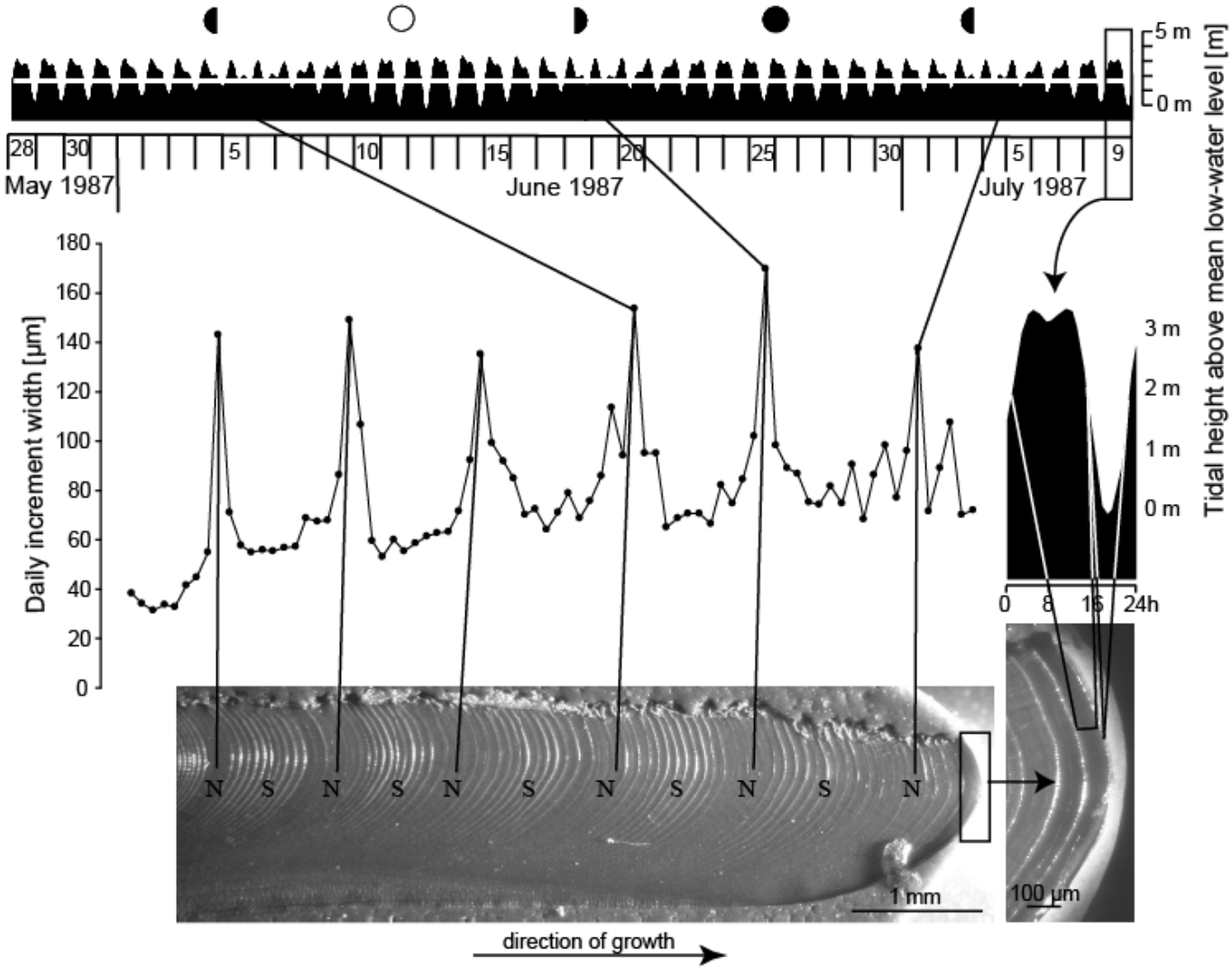


Figure 9. Spring neap tide cycles from 28th May 1987 to 9th July 1987 of Pender Island, southern British Columbia (data generated with WXTide32 ver. 4.7). Daily growth increment width and tidal growth pattern of DeRt-1-0787-A3L reveal information about the collection date, time and location in the intertidal (i.e., approx. water depth and distance from the shoreline). Broad increments are formed during neap tide (N, half moon) and narrow increments with distinct growth lines during spring tide (S, full moon = open circle or new moon = filled circle). The last increment was formed approximately between midnight and late afternoon on July 9th 1987 at a tidal height of more than 2 m (shell was covered with water). The formation of the last microgrowth line at the ventral margin started at a tidal height of less than 2 m during the early evening before this specimen was collected in the evening (shell was exposed to the air). White horizontal line in tidal calendar denotes position on shelf where the shell was collected.

### 3.5.5. Limitations of sclerochronology for identifying seasonality

Reliable identification of lunar daily growth patterns is limited to around the first six years of life, when shells grow at their fastest rates (JONES, 1983). With increasing ontogenetic age, recognition of shell microgrowth patterns becomes more difficult, because individual narrow microgrowth increments cannot be distinguished from each other. In such cases, the season of shellfish collection may only be estimated to the nearest month or so by counting fortnightly bundles of microgrowth increments.

Bivalves from stressful environmental settings (frequently occurring storms, large number of predators etc.) are less suitable for sclerochronological analyses, because they tend to show a large number of disturbance breaks. Consequently, the shell record of several days or weeks may be missing in such specimens precluding a precise estimation of when shellfish were harvested. Several shells from each locality have to be analyzed due to the inter-annual (year-to-year variation of temperature and other environmental factors) and inter-individual variability of shell growth, which may be caused by different micro-site conditions and/or physiological differences.

Reconstructing the season of shell collection with archaeological shells requires considering a change of the tidal regime through time due to changing topography, sea level and astronomical parameters. Also the ocean tide i.e., the boundary between the shelf and the open ocean, has to be considered, which changes throughout time. Therefore the tidal calendar of today is not exactly applicable to the past. If the tidal calendar is available, it is possible to estimate whether shells were collected during day or night.

## *3.6. CONCLUSIONS*

Prior to commencing a seasonality study using stable isotopes, the growth history of the shell must be understood, as well as an understanding of the ecological settings and the environmental conditions that influence shell growth patterns. Inter-annual and inter-individual differences in shell growth have to be taken into account, therefore several specimens from each locality have to be analyzed. It is still not known if *S. gigantea* precipitates its shell in isotopic equilibrium with the ambient seawater, and this may prove problematic for paleoclimate reconstructions. Additionally, the varying salinity on the Pacific Coast of North America will seasonally change the $\delta^{18}O$ of the seawater, which will also make paleotemperature estimates difficult. Thus studies to examine the effects of freshwater

(glacial melt water, precipitation) on the geochemistry and growth pattern of the shells are important.

The application of sclerochronology to archeological shells has the potential to refine seasonality estimates of collection because it increases the precision by combining both geochemical and biological data. With this method, archaeological shells can be analyzed, not only to determine the season of death, but also whether the shell was collected during low or high tides, spring or neap tides, or during the day or night. It is also possible to identify the approximate elevation in the intertidal zone from which the shells were being harvested. The results of this study can be applied to archaeological investigations of seasonality and shellfish collection strategies, which can then be used to interpret the role of shellfish in prehistoric diets, and the nature of coastal economies.

## *3.7. ACKNOWLEDGEMENTS*

Shannon Wood (Simon Fraser University) is kindly acknowledged for providing access to archaeological shells from the Pender Canal Site and laboratory space. We thank Aubrey Cannon (McMaster University) who provided resources at the Fisheries Archaeology Research Centre funded by The Canadian Foundation for Innovation and the Social Sciences Humanities Research Council of Canada, and Andrew Martindale (University of British Columbia) for inviting us to work on the Dundas Islands Project. We thank Henry Schwarcz for helpful comments on preparing this manuscript and reviews of the draft manuscript by Dr. Jeanne Schaaf and Dr. A.L.A. Johnson. We also wish to acknowledge the National Oceanic and Atmospheric Administration for providing the sea surface temperature data (NOAA_OI_SST_V2 data provided by the NOAA/OAR/ESRL PSD, Boulder, Colorado, USA, from their Web site at http://www.cdc.noaa.gov). Financial support for this study was provided by the German Research Foundation, DFG (SCHO 793/3) to BRS; the Exxon Valdez Oil Spill Trustee Council, the U.S. Geological Survey and the National Park Service to GVI. Any mention of trade names is for descriptive purposes only and does not represent endorsement by the U.S. government. This is Geocycles publication number 620.

## 3.8. REFERENCES

ANDRUS, C.F.T., and CROWE, D.E., 2000. Geochemical analysis of *Crassostrea virginica* as a method to determine season of capture. Journal of Archaeological Science 27, 33–42.

BÖHM, F., JOACHIMSKI, M.M., DULLO, W.-Ch., EISENHAUER, A., LEHNERT, H., REITNER, J., and WÖRHEIDE, G., 2000. Oxygen isotope fractionation in marine aragonite of coralline sponges. Geochimica et Cosmochimica Acta 64, 1695–1703.

CANNON, A., and BURCHELL, M., 2009. Clam growth-stage profiles as a measure of harvest intensity and resource management on the Central Coast of British Columbia. Journal of Archaeological Science 36, 1050–1060.

CANNON, A., BURCHELL, M., and BATHURST, R., 2008. Trends and strategies in shellfish gathering on the Pacific Northwest Coast of North America. *In*: ANTCZAK, A., CIPRIANI, R. (eds.), BAR International Series 1865, Archaeopress, Oxford, 7–22.

CLAASSEN, C.P., 1983. Prehistoric shellfishing patterns in North Carolina. *In*: GRIGSON, C., CLUTTON-BROCK, J. (eds.), Animals and Archaeology. Shell Middens, Fishes and Birds, BAR International Series 183, 211–223.

CLARK II, G.R., 1974. Growth lines in invertebrate skeletons. Annual Review of Earth and Planetary Sciences 2, 77–99.

COUPLAND, G., BISSELL, C., and KING, S., 1993. Prehistoric subsistence and seasonality at Prince Rupert Harbour: evidence from the McNichol Creek Site. Canadian Journal of Anthropology 17, 59–73.

COUTTS, P.J.F., 1970. Bivalve-growth patterning as a method for seasonal dating in archaeology. Nature 226, 874.

CRAIG, H., and GORDON, L.I., 1965. Deuterium and oxygen 18 variations in the ocean and the marine atmosphere. *In*: TONGIORGI, E. (ed.), Stable Isotopes in Oceanographic Studies and Paleotemperatures. Consiglio Nazionale delle Ricerche, Spoleto, Italy, 9–130.

CUSTER, J.F., and DOMS, K.R., 1990. Analysis of microgrowth patterns of the American oyster (*Crassostrea virginica*) in the middle Atlantic region of eastern North America: archaeological applications. Journal of Archaeological Science 17, 151–160.

DAVIS, L.G., and MUEHLENBACHS, K., 2001. A late Pleistocene to Holocene record of precipitation reflected in *Margaritifera falcata* shell $\delta^{18}$Oshell from three archaeological sites in the lower Salmon River canyon, Idaho. Journal of Archaeological Science 28, 291–303.

DEITH, M.R., 1983. Molluscan calendars: the use of growth-line analysis to establish seasonality of shellfish collection at the Mesolithic site of Morton, Fife. Journal of Archaeological Science 10, 423–440.

EPSTEIN, S., BUCHSBAUM, R., LOWENSTAM, H.A., and UREY, H.C., 1953. Revised carbonate-water isotopic temperature scale. Bulletin of the Geological Society of America 64, 1315–1326.

EVANS, J.W., 1972. Tidal growth increments in the cockle *Clinocardium nuttalli*. Science 176, 416–417.

GILLIKIN, D.P., DE RIDDER, F., ULENS, H., ELSKENS, M., KEPPENS, E., BAEYENS, W., and DEHAIRS, F., 2005b. Assessing the reproducibility and reliability of estuarine bivalve shells (*Saxidomus giganteus*) for sea surface temperature reconstruction: implications for paleoclimate studies. Palaeogeography Palaeoclimatology Palaeoecology 228, 70–85.

GILLIKIN, D.P., LORRAIN, A., NAVEZ, J., TAYLOR, J.W., ANDRÉ, L., KEPPENS, E., BAEYENS, W., and DEHAIRS, F., 2005a. Strong biological controls on Sr/Ca ratios in aragonitic marine bivalve shells. Geochemistry, Geophysics, Geosystems 6, Q05009, doi:10.1029/2004GC000874.

GROSSMAN, E.L., and KU, T.-L., 1986. Oxygen and carbon isotope fractionation in biogenic aragonite; temperature effects. Chemical Geology (Isotope Geoscience Section) 59, 59–74.

HAM, L., and IRVING, M., 1975. Techniques for determining seasonality of shell middens from marine mollusk remains. Syesis 8, 363–373.

HERBERT, J.M., and STEPONAITIS, L.C., 1998. Estimating the seasonal of harvest of eastern oysters (*Crassostrea virginica*) with shells from Chesapeake Bay. Southeastern Archaeology 17, 53–71.

JONES, D.S., 1983. Sclerochronology: reading the record of the molluscan shell. American Scientist 71, 384–391.

JONES, D.S., and QUITMYER, I.R., 1996. Marking time with bivalve shells: oxygen isotopes and season of annual increment formation. PALAIOS 11, 340–346.

KEEN, S.D., 1979. The growth rings of clam shells from two pentlatch middens as indicators of seasonal gathering. Occasional Paper Number 3, Archaeology Division, Heritage Conservation Branch, Victoria, British Columbia.

KENNETT, D.J., and VOORHIES, B., 1996. Oxygen isotopic analysis of archaeological shells to detect seasonal use of wetlands on the Southern Pacific Coast of Mexico. Journal of Archaeological Science 23, 689–704.

KOIKE, H., 1973. Daily growth lines of the clam *Meretrix lusoria*. Journal of the Anthropological Society of Nippon 81, 122–138.

KOIKE, H., 1975. The use of daily and annual growth lines of the clam *Meretrix lusoria* in estimating seasons of Jomon period shell gathering. Quaternary Studies, The Royal Society of New Zealand 13, 189–193.

KOIKE, H., 1980. Seasonal dating by growth-line counting of the clam *Meretrix lusoria*. University Museum, University of Tokyo, Bulletin 18, 120 p.

MANNINO, M.A., BARUCH, F.S., and THOMAS, K.D., 2003. Sampling shells for seasonality: oxygen isotope analysis of shell carbonates on the intertidal gastropod *Monodonta lineata* (da Costa) from populations across its modern range and from a Mesolithic site in southern Britain. Journal of Archaeological Science 30, 666–679.

MAXWELL, D., 1989. Growth coloration: A method for determining the season of collection of archaeological shellfish. Unpublished master's thesis, Simon Fraser University, British Columbia.

MC LEAN FRASER, M., and SMITH, G.M., 1928. Notes on the ecology of the butter clam, *Saxidomus giganteus* Deshayes. Section V, Transactions of the Royal Society of Canada 3, 271–284.

MILNER, N., 2001. At the cutting edge: using thin sectioning to determine season of death of the European Oyster, *Ostrea edulis*. Journal of Archaeological Science 28, 861–873.

MIYAJI, T., TANABE, K., and SCHÖNE, B.R., 2007. Environmental controls on daily shell growth of *Phacosoma japonicum* (Bivalvia: Veneridae) from Japan. Marine Ecology Progress Series 336, 141–150.

MONKS, G.G., and JOHNSTON, R., 1993. Estimating season of death from growth increment data: a critical review. Archaeozoologica 2, 17–40.

NICKERSON, R.B., 1977. A study of the littleneck clam (*Protothaca staminea* Conrad) and the butter clam (*Saxidomus giganteus* Deshayes) in a habitat permitting coexistence, Prince William Sound, Alaska. Proceedings of the National Shellfisheries Association 67, 85–102.

OHNO, T., 1985. Experimentelle Analysen zur Rhythmik des Schalenwachstums einiger Bivalven und ihre paläobiologische Bedeutung. Palaeontographica 189, 63–123.

PAUL, A.J., PAUL, J.M., and FEDER, H.M., 1976. Age, growth, and recruitment of the butter clam, *Saxidomus gigantea*, on Porpoise Island, Southeast Alaska. Proceedings of the National Shellfisheries Association 66, 26–28.

QUAYLE, D.B., and BOURNE, N., 1972. The clam fisheries of British Columbia. Fisheries Research Board of Canada, Ottawa, Bulletin 179, 70 p.

QUITMYER, I.R., JONES, D.S., and ARNOLD, W.S., 1997. The sclerochronology of hard clams, *Mercenaria spp.*, from the South-Eastern U.S.A.: a method of elucidating the zooarchaeological records of seasonal resource procurement and seasonality in prehistoric shell middens. Journal of Archaeological Science 24, 825–840.

REYNOLDS, R.W., RAYNER, N.A., SMITH, T.M., STOKES, D.C., and WANG, W., 2002. An improved in situ and satellite SST analysis for climate. Journal of Climate 15, 1609–1625.

RHOADS, D.C., and PANNELLA, G., 1970. The use of molluscan shell growth patterns in ecology and paleoecology. Lethaia 3, 143–161.

ROMANEK, C.S., GROSSMAN, E.L., and MORSE, J.W., 1992. Carbon isotopic fractionation in synthetic aragonite and calcite: effects of temperature and precipitation rate. Geochimica et Cosmochimica Acta 56, 419–430.

SARKAR, N., ROYER, T.C., and GROSCH, C.E., 2005. Hydrographic and mixed layer depth variability on the shelf in the northern Gulf of Alaska, 1974–1998. Continental Shelf Research 25, 2147–2162.

SCHÖNE, B.R., DUNCA, E., FIEBIG, J., and PFEIFFER, M., 2005b. Mutvei's solution: an ideal agent for resolving microgrowth structures of biogenic carbonates. Palaeogeography Palaeoclimatology Palaeoecology 228, 149–166.

SCHÖNE, B.R., FIEBIG, J., PFEIFFER, M., GLEß, R., HICKSON, J., JOHNSON, A.L.A., DREYER, W., and OSCHMANN, W., 2005a. Climate records from a bivalve Methuselah (*Arctica islandica*, Mollusca; Iceland). Palaeogeography Palaeoclimatology Palaeoecology 228, 130–148.

SCHÖNE, B.R., GOODWIN, D.H., FLESSA, K.W., DETTMAN, D.L., and ROOPNARINE, P.D., 2002a. Sclerochronology and growth of the bivalve *Chione* (Chionista) *fluctifraga* and *C.* (Chionista) *cortezi* in the northern Gulf of California, Mexico. The Veliger 45, 45–54.

SCHÖNE, B.R., LEGA, J., FLESSA, K.W., GOODWIN, D.H., and DETTMAN, D.L., 2002b. Reconstructing daily temperatures from growth rates of the intertidal bivalve mollusk

*Chione cortezi* (northern Gulf of California, Mexico). Palaeogeography, Palaeoclimatology, Palaeoecology 184, 131–146.

SCHÖNE, B.R., TANABE, K., DETTMAN, D.L., and SATO, S., 2003. Environmental controls on shell growth rates and $\delta^{18}O$ of the shallow-marine bivalve mollusk *Phacosoma japonicum* in Japan. Marine Biology 142, 473–485.

# Executive summary and conclusions

This detailed analysis of life history traits of *Saxidomus gigantea* provides new insights into the seasonal growth of butter clams, which are beneficial for reconstructing paleoenvironments and interpreting the season of shellfish collection. Growth patterns within a species may differ from region to region and therefore they need to be reanalyzed for every new habitat. Furthermore, it is important to consider latitudinal gradients in growth within a species (TANABE and OBA, 1988; HALLMANN et al., 2009).

A significant relationship exists between bivalve shell growth rate and water temperature (e.g., PANNELLA and MCCLINTOCK, 1968; JONES, 1981; JONES et al., 1989; MARCHITTO et al., 2000; SCHÖNE et al., 2003). Seawater temperature is considered to be the most important factor controlling shell growth (GOODWIN et al., 2001; SCHÖNE et al., 2002b). However, besides temperature many other environmental factors, such as salinity, food quality and quantity, water flow, sediment characteristics and biotic interactions affect growth rates of bivalves (KRAEUTER and CASTAGNA, 2001; MARSDEN, 2004). The influence of these environmental parameters on shell growth rates may differ from locality to locality and from time to time.

After the calibration of *S. gigantea* a growth-temperature model was established for Alaskan butter clams. This approach allows the independent measure of water temperature and salinity from variations in the width of lunar daily growth increments of butter clams. The model was calibrated with modern shells and then applied to archaeological shells. A constant recalibration of the growth-temperature model is necessary to improve the precision of the temperature and salinity reconstructions.

# Chapter 4: An improved understanding of the Alaska Coastal Current: The application of a bivalve growth-temperature model to reconstruct freshwater-influenced paleoenvironments

Nadine Hallmann[1], Bernd R. Schöne[1], Gail V. Irvine[2], Meghan Burchell[3], Edward D. Cokelet[4], Michael R. Hilton[5]

[1] Earth System Science Research Centre, Department of Applied and Analytical Paleontology (INCREMENTS), Institute of Geosciences, University of Mainz, Johann-Joachim-Becher-Weg 21, 55128 Mainz, Germany

[2] U.S. Geological Survey, Alaska Science Center, 4210 University Dr., Anchorage, AK 99508, USA

[3] Department of Anthropology, McMaster University, 1280 Main Street West, Hamilton, Ontario, Canada

[4] NOAA/PMEL, 7600 Sand Point Way NE, Seattle, WA 98115-6349, USA

[5] Cotsen Institute of Archaeology at UCLA, A210 Fowler, UCLA, Los Angeles, CA 90095-1510 57730, USA

Accepted by PALAIOS (pending minor to moderate revisions)

## *ABSTRACT*

**Shells of intertidal bivalve mollusks contain subseasonally to inter-annually resolved records of temperature and salinity variations in coastal settings. Such data are essential to understand changing land-sea interactions through time, specifically atmospheric (precipitation rate, glacial meltwater, river discharge) and oceanographic circulation patterns. However, independent temperature and salinity proxies are currently not available. For example, reconstructing temperatures from $\delta^{18}O_{shell}$ values requires a precise knowledge of salinity and the oxygen isotope composition of the water, which is rarely the case for ancient environments. We established a model for reconstructing daily water temperatures with an average standard error of ~1.3°C based on variations in the width of lunar daily growth increments of *Saxidomus gigantea* from south west Alaska. Temperature explains 70% of the variability in shell growth. When used in conjunction with stable oxygen isotope data, this approach can also be used to identify changes in past seawater salinity. This study provides a better understanding of the hydrological changes related to the Alaska Coastal Current (ACC). In combination with $\delta^{18}O_{shell}$ values, increment-derived temperatures were used to estimate salinity changes with an average error of 1.4±1.1 PSU. Our model was calibrated and tested with modern shells and then applied to archaeological specimens. As derived from the model, the time interval of 988-1447 cal yr BP was characterized by ~1-2°C colder and much drier (2-5 PSU) summers. During that time interval, the ACC was likely flowing much slower than at present. In contrast, between 599 and 1014 cal yr BP, the Aleutian low may have been stronger, which resulted in a 3°C temperature decrease during summers and 1-2 PSU fresher conditions than today. The ACC was probably flowing faster at that time.**

**The shell growth-temperature model can be used to estimate seasonal to inter-annual salinity and temperature changes in freshwater-influenced environments through time.**

**Keywords: Paleosalinity, Stable isotopes, Sclerochronology, North Pacific, *Saxidomus gigantea***

## 4.1. INTRODUCTION

Freshwater discharge from coastal mountains into the northern Gulf of Alaska exerts a major control on the Alaska Coastal Current (ACC; ROYER, 1982; JOHNSON et al., 1988; STABENO et al., 2004; WEINGARTNER et al., 2005). The ACC is a narrow swift stream that flows alongshore in a counter-clockwise direction from British Columbia to Unimak Pass (Aleutians) where it enters the Bering Sea (MUENCH et al., 1978; SCHUMACHER et al., 1982; KIPPHUT, 1990; SPIES, 2007). From there, the nutrient-rich, low-salinity waters (25-31 PSU, MUNDY, 2005) reach the Arctic Ocean (WEINGARTNER et al., 2005) and foster the productivity and sea-ice formation in Polar waters (HU et al., 2010). Large freshwater discharges increase the speed of the ACC (ROYER, 1981) and therefore, the amount of low-salinity waters reaching the Arctic seas. In turn, this can increase sea-ice formation and albedo. Hence, freshwater runoff into the Gulf of Alaska can act as a thermostat, affecting processes in the Bering Sea and northward. Despite its importance in the global climate system, past dynamics of the ACC on seasonal to inter-annual time-scales are barely studied due to the lack of high-resolution climate proxy archives. Most available records only report on precipitation patterns on land (dendrochronology: e.g., GARFINKEL and BRUBAKER, 1980; WILES et al., 1996, 1998; BARBER et al., 2004) or only provide low temporal resolution, typically on an annual scale (i.e., pollen: BIGELOW and EDWARDS, 2001; lake deposits: ABBOTT et al., 2000; ANDERSON et al., 2001; foraminifera: KEIGWIN et al., 2006). Recently, coralline red algae have been employed to reconstruct inter-annual temperature and salinity changes at the Aleutians (HALFAR et al., 2007; HETZINGER et al., 2009). However, this record only extends back to the end of the 19$^{th}$ century.

Alternatively, shells of intertidal bivalve mollusks can provide subseasonal to inter-annual records of salinity and temperature changes. Living at the interface between land and the open ocean, bivalves are exposed to changes in freshwater runoff, as mediated by the ACC. Bivalves are highly sensitive to ambient environmental changes and encode a number of environmental parameters in their shells in the form of variable growth rates and geochemical properties (EPSTEIN et al., 1953; WILLIAMS et al., 1982; GOODWIN et al., 2001; SCHÖNE et al., 2005a, 2011; BUTLER et al., 2010). The butter clam *Saxidomus gigantea* (Deshayes) is the most abundant clam on beaches in Alaska, British Columbia and Puget Sound, Washington (RICKETS and CALVIN, 1962). It also is abundant in archaeological shell middens covering almost the entire Holocene. *S. gigantea* inhabits the intertidal and shallow

subtidal zone, lives buried in sandy to gravely sediments ca. 30 cm beneath the sediment-water interface and attains a lifespan of more than twenty years (QUAYLE and BOURNE, 1972).

In Alaska, shell growth of *S. gigantea* ceases for up to six or seven months per year from approximately October/November to April/May (HALLMANN et al., 2009). Daily microgrowth patterns demonstrated that shell growth is strongly linked to the water temperature with fastest rates occurring during the summer and slowest growth during spring and fall (HALLMANN et al., 2009). The lower and upper growth temperature thresholds are ~4-5° and 20°C, respectively (BERNARD, 1983; GILLIKIN et al., 2005a; HALLMANN et al., 2009). Despite its potential importance for paleoclimate studies, the butter clam has rarely been studied by means of sclerochronological techniques (GILLIKIN et al. 2005a, b; KINGSTON et al., 2008; HALLMANN et al., 2009). In its shell, *S. gigantea* produces distinct lunar daily (circadian), fortnightly and annual growth increments, which can be used to assign precise calendar dates to each portion of the shell (HALLMANN et al., 2009). Furthermore, geochemical properties of the shells can provide serviceable environmental proxies. For example, based on three contemporaneous specimens collected alive from Puget Sound, WA, USA, GILLIKIN et al. (2005a) concluded that water temperatures can be estimated from $\delta^{18}O_{shell}$ values to the nearest 0.8°C. However, such estimates require a precise knowledge of salinity and the oxygen isotope composition of the water, which is rarely the case for ancient environments. Unfortunately, independent temperature and salinity proxies are currently not available, which limits use of bivalve shells from freshwater-influenced environments for quantitative paleoclimate reconstructions.

In this study we determined if quantifiable temperature and salinity data can be reconstructed from growth patterns and light stable isotope data of *S. gigantea*. Specifically, we tested the hypotheses that the independent measurement of water temperature and salinity can be used to estimate seasonal to inter-annual changes in paleosalinity and paleotemperature revealed in the sclerochronological records of *S. gigantea* shells. Using shell growth patterns and shell isotope data, $\delta^{18}O_{water}$ and salinity values were reconstructed and compared to modern environmental records. The new model was then applied to archaeological shells (599-1447 cal yr BP) in order to identify paleohydrologic changes through time.

## *4.2. METHODS AND MATERIALS*

A total of 28 specimens of *Saxidomus gigantea* that were collected live from the intertidal zone at four different, but proximate localities in southwestern Alaska (Fig. 1, Tab. 1) were analyzed. These living bivalves were gathered from Little Takli Island (locality 1; Fig. 1) and Mink Island (localities 2-4; Fig. 1) between 1998 and 2008. In addition, five archaeological specimens (single valves) came from a shell midden site on Mink Island (site XMK-030 near sample locality 3; Fig. 1D). Both islands are situated at the entrance of Amalik Bay in the Shelikof Strait and approximately three kilometers away from the Katmai mainland. The Shelikof Strait is a 200 km long and 35 km wide channel between Kodiak Island and the Alaska Peninsula that is dominated by the ACC. A detailed list of shells from each locality is provided in Table 1.

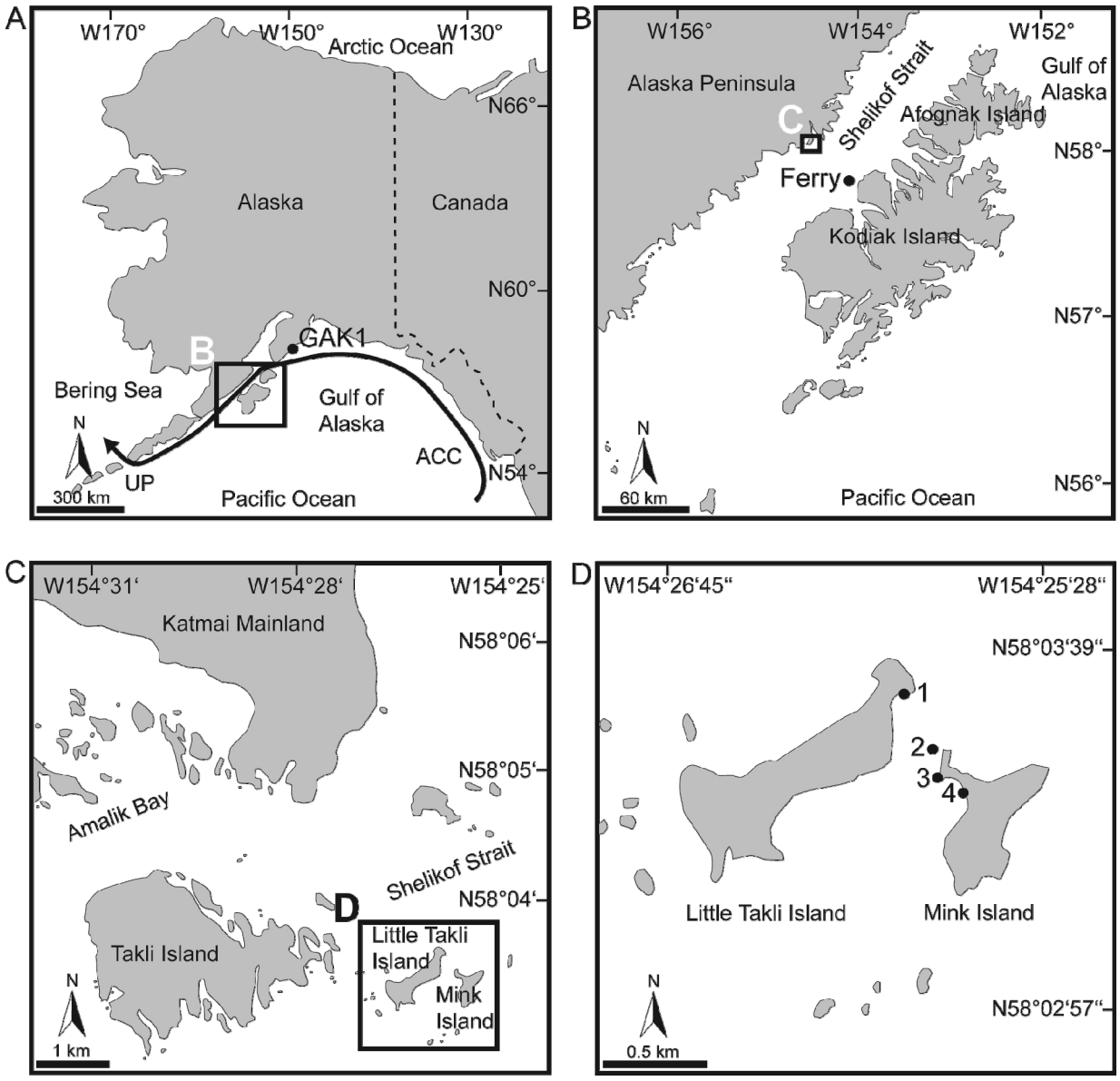


Figure 1. Maps showing sample localities. A) Map of Alaska. ACC = Alaska Coastal Current, UP = Unimak Pass. Sample sites are located in the box. B) Shelikof Strait between the Alaska Peninsula and Kodiak Island and C) the entrance of Amalik Bay where the two study sites, Little Takli Island and Mink Island are located. Water samples, clams and temperature logger data were gathered at four different localities (D).

Table 1. List of modern and archaeological shells used in this study, their locales of origin, ontogenetic ages, shell heights and the types of data generated. LDGI = lunar daily growth patterns. For locality code see Figure 1. Asterisks indicate LDGI data which were used to calibrate the GT model.

| Shell ID | Locality | Ontogenetic age (yrs) | Shell height (mm) | LDGI width (calendar yrs, ontogenetic age) | Isotope samples (#, calendar yrs, ontogenetic age, date of collection) |
|---|---|---|---|---|---|
| GI-MI0898-A5R | 4 | | | | |
| GI-MI0898-A7R | 4 | 17 | 82 | | 8, 1987, 6, 9 Aug 98 |
| GI-MI0903-A2R | 4 | 7 | 38 | | 53, 1998-2002, 2-6, 11 Sep 03 |
| GI-MI0903-A3L | 4 | | | | |
| GI-MI0903-A5L | 4 | | | | |
| GI-MI0903-A6L | 4 | 6 | 33 | | 36, 2000-2002, 3-5, 11 Sep 03 |
| GI1-LTI0707-A1L | 1 | | | | |
| GI1-LTI0707-A2L | 1 | | | 2006, 4 | |
| GI1-LTI0707-A3L | 1 | | | 2005*, 06*, 07, 1-3 | |
| GI1-LTI0707-A4L | 1 | | | | |
| GI1-LTI0707-A5L | 1 | 6 | 34 | | 42, 2004-2007, 3-6, 3 Jul 07 |
| GI1-LTI0707-A6L | 1 | 4 | 31 | | 18, 2005-2006, 2-3, 3 Jul 07 |
| GI1-LTI0707-A7L | 1 | | | | |
| GI2-MI0707-A2L | 2 | 4 | 25 | | 33, 2005-2007, 2-4, 3 Jul 07 |
| GI2-MI0707-A3L | 2 | | | 2006*, 3 | |
| GI1-LTI0907-A1L | 1 | 7 | 37 | 2002-2007, 2-7 | 124, 2003-2007, 3-7, 9 Sep 07 |
| GI1-LTI0907-A2L | 1 | 4 | 30 | 2006*-2007, 3-4 | 38, 2005-2007, 2-4, 9 Sep 07 |
| GI1-LTI0907-A7L | 1 | 5 | 32 | | 24, 2005-2006, 3-4, 9 Sep 07 |

| | | | | | |
|---|---|---|---|---|---|
| GI1-LTI0907-A8L | 1 | | | 2007, 5 | |
| GI4-MI0907-A1L | 4 | | | 2007, 5 | |
| GI4-MI0907-A2L | 4 | | | 2004, 05*, 06, 07, 4-7 | |
| GI4-MI0907-A4L | 4 | 5 | 36 | 2004*, 2; 2007*, 5 | 32, 2005-2007, 3-5, 11 Sep 07 |
| GI4-MI0907-A5L | 4 | 5 | 28 | 2005*, 06*, 07, 3-5 | 25, 2005-2007, 3-5, 11 Sep 07 |
| GI3-MI0808-A3L | 3 | | | 2007, 1 | 21, 2007-2008, 30 Aug 08 |
| GI3-MI0808-A7L | 3 | 4 | 28 | 2007*, 3 | 28, 2007-2008, 3-4, 30 Aug 08 |
| GI2-MI0908-A2L | 2 | 4 | 21 | | 9, 2007, 3, 1 Sep 08 |
| GI2-MI0908-A4L | 2 | 6 | 30 | | 22, 2007-2008, 5-6, 1 Sep 08 |
| GI2-MI0908-A10L | 2 | 5 | 25 | | 11, 2007, 4, 1 Sep 08 |
| | | | | | |
| GI-MI20572-D1R | 3 | 9 | 53 | 4.5 yrs | 49, 2 yrs, 4+8 |
| GI-MI20572-D2L | 3 | 9 | 51 | 2.5 yrs | 33, 3 yrs, 4-6 |
| GI-MI81972-D1L | 3 | 7 | 47 | 2.5 yrs | 36, 3 yrs, 4-6 |
| GI-MIXMK030-D1L | 3 | 10 | 58 | | 37, 4 yrs, 4-7 |
| GI-MI20510-D2R | 3 | 18 | 74 | | 34, 3 yrs, 5+7+9 |

### 4.2.1. Preparation of cross-sectioned valves for sclerochronological analyses

For light stable isotope and growth pattern analyses, one valve of each specimen was mounted on a plexiglass cube with plastic welder (Multipower, GlueTec) and coated with metal epoxy resin (WIKO) to avoid shell fracture during sectioning (Fig. 2A). Two three-millimeter thick slabs were cut from the shells perpendicular to the growth lines and along the axis of maximum growth from the umbo to the ventral margin using a low-speed precision saw (Buehler, IsoMet 1000) and a 0.4 mm thick diamond-coated saw blade (Fig. 2A). Both slabs were mounted with metal epoxy resin on glass slides, ground on glass plates (800, 1200 grit powder) and polished with 1 μm $Al_2O_3$ powder (Fig. 2B). After each grinding and polishing step, the cross-sections were cleaned by ultrasonic rinsing to remove any adhering grinding powder. All samples were then cleaned with de-ionized water and air-dried. For growth pattern analyses, one polished section of each specimen was immersed in Mutvei's solution for twenty minutes under constant stirring at 37°C to 40°C (SCHÖNE et al., 2005b). Mutvei's solution simultaneously etches the shell, and preserves and stains organic matrices (i.e., proteins and sugars) blue. After the staining process, the cross-sections were gently rinsed with de-ionised water and air-dried. The organic-rich growth lines stand out as etch-resistant, dark blue stained ridges, whereas the growth increments between consecutive growth lines are more strongly etched and appear in lighter shades of blue (Fig. 2C); this combination facilitates growth pattern analyses.

To analyze shell growth patterns, digital images were taken of the outer shell layer (Figs 2B and 2C) with a Nikon Coolpix 995 camera attached to a binocular microscope (Wild Heerbrugg M3Z). Lunar daily growth increment widths (Fig. 2C) were measured in the direction of growth to the nearest 2 μm using the image processing software Panopea (© Peinl and Schöne).

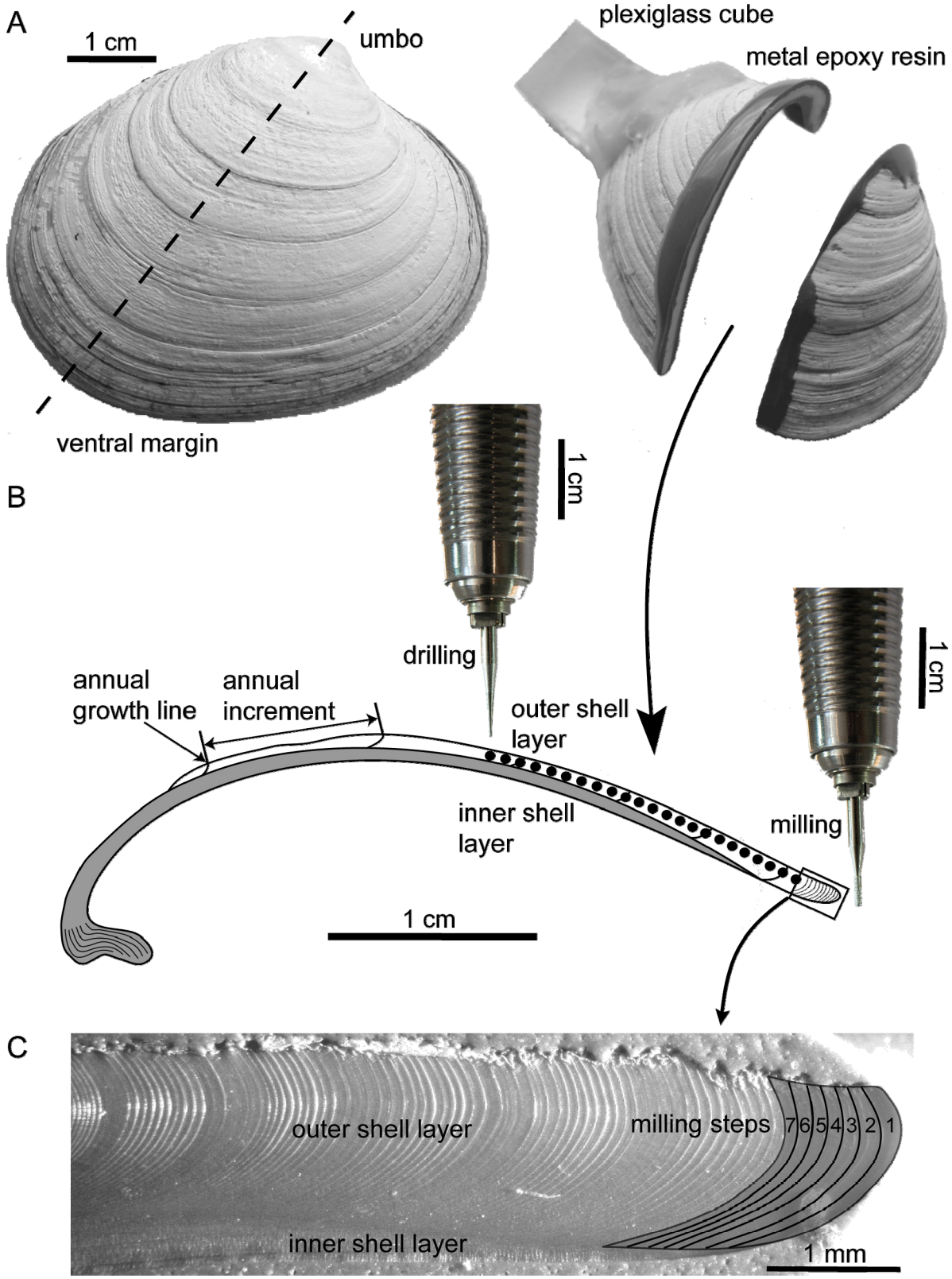


Figure 2. Preparation of *Saxidomus gigantea* shells. A) The valves were cut perpendicular to the growth lines along the axis of maximum growth from the umbo to the ventral margin. B) The outer shell layer of the polished cross sections was sampled for stable isotope analysis using two different sampling techniques, microdrilling and micromilling. Inner shell layer = grey, outer shell layer = white. Black dots denote the drilled holes. C) Microgrowth patterns

in an ontogenetically young shell portion after immersion in Mutvei's solution. Each microgrowth increment represents one lunar day. Microgrowth patterns are arranged in bundles. Distinct bundles were formed during spring tides, less distinct growth patterns during neap tides. Therefore, couplets of distinct and less distinct bundles represent fortnight cycles (see also HALLMANN et al., 2009). Also illustrated is the micromilling technique in the outer shell layer. Milling step sizes measure approximately 100 µm. Typically, micromilling was only applied to slow-growing shell portions of ontogenetically old specimens.

### 4.2.2. Shell stable isotopes

For determination of stable isotope ratios ($\delta^{18}O_{shell}$, $\delta^{13}C_{shell}$), powder samples were hand micromilled and drilled from the outer shell layer of unstained, polished cross-sections. In fast-growing shell portions, samples were obtained by drilling holes with a conical drill bit (300 µm diameter, Komet/Gebr. Brasseler GmbH & Co. KG, model no. H52 104 003; Fig. 2B). The distance between the centers of consecutive sample spots varied between 200 and 500 µm. However, in slow-growing portions of the shell, e.g., near the ventral margin, a cylindrical bit (1 mm diameter; model no. 835 104 010) was used. Individual milling steps contoured the microgrowth patterns and measured in the broadest areas approximately 100 µm in the direction of growth (Fig. 2C). Through high-resolution, equidistant micromilling an uninterrupted isotope record can be obtained. Each powder sample weighed between 30 and 126 µg. The 713 individual samples were processed in a Thermo Finnigan MAT 253 continuous flow – isotope ratio mass spectrometer equipped with a Gas Bench II. Isotope data were calibrated against a NBS-19 calibrated Carrara marble standard ($\delta^{18}O = -1.74‰$ and $\delta^{13}C = 2.01‰$) with a 1σ external reproducibility (= accuracy) of 0.07‰ and 0.03‰ for oxygen and carbon isotope values, respectively. The $\delta^{18}O_{shell}$ and $\delta^{13}C_{shell}$ values are expressed relative to the international VPDB (Vienna Pee Dee Belemnite) standard and are given as parts per mil (‰).

The $\delta^{18}O_{shell}$ values can be used to reconstruct temperature of the ambient water ($T_{\delta^{18}O}$) during shell formation if the oxygen isotope value of the ambient water ($\delta^{18}O_{water}$) is known (EPSTEIN et al., 1953). As indicated by the Feigl test (FEIGL, 1958), all sampled shells consisted of 100% aragonite (see also GILLIKIN et al., 2005b), therefore the paleothermometry equation by BÖHM et al. (2000) was employed.

$$(1) \qquad T_{\delta^{18}O}(°C) = (20 \pm 0.2) - (4.42 \pm 0.1) \cdot (\delta^{18}O_{shell}(VPDB) - \delta^{18}O_{water}(VSMOW))$$

A one per mil shift in $\delta^{18}O_{shell}$ corresponds to a change of ambient water temperature by 4.42°C. We used the equation by BÖHM et al. (2000) instead of that by GROSSMAN and KU (1986) because it reduces the error of the calculated temperature by combining data from synthetic aragonite (TARUTANI et al., 1969), mollusks and foraminifera (GROSSMAN and KU, 1986), gastropods (RAHIMPOUR-BONAB et al., 1997) and coralline sponges (BÖHM et al., 2000). Furthermore, the external precision of the mass spectrometer had to be considered, which resulted in an average $T_{\delta^{18}O}$ error of ±0.3°C.

### 4.2.3. Stable isotope values and salinity of seawater

For calibration of the $\delta^{18}O_{shell}$ and $\delta^{13}C_{shell}$ data, the stable oxygen and carbon isotope composition of the water ($\delta^{18}O_{water}$) and dissolved inorganic carbon (DIC; $\delta^{13}C_{DIC}$) was recorded at the localities where the live bivalves were collected (Fig. 1, Tab. 2). Water samples for $\delta^{18}O_{water}$ and $\delta^{13}C_{DIC}$ measurements were collected during the summer between 2003 and 2008 at a depth of ca. 0.5 m. The $\delta^{18}O_{water}$ and $\delta^{13}C_{DIC}$ are reported in per mil versus VSMOW and VPDB, respectively. The average analytical precision was 0.1‰ (1σ).

Table 2. Oxygen and carbon isotope values and salinity (computed from $Na^+$ concentrations; Fig. 3) of water samples collected between 2003 and 2008 from Little Takli Island (Locality 1; Fig. 1) and Mink Island (MI, Localities 2 to 4). Asterisks indicate water samples toxified with $HgCl_2$.

| Date of collection | Locality | $\delta^{18}O_{water}$ (‰ VSMOW) | Standard deviation (1σ) | $\delta^{13}C_{DIC}$ (‰ VPDB) | Standard deviation (1σ) | $Na^+$ [ppm] | $S_{reco}$ [PSU] |
|---|---|---|---|---|---|---|---|
| 11 Sep 03 | MI | -3.03 | 0.08 | -0.59 | 0.08 | | |
| | | -2.90 | | | | | |
| | | -2.91 | | | | | |
| 20 Aug 05 | 1 | -2.79 | 0.04 | 1.39 | 0.04 | | |
| | | -2.80 | | | | | |
| | | -3.18 | | | | | |
| 20 Aug 05 | 4 | -2.85 | 0.04 | 0.54 | 0.04 | | |
| | | -2.71 | | | | | |
| | | -2.95 | | | | | |
| 2 Jul 07 | 4 | -2.14 | 0.03 | -0.51 | 0.03 | | |
| 3 Jul 07 | 1 | -2.38 | 0.11 | 1.93 | 0.11 | 362 | 29.4 |
| | | -2.06 | | | | 362 | 29.4 |
| | | -1.99 | | | | 362 | 29.4 |
| 10 Sep 07 | 1 | -2.97* | 0.08 | -1.75* | 0.08 | 350 | 28.4 |
| | | -3.05* | 0.03 | -0.58* | 0.03 | 350 | 28.4 |
| | | -2.86 | | | | 350 | 28.4 |
| 10 Sep 07 | 4 | -3.13* | 0.10 | -1.70* | 0.10 | 337 | 27.3 |
| | | -3.20* | 0.07 | 0.04* | 0.07 | 337 | 27.3 |
| | | -2.92 | | | | 337 | 27.3 |
| 30 Aug 08 | 3 | -2.73 | 0.09 | | | 352 | 28.6 |
| | | -2.42* | 0.08 | 1.50* | 0.11 | 352 | 28.6 |
| 1 Sep 08 | 2 | -2.92 | 0.08 | | | 348 | 28.2 |
| | | -2.44* | 0.17 | 1.33* | 0.21 | 348 | 28.2 |

To precisely determine the salinity of the water samples, the sodium ion ($Na^+$) concentration of five water samples (collected in 30 ml Teflon containers, acidified with three drops of 65 vol% ultrapure $HNO_3$) was determined with a Spectro CIROS Vision ICP-OES system. We followed the techniques described by SCHRAG (1999) and DE VILLIERS et al.

(2002). The internal precision (given in relative standard deviation [1σ], %RSD) of quintuplicate measurements of a MERCK multielement standard solution (HC961393) was 1.07 %RSD, the external reproducibility (1σ precision of nine measurements) equaled 3.26 %RSD and accuracy was 6.57 %RSD. These data were then converted into salinity

(2) $$S_{Na}(PSU) = Na^{+}(\mu g \cdot g^{-1}) \cdot 35/10783.7$$

where 10,783.7 µg $g^{-1}$ $Na^{+}$ coincides with a salinity of 35 PSU (DOE, 1994). Sodium-derived salinity ($S_{Na}$) and $\delta^{18}O_{water}$ values were significantly linearly correlated (Fig. 3; $R = 0.83$, $R^2 = 0.68$, $p < 0.001$, $n = 13$) as expressed by equation 3 (model II regression, errors are one standard deviation).

(3) $$\delta^{18}O_{water} = (0.54 \pm 0.08) \cdot S_{Na} - (18.11 \pm 2.41)$$

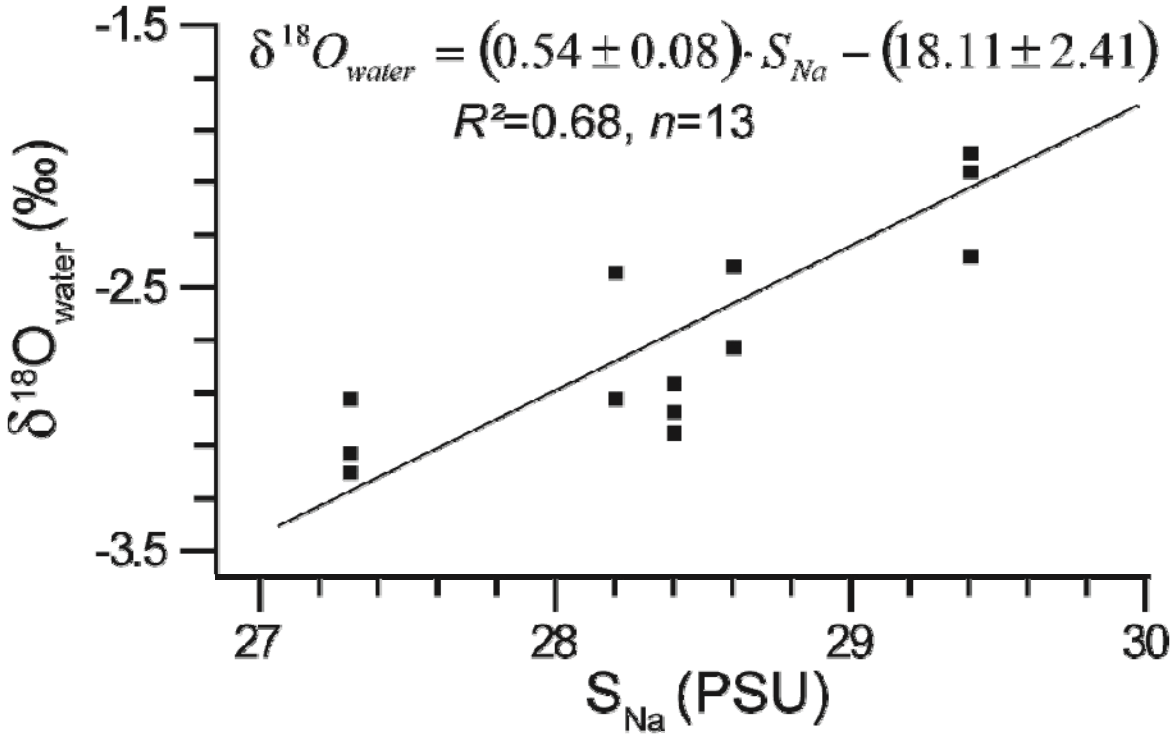


Figure 3. Relationship between oxygen isotope values of the water and salinity (computed from $Na^{+}$ concentration). Errors are one standard deviation.

### 4.2.4. Temperature logger data

Four HOBO temperature loggers were deployed in the intertidal zone (N58°3', W154°25') at the four study localities (Fig. 1). The loggers recorded temperature ($T_{logger}$) every 30 minutes from April 15, 2006 (8:30 PM) to July 3, 2007 (11:30 AM) and September 3, 2006 (8:00 PM) to September 10, 2007 (9:00 AM), respectively (Tab. 3). A set of two new HOBO data loggers were installed on September 9, 2007 and recorded seawater temperatures every hour until August 30, 2008 (8:00 PM) and September 1, 2008 (9:00 PM), respectively (Tab. 3). The resolution was 0.02°C and the accuracy ±0.2°C. For comparison with $\delta^{18}O_{shell}$ values, only temperature logger data recorded during high tide (i.e., when water level was above mean tide level of 2.05 m) were considered, because shells from the intertidal zone grow only when submerged in water during high tide (e.g., EVANS, 1972; OHNO, 1989).

Table 3. Water temperatures recorded during high tide from April 15, 2006 to September 1, 2008 by six HOBO data loggers at four different localities near Mink Island and Little Takli Island, Alaska. MLLW = Mean Lower Low Water (0-ft tide elevation).

| Locality | Logger # | Logger time interval | Relative height MLLW [ft] | Logger interval | $T_{min}$ [°C] | $T_{max}$ [°C] |
|---|---|---|---|---|---|---|
| 1 | 902115 | 3 Sep 06 – 10 Sep 07 | -0.6 to -0.7 | half-hourly | -0.2 | 13.0 |
| 2 | 902116 | 15 Apr 06 – 3 Jul 07 | +1.5 | half-hourly | -0.9 | 13.1 |
| | 1044802 | 9 Sep 07 – 1 Sep 08 | +1.5 | hourly | -1.4 | 13.9 |
| 3 | 902117 | 15 Apr 06 – 3 Jul 07 | +1.5 | half-hourly | -2.2 | 13.9 |
| | 1044800 | 9 Sep 07 – 30 Aug 08 | +1.5 | hourly | -4.6 | 14.9 |
| 4 | 902118 | 3 Sep 06 – 10 Sep 07 | +6 | half-hourly | -1.6 | 13.5 |

For years prior to 2006, high-resolution temperature data ($T_{reco}$) were reconstructed from $T_{logger}$ and satellite-derived sea surface temperature data of 1998-2008, which were recorded at six-hour intervals ($T_{NCEP}$; 2° x 2° grid centered at N54°, W152°; NCEP/DOE AMIP-II Reanalysis obtained from http://www.esrl.noaa.gov/; last accessed on November 26, 2010). The following linear model ($R^2 = 0.97$, $p < 0.0001$) was used to compute $T_{reco}$ from $T_{NCEP}$ (eq. 4).

(4) $$T_{reco} = 1.1038 \cdot T_{NCEP} - 0.6414$$

### 4.2.5. Further environmental data

Salinity measurements were obtained from the oceanographic station GAK1, which is located at the mouth of Resurrection Bay within the ACC (N59°50'42'', W149°28'0''; Fig. 1) (http://www.ims.uaf.edu/gak1/, last accessed on November 26, 2010). The Alaska coastal discharge (total discharge near Seward in $m^3/s$) was also measured by this station. Monthly accumulated rainfall data (mm) with a spatial resolution of 2.5° x 2.5° were gathered from the Global Precipitation Climatology Project (GPCP) for the area of W154°31' to W154°24', N58°02' to N58°04'. The GPCP combined precipitation data were developed and computed by the NASA/Goddard Space Flight Center's Laboratory for Atmospheres as a contribution to the GEWEX Global Precipitation Climatology Project (Available at http://disc2.nascom.nasa.gov/Giovanni/tovas/rain.GPCP.shtml).

Chlorophyll *a* fluorescence was measured in water pumped from a depth of 4 meters on the Alaska Marine Highway System ferry *Tustumena* and converted to chlorophyll concentration from discrete water samples calibrated in the laboratory (COKELET et al., 2010). Chlorophyll *a* measurements in 2006 and 2007 were averaged along 44 transects within a 25 $km^2$ box centered on N57°50'6'', W154°0'0'' – the ferry's nearest approach point southeast of Mink Island (Fig. 1).

### 4.2.6. AMS radiocarbon dating

To obtain the absolute age of the archaeological shells, material was sampled from the ventral margin (most recent years of shell growth) of five *S. gigantea* specimens from the Mink Island shell midden site XMK-030 (near sample locality 3, Fig. 1, Tab. 4). First, the periostracum and the outermost 100 µm of shell carbonate were physically removed, and then 70 to 120 mg of shell carbonate was taken for radiocarbon analysis. Radiometric ages were determined by $^{14}C_{AMS}$ dating performed at the Poznań Radiocarbon Laboratory (Poland). Conventional radiocarbon ages were converted to calibrated $^{14}C_{AMS}$ ages by the program Calib 6.0 (STUIVER and REIMER, 1993) using the Marine09 calibration dataset (REIMER et al., 2009). The local $^{14}C$ marine reservoir effect ($\Delta R$) for the study region is assumed to be 300±100 years (MCNEELY et al., 2006).

Table 4. Uncalibrated and calibrated (cal yr BP) $^{14}C_{AMS}$ ages of five *S. gigantea* specimens from the Mink Island shell midden. Conventional ages were converted to calendar years by the program Calib 6.0 (STUIVER and REIMER, 1993) using the Marine09 calibration dataset by REIMER et al. (2009) and assuming a local calibration value (ΔR) of 300±100 years.

| Shell ID | Laboratory ID | Conventional $^{14}C_{AMS}$ age [yr BP] | 95.4% (2σ) Calibrated age ranges [cal yr BP] |
|---|---|---|---|
| GI-MI20572-D1R | Poz30759 | 1530±30 | 599-994 |
| GI-MI20572-D2L | Poz30760 | 1550±30 | 621-1014 |
| GI-MI81972-D1L | Poz30766 | 1980±30 | 988-1447 |
| GI-MIXMK030-D1L | Poz30767 | 2030±30 | 1057-1508 |
| GI-MI20510-D2R | Poz30758 | 2175±30 | 1237-1680 |

## *4.3. RESULTS*

### 4.3.1. Shell growth of modern and archaeological shells

Overall sizes and ontogenetic ages of modern and archaeological *Saxidomus gigantea* shells from Mink Island and Little Takli Island were similar. On average, the studied specimens were 7±4 years-old and measured 40±16 mm in height (1σ, n = 20, Tab. 1). Annual growth increment widths decreased exponentially with maximum rates occurring during age one to three (Fig. 4A).

Lunar daily (= circatidal) growth increments (LDGI) and fortnight increments were identifiable between annual growth lines of all specimens. However, in only twelve modern and three archaeological shells, the number and widths of LDGI and therefore, the duration of the growing season, and the seasonal growth rate could be reliably determined throughout at least one full growing season (Tab. 1, Fig. 4B). According to these data, modern and archaeological clams from SW Alaska grew for about six to seven and seven to eight months per year, respectively. Live-collected shells with known dates of death were precisely temporally aligned by means of LDGI counts. LDGI curves of other years from live-collected specimens started and ended at 4-5°C. However, the LDGI time-series of the archaeological specimens were aligned so that the curve shapes fitted best to that of modern specimens. Therefore, the growing season of modern shells lasted from late April/early May to late October/early November, whereas archaeological shells started growing in early/mid April and stopped growing in mid/late November. In three year-old modern specimens, LDGI

widths measured ~ 10 µm near the 'winter' lines and were broadest (on average 70 µm in modern shells) about half-way between the annual growth lines.

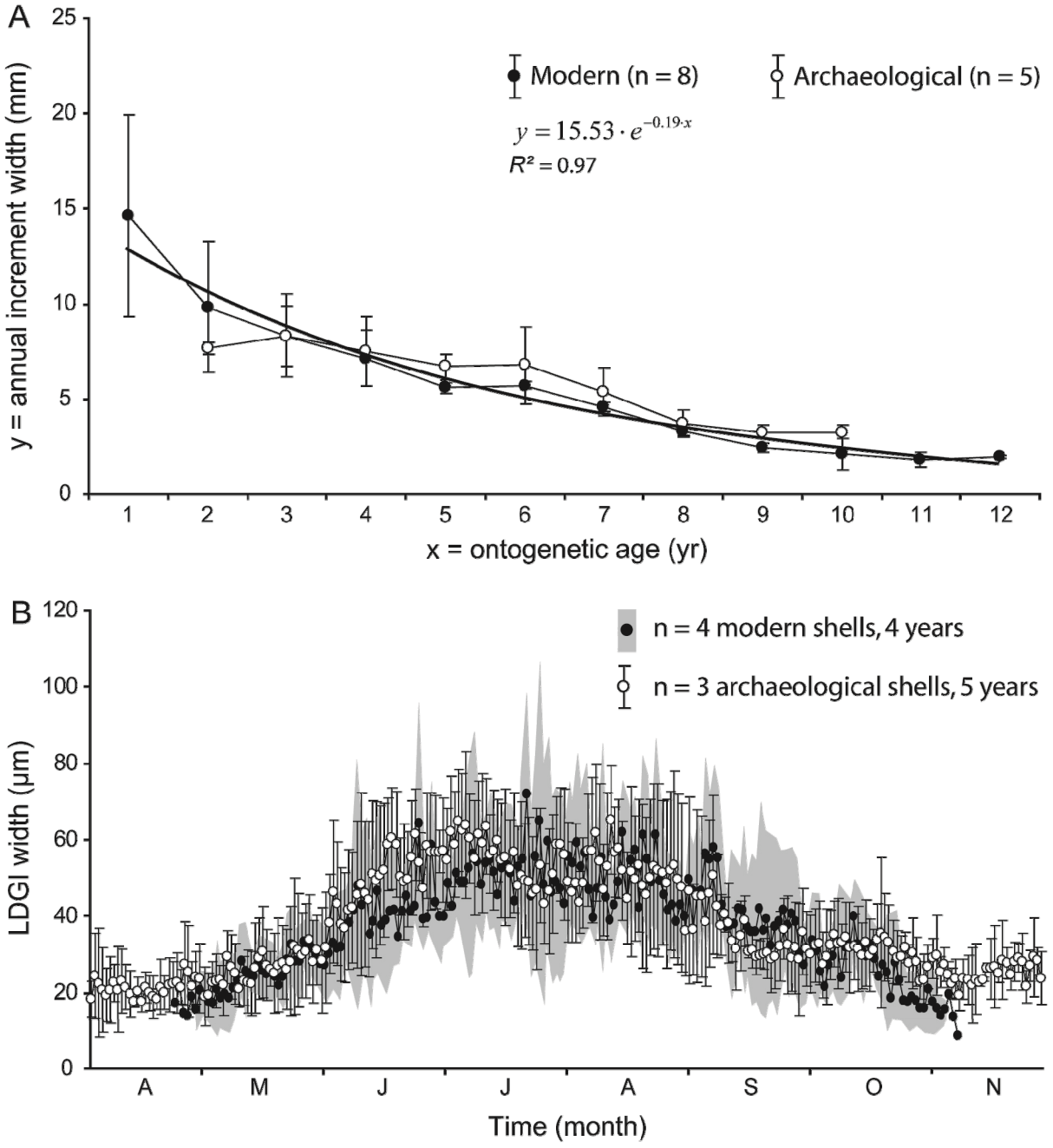


Figure 4. Annual (A) and seasonal (B) shell growth of *Saxidomus gigantea*. A) Annual increment data of eight modern and five archaeological shells were depicted (modern specimens GI1-LTI0707-A1L, -A3L, -A4L, -A7L, GI1-LTI0907-A8L, GI-MI0898-A5R, GI-MI0903-A3L, -A5L). B) The average intra-annual growth curves are based on lunar daily increment width data from a total of four years from four modern shells (GI1-LTI0707-A3L, GI1-LTI0907-A2L, GI3-MI0808-A7L, GI2-MI0707-A3L; ontogenetic age = three) and from a total of five years from three archaeological shells (GI-MI81972-D1L: three years, GI-MI20572-D2L: one year, GI-MI20572-D1R: one year). Variability is shown as 1σ standard

deviation (error bars and grey curve). Live-collected shells with known dates of death were precisely temporally aligned by means of LDGI counts. However, the LDGI time-series of the archaeological specimens were so aligned that the curve shapes fitted best to that of modern specimens.

### 4.3.2. Stable isotope values of modern and archaeological shells

Modern and archaeological specimens showed similar patterns in their seasonal stable isotope profiles. A representative intra-annual isotope profile of a modern shell with a known date of collection is depicted in Figure 5. Shell oxygen isotope ($\delta^{18}O_{shell}$) curves exhibited distinct seasonal cycles with most positive values occurring at the winter growth lines and most negative values occurring during the second half of the year. The seasonal $\delta^{13}C_{shell}$ values showed a similar but more variable pattern than the $\delta^{18}O_{shell}$ chronologies. Ontogenetic age-related trends were not observed in stable oxygen or carbon isotope curves (Fig. 5).

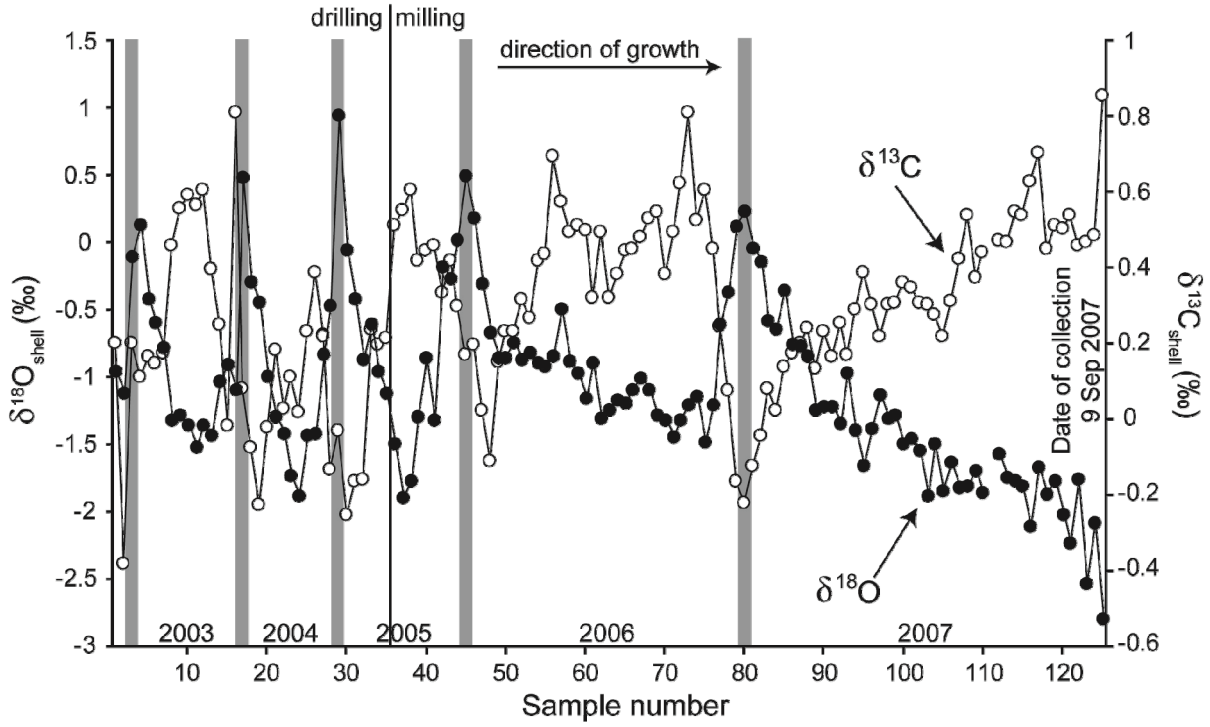


Figure 5. Typical high-resolution stable oxygen and carbon isotope profile of a modern specimen (GI1-LTI0907-A1L). The shell was collected on September 9, 2007 from Little Takli Island, Alaska. Filled circles = $\delta^{18}O_{shell}$; open circles = $\delta^{13}C_{shell}$. Vertical grey bars represent winter growth lines. 1σ external reproducibility (= accuracy) is 0.07‰ and 0.03‰ for oxygen and carbon isotope values, respectively.

Since different powder samples taken for isotope analysis represent different amounts of time, we used a modified mathematical technique of SCHÖNE et al. (2005b) to equalize the amount of time represented by each sample. In most cases, eight isotope samples were obtained from each annual increment. Therefore, this number was set as the required minimum number of samples per year. Any annual increment that did not contain at least eight samples was discarded. Intra-annual $\delta^{18}O_{shell}$ data were then fitted with linear fits, and the curves re-sampled so that each sample represented an approximately equal portion of time. This was achieved by using the average seasonal growth curve for the study area (Fig. 4B). The temporally equalized isotope values ($\delta^{18}O_{shell}$', $\delta^{13}C_{shell}$') were used to directly compare isotope data with each other (Fig. 6).

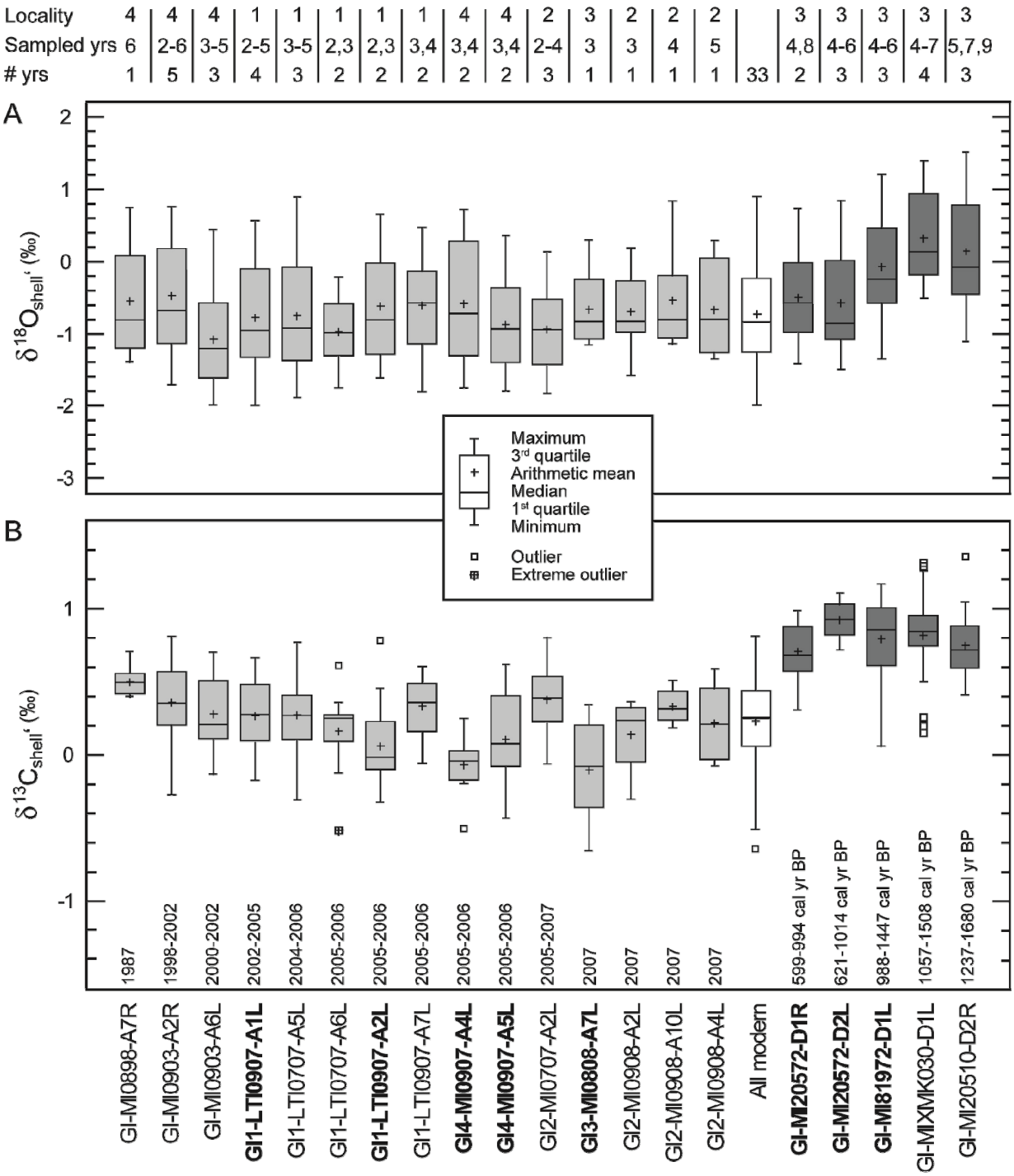


Figure 6. Boxplots showing $\delta^{18}O_{shell}$' (A) and $\delta^{13}C_{shell}$' (B) values of fifteen modern (light grey) and five archaeological (dark grey) specimens. The white box represents the isotope values of all studied modern shells. Prior to the analyses, seasonal isotope values were re-sampled so that each sample represented the same amount of time. This mathematical conversion enabled a direct comparison of the isotope values, but reduced the seasonal amplitudes. Bold font: lunar daily shell growth data available.

In the boxplots in Figure 6, the $\delta^{18}O_{shell}$' and $\delta^{13}C_{shell}$' data of fifteen modern and five archaeological shells are shown including the average, quartiles as well as maximum and minimum values of each specimen. Each box represents up to five years (ontogenetic years two to six in modern and, owing to preservation issues, years four to nine in archaeological shells) of a single specimen, except for the white box that represents the average modern shell. For a more reliable comparison of archaeological shells with modern specimens, it was necessary to characterize the modern environment of the entire study area together with its inter-annual and site-specific variability (Fig. 6). The original isotope data set consisted of 524 powder samples from modern shells and 189 samples from archaeological specimens. As a result of re-sampling (see above), each isotope sample represented nearly the same amount of time (~three to four weeks), which enabled a direct comparison of data acquired by different sampling resolution. This mathematical conversion also reduced the seasonal amplitudes in shell portions that were originally sampled with higher resolution.

The average $\delta^{18}O_{shell}$ and $\delta^{13}C_{shell}$ values (Fig. 6) of all modern specimens equaled −0.73±0.70‰ and 0.24±0.29‰ (arithmetic means ± 1σ), respectively. Average minimum and maximum values were −1.99‰ and 0.91‰ for $\delta^{18}O_{shell}$ values and −0.66‰ and 0.81‰ for $\delta^{13}C_{shell}$ values, respectively. According to ANOVA analyses, there was significantly more variability observed among stable carbon isotope values than oxygen isotope values (Fisher-LSD test, $p < 0.05$).

When comparing modern to archaeological specimens, oxygen isotope values from GI-MI81972-D1L, GI-MIXMK030-D1L and GI-MI20510-D2R differed significantly from the average modern shell (Fisher-LSD test, $p < 0.05$), indicating they are more positive than recent shells (Fig. 6A). This applied to average (+0.7 to +1.1‰) and extreme values (~ +0.3 to +1.5‰). However, the more recent archaeological shells fell within the oxygen isotope range of modern specimens (Fig. 6A). In contrast, all studied archaeological shells were, on average, 0.4 to 0.7‰ more positive than modern specimens in their $\delta^{13}C_{shell}$ signatures (Fig. 6B).

### 4.3.3. Shell growth, light stable isotopes and their relation to the local environment

In order to evaluate the observed differences between modern and archaeological shells (Fig. 6), seasonal shell growth and stable isotope data ($\delta^{18}O_{shell}$, $\delta^{13}C_{shell}$) of seven modern *S. gigantea* specimens (in which LDGI were well developed) were compared to environmental data (Fig. 7).

The seasonal cycle of recorded water temperature ($T_{logger}$; all localities combined) during high tide ranged from −4.6°C (likely, air temperatures were recorded when loggers were not completely immersed) to 14.9°C (Fig. 7). At all studied localities, the highest water temperature occurred in August. The water temperature was well correlated between the four localities ($R = 0.97$ to $0.99$, $p < 0.0001$). However, contemporaneously recorded temperatures at the four localities revealed an average difference of 0.9°C. Maximum differences between the loggers were as high as 4.9°C. Approximately 5% of all data points recorded contemporaneously by all loggers revealed a difference of 2°C.

When placed in temporal context by means of LDGI, shell growth is most strongly associated with water temperature. Simple linear regression analysis (eq. 5, Tab. 5) suggested that water temperature explains the majority (70%) of the variability in shell growth (adjusted $R^2 = 0.70$, $p < 0.0001$, $n = 190$). For this relationship, an average intra-annual growth curve totalling seven years based on LDGI data from five modern shells was used (GI1-LTI0707-A2L: one year, -A3L: two years, GI2-MI0707-A3L: one year, GI4-MI0907-A5L: two years, GI1-LTI0907-A2L: one year; ontogenetic ages = two to four).

(5) $$LDGI = 4.66 \cdot T - 11.77$$

Table 5. Results (statistical values R, adjusted $R^2$, p and n) of simple and multiple regressions for LDGI, $\delta^{18}O_{shell}$, $\delta^{13}C_{shell}$ and the environmental parameters temperature (T), precipitation (P), discharge (D), salinity (S) and chlorophyll (Chl).

| Parameters | Statistical values | | | |
|---|---|---|---|---|
| | R | $R^2$ | p | n |
| Simple regressions | | | | |
| LDGI~T | 0.84 | 0.70 | < 0.0001 | 190 |
| $\delta^{18}O_{shell}$~T | -0.96 | 0.92 | < 0.0001 | 72 |
| $\delta^{18}O_{shell}$~P | -0.14 | 0.46 | > 0.05 | 72 |
| $\delta^{18}O_{shell}$~D | -0.32 | 0.09 | < 0.01 | 72 |
| $\delta^{13}C_{shell}$~S | 0.88 | 0.78 | < 0.0001 | 72 |
| $\delta^{13}C_{shell}$~Chl | 0.54 | 0.29 | < 0.0001 | 72 |
| T~S | -0.87 | 0.75 | < 0.0001 | 200 |
| T~Chl | -0.82 | 0.67 | < 0.0001 | 178 |
| S~Chl | 0.82 | 0.67 | < 0.0001 | 178 |
| | | | | |
| Multiple regressions | | | | |
| $\delta^{18}O_{shell}$~T, P, D | | 0.96 | < 0.0001 | 72 |
| $\delta^{13}C_{shell}$~S, Chl | | 0.81 | < 0.001 | 72 |

Fastest shell growth (on average ~70 µm per day in three year-old specimens) occurred during July at average temperatures of 12°C (and extreme temperatures of nearly 15°C) and slowest growth (~10 µm per day) during periods of colder temperatures. Little to no growth was observed below ~4-5°C, which is in agreement with previous findings (BERNARD, 1983; GILLIKIN et al., 2005a; HALLMANN et al., 2009).

Most negative $\delta^{18}O_{shell}$ values occurred in August and most positive values in April and October. Even though some contemporaneous specimens grew in close proximity, shell oxygen isotope values differed on average by ca. 1‰. This difference was slightly larger during the summer. When oxygen isotope values of the water were available (Tab. 2), the $\delta^{18}O_{shell}$-derived water temperatures ($T_{\delta^{18}O}$) resembled the instrumental temperatures ($T_{logger}$) to the nearest ~0.5 to 1°C (Fig. 7) confirming previous findings that *S. gigantea* precipitates its shell near oxygen isotopic equilibrium with the ambient water (GILLIKIN et al., 2005a).

Assuming that the $\delta^{18}O_{water}$ values remained unchanged (−2.86‰ as measured on September 10, 2007), water temperatures were underestimated by ~3°C during the spring and fall of 2006, but were overestimated by about 3° to 5°C in early summer of 2007 (Fig. 7). This discrepancy in temperature estimates likely corresponds to shifting seasonal freshwater discharge and lower salinity (Fig. 7). Despite varying seasonal $T_{\delta^{18}O}$ amplitudes, the measured and reconstructed seasonal temperature profiles were in phase (Fig. 7).

A significant (stepwise multiple regression, $p < 0.0001$, $n = 72$) statistical relationship was observed between $\delta^{18}O_{shell}$ (average curve: 22 years from 9 specimens), temperature (T), precipitation (P) and discharge (D, eq. 6, Tab. 5). Temperature accounted for 92% of the variation in $\delta^{18}O_{shell}$ (simple linear regression). All parameters together accounted for 96% of the variance.

(6) $$\delta^{18}O_{shell} = -0.33 \cdot T + 0.01 \cdot P - 3 \cdot 10^{-5} \cdot D + 2.19$$

In contrast to oxygen isotopes, the $\delta^{13}C_{shell}$ curves exhibited a greater variability. Most positive $\delta^{13}C_{shell}$ values typically occurred in shell portions that were formed between July and September. However, shell stable carbon isotope values varied by more than 1‰ between different specimens (Fig. 7). In addition, $\delta^{13}C_{shell}$ values deviated from measured $\delta^{13}C_{DIC}$ values by up to +2.56‰ and −2.59‰. Even with these discrepancies, a highly significant (stepwise multiple regression, $p < 0.001$, $n = 72$) statistical relationship was observed between $\delta^{13}C_{shell}$ (average curve: 22 years from nine specimens), salinity (S) and chlorophyll *a* (eq. 7, Tab. 5). Chlorophyll accounted for 29% and salinity 78% of the variance (simple linear regressions). Some of the variation in $\delta^{13}C_{shell}$ may be simultaneously explained by both variables. Both parameters together accounted for 81% of the variance.

(7) $$\delta^{13}C_{shell} = -0.08 \cdot S + 0.01 \cdot Chl + 2.44$$

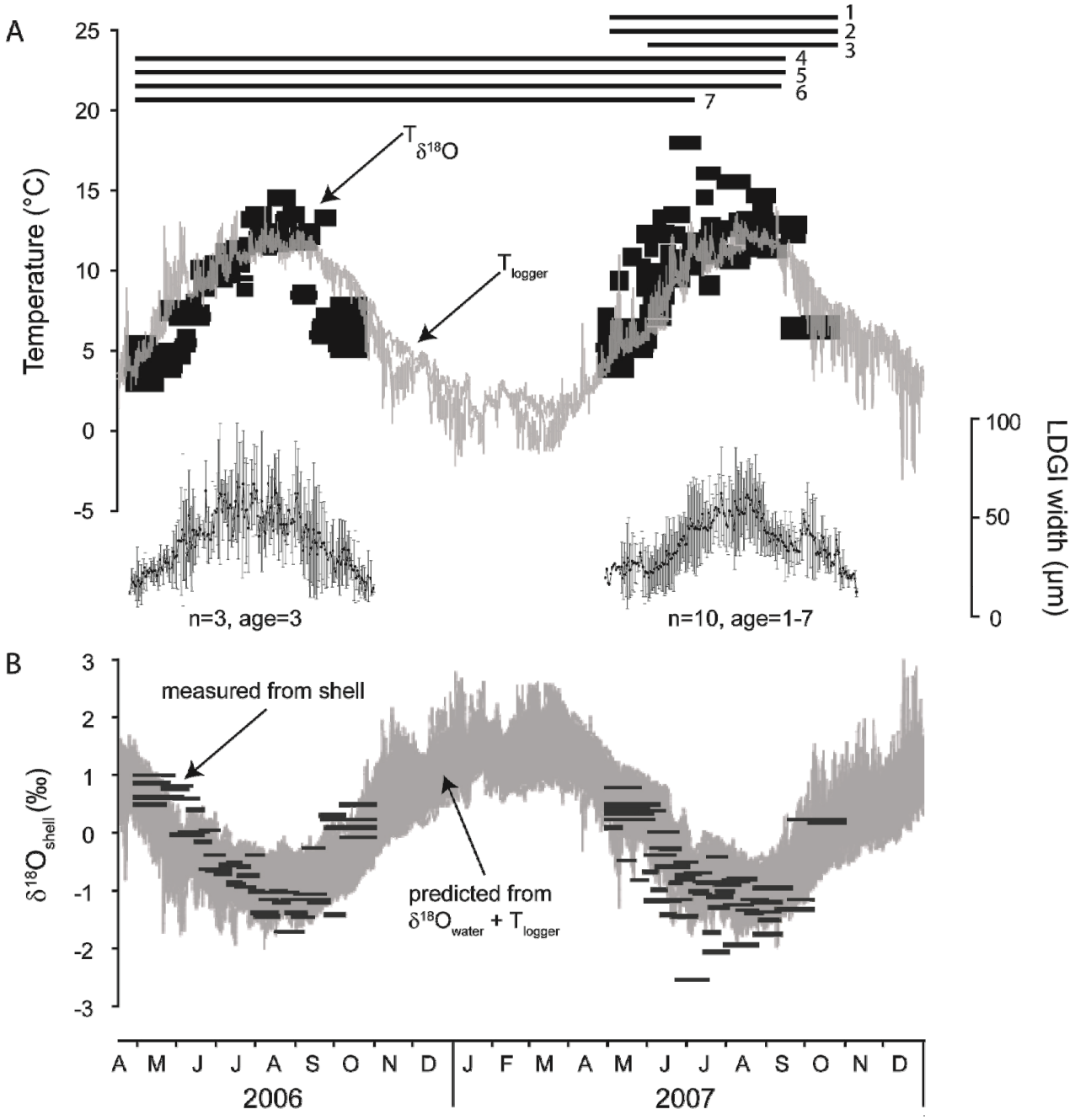
A
B
Temperature (°C)
LDGI width (µm)
T δ18O
T logger
n=3, age=3
n=10, age=1-7
δ18Oshell (‰)
measured from shell
predicted from
δ18Owater + Tlogger
A M J J A S O N D J F M A M J J A S O N D
2006
2007

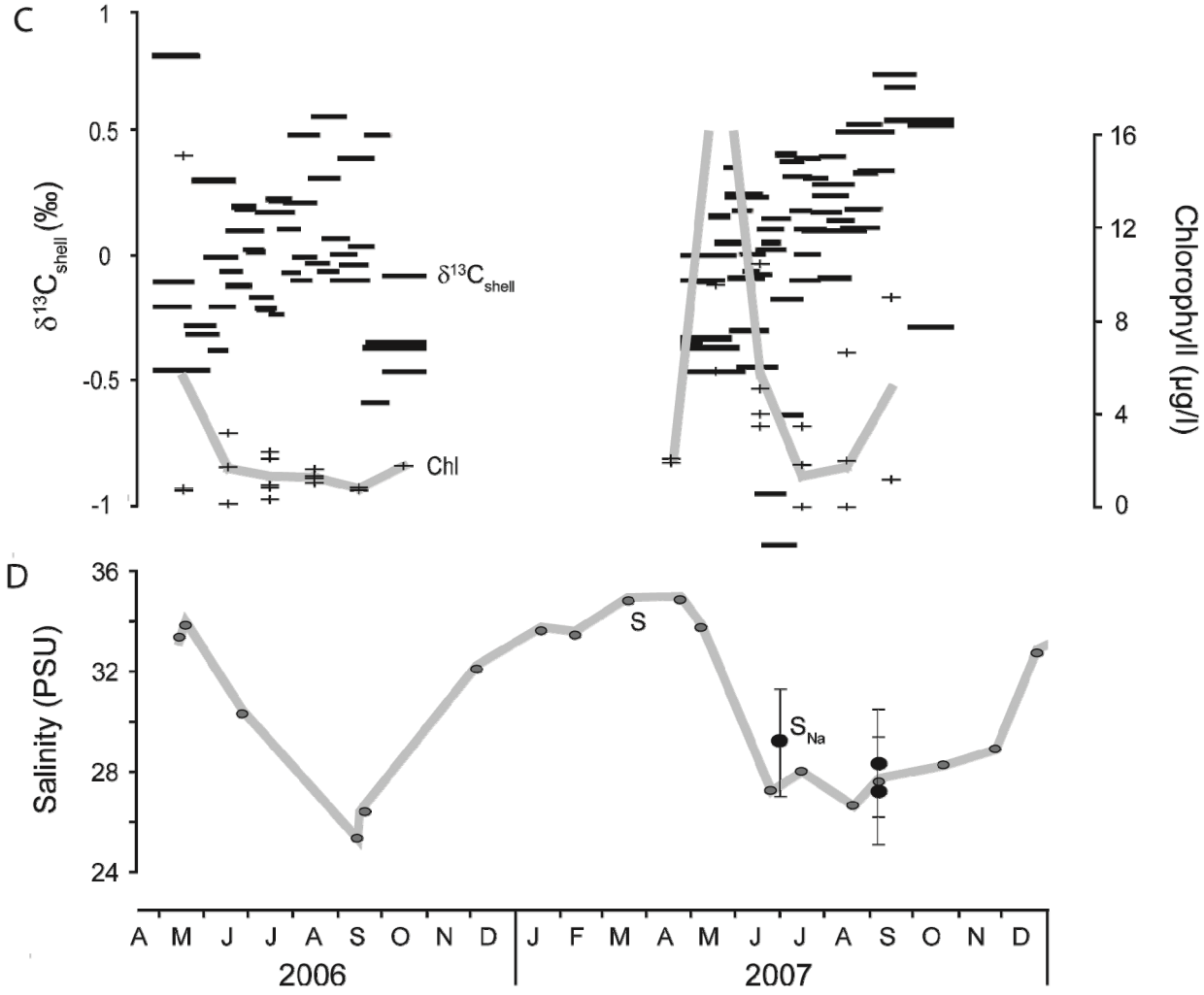


Figure 7. Lunar daily shell growth (LDGI) and stable oxygen isotope data of *Saxidomus gigantea* in comparison to environmental data (temperature, chlorophyll *a* and salinity). Horizontal lines on top denote temporal coverage of the seven bivalve specimens used in this figure (GI1-LTI0707-A5L, GI1-LTI0907-A2L, GI4-MI0907-A4L, -A5L, GI3-MI0808-A3L, -A7L, GI2-MI0908-A4L). A) To compute shell oxygen isotope-derived temperatures ($T_{\delta^{18}O}$; black bars in upper graph; vertical extension denotes error range (95% confidence interval) as given by the paleothermometry equation of Böhm et al., 2000; horizontal extension of bars denote time represented by $T_{\delta^{18}O}$), a $\delta^{18}O_{water}$ value of −2.86‰ was used (measured on September 10, 2007; Tab. 2). Measured temperatures ($T_{logger}$) from six loggers are shown in grey. Note the good agreement between LDGI curves, $T_{\delta^{18}O}$ and $T_{logger}$. B) Measured shell oxygen isotope data ($\delta^{18}O_{shell}$, black horizontal lines; extension of lines denote time represented by $\delta^{18}O_{shell}$ value) were plotted against predicted $\delta^{18}O_{shell}$ values (grey), which were calculated with $\delta^{18}O_{water}$ values of −3.2 and −1.99‰ (Tab. 2), the minimum and maximum values that were recorded during 2007. C) $\delta^{13}C_{shell}$ data (black horizontal lines) in comparison with chlorophyll *a* data recorded by a ferry (crosses, solid lines, grey shading; Fig. 1). There is a chlorophyll *a* peak in May 2007 of 21.4 µg/l. D) Salinity data recorded at coastal station GAK1 (Fig. 1) and salinity computed from sodium concentration in water samples ($S_{Na}$).

It still remains unanswered why $\delta^{18}O_{shell}$ values of three archaeological shells were significantly more positive than that of all modern shells from the same region. Were temperatures lower and/or waters more saline (i.e., less freshwater influx = more positive $\delta^{18}O_{water}$ values) between ~988 and 1680 cal yr BP? To solve this question, a growth-temperature (GT) model adapted from SCHÖNE et al. (2002) was used to estimate water temperatures from daily shell growth rates (Fig. 8). Ten intra-annual LDGI time-series of seven modern shells that lived between 2004 and 2007 were used to calibrate the model (Tab. 1). Each LDGI time-series was corrected for fortnightly variations and the age-related decline in shell growth. Likewise, $T_{logger}$ chronologies exhibited tide-related variations, which were removed in Fourier space and the data back-transformed to the time domain.

Filtered and detrended lunar daily shell growth data (LDGI') of a total of ten years from seven modern specimens were plotted against filtered $T_{logger}$ data ($T_{logger}$'). As seen from Figure 8, LDGI' and $T_{logger}$' exhibit a highly significant positive correlation ($p < 0.0001$). During the first half of the growing season, i.e., until fastest growth rates were attained, the LDGI'– $T_{logger}$' relationship (eq. 8) was only slightly different from that of the second half of the growing season (eq. 9), indicating that shells grew as fast during the first half of the growing season as during the remaining part of the year despite 2°C lower temperatures.

(8) $$T_{inc} = 3 \cdot 10^{-5} \cdot (LDGI')^3 - 0.006 \cdot (LDGI')^2 + 0.441 \cdot (LDGI') - 1.484$$
$$(R^2 = 0.89)$$

(9) $$T_{inc} = 2 \cdot 10^{-6} \cdot (LDGI')^3 - 0.003 \cdot (LDGI')^2 + 0.308 \cdot (LDGI') + 2.232$$
$$(R^2 = 0.92)$$

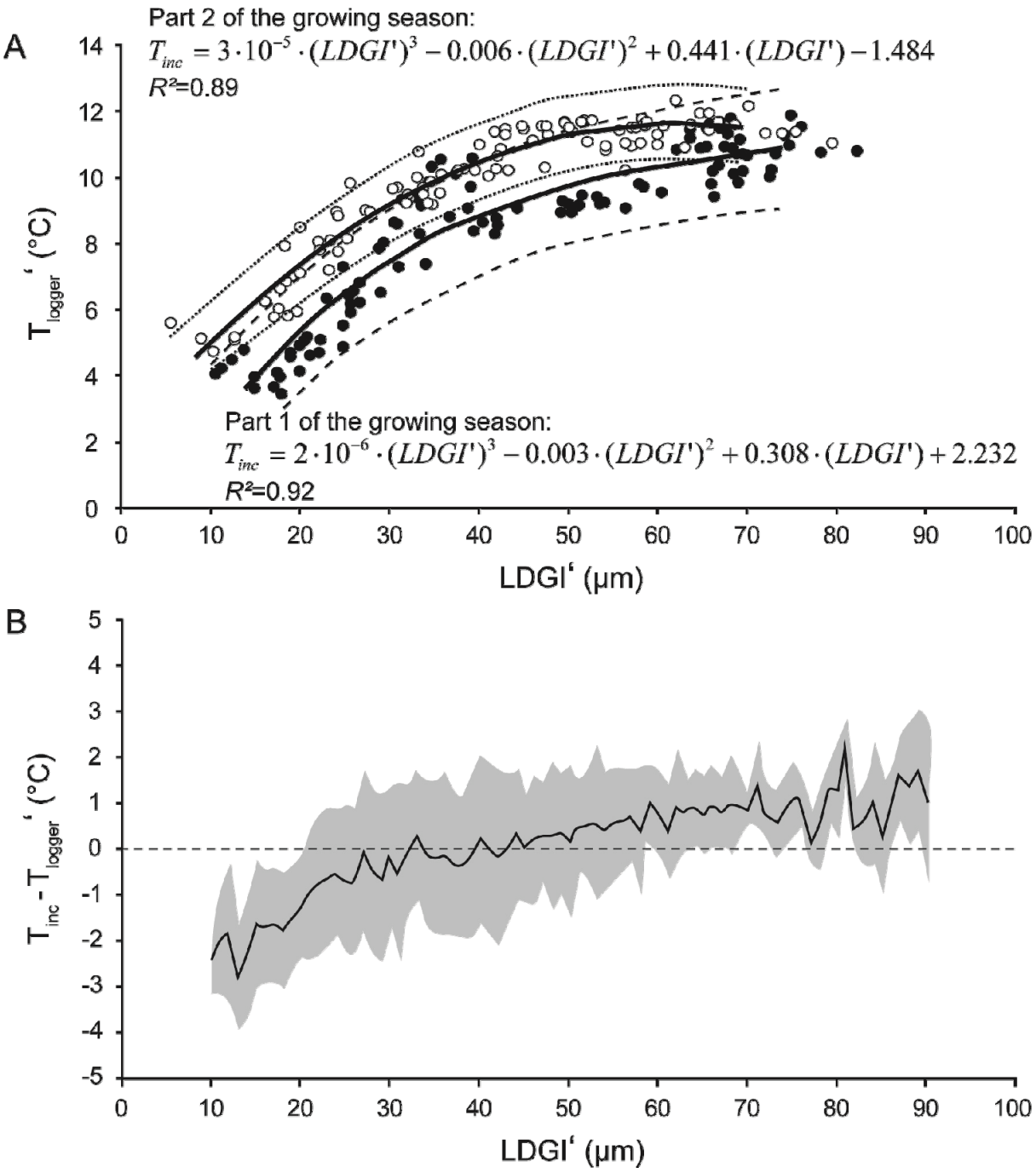


Figure 8. Growth-temperature (GT) model. (A) Tidal-cycle corrected and age-detrended average lunar daily shell growth data (LDGI') of a total of ten years from seven modern specimens of *Saxidomus gigantea* plotted against tidal-cycle corrected temperature logger data ($T_{logger}$'). LDGI' and $T_{logger}$' exhibit a highly significant positive correlation ($p < 0.0001$). During the first half of the growing season, i.e., until fastest growth rates were attained, the LDGI'– $T_{logger}$' relationship was only slightly different from that of the second half of the growing season, indicating that shells grew as fast during the first half of the growing season as during the remaining part of the year despite 2°C lower temperatures. Equations shown in this graph can be used to reconstruct increment-derived water temperatures ($T_{inc}$) from LDGI'. Dashed lines represent 95% confidence interval. (B) Deviations of $T_{inc} - T_{logger}$' vs. LDGI' for the seven specimens. The grey curve is one standard deviation.

The GT model enables temperature estimates ($T_{inc}$) from shell growth data. The relative standard error (SE) associated with daily increment-derived temperatures was computed as follows.

(10) $$SE(\%) = \frac{\left| T_{inc} - T_{logger} \right|}{T_{logger}} \cdot 100$$

By using $T_{inc}$ and $\delta^{18}O_{shell}$ values, it is possible to reconstruct $\delta^{18}O_{water}$ signatures during shell deposition. In turn, $\delta^{18}O_{water}$ values are strongly positively correlated to salinity (Fig. 3). Therefore, increment-derived water temperature estimates and shell oxygen isotope data can be used to estimate salinity ($S_{inc}$; Fig. 9).

We tested the GT model with the modern shell, GI1-LTI0907-A1L (years 2-7, 2002-2007; Fig. 9A). Reconstructed ($T_{inc}$) and measured temperatures ($T_{logger}$) as well as $T_{inc}$ and $T_{reco}$ revealed a highly significant correlation ($R = 0.80$, $R^2 = 0.65$, $p < 0.0001$, $n = 200$). As seen in Figure 9A, the curve shapes of $T_{inc}$ and $T_{logger}$ as well as $T_{inc}$ and $T_{reco}$ closely resembled each other. The average relative standard error was 20% (= 1.3°C). Minimum and maximum reconstructed temperatures ($T_{inc}$) equaled 2.9° and 14.6°C, respectively; during the same time interval, $T_{logger}$ ranged from −0.2° to 13.0°C (Tab. 3; low winter temperatures are likely air temperatures). In combination with $T_{inc}$, measured $\delta^{18}O_{shell}$ values enabled the reconstruction of $\delta^{18}O_{water}$ values by using equation 1, which, in turn, were used to compute $S_{inc}$ by using equation 3. The increment-derived salinity range of 23.8 to 30.7 PSU was in the range of the observed salinity at station GAK1 and $S_{Na}$ (25.7 to 31 PSU) during 2007 (Fig. 9A). The maximum difference between $S_{inc}$ and salinity measured at the station GAK1 was 3.5 PSU. The average error for the reconstruction of salinity from growth increments was 1.4±1.1 PSU (1 sigma). It should be noted that salinity exhibited large variations of up to ca. 4 PSU within a single month (Fig. 9A). For years with too few salinity data from station GAK1 and without $S_{Na}$ values, $S_{inc}$ were compared to monthly salinity at GAK1 averaged over 1998-2007.

In a further step, the GT model was applied to three archaeological specimens (GI-MI20572-D1R, GI-MI20572-D2L and GI-MI81972-D1L; Figs 9B-D) with distinctly developed LDGI (cf. Fig. 4). Although minimum and maximum $T_{inc}$ of all three shells were in

the same range as in modern specimens, i.e., ~3-4° to 15.1°C, respectively, the seasonal $T_{inc}$ curves differed from each other and from modern temperatures (seasonal $T_{reco}$ curves of 1998-2008) of the study area (Figs 9B-D). The oldest studied shell, which was alive during 988-1447 cal yr BP, showed ~1-2°C lower water temperatures during summer (Fig. 9D). In contrast, the more recent archaeological shells (GI-MI20572-D1R and GI-MI20572-D2L) alive during 599-1014 cal yr BP suggested up to 3°C lower temperatures than at present (Figs 9B and 9C). The salinity amplitude (27.1 to 32.0 PSU) reconstructed from the oldest of the three shells was much lower than at present (1998-2007 monthly averages at GAK1), and late summer values remained 2 to 5 PSU above modern values (Fig. 9D). On the contrary, the more recent archaeological shells suggested up to 1-2 PSU fresher than modern conditions prevailed during 599-1014 cal yr BP (Figs 9B and 9C).

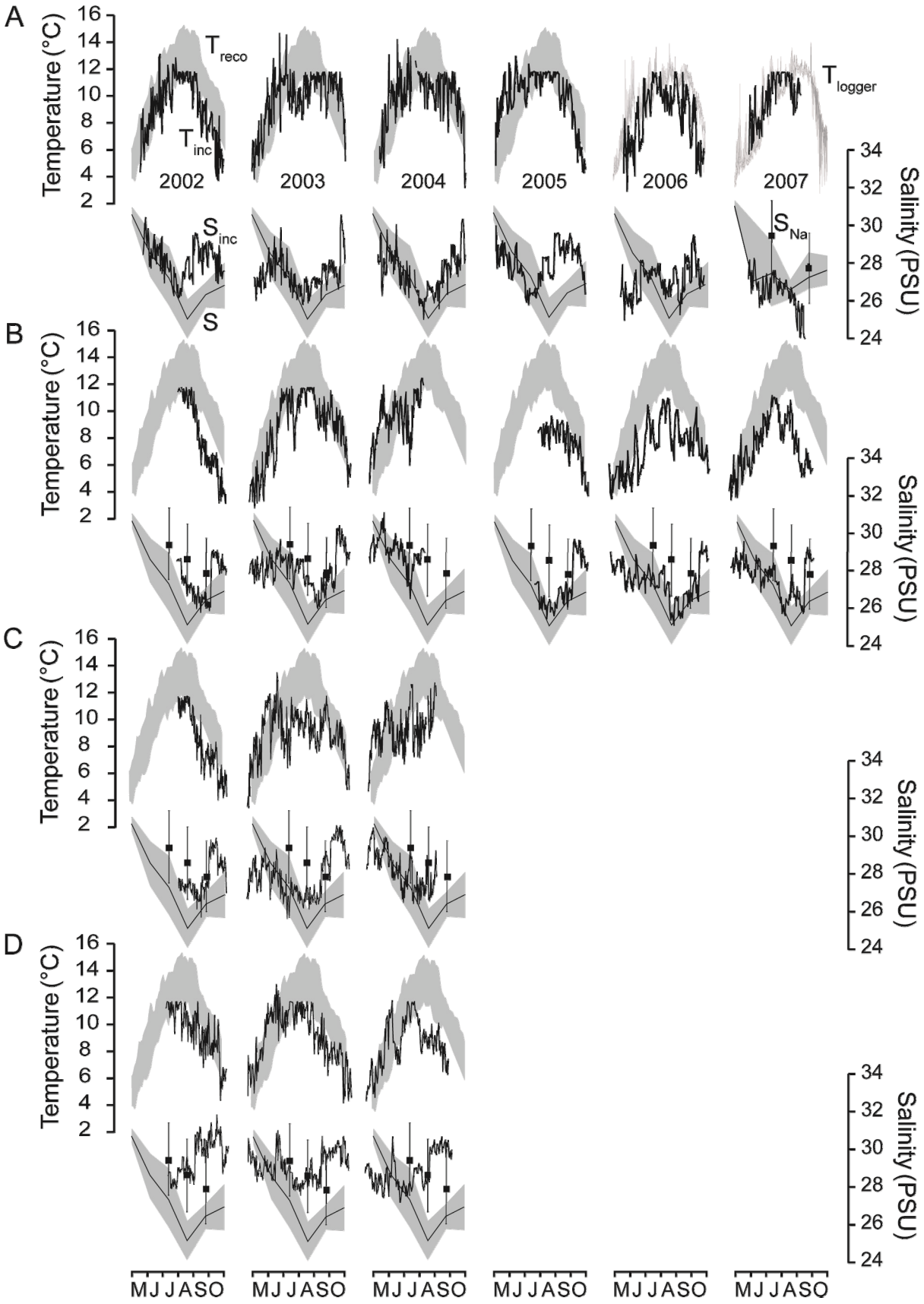


Figure 9. GT model from Figure 8 applied to a modern (A: GI1-LTI0907-A1L) and archaeological shells (B: 599-994 cal yr BP; C: 621-1014 cal yr BP; D: 988-1447 cal yr BP; Tab. 4). Increment-derived temperature ($T_{inc}$) and salinity ($S_{inc}$) data are depicted in black,

whereas measured temperature ($T_{logger}$), modeled temperature ($T_{reco}$) and monthly salinity data (coastal station GAK1; Fig. 1) are given in grey. For modern (2002-2005) and archaeological shells, seasonal $T_{reco}$ curves for the time interval of 1998-2008 are shown. For years prior to 2007, monthly GAK1 salinity data during 1998-2007 were used for comparison with $S_{inc}$. Black squares represent sodium-derived salinities.

## *4.4. DISCUSSION*

Most previous paleoseasonality studies using shells of bivalve mollusks were solely based on geochemical data (e.g., CULLETON et al., 2009; NÜTZEL et al., 2010) and only a few employed daily growth patterns (e.g., KOIKE, 1975; KENNISH and OLSSON, 1975; LAZARETH et al., 2006). However, when combined with microgrowth pattern analysis, the quality of information extracted from the shells can be significantly improved. Specifically, it becomes possible to disentangle the influence of freshwater and temperature on $\delta^{18}O_{shell}$ values of *Saxidomus gigantea* by reconstructing temperature data from shell growth rates. So far, the ambiguity of shell oxygen isotope data has severely limited the use of bivalves from freshwater influenced habitats (SURGE and LOHMANN, 2002) and propelled the search for independent geochemical temperature proxies. Unfortunately, Sr/Ca and Mg/Ca ratios of many bivalve species including *S. gigantea* (GILLIKIN et al., 2005b) do not seem to provide reliable paleotemperature estimates. The growth-temperature model presented here is an inexpensive alternative to currently assessed sophisticated geochemical paleothermometers such as the $\Delta_{47}$ or $^{44/40}Ca$ values (GHOSH et al. 2006; NAGLER et al., 2006).

### 4.4.1. Growth-temperature model and salinity estimates: accuracy and applicability

As indicated by simple linear regression analysis, temperature dominates the variability of age- and tide-detrended shell growth of *S. gigantea*. This is in good agreement with numerous previous studies on other bivalve species (e.g., DAVENPORT 1938; GUNTER, 1957; BERRY and BARKER, 1968). However, 30% of the variability in daily shell growth of *S. gigantea* is unrelated to temperature and controlled by other environmental parameters. GILLIKIN et al. (2005a) noticed a growth cessation during low salinity periods in this species, which we did not find in the specimens from SW Alaska. However, laboratory studies by MARSDEN (2004) revealed that reduced phytoplankton quantities stress a New Zealand bivalve more than lowered salinity. Additional laboratory experiments are required to test how salinity influences shell growth of *S. gigantea*.

Provided that the observed relationship between environmental parameters and shell growth has remained unchanged through time, daily increment widths of archaeological shells can provide information on past water temperatures with an error of about 1.3°C. Besides temperature, many other environmental factors such as salinity, food quality and quantity, water flow, sediment characteristics and biotic interactions affect growth rates of bivalves (KRAEUTER and CASTAGNA, 2001; MARSDEN, 2004). For example, in *Mercenaria mercenaria* temperature sets the limits and – together with food availability – controls the rate at which the shell can grow (ANSELL, 1968; JONES et al., 1989). However, severe food shortage is unlikely to occur at the study sites in SW Alaska. Aside from nutrient- and organic particle-rich terrestrial runoff, nutrients are brought to the surface layers by wind-mixing, mixing by tidal currents over banks and in narrow passages, wind-driven Ekman transport, episodic upwelling events in summer when the winds relax, eddies and topographic steering (STABENO et al., 2004). This fosters phytoplankton growth. Therefore, the GT model can most likely be applied to fossil shells.

However, in order to apply the growth–temperature model to butter clams (or other species) from other habitats, a new calibration of shell growth and environmental variables is required. It cannot be ruled out that other environmental forcings than studied in the present paper influence shell growth of this species. For example, population density may negatively affect growth rates (PETERSON, 1982). More importantly, in settings where the optimum growth temperature of this species is exceeded, the model returns ambiguous temperature data for similar daily increment widths. Similar studies on other bivalves have shown that shell growth slows down between the optimum growth temperature and the upper shutdown temperature (SCHÖNE et al., 2003). BERNARD (1983) reported an upper growth temperature of 20°C for this species. In southern British Columbia, summer temperatures of ~15°C had no negative effect on shell growth, so that the optimum growth temperature is likely between 15° and 20°C.

In conjunction with increment-derived water temperatures, $\delta^{18}O_{shell}$ values can be used to compute past salinity variations. Prior to such reconstructions, it has to be confirmed that the bivalves precipitate their shells in oxygen isotopic equilibrium with the ambient water. As seen from Table 1, $\delta^{18}O_{water}$ values of coastal settings determined only a few tens of meters apart at nearly the exact same time can be highly variable. Up to ~0.5 ‰ differences have

been observed at the studied localities, which translate into a salinity difference of 1.1 PSU or a temperature difference of more than 2.2°C. These microsite differences may be partly induced by groundwater (ELLIOT et al., 2003) and small rivulets with a more negative $\delta^{18}O_{water}$ signature reaching the coastal area. Therefore, in coastal settings a large number of shells and water samples may be required to confirm equilibrium deposition of shell carbonate.

Furthermore, a careful analysis of life history traits must precede the use of the GT model. If the duration of the growing season changes through life, annual increments of younger-age portions of the shells cannot be directly compared to years formed during later ontogenetic stages. For example, with progressive ontogenetic age, *Phacosoma japonicum* from Japan seems to start growing shell later in the year and seems to stop growing shell earlier (MIYAJI et al., 2007). Shell growth is then biased toward summer as the bivalve grows older and 'annual' average $\delta^{18}O_{shell}$ values would exhibit a trend toward more negative values. For *Saxidomus gigantea* an ontogenetic trend in the number of LDGI was not observed. With increasing ontogenetic age, increment widths decreases linearly. Also, later ontogenetic years sampled by micromilling yielded the same $\delta^{18}O_{shell}$ ranges as obtained by drilling of younger-age portions of the shells.

By using the growth-temperature model in conjunction with LDGI and $\delta^{18}O_{shell}$ values, past seasonal salinity variations can be computed, and the time interval during which a certain temperature and salinity range persisted can be reliably determined. However, no precise calendar dates can be assigned to reconstructed temperatures and salinity data of fossil shells, because the date of death can only be determined to the nearest two to four weeks or so by means of lunar daily growth pattern analysis (HALLMANN et al., 2009).

### 4.4.2. Modern and past environmental conditions in coastal SW Alaska

Despite different localities and years that were analyzed, the average $\delta^{18}O_{shell}$ values were remarkably uniform (Fig. 6). As indicated by comparison with environmental variables, the observed differences among the minimum and maximum values were most likely the result of changing $\delta^{18}O_{water}$ signature caused by freshwater influx and microsite differences. However, the stable carbon isotope values were much more variable among the studied specimens than oxygen isotope ratios. These differences cannot be attributed to ontogenetic age-related

$\delta^{13}C_{shell}$ changes. Firstly, in agreement with GILLIKIN et al. (2005a), the butter clam does not show ontogenetic trends in its shell carbon isotope signatures (Fig. 5). Secondly, same ontogenetic years of different specimens that lived close to each other exhibited significant differences in $\delta^{13}C_{shell}$ values (Fig. 6). Likewise, GILLIKIN et al. (2005a) found inconsistencies in $\delta^{13}C_{shell}$ values among different contemporaneous specimens of *S. gigantea* from the exact same locality at Puget Sound. However, these authors also noted a strong agreement of the $\delta^{13}C_{shell}$ curves in other years. This may suggest that the shells are capable of recording the isotopic signature of the ambient DIC (with the well-known 2.7‰ offset due to fractionation between aragonite and bicarbonate; ROMANEK et al., 1992).

As indicated by isotope signatures of the studied archaeological shells, climate and environmental conditions were different between 599-1680 cal yr BP and present. Three of the five studied archaeological shells alive during 988-1680 cal yr BP were significantly more positive in $\delta^{18}O_{shell}$ than modern specimens. Based on the growth-temperature model and reconstruction of salinity values for one of these shells (GI-MI81972-D1L; 988-1447 cal yr BP; Fig. 9D), the observed difference was largely attributed to a reduced freshwater discharge, i.e., drier and 2 to 5 PSU more saline conditions prevailed in the past during August through October (Fig. 9D). In addition, temperatures were ~1-2°C lower than today during summer. This may have been sufficient to reduce the amount of meltwater reaching the ocean during these seasons of the year and increase the amount of precipitation stored in glaciers (ROYER, 1979, 1982, 2005; KIPPHUT, 1990; MUNDY, 2005; SPIES, 2007). This interpretation agrees well with the advance of glaciers in the Kenai Mountains (approx. 300 km northeast of our study site) around 1350 cal yr BP (WILES and CALKIN, 1994). As a result of reduced freshwater influx, the Alaska Coastal Current was probably flowing slower than at present, so that lower amounts of freshwater were delivered to Polar waters.

Greater amounts of freshwater would increase the flow speed of the ACC leading to an enhanced vertical mixing, and the transport of nutrient-rich subsurface waters to the coast (ROYER et al., 2001). Cross-shelf transport, vertical mixing (KILLINGLEY and BERGER, 1979) and terrestrial runoff would significantly increase the relative amount of light carbon isotopes in surface waters and would therefore be associated with a strong negative $\delta^{13}C_{DIC}$ and $\delta^{13}C_{shell}$ shift [see discussion above on a potential salinity control of $\delta^{13}C_{shell}$]. High input of nutrients would have resulted in a primary productivity pulse, which would have driven the

stable carbon isotope values of DIC and the shells toward more positive values. However, such strong $\delta^{13}C_{shell}$ shifts have not been observed. The $\delta^{13}C_{shell}$ values of all five studied archaeological shells were consistently more positive than modern shells, even in specimens with a modern $\delta^{18}O_{shell}$ range and similar LDGI values (Fig. 6B).

Most of the positive $\delta^{13}C_{shell}$ offset between modern and archaeological shells is more likely explained as a result of the Suess effect. Combustion of fossil fuels, deforestation and land use change has shifted atmospheric $\delta^{13}C$ values by ca. −1.8‰ (FRIEDLI et al., 1986; FRANCEY et al., 1999; KEELING et al., 2005) since 1790. Admixture of anthropogenic $CO_2$ has also resulted in a significant negative $\delta^{13}C_{DIC}$ shift (NOZAKI et al., 1978; DRUFFEL and BENAVIDES, 1986) known as the oceanic Suess effect (GRUBER et al., 1999). However, the observed difference between modern and pre-1790 $\delta^{13}C_{shell}$ values of 0.4 to 0.7‰ cannot be solely explained by the Suess effect, because it is slightly lower than the negative $\delta^{13}C_{shell}$ shift of ~0.77 to 0.93‰ between the beginning of the industrialization and 2003 observed in other bivalves from the North Atlantic (BUTLER et al., 2009; SCHÖNE et al., 2011). It seems reasonable to assume that higher primary productivity has partly counterbalanced the Suess effect. If freshwater fluxes from land were reduced, the required nutrients were likely supplied by cross-shelf transport and vertical mixing.

Assuming that the multivariate analyses (eq. 7) hold true and nearly $4/5^{th}$ of the variability in shell stable carbon isotope values was governed by salinity changes, one might suggest using $\delta^{13}C_{shell}$ values for salinity reconstructions. However, given the likely influence on $\delta^{13}C_{shell}$ by the Suess effect, this does not seem a feasible approach.

The two remaining, more recent archaeological shells (GI-MI20572-D1R and GI-MI20572-D2L) alive during 599-1014 cal yr BP were statistically indistinguishable from the $\delta^{18}O_{shell}$ ranges of modern specimens (Fig. 6). However, reconstructed summer temperatures were up to 3°C lower and salinity 1 to 2 PSU lower than at modern times (Figs 9B and 9C). These data imply that terrestrial freshwater discharge was probably larger during that time interval than nowadays and was likely caused by an increased amount of precipitation (in the form of rain) rather than meltwater (because of reduced temperatures), and, accordingly, by a

stronger Aleutian low pressure system (ROYER, 1979; MUNDY, 2005). As a consequence of fresher conditions at that time, the ACC was probably flowing faster than today.

Interestingly, the growing season of the studied archaeological shells was up to one month longer than today (Fig. 6B). Since *S. gigantea* stops growing shell when temperatures drop below 4° to 5°C, the time interval during which higher temperatures prevailed was longer than present day. It should be pointed out, however, that only a limited number of years in a few archaeological shells have been studied herein and additional studies with larger sample sizes are required to draw a more reliable and complete picture of the past.

## *4.5. CONCLUSIONS*

The results of this study indicate an integrated growth pattern and isotope approach can yield quantifiable temperature and salinity data from bivalve shells in freshwater-influenced habitats of coastal SW Alaska. Specifically, it was possible to disentangle the influence of freshwater and temperature on $\delta^{18}O_{shell}$ values by reconstructing water temperature independently from shell growth rates.

The combined use of shell stable isotopes and growth patterns along with contemporary environmental data were also essential to determine or confirm (1) the precise duration of the growing season and potential ontogenetic changes, (2) optimum and shutdown temperatures for growth, (3) the precise timing of growth line and growth increment formation, and (4) if the shells were precipitated in isotopic equilibrium with the ambient water.

Application of the growth-temperature model to archaeological shells revealed differences in seasonal temperature regimes. Between 599 and 1447 cal yr BP temperatures remained above 4-5°C for eight months, i.e., one month longer than at present. The time interval of 988-1447 cal yr BP was characterized by ~1-2°C colder and much drier (2-5 PSU) summers. The ACC was likely flowing much slower than presently. In contrary, from 599 to 1014 cal yr BP, the Aleutian low may have been stronger, which resulted in up to 3°C colder summer temperatures and up to 1-2 PSU fresher conditions than today. The ACC was probably flowing faster.

Future laboratory experiments should test which other factors than temperature govern shell growth. This may result in a multivariate growth-temperature model and improve temperature estimates from bivalve shells that were influenced by changing salinity. In particular, the influence of salinity on $\delta^{13}C_{shell}$ should be studied. Moreover, errors in temperature estimates may be further reduced when the growth-temperature model is applied to different contemporaneous species from the same locality.

## *4.6. ACKNOWLEDGEMENTS*

Financial support for this study was provided by the German Research Foundation, DFG (SCHO 793/3) to BRS; the *Exxon Valdez* Oil Spill Trustee Council, the U.S. Geological Survey and the National Park Service to GVI. Any mention of trade names is for descriptive purposes only and does not represent endorsement by the U.S. government. Satellite-derived sea surface temperature data (NCEP/DOE AMIP-II Reanalysis, "skin temperature") were provided by Physical Sciences Division, Earth System Research Laboratory, NOAA, Boulder, Colorado, from their Web site at http://www.esrl.noaa.gov/. GAK1 salinity data came from the Institute of Marine Science at the University of Alaska Fairbanks (http://www.ims.uaf.edu). We kindly thank Jens Fiebig (University of Frankfurt/Main, Germany) and Christopher S. Romanek (University of Kentucky, USA) for conducting most of the isotope analyses of carbonates and water, respectively. Thanks go also to Kazushige Tanabe and Marta E. Torres for reviews of the draft manuscript. We are grateful for suggestions by two anonymous reviewers and Adam Tomasovych, which significantly improved the quality of the manuscript. This is contribution number 3662 from the Pacific Marine Environmental Laboratory, NOAA.

## 4.7. REFERENCES

ABBOTT, M.B., FINNEY, B.P., EDWARDS, M.E., and KELTS, K.R., 2000. Lake-level reconstructions and paleohydrology of Birch Lake, Central Alaska, based on seismic reflection profiles and core transects. Quaternary Research 53, 154–166.

ANDERSON, L., ABBOTT, M.B., and FINNEY, B.P., 2001. Holocene climate inferred from oxygen isotope ratios in lake sediments, Central Brooks Range, Alaska. Quaternary Research 55, 313–321.

ANSELL, A.D., 1968. The rate of growth of the hard clam *Mercenaria mercenaria* (L) throughout the geographic range. Journal du Conseil internationale pour l'Exploration de la Mer 31, 364–409.

BARBER, V.A., JUDAY, G.P., FINNEY, B.P., and WILMKING, M., 2004. Reconstruction of summer temperatures in interior Alaska from tree-ring proxies: Evidence for changing synoptic climate regimes. Climatic Change 63, 91–120.

BERNARD, F.R., 1983. Physiology and the mariculture of some northeastern Pacific bivalve mollusks. Canadian Special Publication of Fisheries and Aquatic Sciences 63, 1–24.

BERRY, W.B.N., and BARKER, R.M., 1968. Fossil bivalve shells indicate longer month and year in Cretaceous than Present. Nature 217, 938–939.

BIGELOW, N.H., and EDWARDS, M.E., 2001. A 14,000 yr paleoenvironmental record from Windmill Lake, Central Alaska: Lateglacial and Holocene vegetation in the Alaska range: Quaternary Science Reviews 20, 203–215.

BÖHM, F., JOACHIMSKI, M.M., DULLO, W.-Ch., EISENHAUER, A., LEHNERT, H., REITNER, J., and WÖRHEIDE, G., 2000. Oxygen isotope fractionation in marine aragonite of coralline sponges. Geochimica et Cosmochimica Acta 64, 1695–1703.

BUTLER, P.G., SCOURSE, J.D., RICHARDSON, C.A., WANAMAKER, A.D.JR., BRYANT, C., and BENNELL, J.D., 2009. Continuous marine radiocarbon reservoir calibration and the $^{13}C$ Suess effect in the Irish Sea: results from the first multi-centennial shell-based marine master chronology. Earth and Planetary Science Letters 279, 230–241.

COKELET, E.D., MORDY, C.W., JENKINS, A.J., and PEGAU, W.S., 2010, Biophysical observations aboard Alaska Marine Highway System ferries, *Exxon Valdez* Oil Spill Gulf Ecosystem Monitoring and Research Project 040699 Final Report, Alaska Department of Fish and Game, Habitat Restoration Division, Anchorage, Alaska, 67 p.

CULLETON, B., KENNETT, D.J., and JONES, T.L., 2009. Oxygen isotope seasonality in a temperate estuarine shell midden: a case study from CA-ALA-17 on the San Francisco Bay, California. Journal of Archaeological Science 36, 1354–1363.

DAVENPORT, C.B., 1938. Growth lines in fossil pectens as indicators of past climates: Journal of Paleontology 12, 514–515.

DE VILLIERS, S., GREAVES, M., and ELDERFIELD, H., 2002. An intensity ratio calibration method for the accurate determination of Mg/Ca and Sr/Ca of marine carbonates by ICP-AES. Geochemistry Geophysics Geosystems 3, doi: 10.1029/2001GC000169.

DOE, 1994, Handbook of methods for the analysis of the various parameters of the carbon dioxide system in sea water: Version 2, DICKSON, A.G., GOYET, C. (eds.), ORNL/CDIAC-74. [Available online at http://132.239.122.17/co2qc/handbook.html]

DRUFFEL, E.M., and BENAVIDES, L.M., 1986. Input of excess $CO_2$ to the surface ocean based on $^{13}C/^{12}C$ ratios in a banded Jamaican sclerosponge. Nature 321, 58–61.

ELLIOT, M., DEMENOCAL, P.B., LINSLEY, B.K., and HOWE, S.S., 2003. Environmental controls on the stable isotopic composition of *Mercenaria mercenaria*: potential application to paleoenvironmental studies. Geochemistry Geophysics Geosystems 4, 1–16.

EPSTEIN, S., BUCHSBAUM, R., LOWENSTAM, H.A., and UREY, H.C., 1953. Revised carbonate-water isotopic temperature scale. Bulletin of the Geological Society of America 64, 1315–1326.

EVANS, J.W., 1972. Tidal growth increments in the cockle *Clinocardium nuttalli*. Science 176, 416–417.

FEIGL, F., 1958. Spot tests in inorganic analysis. Elsevier, Amsterdam, 600 p.

FRANCEY, R.J., ALLISON, C.E., ETHERIDGE, D.M., TRUDINGER, C.M., ENTING, I.G., LEUENBERGER, M., LANGENFELDS, R.L., MICHEL, E., and STEELE, L.P., 1999. A 1000-year high precision record of $\delta^{13}C$ in atmospheric $CO_2$. Tellus 51B, 170–193.

FRIEDLI, H., LOTSCHER, H., OESCHGER, H., SIEGENTHALER, U., and STAUFFER, B., 1986. Ice core record of the $^{13}C/^{12}C$ ratio of atmospheric $CO_2$ in the past two centuries. Nature 324, 237–238.

GARFINKEL, H.L., and BRUBAKER, L.B., 1980. Modern climate−tree-growth relationships and climatic reconstruction in sub-Arctic Alaska. Nature 286, 872–874.

GHOSH, P., ADKINS, J., AFFEK, H., BALTA, B., GUO, W., SCHAUBLE, E.A., SCHRAG, D., and EILER, J.M., 2006. $^{13}C$-$^{18}O$ bonds in carbonate minerals: A new kind of paleothermometer. Geochimica et Cosmochimica Acta 70, 1439–1456.

GILLIKIN, D.P., DE RIDDER, F., ULENS, H., ELSKENS, M., KEPPENS, E., BAEYENS, W., and DEHAIRS, F., 2005. Assessing the reproducibility and reliability of estuarine bivalve shells (*Saxidomus giganteus*) for sea surface temperature reconstruction: implications

for paleoclimate studies. Palaeogeography Palaeoclimatology Palaeoecology 228, 70–85.

GILLIKIN, D.P., LORRAIN, A., NAVEZ, J., TAYLOR, J.W., ANDRÉ, L., KEPPENS, E., BAEYENS, W., and DEHAIRS, F., 2005b. Strong biological controls on Sr/Ca ratios in aragonitic marine bivalve shells. Geochemistry, Geophysics, Geosystems 6, Q05009, doi:10.1029/2004GC000874.

GOODWIN, D.H., FLESSA, K.W., SCHÖNE, B.R., and DETTMAN, D.L., 2001. Cross-calibration of daily growth increments, stable isotope variation, and temperature in the Gulf of California bivalve mollusk *Chione cortezi*: implications for paleoenvironmental analysis. PALAIOS 16, 387–398.

GROSSMAN, E.L., and KU, T.-L., 1986. Oxygen and carbon isotope fractionation in biogenic aragonite; temperature effects. Chemical Geology (Isotope Geoscience Section) 59, 59–74.

GRUBER, N., KEELING, C.D., BACASTOW, R.B., GUENTHER, P.R., LUEKER, T.J., WAHLEN, M., MEIJER, H.A.J., MOOK, W.G., and STOCKER, T.F., 1999. Spatiotemporal patterns of carbon-13 in the global surface oceans and the oceanic Suess effect: Global Biogeochemical Cycles 13, 307–335.

GUNTER, G., 1957. Temperature. Memoir of the Geological Society of America 67, 159–184.

HALFAR, J., STENECK, R., SCHÖNE, B.R., MOORE, G.W.K., JOACHIMSKI, M., KRONZ, A., FIETZKE, J., and ESTES, J., 2007. Coralline alga reveals first marine record of subarctic North Pacific climate change. Geophysical Research Letters 34, L07702, doi:10.1029/2006GL028811.

HALLMANN, N., BURCHELL, M., SCHÖNE, B.R., IRVINE, G.V., and MAXWELL, D., 2009. High-resolution sclerochronological analysis of the bivalve mollusk *Saxidomus gigantea* from Alaska and British Columbia: techniques for revealing environmental archives and archaeological seasonality. Journal of Archaeological Science 36, 2353–2364.

HETZINGER, S., HALFAR, J., KRONZ, A., STENECK, R.S., ADEY, W., LEBENDNIK, A., and SCHÖNE, B.R., 2009. High-resolution Mg/Ca ratios in a coralline red alga as a proxy for Bering Sea temperature variations from 1902 to 1967. PALAIOS 24, 406–412.

HU, A., MEEHL, G.A., OTTO-BLIESNER, B.L., WAELBROECK, C., HAN, W., LOUTRE, M.-F., LAMBECK, K., MITROVICA, J.X., and ROSENBLOOM, N., 2010. Influence of Bering Strait flow and North Atlantic circulation on glacial sea-level changes. Nature Geoscience 3, 118–121.

JOHNSON, W.R., ROYER, T.C., and LUICK, J.L., 1988. On the seasonal variability of the Alaska Coastal Current. Journal of Geophysical Research 93, 12423–12437.

JONES, D.S., Arthur, M.A., and Allard, D.J., 1989, Sclerochronological records of temperature and growth from shells of Mercenaria mercenaria from Narragansett Bay, Rhode Island: Marine Biology, v. 102, p. 225–234.

KEELING, C.D., PIPER, S.C., BACASTOW, R.B., WAHLEN, M., WHORF, T.P., HEIMANN, M., and MEIJER, H.A., 2005. Atmospheric $CO_2$ and $^{13}CO_2$ exchange with the terrestrial biosphere and oceans from 1978 to 2000: observations and carbon cycle implications. Ecological Studies 177, 83–113.

KEIGWIN, L.D., DONNELLY, J.P., COOK, M.S., DRISCOLL, N.W., and BRIGHAM-GRETTE, J., 2006. Rapid sea-level rise and Holocene climate in the Chukchi Sea. Geology 34, 861–864.

KENNISH, M.J., and OLSSON, R.K., 1975. Effects of thermal discharges on the microstructural growth of *Mercenaria mercenaria*. Environmental Geology (Springer) 1, 41–64.

KILLINGLEY, J.S., and BERGER, W.H., 1979. Stable isotopes in a mollusk shell: Detection of upwelling events. Science 205, 186–188.

KINGSTON, A.W., GRÖCKE, D.R., and BURCHELL, M., 2008. A multiaxial growth analysis of stable isotopes in the modern shell of *Saxidomus gigantea*: Implications for sclerochronology studies. Geochemistry, Geophysics, Geosystems 9, Q01007, doi:10.1029/2007GC001807.

KIPPHUT, G.W., 1990. Glacial meltwater input to the Alaska coastal current: Evidence from oxygen isotope measurements. Journal of Geophysical Research 95, 5177–5181.

KOIKE, H., 1975. The use of daily and annual growth lines of the clam *Meretrix lusoria* in estimating seasons of Jomon period shell gathering. Quaternary Studies, The Royal Society of New Zealand 13, 189–193.

LAZARETH, C.E., LASNE, G., and ORTLIEB, L., 2006. Growth anomalies in *Protothaca thaca* (Mollusca, Veneridae) shells as markers of ENSO conditions. Climate Research 30, 263–269.

MARSDEN, I.D., 2004. Effects of reduced salinity and seston availability on growth of the New Zealand little-neck clam *Austrovenus stutchburyi*. Marine Ecology Progress Series 266, 157–171.

MCNEELY, R., DYKE, A.S., and SOUTHON, J. R., 2006. Canadian marine reservoir ages, preliminary data assessment. Geological Survey Canada, Open File 5049.

MIYAJI, T., TANABE, K., and SCHÖNE, B.R., 2007. Environmental controls on daily shell growth of *Phacosoma japonicum* (Bivalvia: Veneridae) from Japan. Marine Ecology Progress Series 336, 141–150.

MUENCH, R.D., MOFJIELD, H.O., and CHARNELL, R.L., 1978. Oceanographic conditions in lower Cook Inlet: spring and summer 1973. Journal of Geophysical Research 83, 5090–5098.

MUNDY, P.R. (ed.), 2005. The Gulf of Alaska: Biology and Oceanography. Alaska Sea Grant College Program, University of Alaska Fairbanks, 214 p.

NAGLER, T.F., HART, S.F., and HIPPLER, D., 2006. Seasonal Sr/Ca, and $^{44}Ca/^{40}Ca$ co-variation in *Arctica islandica*. Geophysical Research Abstracts 8, 02256.

NOZAKI, Y., RYE, D.M., TUREKIAN, K.K., and DODGE, R.E., 1978. A 200 year record of carbon-13 and carbon-14 variations in a Bermuda coral. Geophysical Research Letters 5, 826–828.

NÜTZEL, A., JOACHIMSKI, M., and LÓPEZ-CORREA, M., 2010. Seasonal climatic fluctuations in the Late Triassic tropics—High-resolution oxygen isotope records from aragonitic bivalve shells (Cassian Formation, Northern Italy). Palaeogeography, Palaeoclimatology, Palaeoecology 285, 194–204.

OHNO, T., 1989. Palaeotidal characteristics determined by micro-growth patterns in bivalves. Palaeontology 32, 237–263.

PETERSON, C., 1982. The importance of predation and intra- and interspecific competition in the population biology of two infaunal suspension-feeding bivalves, *Protothaca staminea* and *Chione undatella*. Ecological Monographs 52, 437–475.

QUAYLE, D.B., and BOURNE, N., 1972. The clam fisheries of British Columbia. Fisheries Research Board of Canada, Ottawa, Bulletin 179, 70 p.

RAHIMPOUR-BONAB, H., BONE, Y., and MOUSSAVI-HARAMI, R., 1997. Stable isotope aspects of modern molluscs, brachiopods, and marine cements from cool-water carbonates, Lacepede Shelf, South Australia. Geochimica et Cosmochimica Acta 61, 207–218.

REIMER, P.J., BAILLIE, M.G.L., BARD, E., BAYLISS, A., BECK, J.W., BLACKWELL, P.G., BRONK RAMSEY, C., BUCK, C.E., BURR, G.S., EDWARDS, R.L., FRIEDRICH, M., GROOTES, P.M., GUILDERSON, T.P., HAJDAS, I., HEATON, T.J., HOGG, A.G., HUGHEN, K.A., KAISER, K.F., KROMER, B., MCCORMAC, F.G., MANNING, S.W., REIMER, R.W., RICHARDS, D.A., SOUTHON, J.R., TALAMO, S., TURNEY, C.S.M., VAN DER PLICHT, J., and WEYHENMEYER, C.E., 2009. IntCal09 and Marine09 radiocarbon age calibration curves, 0 - 50,000 years cal BP. Radiocarbon 51, 1111–1150.

RICKETS, E.F., and CALVIN, J., 1962. Between Pacific tides. Stanford University Press, Stanford, 515 p.

ROMANEK, C.S., GROSSMAN, E.L., and MORSE, J.W., 1992. Carbon isotopic fractionation in synthetic aragonite and calcite: effects of temperature and precipitation rate. Geochimica et Cosmochimica Acta 56, 419–430.

ROYER, T.C., 1979. On the effect of precipitation and runoff on coastal circulation in the Gulf of Alaska. Journal of Physical Oceanography 9, 555–563.

ROYER, T.C., 1981. Baroclinic transport in the Gulf of Alaska. Part II. A fresh water driven coastal current. Journal of Marine Research 39, 251–266.

ROYER, T.C., 1982. Coastal fresh water discharge in the Northeast Pacific. Journal of Geophysical Research 87, 2017–2021.

ROYER, T.C., 2005. Hydrographic responses at a coastal site in the northern Gulf of Alaska to seasonal and interannual forcing. Deep Sea Research Part II, Topical Studies in Oceanography 52, 267–288.

ROYER, T.C., GROSCH, C.E., and MYSAK, L.A., 2001. Interdecadal variability of Northeast Pacific coastal freshwater and its implications on biological productivity. Progress in Oceanography 49, 95–111.

SCHÖNE, B.R., DUNCA, E., FIEBIG, J., and PFEIFFER, M., 2005a. Mutvei's solution: an ideal agent for resolving microgrowth structures of biogenic carbonates. Palaeogeography Palaeoclimatology Palaeoecology 228, 149–166.

SCHÖNE, B.R., FIEBIG, J., PFEIFFER, M., GLEß, R., HICKSON, J., JOHNSON, A.L.A., DREYER, W., and OSCHMANN, W., 2005b. Climate records from a bivalve Methuselah (*Arctica islandica*, Mollusca; Iceland). Palaeogeography Palaeoclimatology Palaeoecology 228, 130–148.

SCHÖNE, B.R., LEGA, J., FLESSA, K.W., GOODWIN, D.H., and DETTMAN, D.L., 2002. Reconstructing daily temperatures from growth rates of the intertidal bivalve mollusk *Chione cortezi* (northern Gulf of California, Mexico). Palaeogeography, Palaeoclimatology, Palaeoecology 184, 131–146.

SCHÖNE, B.R., TANABE, K., DETTMAN, D.L., and SATO, S., 2003. Environmental controls on shell growth rates and $\delta^{18}O$ of the shallow-marine bivalve mollusk *Phacosoma japonicum* in Japan. Marine Biology 142, 473–485.

SCHÖNE, B.R., WANAMAKER, A.D. JR., FIEBIG, J., THÉBAULT, J., and KREUTZ, K.J., 2011. Annually resolved $\delta^{13}C_{shell}$ chronologies of long-lived bivalve mollusks (*Arctica islandica*) reveal oceanic carbon dynamics in the temperate North Atlantic during

recent centuries: Palaeogeography, Palaeoclimatology, Palaeoecology, In press, doi:10.1016/j.palaeo.2010.02.002.

SCHRAG, D.P., 1999. Rapid analysis of high-precision Sr/Ca ratios in corals and other marine carbonates. Paleoceanography 14, 97–102.

SCHUMACHER, J.D., PEARSON, C.A., and OVERLAND, J.E., 1982. Exchange of water between the Gulf of Alaska and the Bering Sea through Unimak Pass. Journal of Geophysical Research 87, 5785–5795.

SPIES, R.B., 2007. Long-term ecological change in the Northern Gulf of Alaska. Elsevier Science, Amsterdam, 589 p.

STABENO, P.J., BOND, N.A., HERMANN, A.J., KACHEL, N.B., MORDY, C.W., and OVERLAND, J.E., 2004. Meteorology and oceanography of the Northern Gulf of Alaska. Continental Shelf Research 24, 859–897.

STUIVER, M., and REIMER, P. J., 1993. Extended $^{14}C$ database and revised CALIB 3.0 $^{14}C$ age calibration program. Radiocarbon 35, 215–230.

SURGE, D.M., and LOHMANN, K.C., 2002. Temporal and spatial differences in salinity and water chemistry in SW Florida estuaries: Effects of human-impacted watersheds. Estuaries 25, 393–408.

TARUTANI, T., CLAYTON, R.N., and MAYEDA, T.K., 1969. The effect of polymorphism and magnesium substitution on oxygen isotope fractionation between calcium carbonate and water. Geochimica et Cosmochimica Acta 33, 987–996.

WEINGARTNER, T.J., DANIELSON, S.L., and ROYER, T.C., 2005. Freshwater variability and predictability in the Alaska Coastal Current. Deep-Sea Research II 52, 169–191.

WILES, G.C., and CALKIN, P.E., 1994. Late Holocene, high-resolution glacial chronologies and climate, Kenai Mountains, Alaska. Geological Society of America Bulletin 106, 281–303.

WILES, G.C., D'ARRIGO, R.D., and JACOBY, G.C., 1996. Temperature changes along the Gulf of Alaska and the Pacific Northwest coast modeled from coastal tree rings. Canadian Journal of Forest Research 26, 474–481.

WILES, G.C., D'ARRIGO, R.D., and JACOBY, G.C., 1998. Gulf of Alaska atmosphere-ocean variability over recent centuries inferred from coastal tree-ring records. Climatic Change 38, 289–306.

WILLIAMS, D.F., ARTHUR, M.A., JONES, D.S., and HEALY-WILLIAMS, N., 1982. Seasonality and mean annual sea surface temperatures from isotopic and sclerochronological records. Nature 296, 432–434.

# 5. SUMMARY AND CONCLUSIONS

This study shows that bivalve mollusk shells are useful tools for multi-species and multi-proxy paleoenvironmental reconstructions with a high temporal and spatial resolution. A major component of this Ph.D. research is calibration studies, which are essential in order to ascertain the usefulness of selected bivalve species as paleoclimate proxy archives. The results of these calibration studies can be summarized as follows:

- The sclerochronology and oxygen isotope ratios of different shell layers of *Panopea abrupta* were studied in order to test the reliability of this species as a climate archive and to reconstruct temperatures. Shell growth pattern analysis revealed that *P. abrupta* grows shell carbonate from March/April to November/December. Geoducks cease growth during the cold winter months and form major growth lines. These annual lines allow the determination of the ontogenetic ages of the shells and are clearly discernable in umbonal shell portions, but less so in the outer shell layer. The inner aragonitic shell layer of *P. abrupta* is formed in disequilibrium with the ambient water and therefore this shell portion is not suitable as a proxy for the reconstruction of past climate. However, temperatures are reliably recorded by the oxygen isotope ratios of the outer aragonitic shell layer. Sampling should therefore be confined to this shell layer. Furthermore, the high intra-specific variability requires the use of multiple contemporaneous specimens for a reliable reconstruction of paleotemperatures.

- By using archaeological *Saxidomus gigantea* shells it is possible to reconstruct variability in climate and seasonality during the Holocene with a high temporal resolution. A combination of geochemical and sclerochronological data refines estimates for season of shellfish collection and helps to distinguish between annual growth lines and disturbance lines, which can be caused by storms or predators. Bivalves from stressful environments have more disturbance lines and are therefore less suitable for archaeological purposes, specifically the identification of the season of shellfish collection. The comparison of shell growth patterns and an appropriate tidal calendar permits an estimation of a precise collection circumstance, such as low or high tide, springs or neaps, day- or nighttime and the identification of the relative position in the intertidal zone where the shells were collected. The butter clam is a valuable proxy archive to detect past environmental changes with a high temporal

resolution (subseasonal up to daily) and also to gain new insights into the settlement and subsistence economies of coastal hunter-gatherers. When these data are combined, it is possible to detect climate and cultural changes. However, the analysis of several shells from each locality is necessary due to intra-specific variability.

- The established growth-temperature model based on *S. gigantea* shells from south west Alaska helps to better understand hydrological changes related to the Alaska Coastal Current (ACC). An integrated growth pattern and oxygen isotope approach can yield quantifiable temperature and salinity data from bivalve shells in freshwater-influenced habitats. It was possible to disentangle the influence of freshwater and temperature on $\delta^{18}O_{shell}$ values by reconstructing water temperature independently from shell growth rates. The application of the model to archaeological shells revealed changes in seasonal temperature and salinity regimes. The time period between 988 and 1447 cal yrs BP was characterized by colder (~1-2°C) and much drier (2-5 PSU) summers, and a likely much slower flowing ACC than at present. In contrast, the summers during the time interval of 599-1014 cal yrs BP were colder (up to 3°C) and fresher (1-2 PSU) than today. The Aleutian Low may have been stronger and the ACC was probably flowing faster during this time. Errors in the reconstruction of paleotemperature and paleosalinity may be reduced by applying the growth-temperature model to more contemporaneous *S. gigantea* shells and to different species from the same locality. Further research is necessary to study the factors affecting shell growth and to reconstruct a multivariate growth-temperature model.

The overall aim of the project (of which this dissertation thesis is part of) is the construction of a paleoclimate network of proxy data for the North Pacific that can be used to examine large-scale Holocene climate variability. In order to reconstruct Holocene climate variability and environmental changes, stable oxygen and carbon isotopes have been measured in modern and fossil marine bivalve shells of the hard clam *Meretrix lusoria* and the Manila clam *Ruditapes philippinarum* from Japan and the butter clam *Saxidomus gigantea* from Alaska and British Columbia. These studies have not yet been completed. Initial results are briefly reported in the following.

Accordingly, oxygen isotopes were analyzed in both modern and Holocene *S. gigantea* shells from the Dundas Islands group on the northern coast of British Columbia

(BC), in the traditional territory of the Coast Tsimshian. The negative $\delta^{18}O$ summer values (lower quartiles and negative extremes) observed in the early and late Holocene become considerably more negative during the mid Holocene around 3000 and 5500 cal yr BP (Fig. 1). Oxygen isotope values become 2‰ more negative from 1500-3000 cal yr BP and 1‰ more negative from 7500-5500 cal yr BP (Fig. 1). The $\delta^{18}O_{shell}$ values from the mid Holocene are up to 2‰ more negative than today. This may imply a much fresher mid Holocene than early and late Holocene. Increased amounts of precipitation and melt water are possibly linked to warmer summers during this time period. The minimum $\delta^{18}O$ summer values are far more variable than the positive fall to spring values (upper quartiles and positive extremes), which remain relatively constant throughout the Holocene, indicating a year-to-year freshwater variation in summer. This mid Holocene climate transition observed in the $\delta^{18}O_{shell}$ record is consistent with environmental changes reported for British Columbia. The mid-Holocene was a period of climate transition on the Northwest coast of North America. For most coastal areas an increase in precipitation is reported for this time period. There is evidence from northern BC lake sediments for a cooling and an increase in precipitation for 6000 to 3000 cal yrs BP (SPOONER et al., 2002).

Furthermore, *S. gigantea* shells from different sites in central BC have been studied. They have 1-2‰ and 1-3‰ more negative fall to spring $\delta^{18}O_{shell}$ values (upper quartiles and positive extremes) around 1000 cal yr BP compared to today and the time period between 1500 and ~3800 cal yr BP, respectively (Fig. 1). This time around 1000 years ago was possibly characterized by higher temperatures and a higher freshwater influx. This agrees well with the ENSO peak (high frequency and amplitude) observed around 1200 years ago (MOY et al., 2002; WANNER et al., 2008).

Carbon isotope values of modern *S. gigantea* shells are 1-2‰ and 1-2.5‰ more negative than in archaeological shells from central and northern BC, respectively (Fig. 2). This possibly indicates a lower primary productivity today than in the past, which could be due to the higher freshwater influx and consequently a higher stratification and less nutrients in surface waters. Modern $\delta^{13}C_{shell}$ values are approximately 0.8‰ more negative due to the Suess-effect (SCHÖNE et al., 2011).

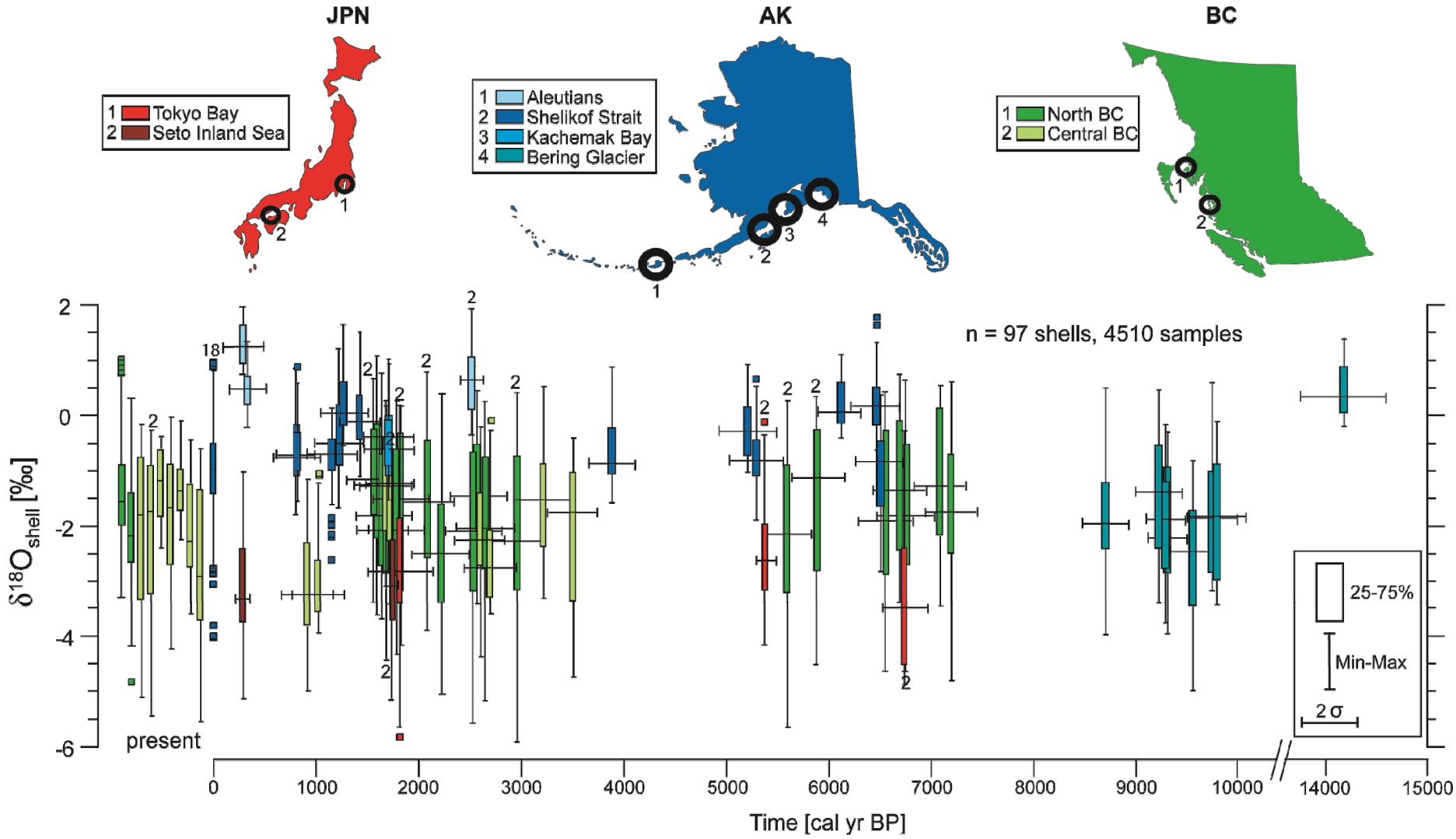


Figure 1. Oxygen isotope data of *Meretrix lusoria* shells from Japan (JPN) and *Saxidomus gigantea* shells from Alaska and British Columbia (BC). Each box represents one specimen (number of specimens, n, is shown if n > 1. Squares indicate outliers. Radiocarbon ages are shown as 2σ calibrated years BP (horizontal bars).

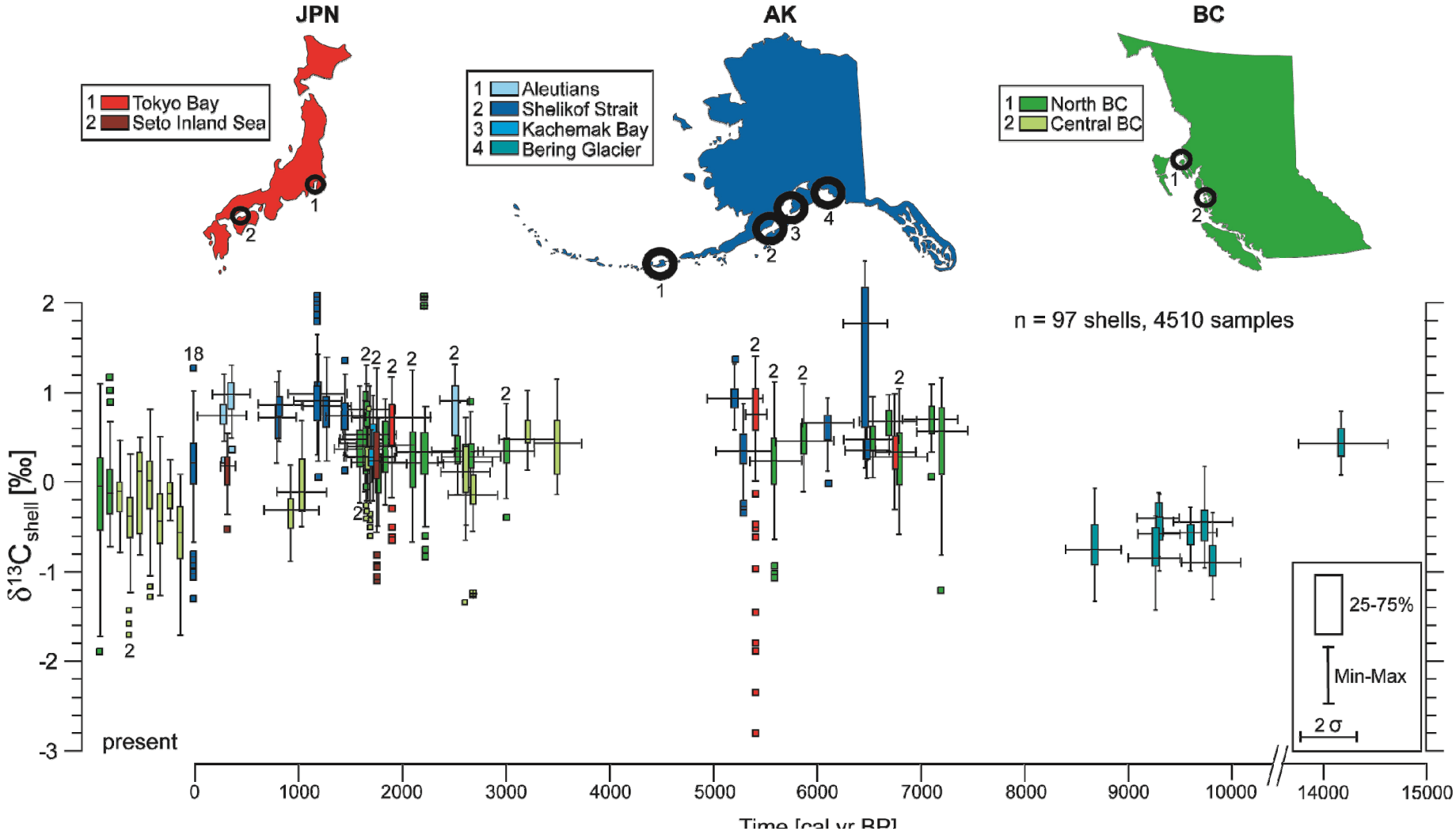


Figure 2. Carbon isotope data of *Meretrix lusoria* shells from Japan (JPN) and *Saxidomus gigantea* shells from Alaska and British Columbia (BC). Each box represents one specimen (number of specimens, n, is shown if n > 1. Squares indicate outliers. Squares with a cross are extreme outliers. Radiocarbon ages are shown as 2σ calibrated years BP (horizontal bars).

*S. gigantea* shells from the Bering Glacier (Alaska) indicate a climate shift between 10 000 and 14 000 cal yr BP. Shells from 14 000 to 14 500 cal yr BP have 3-5‰ and 1-1.5‰ more positive $\delta^{18}O_{shell}$ and $\delta^{13}C_{shell}$ values than shells from 8500-10 000 cal yr BP (Figs 1 and 2). This change in the isotopic composition of the shells reveals the last glacial-interglacial transition around 12 000 years ago (e.g., HU and SHEMESH, 2003). Furthermore, *S. gigantea* shells from Alaska (Shelikof Strait) indicate warmer and fresher modern than past conditions. Oxygen and carbon isotopes of modern shells are 1-3‰ and 1-1.5‰ more negative than in all archaeological shells, respectively (Figs 1 and 2). These first results are consistent with the warming and freshening trend observed in the Gulf of Alaska (ROYER and GROSCH, 2006). The freshening of the Alaska Coastal Current can also be detected in coralline red algae (HALFAR et al., 2007; HETZINGER et al., 2009). This warming and freshening could affect the global ocean circulation and therefore provides an interesting and important research field.

Japan provides a high density of archaeological sites from which bivalve shells can be obtained. Holocene shell middens in Japan are well studied and radiocarbon dated (MATSUSHIMA, 1982; MATSUSHIMA and KAWAGUCHI, 1991; MATSUSHIMA and KAWAKAMI, 1995). However, only few archaeological bivalve shell samples from Japan were analyzed (KOIKE, 1980; SCHÖNE et al., 2004b, 2005c; MIYAJI et al., 2010). This study analyzes common bivalve species from Japan, such as *M. lusoria* and *R. philippinarum*. These species are abundant in archaeological sites and therefore in the main focus of research. Life history traits of these two typical bivalve species were already well studied (KOIKE, 1980; RICHARDSON, 1987, 1988a; KANAZAWA and SATO, 2008; POULAIN et al., 2011). So far, oxygen and carbon isotope analysis of *M. lusoria* shells reveals no environmental changes during the Holocene, because only a few shells (n = 8) were analyzed up until now (Figs 1 and 2). Stable isotope analysis in *R. philippinarum* shells is ongoing research.

Future research should include:

- The analyses of more bivalve shells from British Columbia, Alaska and Japan to validate the obtained results. It is necessary to analyze many shells from each locality and from each time period due to their intra-specific variability. This approach increases the precision of paleoenvironmental reconstructions.

- The interpretation of proxy archives can be advanced by extensive analyses of modern data, which would reduce uncertainties of our knowledge of past environmental and climate changes.

- The improvement of the calibration between proxy and environmental data. This is necessary because proxy data may also contain non-climatic information, which is difficult to estimate.

- The study of more species to prove the results and further understand any local environmental variability.

- A construction of a multi-proxy network for a better global coverage and a better understanding of past climate. This multi-species and multi-proxy approach, i.e. the analysis of several taxa and several proxies, such as growth increments, stable isotopes and trace elements, within one organism improves the accuracy and reliability of paleoecological reconstructions. For, example, BLACK et al. (2009) provide a good approach in their reconstruction of sea surface temperature (SST) for the northeast Pacific from trees and *Panopea abrupta* shells. However, it is also important to consider the limitations of each proxy type and which proxy data should be used in a multi-proxy climate reconstruction. Furthermore, the correct calibration of these archives is necessary because they provide different timescales (MANN and JONES, 2003; MOBERG et al., 2005). The reconstruction of past climate requires an understanding of the proxy archives, e.g., individual differences, inter-annual variability and different localities have to be considered.

- The development of new proxy data, which is necessary to improve the accuracy of paleoenvironmental reconstructions.

- A combined analysis of shell growth increments, stable isotopes, trace elements and environmental data for environmental reconstructions from bivalve shells is required. Therefore, another topic of further research is the analysis of trace elements. Besides growth pattern and stable isotope analysis for the reconstruction of paleotemperature, paleosalinity and paleoproductivity, trace element ratios, e.g., Sr/Ca and Mg/Ca, can be used to validate these data. Furthermore, clumped isotopes may be used to reconstruct paleotemperatures. The advantage of reconstructing temperatures from

clumped isotopes instead from traditional oxygen isotopes is that the isotope value of the water in which the shell was precipitated has not to be assumed.

- The comparison of proxy data from different study regions and the comparison of regional shell records to other proxy archives, such as tree rings and lake sediments in order to detect large-scale climate patterns, to investigate land-sea interactions and to study teleconnections between Japan, Alaska, British Columbia and further study areas in the North Pacific. Knowledge of regional and local climate is essential to understand prehistoric shellfish gathering strategies and to gain insight into site occupation and seasonal mobility patterns of past people. However, local climate does not have to present large-scale climate.

- The comparison of the obtained results from *M. lusoria* and *R. philippinarum* with the environmental reconstructions of MIYAJI et al. (2010) from Holocene shells of the bivalve *Phacosoma japonicum*.

- Sclerochronological and geochemical methods improved considerably since the studies of KOIKE (1980) permitting new insights into past climate and seasonality patterns. Future research will extend these studies by applying modern sclerochronological and geochemical techniques to reconstruct past environmental and climatic changes (e.g., to reconstruct monsoon) and to resolve many archaeological questions, e.g., to determine the season, timing and water depth of shellfish collection. This sclerochronological analysis is essential to understand seasonal shellfish procurement strategies, settlement patterns of prehistoric peoples, the cultural development and reasons for sociocultural changes. The data may provide insights into the Jomon (ca. 12 000 to 2000 BP) and Yayoi (ca. 2000 BP to 300 AD) culture in Japan. Coastal communities are particularly important for the cultural development of this island country. People settled along the coast and marine resources provided the basis for their life.

# 6. REFERENCES

ABBOTT, M.B., FINNEY, B.P., EDWARDS, M.E., and KELTS, K.R., 2000. Lake-level reconstructions and paleohydrology of Birch Lake, Central Alaska, based on seismic reflection profiles and core transects. Quaternary Research 53, 154–166.

ALLEY, N.F., 1976. The palynology and palaeoclimatic significance of a dated core of Holocene peat, Okanagan Valley, southern British Columbia. Canadian Journal of Earth Sciences 13, 1131–1144.

BAILEY, G.N., 1975. The role of molluscs in coastal economies: The results of midden analysis in Australia. Journal of Archaeological Science 2, 45–62.

BAILEY, G.N., DEITH, M.R., and SHACKLETON, N.J., 1983. Oxygen isotope analysis and seasonality determinations: limits and potential of a new technique. American Antiquity 48, 390–398.

BARBER, V.A., JUDAY, G.P., FINNEY, B.P., and WILMKING, M., 2004. Reconstruction of summer temperatures in interior Alaska from tree-ring proxies: Evidence for changing synoptic climate regimes. Climatic Change 63, 91–120.

BARCLAY, D.J., WILES, G.C., and CALKIN, P.E., 1999. A 1119-year tree-ring-width chronology from western Prince William Sound, southern Alaska. The Holocene 9, 79–84.

BARNETT, T.P., PIERCE, D.W., LATIF, M., DOMMENGET, D., and SARAVANAN, R., 1999. Interdecadal interactions between the tropics and midlatitudes in the Pacific basin. Geophysical Research Letters 26, 615–618.

BARRON, J.A., and ANDERSON, L., 2010. Enhanced Late Holocene ENSO/PDO expression along the margins of the eastern North Pacific. Quaternary International, doi: 10.1016/j.quaint.2010.02.026.

BATTLE M., BENDER M., SOWERS T., TANS, P.P., BUTLER, J.H., ELKINS, J.W., ELLIS, J.T., CONWAY, T., ZHANG, N., LANG, P., and CLARKET, A.D., 1996. Atmospheric gas concentrations over the past century measured in air from firn at the South Pole. Nature 383, 231–235.

BEAMISH, R.J., and BOUILLON, D.R., 1993. Pacific salmon production trends in relation to climate. Canadian Journal of Fisheries and Aquatic Sciences 50, 1002–1016.

BECK, J.W., EDWARDS, R.L., ITO, E., TAYLOR, F.W., RECY, J., ROUGERIE, F., JOANNOT, P., and HENIN, C., 1992. Sea-surface temperature from coral skeletal strontium/calcium ratios. Science 257, 644–647.

BECKER, B., KRONER, B. and TRIMBORN, P., 1991. A stable isotope tree-ring timescale of the Late Glacial/Holocene boundary. Nature 353, 647–649.

BLACK, B.A., COPENHEAVER, C.A., FRANK, D.C., STUCKEY, M.J., and KORMANYOS, R.E., 2009. Multi-proxy reconstructions of northeastern Pacific sea surface temperature data from trees and Pacific geoduck. Palaeogeography, Palaeoclimatology, Palaeoecology 278, 40–47.

BÖHM, F., JOACHIMSKI, M.M., DULLO, W.-Ch., EISENHAUER, A., LEHNERT, H., REITNER, J., and WÖRHEIDE, G., 2000. Oxygen isotope fractionation in marine aragonite of coralline sponges. Geochimica et Cosmochimica Acta 64, 1695–1703.

BOENING, D.W., 1999. An evaluation of bivalves as biomonitors of heavy metals pollution in marine waters. Environmental Monitoring and Assessment 55, 459–470.

BONOMO, M., and AGUIRRE, M.L., 2009. Holocene molluscs from archaeological sites of the Pampean region of Argentina: Approaches to past human uses. Geoarchaeology 24, 59–85.

BRIFFA, K.R., BARTHOLIN, T.S., ECKSTEIN, D., JONES, P.D., KARLÉN, W., SCHWEINGRUBER, F.H., and ZETTERBERG, P., 1990. A 1,400–year tree–ring record of summer temperatures in Fennoscandia. Nature 346, 434–439.

BUDDEMEIER, R.W., 1975. Sclerochronology: a data source for reef systems models. Pacific Science Congress Record Of Proceedings 13, 124.

BUREAU, D., HAJAS, W., SURRY, N.W., HAND, C.M., DOVEY, G., and CAMPBELL, A., 2002. Age, size structure and growth parameters of geoducks (*Panopea abrupta*, Conrad 1849) from 34 locations in British Columbia sampled between 1993 and 2000. Canadian Technical Report of Fisheries and Aquatic Sciences 2413, 1–84.

BUTLER, P.G., RICHARDSON, C.A., SCOURSE, J.D., WANAMAKER JR., A.D., SHAMMON, T.M., and BENNELL, J.D., 2010. Marine climate in the Irish Sea: analysis of a 489-year marine master chronology derived from growth increments in the shell of the clam *Arctica islandica*. Quaternary Science Reviews 29, 1614–1632.

BUTLER, P.G., SCOURSE, J.D., RICHARDSON, C.A., WANAMAKER, A.D.JR., BRYANT, C., and BENNELL, J.D., 2009. Continuous marine radiocarbon reservoir calibration and the $^{13}C$ Suess effect in the Irish Sea: results from the first multi-centennial shell-based marine master chronology. Earth and Planetary Science Letters 279, 230–241.

CALKIN, P.E., WILES, G.C., and BARCLAY, D.J., 2001. Holocene coastal glaciation of Alaska. Quaternary Science Reviews 20, 449–461.

CANE, M.A., 2005. The evolution of El Niño, past and future. Earth and Planetary Science Letters 230, 227-240.

CARRÉ, M., BENTALEB, I., BLAMART, D., OGLE, N., CARDENAS, F., ZEVALLOS, S., KALIN, R.M., ORTLIEB, L., and FONTUGNE, M., 2005. Stable isotopes and sclerochronology of the bivalve *Mesodesma donacium*: Potential application to Peruvian paleoceanographic reconstructions. Palaeogeography, Palaeoclimatology, Palaeoecology 228, 4–25.

CHANG, A.S., and PATTERSON, R.T., 2005. Climate shift at 4400 years BP: Evidence from high-resolution diatom stratigraphy, Effingham Inlet, British Columbia, Canada. Palaeogeography, Palaeoclimatology, Palaeoecology 226, 72–92.

CHASE, M., BLESKIE, C., WALKER, I.R., GAVIN, D.G., and HU, F.S., 2008. Midge-inferred Holocene summer temperatures in Southeastern British Columbia, Canada. Palaeogeography, Palaeoclimatology, Palaeoecology 257, 244–259.

CHINZEI, K., KOIKE, H., OBA, T., MATSUSHIMA, Y., and KITAZATO, H., 1987. Secular changes in the oxygen isotope ratios of mollusk shells during the Holocene of Central Japan. Palaeogeography, Palaeoclimatology, Palaeoecology 61, 155–166.

CLARK II, G.R., 1974. Growth lines in invertebrate skeletons. Annual Review of Earth and Planetary Sciences 2, 77–99.

CLARK II, G.R., 1975. Periodic growth and biological rhythms in experimentally grown bivalves. *In*: ROSENBERG, G.D., RUNCORN, S.K. (eds.), Growth Rhythms and the History of the Earth's Rotation. Wiley, London, 103–117.

D'ARRIGO, R.D., and JACOBY, G.C., 1991. A 1000-year record of winter precipitation from northwestern New Mexico, USA: a reconstruction from tree-rings and its relation to El Niño and the Southern Oscillation. The Holocene 1, 95–101.

D'ARRIGO, R.D., VILLALBA, R., and WILES, G., 2001. Tree-ring estimates of Pacific decadal climate variability. Climate Dynamics 18, 219–224.

DAVENPORT, C.B., 1938. Growth lines in fossil pectens as indicators of past climates: Journal of Paleontology 12, 514–515.

DAVIS, H.C., and CALABRESE, A., 1964. Combined effects of temperature and salinity on development of eggs and growth of larvae of *M. mercenaria* and *C. virginica*. Fishery Bulletin 63, 643–655.

DAVIS, L.G., and MUEHLENBACHS, K., 2001. A late Pleistocene to Holocene record of precipitation reflected in *Margaritifera falcata* shell $\delta^{18}$Oshell from three archaeological sites in the lower Salmon River canyon, Idaho. Journal of Archaeological Science 28, 291–303.

DEMENOCAL, P.B., 2001. Cultural responses to climate change during the Late Holocene. Science 292, 667–673.

DETTINGER, M.D., BATTISTI, D.S., GARREAUD, R.D., MCCABE, G.J., and BITZ, C.M., 2001. Interhemispheric effects of interannual and decadal ENSO-like climate variations on the Americas. *In*: MARKGRAF, V. (ed.), Interhemispheric climate linkages: Present and Past Climates in the Americas and their Societal Effects. Academic Press, 1–16.

DETTMAN, D.L., and LOHMANN, K.C., 1995. Microsampling carbonates for stable isotope and minor element analysis; physical separation of samples on a 20 micrometer scale. Journal of Sedimentary Research 65, 566–569.

DETTMAN, D.L., REISCHE, A.K., and LOHMANN, K.C., 1999. Controls on the stable isotope composition of seasonal growth bands in aragonitic fresh-water bivalves (unionidae). Geochimica et Cosmochimica Acta 63, 1049–1057.

ELLIS, D.W., and SWAN, L., 1981. Teaching of the tides: uses of marine invertebrates by the Manhousat people. Theytus Books, Chapter 3.

EMERY, W.J., and HAMILTON, K., 1985. Atmospheric forcing of interannual variability in the Northeast Pacific Ocean: Connections with El Niño. Journal of Geophysical Research 90, 857–868.

ENGSTROM, D.R., and NELSON, S.R., 1991. Paleosalinity from trace metals in fossil ostracodes compared with observational records at Devils Lake, North Dakota, USA. Palaeogeography, Palaeoclimatology, Palaeoecology 83, 295–312.

EPSTEIN, S., BUCHSBAUM, R., LOWENSTAM, H.A., and UREY, H.C., 1953. Revised carbonate-water isotopic temperature scale. Bulletin of the Geological Society of America 64, 1315–1326.

EVANS, J.W., 1972. Tidal growth increments in the cockle *Clinocardium nuttalli*. Science 176, 416–417.

FALLON, S.J., MCCULLOCH, M.T., and GUILDERSON, T.P., 2005. Interpreting environmental signals from the coralline sponge *Astrosclera willeyana*. Palaeogeography, Palaeoclimatology, Palaeoecology 228, 58–69.

FRANCIS, R.C., HARE, S.R., HOLLOWED, A.B., and WOOSTER, W.S., 1998. Effects of interdecadal climate variability on the oceanic ecosystems of the Northeast Pacific. Fisheries Oceanography 7, 1–21.

FREITAS, P., CLARKE, L.J., KENNEDY, H., RICHARDSON, C., and ABRANTES, F., 2005. Mg/Ca, Sr/Ca, and stable-isotope ($\delta^{18}O$ and $\delta^{13}C$) ratio profiles from the fan mussel *Pinna nobilis*: Seasonal records and temperature relationships. Geochemistry, Geophysics, Geosystems 6, Q04D14, doi:10.1029/2004GC000872.

FRIEDLI, H., LOTSCHER, H., OESCHGER, H., SIEGENTHALER, U., and STAUFFER, B., 1986. Ice core record of the $^{13}C/^{12}C$ ratio of atmospheric $CO_2$ in the past two centuries. Nature 324, 237–238.

FRITTS, H.C., 1976. Tree rings and climate. Academic Press, London, 1–567 p.

GEDALOF, Z., MANTUA, N. J., and PETERSON D. L., 2002. A multi-century perspective of variability in the Pacific Decadal Oscillation: new insights from tree rings and coral. Geophysical Research Letters 29, 2204, doi:10.1029/2002GL015824.

GERSHUNOV, A., and BARNETT, T.P., 1998. Interdecadal modulation of ENSO teleconnections. Bulletin of the American Meteorological Society 79, 2715–2725.

GILLIKIN, D.P., LORRAIN, A., BOUILLON, S., WILLENZ, P., and DEHAIRS, F., 2006. Shell carbon isotopic composition of *Mytilus edulis* shells: relation to metabolism, salinity, $\delta^{13}C_{DIC}$ and phytoplankton. Organic Geochemistry 37, 1371–1382.

GILLIKIN, D.P., LORRAIN, A., NAVEZ, J., TAYLOR, J.W., ANDRÉ, L., KEPPENS, E., BAEYENS, W., and DEHAIRS, F., 2005. Strong biological controls on Sr/Ca ratios in aragonitic marine bivalve shells. Geochemistry, Geophysics, Geosystems 6, Q05009, doi:10.1029/2004GC000874.

GOODWIN, D.H., FLESSA, K.W., SCHÖNE, B.R., and DETTMAN, D.L., 2001. Cross-calibration of daily growth increments, stable isotope variation, and temperature in the Gulf of California bivalve mollusk *Chione cortezi*: implications for paleoenvironmental analysis. PALAIOS 16, 387–398.

GRAUMLICH, L.J., 1987. Precipitation Variation in the Pacific Northwest (1675–1975) as Reconstructed from Tree Rings. Annals of the Association of American Geographers 77, 19–29.

GROSSMAN, E.L., and KU, T.-L., 1986. Oxygen and carbon isotope fractionation in biogenic aragonite; temperature effects. Chemical Geology (Isotope Geoscience Section) 59, 59–74.

HALFAR, J., HETZINGER, S., ADEY, W., ZACK, T., GAMBOA, G., KUNZ, B., WILLIAMS, B., and JACOB, D.E., 2011. Coralline algal growth-increment widths archive North Atlantic climate variability. Palaeogeography, Palaeoclimatology, Palaeoecology 302, 71–80.

HALFAR, J., STENECK, R., SCHÖNE, B.R., MOORE, G.W.K., JOACHIMSKI, M., KRONZ, A., FIETZKE, J., and ESTES, J., 2007. Coralline alga reveals first marine record of subarctic North Pacific climate change. Geophysical Research Letters 34, L07702, doi:10.1029/2006GL028811.

HALLMANN, N., BURCHELL, M., SCHÖNE, B.R., IRVINE, G.V., and MAXWELL, D., 2009. High-resolution sclerochronological analysis of the bivalve mollusk *Saxidomus gigantea* from Alaska and British Columbia: techniques for revealing environmental archives and archaeological seasonality. Journal of Archaeological Science 36, 2353–2364.

HARE, S.R., and MANTUA, N.J., 2000. Empirical evidence for North Pacific regime shifts in 1977 and 1989. Progress in Oceanography 47, 103–146.

HARE, S.R, MANTUA, N.J., and FRANCIS, R.C., 1999. Inverse Production Regimes: Alaska and West Coast pacific salmon. Fisheries 24, 6–14.

HEBDA, R.J., 1995. British Columbia vegetation and climate history with focus on 6 ka BP. Géographique physique et Quaternaire 49, 55–79.

HEINRICHS, M.L.,WILSON, S.E., WALKER, I.R., SMOL, J.P., MATHEWES, R.W., and HALL, K.J., 1997. Midge- and diatom-based palaeosalinity reconstructions for Mahoney Lake, Okanagaan Valley, British Columbia, Canada. International Journal of Salt Lake Research 6, 249–267.

HENDY, C.H., and WILSON, A.T., 1968. Palaeoclimatic data from speleothems. Nature 219, 48–51.

HETZINGER, S., HALFAR, J., KRONZ, A., STENECK, R.S., ADEY, W., LEBENDNIK, A., and SCHÖNE, B.R., 2009. High-resolution Mg/Ca ratios in a coralline red alga as a proxy for Bering Sea temperature variations from 1902 to 1967. PALAIOS 24, 406–412.

HEUSSER, C.J., HEUSSER, L.E., and PETEET, D.M., 1985. Late-Quaternary climate change on the American North Pacific Coast. Nature 315, 485–487.

HOUGH, J.L., 1953. Pleistocene Climatic Record in a Pacific Ocean Core Sample. Journal of Geology 61, 252–262.

HU, F.S., ITO, E., BRUBAKER, L.B., and ANDERSON, P.M., 1998. Ostracode geochemical record of Holocene climatic change and implications for vegetational response in the Northwestern Alaska Range. Quaternary Research 49, 86–95.

HU, A., MEEHL, G.A., OTTO-BLIESNER, B.L., WAELBROECK, C., HAN, W., LOUTRE, M.-F., LAMBECK, K., MITROVICA, J.X., and ROSENBLOOM, N., 2010. Influence of Bering Strait flow and North Atlantic circulation on glacial sea-level changes. Nature Geoscience 3, 118–121.

HU, F.S., and SHEMESH, A., 2003. A biogenic-silica $\delta^{18}O$ ercord of climatic change during the last glacial-interglacial transition in southwestern Alaska. Quaternary Research 59, 379-385.

HUDSON, J.H., SHINN, E., HALLEY, R., and LIDZ, B., 1976. Sclerochronology: a new tool for interpreting past environments. Geology 4, 361–364.

JOHNSEN, S.J., DAHL-JENSEN, D., DANSGAARD, W., and GUNDESTRUP, N., 1995. Greenland palaeotemperatures derived from GRIP bore hole temperature and ice core isotope profiles. Tellus B, 47, 624–629.

JOHNSON, W.R., ROYER, T.C., and LUICK, J.L., 1988. On the seasonal variability of the Alaska Coastal Current. Journal of Geophysical Research 93, 12423–12437.

JONES, D.S., 1980. Annual cycle of shell growth increment formation in two continental shelf bivalves and its paleoecologic significance. Paleobiology 6, 331–340.

JONES, D.S., 1981. Annual growth increments in shells of *Spisula solidissima* record marine temperature variability. Science 211, 165–166.

JONES, D.S., 1983. Sclerochronology: reading the record of the molluscan shell. American Scientist 71, 384–391.

JONES, D.S., and ALLMON, W.D., 1995. Records of upwelling, seasonality and growth in stable-isotope profiles of Pliocene mollusk shells from Florida. Lethaia 28, 61–74.

JONES, D.S., ARTHUR, M.A., and ALLARD, D.J., 1989. Sclerochronological records of temperature and growth from shells of *Mercenaria mercenaria* from Narragansett Bay, Rhode Island. Marine Biology 102, 225–234.

JONES, D.S., and QUITMYER, I.R., 1996. Marking time with bivalve shells: oxygen isotopes and season of annual increment formation. PALAIOS 11, 340–346.

JONES, D.S., WILLIAMS, D.F., and ARTHUR, M.A., 1983. Growth history and ecology of the Atlantic surf clam, *Spisula solidissima* (Dillwyn), as revealed by stable isotopes and annual shell increments. Journal of Experimental Marine Biology and Ecology 73, 225–242.

JONES, D.S., WILLIAMS, D.F., ARTHUR, M.A., and KRANTZ, D.E., 1984. Interpreting the paleoenvironmental, paleoclimatic and life history records in mollusk shells. Geobios 17, 333–339.

KALISH, J.M., 1991. $^{13}C$ and $^{18}O$ isotopic disequilibria in fish otoliths: metabolic and kinetic effects. Marine Ecology Progress Series 75, 191–203.

KANAZAWA, T., and SATO, S., 2008. Environmental and physiological controls on shell microgrowth pattern of *Ruditapes philippinarum* (Bivalvia: Veneridae) from Japan. Journal of Molluscan Studies 74, 89–95.

KEIGWIN, L.D., and Cook, M.S., 2007. A role for North Pacific salinity in stabilizing North Atlantic climate. Paleooceanography 22, PA3102, doi:10.1029/2007PA001420.

KENNETT, D.J., and VOORHIES, B., 1996. Oxygen isotopic analysis of archaeological shells to detect seasonal use of wetlands on the Southern Pacific Coast of Mexico. Journal of Archaeological Science 23, 689–704.

KENNISH, M.J., and OLSSON, R.K., 1975. Effects of thermal discharges on the microstructural growth of *Mercenaria mercenaria*. Environmental Geology (Springer) 1, 41–64.

KHIM, B.-K., IKEHARA, K., and SHIN, Y., 2005. Unstable Holocene climate in the northeastern East Sea (Sea of Japan): evidence from a diatom record. Palaeogeography, Palaeoclimatology, Palaeoecology 216, 251–265.

KILLINGLEY, J.S., 1981. Seasonality of mollusk collecting determined from O-18 profiles of midden shells. American Antiquity 46, 152–158.

KILLINGLEY, J.S., and BERGER, W.H., 1979. Stable isotopes in a mollusk shell: Detection of upwelling events. Science 205, 186–188.

KIPPHUT, G.W., 1990. Glacial meltwater input to the Alaska coastal current: Evidence from oxygen isotope measurements. Journal of Geophysical Research 95, 5177–5181.

KITTS, D.D., SMITH, D.S., BEITLER, M.K., and LISTON, J., 1992. Presence of paralytic shellfish poisoning toxins and soluble proteins in toxic butter clams (*Saxidomus giganteus*). Biochemical and Biophysical Research Communications 184, 511–517.

KOIKE, H., 1980. Seasonal dating by growth-line counting of the clam *Meretrix lusoria*. University Museum, University of Tokyo, Bulletin 18, 120 p.

KRAEUTER, J.N., and CASTAGNA, M. (eds.), 2001. Biology of the hard clam: Elsevier Science, Amsterdam, 755 p.

KRANTZ, D.E., WILLIAMS, D.F., and JONES, D.S., 1987. Ecological and paleoenvironmental information using stable isotope profiles from living and fossil molluscs. Palaeogeography, Palaeoclimatology, Palaeoecology 58, 249–266.

KVITEK, R.G., 1991. Paralytic shellfish toxins sequestered by bivalves as a defense against siphon-nipping fish. Marine Biology 111, 369–374.

KVITEK, R.G., and BEITLER, M.K., 1991. Relative insensitivity of butter clam neurons to saxitoxin: A pre-adaptation for sequestering paralytic shellfish poisoning toxins as a chemical defense. Marine Ecology Progress Series 69, 47–54.

KVITEK, R., and BRETZ, C., 2004. Harmful algal bloom toxins protect bivalve populations from sea otter predation. Marine Ecology Progress Series 271, 233–243.

LAMOUREUX, S., 2000. Five centuries of interannual sediment yield and rainfall-induced erosion in the Canadian High Arctic recorded in lacustrine varves. Water Resources Research 36, 309–318.

LAROCQUE, S.J., and SMITH, D.J., 2005. A dendroclimatological reconstruction of climate since AD 1700 in the Mt. Waddington area, British Columbia Coast Mountains, Canada. Dendrochronologia 22, 93–106.

LAURITZEN, S.-E., and LUNDBERG, J. 1999. Speleothems and climate: a special issue of The Holocene. The Holocene 9, 643–647.

LAZARETH, C.E., LASNE, G., and ORTLIEB, L., 2006. Growth anomalies in *Protothaca thaca* (Mollusca, Veneridae) shells as markers of ENSO conditions. Climate Research 30, 263–269.

LEVY, L.B., KAUFMAN, D.S., and WERNER, A., 2004. Holocene glacier fluctuations, Waskey Lake, northeastern Ahklun Mountains, southwestern Alaska. The Holocene 14, 185–193.

LORRAIN, A., PAULET, Y.-M., CHAUVAUD, L., DUNBAR, R., MUCCIARONE, D., and FONTUGNE, M., 2004. $\delta^{13}C$ variation in scallop shells: increasing metabolic carbon contribution with body size. Geochimica et Cosmochimica Acta 68, 3509–3519.

LOUGH, J.M., and FRITTS, H.C., 1985. The Southern Oscillation and tree rings: 1600-1961. Journal of Applied Meteorology 24, 952–966.

LUTAENKO, K.A., ZHUSHCHIKHOVSKAYA, I.S., MIKISHIN, Y.A., and POPOV, A.N., 2007. Mid-Holocene climatic changes and cultural dynamics in the basin of the Sea of Japan and adjacent areas. *In*: ANDERSON, D.G., MAASCH, K.A., SANDWEISS, D.H. (eds.), Climate change and cultural dynamics: A global perspective on Mid-Holocene transitions. 331–406.

LUTZ, R.A., and RHOADS, D.C., 1980. Growth patterns within the Molluscan shell: An overview. *In*: Rhoads, D.C., Lutz, R.A. (eds.), Skeletal Growth of Aquatic Organisms: Biological records of environmental change. Plenum, New York, 203–254.

MANN, D.H., and HAMILTON, T.D., 1995. Late Pleistocene and Holocene paleoenvironments of the North Pacific Coast. Quaternary Science Reviews 14, 449–471.

MANN, M.E., and JONES, P.D., 2003. Global surface temperatures over the past two millennia. Geophysical Research Letters 30, 1820, doi:10.1029/2003GL017814.

MANTUA, N.J., and HARE, S.R., 2002. The Pacific Decadal Oscillation. Journal of Oceanography 58, 35–44.

MANTUA, N.J., HARE, S.R., ZHANG, Y., WALLACE, J.M., and FRANCIS, R.C., 1997. A Pacific decadal climate oscillation with impacts on salmon. Bulletin of the American Meteorological Society 78, 1069–1079.

MARCHITTO, T.A., JONES, G.A., GOODFRIEND, G.A., and WEIDMAN, C.R., 2000. Precise temporal correlation of Holocene mollusk shells using sclerochronology. Quaternary Research 53, 236–246.

MARSDEN, I.D., 2004. Effects of reduced salinity and seston availability on growth of the New Zealand little-neck clam *Austrovenus stutchburyi*. Marine Ecology Progress Series 266, 157–171.

MARTINDALE, A., LETHAM, B., MCLAREN, D., ARCHER, D., BURCHELL, M., and SCHÖNE, B.R., 2009. Mapping of subsurface shell midden components through percussion coring: examples from the Dundas Islands. Journal of Archaeological Science 36, 1565–1575.

MATHEWES, R.W., and HEUSSER, L.E., 1981. A 12 000 year palynological record of temperature and precipitation trends in southwestern British Columbia. Canadian Journal of Botany 59, 707–710.

MATHEWES, R.W., and KING, M., 1989. Holocene vegetation, climate, and lake-level changes in the interior Douglas-fir Biogeoclimatic Zone, British Columbia. Canadian Journal of Earth Sciences 26, 1811–1825.

MATSUSHIMA, Y., 1982. Radiocarbon ages of the Holocene marine deposits along Kucharo Lake, Northern Hokkaido. Bulletin of the Kanagawa Prefectural Museum 13, 51–66.

MATSUSHIMA, Y., and KAWAGUCHI, T., 1991. Radiocarbon ages and the Molluscan fauna from the Holocene marine deposits in the "Seto Jinja" site, Kanazawahakkei, Yokohama. Bulletin of the Kanagawa Prefectural Museum 20, 31–49.

MATSUSHIMA, Y., and KAWAKAMI, J., 1995. Radiocarbon age of the Molluscan shells from the Holocene marine deposits in the Nemuro Peninsula, Eastern Hokkaido. Bulletin of the Kanagawa Prefectural Museum 24, 39–46.

MCCONNAUGHEY, T., 1989a. $^{13}C$ and $^{18}O$ isotopic disequilibrium in biological carbonates: I. Patterns. Geochimica et Cosmochimica Acta 53, 151–162.

McCONNAUGHEY T., 1989b. $^{13}C$ and $^{18}O$ isotopic disequilibrium in biological carbonates. II: In *vitro* simulation of kinetic isotope effects. Geochimica et Cosmochimica Acta 53, 163–171.

McCONNAUGHEY, T.A., BURDETT, J., WHELAN, J.F., and PAULL, C.K., 1997. Carbon isotopes in biological carbonates: respiration and photosynthesis. Geochimica et Cosmochimica Acta 61, 611–622.

McCONNAUGHEY, T.A., and GILLIKIN, D.P., 2008. Carbon isotopes in mollusk shell carbonates. Geo-Marine Letters 28, 287–299.

McDERMOTT, F., 2004. Palaeo-climate reconstruction from stable isotope variations in speleothems: a review. Quaternary Science Reviews 23, 901–918.

Mc LEAN FRASER, M., and SMITH, G.M., 1928. Notes on the ecology of the butter clam, *Saxidomus giganteus* Deshayes. Section V, Transactions of the Royal Society of Canada 3, 271–284.

MITSUGUCHI, T., MATSUMOTO, E., ABE, O., UCHIDA, T., and ISDALE, P.J., 1996. Mg/Ca thermometry in coral skeletons. Science 274, 961–963.

MIYAJI, T., TANABE, K., MATSUSHIMA, Y., SATO, S., YOKOYAMA, Y., and MATSUZAKI, H., 2010. Response of daily and annual shell growth patterns of the intertidal bivalve *Phacosoma japonicum* to Holocene coastal climate change in Japan. Palaeogeography, Palaeoclimatology, Palaeoecology 286, 107–120.

MOBERG, A., SONECHKIN, D.M., HOLMGREN, K., DATSENKO, N.M., and KARLÉN, W., 2005. Highly variable Northern Hemisphere temperatures reconstructed from low- and high-resolution proxy data. Nature 433, 613–617.

MONNIN, E., STEIG, E.J., SIEGENTHALER, U., KAWAMURA, K., SCHWANDER, J., STAUFFER, B., STOCKER, T.F., MORSE, D.L., BARNOLA, J.-M., BELLIER, B., RAYNAUD, D., and FISCHER, H., 2004. Evidence for substantial accumulation rate variability in Antarctica during the Holocene, through synchronization of $CO_2$ in the Taylor Dome, Dome C and DML ice cores. Earth and Planetary Science Letters 224, 45–54.

MOOK, W.G., and VOGEL, J.C., 1968. Isotopic equilibrium between shells and their environment. Science 159, 874–875.

MOORE, J.J., HUGHEN, K.A., MILLER, G.H., and OVERPECK, J.T., 2001. Little Ice Age recorded in summer temperature reconstruction from varved sediments of Donard Lake, Baffin Island, Canada. Journal of Paleolimnology 25, 503–517.

MOSS, M.L., PETEET, D.M., and WHITLOCK, C., 2007. Mid-Holocene culture and climate on the Northwest Coast of North America. *In*: ANDERSON, D., MAASCH, K., SANDWEISS,

D. (eds.), Climate change and cultural dynamics: A Global Perspective on Mid-Holocene Transitions. Academic Press, London, 491–530.

MOY, C.M., SELTZER, G.O., RODBELL, D.T., and ANDERSON, D.M., 2002. Variability of El Niño/Southern Oscillation activity at millennial timescales during the Holocene epoch. Nature 420, 162–165.

MUDIE, P.J., ROCHON, A., and LEVAC, E., 2002. Palynological records of red-tide producing species in Canada: past trends and implications for the future. Palaeogeography, Palaeoclimatology, Palaeoecology 180, 159–186.

MUENCH, R.D., MOFJIELD, H.O., and CHARNELL, R.L., 1978. Oceanographic conditions in lower Cook Inlet: spring and summer 1973. Journal of Geophysical Research 83, 5090–5098.

MUNDY, P.R. (ed.), 2005. The Gulf of Alaska: Biology and Oceanography. Alaska Sea Grant College Program, University of Alaska Fairbanks, 214 p.

NEDERBRAGT, A.J., and THUROW, J.W., 2001. A 6000 yr varve record of Holocene climate in Saanich Inlet, British Columbia, from digital sediment colour analysis of ODP Leg 169S cores. Marine Geology 174, 95–110.

NICKERSON, R.B., 1977. A study of the littleneck clam (*Protothaca staminea* Conrad) and the butter clam (*Saxidomus giganteus* Deshayes) in a habitat permitting coexistence, Prince William Sound, Alaska. Proceedings of the National Shellfisheries Association 67, 85–102.

NOAKES, D.J., and CAMPBELL, A., 1992. Use of geoduck clams to indicate changes in the marine environment of Ladysmith Harbor, British Columbia. Environmetrics 3, 81–97.

OHNO, T., 1985. Experimentelle Analysen zur Rhythmik des Schalenwachstums einiger Bivalven und ihre paläobiologische Bedeutung. Palaeontographica 189, 63–123.

OVERLAND, J.E., ADAMS, J.M., and BOND, N.A. 1999. Decadal Variability of the Aleutian Low and Its Relation to High-Latitude Circulation. Journal of Climate 12, 1542–1548.

OWEN, R., KENNEDY, H., and RICHARDSON, C., 2002. Isotopic partitioning between scallop-shell calcite and seawater: effect of shell-growth rate. Geochimica et Cosmochimica Acta 66, 1727–1737.

OWEN, E.F., WANAMAKER JR., A.D., FEINDEL, S.C., SCHÖNE, B.R., and RAWSON, P.D., 2008. Stable carbon and oxygen isotope fractionation in bivalve (*Placopecten magellanicus*) larval aragonite. Geochimica et Cosmochimica Acta 72, 4687–4698.

PAERL, H.W., STEPPE, T.F., BUCHAN, K.C., and POTTS, M., 2003. Hypersaline cyanobacterial mats as indictors of elevated Tropical Hurricane Activity and Associated Climate Change. Ambio 32, 87–90.

PALMER, S., WALKER, I., HEINRICHS, M., HEBDA, R., and SCUDDER, G., 2002. Postglacial midge community change and Holocene palaeotemperature reconstructions near treeline, southern British Columbia (Canada). Journal of Paleolimnology 28, 469–490.

PANNELLA, G., 1976. Tidal growth patterns in recent and fossil mollusk bivalve shells: a tool for the reconstruction of paleotides. Naturwissenschaften 63, 539–543.

PANNELLA, G., and MACCLINTOCK, C., 1968. Biological and environmental rhythms reflected in molluscan shell growth. Paleontological Society Memoirs 42, 64–80.

PAUL, A.J., PAUL, J.M., and FEDER, H.M., 1976. Age, growth, and recruitment of the butter clam, *Saxidomus gigantea*, on Porpoise Island, Southeast Alaska. Proceedings of the National Shellfisheries Association 66, 26–28.

PELLATT, M.G., HEBDA, R.J., and MATHEWES, R.W., 2001. High-resolution Holocene vegetation history and climate from Hole 1034B, ODP leg 169S, Saanich Inlet, Canada. Marine Geology 174, 211–226.

PELLAT, M.G., and MATHEWES, R.W., 1994. Paleoecology of postglacial tree line fluctuations on the Queen Charlotte Islands, Canada. Ecoscience 1, 71–81.

PELLATT, M.G., SMITH, M.J., MATHEWES, R.W., WALKER, I.R., and PALMER, S.L., 2000. Holocene treeline and climate change in the subalpine zone near Stoyoma Mountain, Cascade Mountains, southwestern British Columbia, Canada. Arctic, Antarctic, and Alpine Research 32, 73–83.

PETIT, J.R., JOUZEL, J., RAYNAUD, D., BARKOV, N.I., BARNOLA, J.-M., BASILE, I., BENDER, M., CHAPELLAZ, J., DAVIS, J., DELAYGUE, G., DELMOTTE, M., KOTLYAKOV, V.M., LEGRAND, M., LIPENKOV, V., LORIUS, C., PÉPIN, L., RITZ, C., SALTZMAN, E., and STIEVENARD, M., 1999. Climate and atmospheric history of the past 420,000 years from the Vostok ice core, Antarctica. Nature 399, 429–436.

PETIT, J.R., MOUNIER, L., JOUZEL, J., KOROTKEVICH, Y.S., KOTLYAKOV, V.I., and LORIUS, C., 1990. Palaeoclimatological and chronological implications of the Vostok core dust record. Nature 343, 56–58.

PFEIFFER, M., DULLO, W.-Ch., ZINKE, J., and GARBE-SCHÖNBERG, D., 2009. Three monthly coral Sr/Ca records from the Chagos Archipelago covering the period of 1950-1995 A.D.: reproducibility and implications for quantitative reconstructions of sea surface

temperature variations. International Journal of Earth Sciences (Geologische Rundschau) 98, 53–66.

PITTENDRIGH, C.S., 1979. Some functional aspects of circadian pacemakers. *In*: SUDA, M., HAYAISHI, O., NAKAGAWA, H. (eds.), Biological rhythms and their central mechanism. Elsevier, Netherlands, 3–12.

POULAIN, C., LORRAIN, A., FLYE-SAINTE-MARIE, J., AMICE, E., MORIZE, E., and PAULET, Y.-M., 2011. An environmentally induced tidal periodicity of microgrowth increment formation in subtidal populations of the clam *Ruditapes philippinarum*. Journal of Experimental Marine Biology and Ecology 397, 58–64.

PRICE, G.D., and PEARCE, N.J.G., 1997. Biomonitoring of pollution by *Cerastoderma edule* from the British Isles: a Laser Ablation ICP-MS study. Marine Pollution Bulletin 34, 1025–1031.

QUAYLE, D.B., and BOURNE, N., 1972. The clam fisheries of British Columbia. Fisheries Research Board of Canada, Ottawa, Bulletin 179, 70 p.

RAHIMPOUR-BONAB, H., BONE, Y., and MOUSSAVI-HARAMI, R., 1997. Stable isotope aspects of modern molluscs, brachiopods, and marine cements from cool-water carbonates, Lacepede Shelf, South Australia. Geochimica et Cosmochimica Acta 61, 207–218.

REIMER, P.J., BAILLIE, M.G.L., BARD, E., BAYLISS, A., BECK, J.W., BLACKWELL, P.G., BRONK RAMSEY, C., BUCK, C.E., BURR, G.S., EDWARDS, R.L., FRIEDRICH, M., GROOTES, P.M., GUILDERSON, T.P., HAJDAS, I., HEATON, T.J., HOGG, A.G., HUGHEN, K.A., KAISER, K.F., KROMER, B., MCCORMAC, F.G., MANNING, S.W., REIMER, R.W., RICHARDS, D.A., SOUTHON, J.R., TALAMO, S., TURNEY, C.S.M., VAN DER PLICHT, J., and WEYHENMEYER, C.E., 2009. IntCal09 and Marine09 radiocarbon age calibration curves, 0 - 50,000 years cal BP. Radiocarbon 51, 1111–1150.

REN, L., LINSLEY, B.K., WELLINGTON, G.M., SCHRAG, D.P., and HOEGH-GULDBERG, O., 2003. Deconvolving the $\delta^{18}O$ and Sr/Ca at Rarotonga in the southwestern subtropical Pacific for the period 1726 to 1997. Geochimica et Cosmochimica Acta 67, 1609–1621.

RHOADS, D.C., and PANNELLA, G., 1970. The use of molluscan shell growth patterns in ecology and paleoecology. Lethaia 3, 143–161.

RICHARDSON, C.A., 1987. Tidal bands in the shell of the clam *Tapes philippinarum* (Adams & Reeve, 1850). Proceedings of the Royal Society of London, Series B, Biological Sciences 230, 367–387.

RICHARDSON, C.A., 1988a. Exogenous and endogenous rhythms of band formation in the shell of the clam *Tapes philippinarum* (Adams et Reeve, 1850). Journal of Experimental Marine Biology and Ecology 122, 105–126.

RICHARDSON, C.A., 1988b. Tidally produced growth bands in the subtidal bivalve *Spisula subtruncata* (da Costa). Journal of Molluscan Studies 54, 71–82.

RODLAND, D.L., SCHÖNE, B.R., HELAMA, S., NIELSEN, J.K., and BAIER, S., 2006. A clockwork mollusc: ultradian rhythms in bivalve activity revealed by digital photography. Journal of Experimental Marine Biology and Ecology 334, 316–323.

ROSENBERG, S.M., WALKER, I.R., MATHEWES, R.W., and HALLETT, D.J., 2004. Midge-inferred Holocene climate history of two subalpine lakes in southern British Columbia, Canada. The Holocene 14, 258–271.

ROSENHEIM, B.E., SWART, P.K., THORROLD, S.R., EISENHAUER, A., and WILLENZ, P., 2005. Salinity change in the subtropical Atlantic: Secular increase and teleconnections to the North Atlantic Oscillation. Geophysical Research Letters 32, L02603, doi:10.1029/2004GL021499.

ROSENHEIM, B.E., SWART, P.K., THORROLD, S.R., WILLENZ, P., BERRY, L., and LATKOCZY, C., 2004. High-resolution Sr/Ca records in sclerosponges calibrated to temperature in situ. Geology 32, 145–148.

ROYER, T.C., 1981. Baroclinic transport in the Gulf of Alaska. Part II. A fresh water driven coastal current. Journal of Marine Research 39, 251–266.

ROYER, T.C., 1982. Coastal fresh water discharge in the Northeast Pacific. Journal of Geophysical Research 87, 2017–2021.

ROYER, T.C., and GROSCH, C.E., 2006. Ocean warming and freshening in the northern Gulf of Alaska. Geophysical Research Letters 33, L16605, doi: 10.1029/2006GL026767.

SAKAGUCHI, Y., 1983. Climatic variability during the Holocene epoch in Japan and its causes. University of Tokyo, Bulletin of the Department of Geography 15, 1–27.

SATO, S., 1997. Shell microgrowth patterns of bivalves reflecting seasonal change of phytoplankton abundance. Paleontological Research 1, 260–266.

SCHELSKE, C.L., ROBBINS, J.A., GARDNER, W.S., CONLEY, D.J., and BOURBONNIERE, R.A., 1988. Sediment record of biogeochemical responses to anthropogenic perturbations of nutrient cycles in Lake Ontario. Canadian Journal of Fisheries and Aquatic Sciences 45, 1291–1303.

SCHÖNE, B.R., 2008. The curse of physiology—challenges and opportunities in the interpretation of geochemical data from mollusk shells. Geo-Marine Letters, doi: 10.1007/s00367-008-0114-6.

SCHÖNE, B.R., DUNCA, E., FIEBIG, J., and PFEIFFER, M., 2005a. Mutvei's solution: an ideal agent for resolving microgrowth structures of biogenic carbonates. Palaeogeography Palaeoclimatology Palaeoecology 228, 149–166.

SCHÖNE, B.R., FREYRE CASTRO, A.D., FIEBIG, J., HOUK, S., OSCHMANN, W., and KRÖNCKE, I., 2004a. Sea surface temperatures over the period 1884–1983 reconstructed from oxygen isotope ratios of a bivalve mollusk shell (*Arctica islandica*, southern North Sea). Palaeogeography Palaeoclimatology Palaeoecology 212, 215–232.

SCHÖNE, B.R., GOODWIN, D.H., FLESSA, K.W., DETTMAN, D.L., and ROOPNARINE, P.D., 2002a. Sclerochronology and growth of the bivalve *Chione* (Chionista) *fluctifraga* and *C.* (Chionista) *cortezi* in the northern Gulf of California, Mexico. The Veliger 45, 45–54.

SCHÖNE, B.R., HICKSON, J., and OSCHMANN, W., 2005c. Reconstruction of subseasonal environmental conditions using bivalve mollusk shells—A graphical model. *In*: MORA, G., SURGE, D. (eds.), Isotopic and elemental tracers of Cenozoic climate change. Geological Society of America Special Paper 395, 21–31.

SCHÖNE, B.R., LEGA, J., FLESSA, K.W., GOODWIN, D.H., and DETTMAN, D.L., 2002b. Reconstructing daily temperatures from growth rates of the intertidal bivalve mollusk *Chione cortezi* (northern Gulf of California, Mexico). Palaeogeography, Palaeoclimatology, Palaeoecology 184, 131–146.

SCHÖNE, B.R., OSCHMANN, W., TANABE, K., DETTMAN, D., FIEBIG, J., HOUK, S.D., and KANIE, Y., 2004b. Holocene seasonal environmental trends at Tokyo Bay, Japan, reconstructed from bivalve mollusk shells—implications for changes in the east Asian monsoon and latitudinal shifts of the Polar Front. Quaternary Science Reviews 23, 1137–1150.

SCHÖNE, B.R., PFEIFFER, M., POHLMANN, T., and SIEGISMUND, F., 2005b. A seasonally resolved bottom-water temperature record for the period AD 1866–2002 based on shells of *Arctica islandica* (Mollusca, North Sea). International Journal of Climatology 25, 947–962.

SCHÖNE, B.R., TANABE, K., DETTMAN, D.L., and SATO, S., 2003. Environmental controls on shell growth rates and $\delta^{18}O$ of the shallow-marine bivalve mollusk *Phacosoma japonicum* in Japan. Marine Biology 142, 473–485.

SCHÖNE, B.R., WANAMAKER, A.D. JR., FIEBIG, J., THÉBAULT, J., and KREUTZ, K.J., 2011. Annually resolved $\delta^{13}C_{shell}$ chronologies of long-lived bivalve mollusks (*Arctica islandica*) reveal oceanic carbon dynamics in the temperate North Atlantic during recent centuries: Palaeogeography, Palaeoclimatology, Palaeoecology, In press, doi:10.1016/j.palaeo.2010.02.002.

SCHUMACHER, J.D., PEARSON, C.A., and OVERLAND, J.E., 1982. Exchange of water between the Gulf of Alaska and the Bering Sea through Unimak Pass. Journal of Geophysical Research 87, 5785–5795.

SHACKLETON, N.J., 1973. Oxygen isotope analysis as a means of determining season of occupation of prehistoric midden sites. Archaeometry 15, 133–141.

SPIES, R.B., 2007. Long-term ecological change in the Northern Gulf of Alaska. Elsevier Science, Amsterdam, 589 p.

SPÖTL, C., and MATTEY, D., 2006. Stable isotope microsampling of speleothems for palaeoenvironmental studies: A comparison of microdrill, micromill and laser ablation techniques. Chemical Geology 235, 48–58.

SPOONER, I., MAZZUCCHI, D., OSBORN, G., GILBERT, R., and LAROCQUE, I., 2002. A multi-proxy Holocene record of environmental change from the sediments of Skinny Lake, Iskut region, northern British Columbia, Canada. Journal of Paleolimnology 28, 419–431.

STABENO, P.J., BOND, N.A., HERMANN, A.J., KACHEL, N.B., MORDY, C.W., and OVERLAND, J.E., 2004. Meteorology and oceanography of the Northern Gulf of Alaska. Continental Shelf Research 24, 859–897.

STEIG, E.J., GROOTES, P.M., and STUIVER, M., 1994. Seasonal precipitation timing and ice core records. Science 266, 1885–1886.

STENSETH, N.C., MYSTERUD, A., OTTERSEN, G., HURRELL, J.W., CHAN, K.-S., and LIMA, M., 2002. Ecological effects of climate fluctuations. Science 297, 1292–1296.

STROM, A., FRANCIS, R.C., MANTUA, N.J., MILES, E.L., and PETERSON, D.L., 2004. North Pacific climate recorded in growth rings of geoduck clams: a new tool for paleoenvironmental reconstruction. Geophysical Research Letters 31, L06206, doi:10.1029/2004GL019440.

STUIVER, M., and REIMER, P. J., 1993. Extended $^{14}C$ database and revised CALIB 3.0 $^{14}C$ age calibration program. Radiocarbon 35, 215–230.

TANABE, K., and OBA, T., 1988. Latitudinal variation in shell growth patterns of *Phacosoma japonicum* (Bivalvia: Veneridae) from the Japanese coast. Marine Ecology Progress Series 47, 75–82.

TANAKA, N., MONAGHAN, M.C., and RYE, D.M., 1986. Contribution of metabolic carbon to mollusc and barnacle shell carbonate. Nature 320, 520–523.

THOMPSON, L.G., DAVIS, M.E., MOSLEY-THOMPSON, E., SOWERS, T.A., HENDERSON, K.A., ZAGORODNOV, V.S., LIN, P.-N., MIKHALENKO, V.N., CAMPEN, R.K., BOLZAN, J.F., COLE-DAI, J., and FRANCOU, B., 1998. A 25,000-year tropical climate history from Bolivian ice cores. Science 282, 1858–1864.

TRENBERTH, K.E., and HURRELL, J.W., 1994. Decadal atmosphere-ocean variations in the Pacific. Climate Dynamics 9, 303–319.

TRUTSCHLER, K., and SAMTLEBEN, C., 1988. Shell growth of *Astarte elliptica* (Bivalvia) from Kiel Bay (Western Baltic Sea). Marine Ecology Progress Series 42, 155–162.

TURNER, J.V., 1982. Kinetic fractionation of carbon-13 during calcium carbonate precipitation. Geochimica et Cosmochimica Acta 46, 1183–1191.

ULLMANN, C.V., WIECHERT, U., and KORTE, C., 2010. Oxygen isotope fluctuations in a modern North Sea oyster (*Crassostrea gigas*) compared with annual variations in seawater temperature: Implications for palaeoclimate studies. Chemical Geology 277, 160–166.

URBAN, F.E., COLE, J.E., and OVERPECK, J.T., 2000. Influence of mean climate change on climate variability from a 155-year tropical Pacific coral record. Nature 407, 989–993.

UREY, H.C., 1947. The thermodynamic properties of isotopic substances. Journal of the Chemical Society (London) 562–581.

VIMEUX, F., CUFFEY, K.M., and JOUZEL, J., 2002. New insights into Southern Hemisphere temperature changes from Vostok ice cores using deuterium excess correction. Earth and Planetary Science Letters 203, 829–843.

WALKER, I.R., and CWYNAR, L.C., 2006. Midges and palaeotemperature reconstruction—the North American experience. Quaternary Science Reviews 25, 1911–1925.

WALKER, I.R., and MATHEWES, R.W., 1987. Chironomidae (Diptera) and Postglacial climate at Marion Lake British Columbia, Canada. Quaternary Research 27, 89–102.

WALKER, I.R., and PELLATT, M.G., 2003. Climate change in coastal British Columbia— A paleoenvironmental perspective. Canadian Water Resources Journal 28, 531–566.

WALLACE, J.M., and GUTZLER, D.S., 1981. Teleconnections in the geopotential height field during the Northern Hemisphere winter. Monthly Weather Review 109, 784–812.

WANAMAKER JR., A.D., HEINEMEIER, J., SCOURSE, J.D., RICHARDSON, C.A., BUTLER, P.G., EIRÍKSSON, J., and KNUDSEN, K.L., 2008a. Very long-lived mollusks confirm 17th century AD tephra-based radiocarbon reservoir ages for north Icelandic shelf waters. Radiocarbon 50, 399–412.

WANAMAKER JR., A.D., KREUTZ, K.J., SCHÖNE, B.R., MAASCH, K.A., PERSHING, A.J., BORNS, H.W., INTRONE, D.S., and FEINDEL, S., 2009. A late Holocene paleo-productivity record in the western Gulf of Maine, USA, inferred from growth histories of the long-lived ocean quahog (*Arctica islandica*). International Journal of Earth Sciences (Geologische Rundschau) 98, 19–29.

WANAMAKER JR., A.D., KREUTZ, K.J., SCHÖNE, B.R., PETTIGREW, N., BORNS, H.W., INTRONE, D.S., BELKNAP, D., MAASCH, K.A., and FEINDEL, S., 2008b. Coupled North Atlantic slope water forcing on Gulf of Maine temperatures over the past millennium. Climate Dynamics 31, 183–194.

WANNER, H., BEER, J., BÜTIKOFER, J., CROWLEY, T.J., CUBASCH, U., FLÜCKIGER, J., GOOSSE, H., GROSJEAN, M., JOOS, F., KAPLAN, J.O., KÜTTEL, M., MÜLLER, S.A., PRENTICE, I.C., SOLOMINA, O., STOCKER, T.F., TARASOV, P., WAGNER, M., and WIDMANN, M., 2008. Mid- to Late Holocene climate change: an overview. Quaternary Science Reviews 27, 1791–1828.

WEFER, G., and BERGER, W.H., 1991. Isotope paleontology: growth and composition of extant calcareous species. Marine Geology 100, 207–248.

WILES, G.C., D'ARRIGO, R.D., and JACOBY, G.C., 1996. Temperature changes along the Gulf of Alaska and the Pacific Northwest coast modeled from coastal tree rings. Canadian Journal of Forest Research 26, 474–481.

WILES, G.C., D'ARRIGO, R.D., and JACOBY, G.C., 1998. Gulf of Alaska atmosphere-ocean variability over recent centuries inferred from coastal tree-ring records. Climatic Change 38, 289–306.

WILLIAMS, D.F., ARTHUR, M.A., JONES, D.S., and HEALY-WILLIAMS, N., 1982. Seasonality and mean annual sea surface temperatures from isotopic and sclerochronological records. Nature 296, 432–434.

WILLIAMS, H.F.L., and HEBDA, R.J., 1991. Palynology of Holocene top-set aggradational sediments of the Fraser River Delta, British Columbia. Palaeogeography, Palaeoclimatology, Palaeoecology 86, 297–311.

WURSTER, C.M., and PATTERSON, W.P., 2001. Late Holocene climate change for the eastern interior United States: evidence from high-resolution $\delta^{18}O$ values of sagittal otoliths Palaeogeography, Palaeoclimatology, Palaeoecology 170, 81–100.

WURSTER, C.M., PATTERSON, W.P., and CHEATHAM, M.M., 1999. Advances in micromilling techniques: a new apparatus for acquiring high-resolution oxygen and carbon stable isotope values and major/minor elemental ratios from accretionary carbonate. Computers & Geosciences 25, 1159–1166.

ZHANG, Y., WALLACE, J.M., and BATTISTI, D.S., 1997. ENSO-like interdecadal variability: 1900-93. Journal of Climate 10, 1004–1020.

ZINKE, J., PFEIFFER, M., TIMM, O., DULLO, W.-Ch., and BRUMMER, G.J.A., 2009. Western Indian Ocean marine and terrestrial records of climate variability: a review and new concepts on land-ocean interactions since AD 1660. International Journal of Earth Sciences (Geologische Rundschau) 98, 115–133.

# 7. LIST OF ABBREVIATIONS AND SYMBOLS

| | |
|---|---|
| ACC | Alaska Coastal Current |
| AD | Anno Domini |
| AK | Alaska |
| AL | Aleutian Low |
| $Al_2O_3$ | Aluminium oxide |
| ALPI | Aleutian Low Pressure Index |
| AM | Ante meridiem (before noon) |
| ANOVA | Analysis of variance |
| approx. | Approximately |
| Apr | April |
| Aug | August |
| AVHRR | Advanced Very High Resolution Radiometer |
| BC | British Columbia |
| BP | Before present (present = 1950) |
| CA | California |
| ca. | Circa |
| CAA | Canadian Archaeological Association |
| $CaCO_3$ | Calcium carbonate |
| cal yrs BP | Calibrated years before present (present = 1950) |
| cf. | Conferre (compare) |
| Chl | Chlorophyll *a* |
| cm | Centimeter |
| $CO_2$ | Carbon dioxide |
| CT | Cardinal tooth |
| D | Discharge |

| | |
|---|---|
| DB | Discovery Bay |
| DFG | Deutsche Forschungsgemeinschaft (German Research Foundation) |
| DIC | Dissolved inorganic carbon |
| dog | Direction of growth |
| ed. | Editor |
| eds. | Editors |
| e.g. | For example |
| EGU | European Geosciences Union |
| ENSO | El Niño/Southern Oscillation |
| EPF | Extrapallial fluid |
| eq. | Equation |
| et al. | Et aliae (feminine), et alii (masculine) or et alia (neuter) (and others) |
| F | F-value (variance) |
| Feb | February |
| Fig./Figs | Figure/s |
| *g* | Growing season |
| g | Gram |
| GmbH | Gesellschaft mit beschränkter Haftung |
| GSA | Geological Society of America |
| GT | Growth-temperature |
| h | Hour |
| $HgCl_2$ | Mercuric chloride |
| $HNO_3$ | Nitric acid |
| *i* | Number of lunar daily growth increments |
| ICP-MS | Inductively coupled plasma mass spectrometry |
| ICP-OES | Inductively coupled plasma optical emission spectrometry |
| ID | Idaho |

| | |
|---|---|
| i.e. | That is |
| ISC | International Sclerochronology Conference |
| Jan | January |
| JSPS | Japan Society for the Promotion of Science |
| Jul | July |
| Jun | June |
| km | Kilometer |
| $km^2$ | Square kilometer |
| LDGI | Lunar daily growth increments |
| LDGI' | Filtered and detrended LDGI data |
| Mar | March |
| m | Meter |
| mg | Milligram |
| Mg/Ca | Magnesium-calcium ratio |
| MI | Mink Island |
| min | Minute |
| ml | Milliliter |
| mm | Millimeter |
| n | Number of samples/data points |
| N | North |
| N | Neap tide |
| $Na^+$ | Sodium ion |
| NASA | National Aeronautics and Space Administration |
| NBS | National Bureau of Standards |
| NCEP | National Centers for Environmental Prediction |
| no. | Number |
| NOAA | National Oceanic and Atmospheric Administration |

| | |
|---|---|
| Nov | November |
| NPH | North Pacific High |
| NPI | North Pacific Index |
| NRF | National Research Foundation |
| NW | North-west |
| Oct | October |
| OR | Oregon |
| OSL | Outer shell layer |
| p | p-value (probability) |
| p. | Page |
| P | Precipitation |
| PDO | Pacific Decadal Oscillation |
| PI | Protection Island |
| PM | Post meridiem (after noon) |
| PMEL | Pacific Marine Environmental Laboratory |
| PNA | Pacific/North American teleconnection index |
| PO.DAAC | Physical Oceanography Distributed Active Archive Centre |
| ppm | Parts per million |
| PSU | Practical salinity units |
| R | R-value (correlation coefficient) |
| $R^2$ | $R^2$-value (coefficient of determination) |
| RR | Race Rocks |
| S | Spring tide |
| S | Salinity |
| $S_{inc}$ | Increment-derived salinity |
| $S_{Na}$ | Sodium derived salinity |
| $S_{reco}$ | Reconstructed salinity |

| | |
|---|---|
| SD | Standard deviation |
| SE | Standard error |
| Sep | September |
| s.l. | Sensu lato (in the stricter sense) |
| SLP | Sea level pressure |
| spp. | Species (plural) |
| Sr/Ca | Strontium-calcium ratio |
| SST | Sea surface temperature |
| $SST_{satellite}$ | Satellite-measured sea surface temperature |
| *St* | Storm |
| SW | South west |
| T | Temperature |
| $T_{inc}$ | Increment-derived temperature |
| $T_{\delta 18O}$ | Temperatures reconstructed from oxygen isotope values |
| $T\delta^{18}O_{CT}$ | Temperatures reconstructed from oxygen isotope values of the cardinal tooth portion |
| $T\delta^{18}O_{OSL}$ | Temperatures reconstructed from oxygen isotope values of the outer shell layer |
| $T_{logger}$ | Temperature recorded by a logger |
| $T_{logger}$' | Filtered $T_{logger}$ data |
| $T_{NCEP}$ | Satellite derived sea surface temperature |
| $T_{reco}$ | Reconstructed temperature |
| Tab./Tabs | Table/s |
| UP | Unimak Pass |
| vol% | Volume percent |
| VPDB | Vienna Pee Dee Belemnite |
| vs. | Versus |
| VSMOW | Vienna Standard Mean Ocean Water |

| | |
|---|---|
| *w* | Winter growth line |
| W | West |
| WA | Washington State |
| WDFW | Washington Department of Fish and Wildlife |
| yr(s) | Year(s) |
| YT | Yukon Territory |

| | |
|---|---|
| $^{14}C_{AMS}$ | Carbon-14 Accelerator Mass Spectrometry radiocarbon dating |
| $^{14}C$ yrs BP | Carbon-14 years before present (present = 1950) |
| $^{16}O$ | Oxygen-16 |
| $^{18}O$ | Oxygen-18 |
| $^{44/40}Ca$ | Ratio of calcium isotopes calcium-44 to calcium-40 |
| $\delta$ | Delta |
| $\delta^{18}O$ | Ratio of stable oxygen isotopes ($^{18}O/^{16}O$) relative to a standard |
| $\delta^{18}O_{shell}$ | Ratio of stable oxygen isotopes ($^{18}O/^{16}O$) of shell carbonate relative to the standard (VPDB) |
| $\delta^{18}O_{shell}$' | Temporally equalized $\delta^{18}O_{shell}$ values |
| $\delta^{18}O_{CT}$ | Ratio of stable oxygen isotopes ($^{18}O/^{16}O$) of the cardinal tooth relative to the standard (VPDB) |
| $\delta^{18}O_{OSL}$ | Ratio of stable oxygen isotopes ($^{18}O/^{16}O$) of the outer shell layer relative to the standard (VPDB) |
| $\delta^{18}O_{exp}$ | Expected ratio of stable oxygen isotopes ($^{18}O/^{16}O$) relative to a standard |
| $\delta^{18}O_{water}$ | Ratio of stable oxygen isotopes ($^{18}O/^{16}O$) of sea water relative to the standard (VSMOW) |
| $\delta^{18}O_{water, reco}$ | Reconstructed ratio of stable oxygen isotopes ($^{18}O/^{16}O$) of sea water relative to the standard (VSMOW) |
| $\delta^{13}C$ | Ratio of stable carbon isotopes ($^{13}C/^{12}C$) relative to a standard |
| $\delta^{13}C_{DIC}$ | Ratio of stable carbon isotopes ($^{13}C/^{12}C$) of dissolved inorganic carbon relative to the standard (VPDB) |
| $\delta^{13}C_{shell}$ | Ratio of stable carbon isotopes ($^{13}C/^{12}C$) of shell carbonate relative to the standard (VPDB) |
| $\delta^{13}C_{shell}$ | Temporally equalized $\delta^{13}C_{shell}$ values |
| $\Delta 47$ | Abundances of mass-47 isotopologues of $CO_2$ (clumped isotopes): Difference between the measured 47/44 ratio of the sample and the expected ratio for that sample if all carbon and oxygen isotopes were randomly distributed among the isotopologues (in ‰) |

| | |
|---|---|
| ΔR | Local correction value of the marine reservoir effect |
| µg | Microgram |
| µg/l | Microgram per liter |
| µm | Micrometer |
| ° | Degree |
| °C | Degree Celsius |
| % | Per cent |
| %RSD | Relative standard deviation in % |
| ‰ | Per mil |
| & | And |
| ± | Plus-minus |
| = | Equals |
| ~ | Approximately |
| > | Greater than |
| # | Number |
| σ | Sigma |
| © | Copyright |

# 8. CURRICULUM VITAE

For reasons of data protection the curriculum vitae is not displayed in the online version of this thesis.

# 9. PEER-REVIEWED PUBLICATIONS

**HALLMANN, N.**, SCHÖNE, B.R., IRVINE, G.V., BURCHELL, M., COKELET, E.D., and HILTON, M., 2011. An improved understanding of the Alaska Coastal Current: The application of a bivalve growth-temperature model to reconstruct freshwater-influenced paleoenvironments. PALAIOS, In press.

SEIDENDORF, B., **MEIER [HALLMANN], N.**, PETRUSEK, A., BOERSMA, M., STREIT, B., and SCHWENK K., 2010. Sensitivity of *Daphnia* species to phosphorus-deficient diets. Oecologia 162, 349–357.

**HALLMANN, N.**, BURCHELL, M., SCHÖNE, B.R., IRVINE, G.V., and MAXWELL, D., 2009. High-resolution sclerochronological analysis of the bivalve mollusk *Saxidomus gigantea* from Alaska and British Columbia: Techniques for revealing environmental archives and archaeological seasonality. Journal of Archaeological Science 36, 2353–2364.

THÉBAULT, J., SCHÖNE, B.R., **HALLMANN, N.**, BARTH ,M., and NUNN, E.V., 2009. Investigation of Li/Ca variations in aragonitic shells of the ocean quahog *Arctica islandica*, northeast Iceland. Geochemistry, Geophysics, Geosystem*s* 10, Q12008, doi:10.1029/2009GC002789.

**HALLMANN, N.**, SCHÖNE, B.R., STROM, A., and FIEBIG, J., 2008. An intractable climate archive - Sclerochronological and shell oxygen isotope analyses of the Pacific geoduck, *Panopea abrupta* (bivalve mollusk) from Protection Island (Washington State, USA). Palaeogeography, Palaeoclimatology, Palaeoecology 269, 115–126.

**IN REVIEW:**

BURCHELL, M., **HALLMANN, N.**, SCHÖNE, B.R., CANNON, A., and SCHWARCZ, H. Biogeochemical signatures of archaeological shells: Implications for interpreting seasonality at shell midden sites. Book chapter.

**IN PREPARATION:**

**HALLMANN, N.**, BURCHELL, M., SCHÖNE, B.R., MARTINDALE, A., and SCHWARCZ, H.P. Holocene climate changes at Dundas Islands, northern British Columbia, reconstructed from the bivalve mollusk *Saxidomus gigantea*.

# 10. CONFERENCE CONTRIBUTIONS

## Oral presentations held at international meetings

**HALLMANN, N.**, BURCHELL, M., SCHÖNE, B.R., MARTINDALE, A., CANNON, A. and SCHWARCZ, H..P., 2010. Holocene climate changes in British Columbia and seasonality estimates reconstructed from the bivalve *Saxidomus gigantea* using high-resolution isotope sclerochronology. *In*: SCHÖNE, B.R., NUNN, E.V. (eds.) Program and Abstracts, 2nd International Sclerochronology Conference 2010, July 24-28, Mainz, Germany, p.50.

**MEIER [HALLMANN], N.**, SCHÖNE, B.R., STROM, A., and FIEBIG, J., 2008. Sclerochronological and isotope ($\delta^{18}O$) analyses of *Panopea abrupta* (bivalve mollusk) shells from Protection Island (Washington, USA). Geophysical Research Abstracts Vol. 10, EGU2008-A-09537, EGU General Assembly 2008, April 13-18, Vienna, Austria.

## Co-authored oral presentations held at international meetings

BURCHELL, M.*, CANNON, A., **HALLMANN, N.**, SCHÖNE, B.R., and MARTINDALE, A., 2010. Understanding ancient shellfish use in British Columbia, Canada through high-resolution sclerochronology and oxygen isotope profiles. *In*: SCHÖNE, B.R., NUNN, E.V. (eds.) Program and Abstracts, 2nd International Sclerochronology Conference 2010, July 24-28, Mainz, Germany, p.34.

THÉBAULT, J.*, SCHÖNE, B.R., CHAUVAUD, L., **HALLMANN, N.**, RICHARD, M., BARTH, M., NUNN, E.V., and BASSOULLET, C. 2010. Investigation of Li/Ca ratio temporal variations in shells of two marine bivalves: *Arctica islandica* (Iceland) and *Pecten maximus* (France). *In*: SCHÖNE, B.R., NUNN, E.V. (eds.) Program and Abstracts, 2nd International Sclerochronology Conference 2010, July 24-28, Mainz, Germany, p.81.

BURCHELL, M.*, **HALLMANN, N.**, SCHÖNE, B.R., MARTINDALE, A., CANNON, A., and SCHWARCZ, H.P., 2010. Improving seasonality estimates at shell midden sites: a case study from British Columbia using high-resolution isotope sclerochronology. 43rd Annual Meeting Canadian Archaeological Association (CAA) 2010, April 28-May 02, Calgary, Alberta, Canada.

BURCHELL, M.*, **HALLMANN, N.**, SCHÖNE, B.R., and SCHWARCZ, H.P., 2009. Improving the precision of seasonality estimates using high-resolution sclerochronology and oxygen isotope analysis: A case study from the Pacific Northwest Coast. Developing International Geoarchaeology (DIG) 2009, May 25-29, Hamilton, Ontario, Canada.

**HALLMANN, N.**, BURCHELL, M., SCHÖNE, B.R.*, and MAXWELL, D., 2008. Life history traits of the bivalve mollusk *Saxidomus giganteus* from the coast of British Columbia: Insights for paleoclimate and archaeological applications. Geological Society of America (GSA) – Joint Annual Meeting 2008, October 05-09, Houston, Texas, USA.

*Presenting author

## Poster presentations with published abstracts

**HALLMANN, N.**, SCHÖNE, B.R., BURCHELL, M., TANABE, K., IRVINE, G.V., CANNON, A., MIYAJI, T., and MARTINDALE, A., 2010. Reconstruction of North Pacific Holocene climate using marine bivalves from shell midden deposits. *In*: SCHÖNE, B.R., NUNN, E.V. (eds.) Program and Abstracts, 2nd International Sclerochronology Conference 2010, July 24-28, Mainz, Germany, p.118.

**HALLMANN, N.**, BURCHELL, M., SCHÖNE, B.R., and MAXWELL, D., 2010. Life history traits of the bivalve mollusk *Saxidomus giganteus* from the coast of British Columbia: Insights for paleoclimate and archaeological applications. Geophysical Research Abstracts Vol. 12, EGU2010-4602, EGU General Assembly 2010, May 02-07, Vienna, Austria.

**MEIER [HALLMANN], N.**, HEUBACH, K., BREDE, N., and SCHWENK, K., 2006. Coexistence of *Daphnia* hybrids and parental species: variation in life history strategies of ex-ephippial and parthenogenetic females. Symposium on Hybridization in Animals – Extent, Processes and Evolutionary Impact 2006, October 12-14, Frankfurt, Germany.